

AN ABSTRACT OF THE THESIS OF

Lisa C. McNeill for the degree of Doctor of Philosophy in Geology presented on October 12, 1998.

Title: Structure and Seismic Hazards of the Offshore Cascadia Forearc and Evolution of the Neogene Forearc Basin.

Redacted for Privacy

Abstract approved: _____

Robert S. Yeats

The Cascadia subduction zone has been characterized as a typical Chilean-type subduction zone based on qualitative comparisons of plate age and convergence rate, with simple forearc structure. However, the discovery of unusual structural styles of deformation, variations in the morphology of the forearc, and its absence of seismic activity suggest differences from the Chilean analog. The manuscripts presented here (McNeill et al., 1997, in press, submitted) illustrate this complexity and provide examples of contrasting deformation throughout the offshore forearc. The Washington and northern Oregon shelf and upper slope are characterized by extension in the form of listric normal faults. These faults have been active since the late Miocene and are driven by detachment and extension of the underlying overpressured mélangé and broken formation. This region of the forearc is partly to wholly decoupled from convergence-driven compression which dominates deformation elsewhere in the forearc. One exception to convergence-driven compression is a region of N-S compression of the inner shelf and coastal region which reflects the regional stress field. N-S compressional structures apparently influence the positions of coastal lowlands and uplands and may contribute to the record of coastal marsh burials interpreted as the result of coseismic subsidence during subduction zone earthquakes. Modeling of subduction zone earthquake characteristics based on marsh stratigraphy is likely to be inaccurate in terms of rupture zone position, magnitude, and recurrence interval. The Cascadia shelf and upper slope are underlain by a sequence of deformed basinal strata which reflects the tectonic evolution of the margin. The surface of a regional late Miocene angular unconformity (7.5-6 Ma: a global hiatus) indicates deformation by uplifted submarine banks and subsided synclines (coincident with low recent uplift onshore), which control the current shelf break position. The basin is

currently filled behind a N-S-trending outer-arc high, which uplifted in the early-middle Pliocene following truncation and erosion of the seaward edge of the basin. Breaching of the outer-arc high occurred in the early Pleistocene leading to the formation of the Astoria Submarine Fan and increased growth rates of the accretionary wedge.

© Copyright Lisa C. McNeill
October 12, 1998
All Rights Reserved

**Structure and Seismic Hazards of the Offshore Cascadia Forearc and
Evolution of the Neogene Forearc Basin**

by

Lisa C. McNeill

A Thesis Submitted

to

Oregon State University

In Partial Fulfillment of
the requirements for the
degree of

Doctor of Philosophy

Presented October 12, 1998

Commencement June, 1999

Doctor of Philosophy thesis of Lisa C. McNeill presented on October 12, 1998

Approved:

Redacted for Privacy

Major Professor, representing Geology

Redacted for Privacy

Chair of Department of Geosciences

Redacted for Privacy

Dean of Graduate School

I understand that my thesis will become part of the permanent collection of Oregon State University libraries. My signature below authorizes release of my thesis to any reader upon request.

Redacted for Privacy

Lisa C. McNeill, Author

Acknowledgments

I would like to thank my five committee members, Bob Yeats, Vern Kulm, Chris Goldfinger, Alan Niem, and Robert Jarvis for the time and trouble they have taken in reading and reviewing this thesis. Extreme appreciation is extended, in particular, to Bob Yeats, Vern Kulm, and Chris Goldfinger who have provided countless hours of their time in guiding this research, discussing ideas, providing encouragement at crucial moments, and always being available and interested to help and advise. This project would not have been possible without their assistance. I would also like to particularly thank Chris Goldfinger for his invaluable assistance in the lab, with scientific and computer problems alike. I am grateful to all three for involving me in many other projects outside my thesis, giving me a much broader understanding of oceanographic and neotectonic research and a more rewarding five years than I might otherwise have experienced. I would also like to take this opportunity to thank two members who served on my committee until the defense, for which they were unfortunately unavailable: Robert Lillie and Wayne Huber.

I would like to extend a special thank you to the Minerals Management Service (in particular, Ken Piper and Scott Drewry) for providing data without which this research would not have been possible. Many others have contributed technical advice and scientific insight during the last five years which has vastly improved my understanding of the Cascadia subduction zone, including Brian Atwater, Steve Dickenson, Harvey Kelsey, Pat McCrory, Ken Piper, George Priest, Glenn Thackray, and Anne Tréhu. Katrina Petersen spent a summer working on the dataset for the third manuscript, for which I am extremely grateful. Thanks also to Cheryl Hummon for her assistance at the beginning of my studies.

Numerous wonderful friends have made this time an unforgettable one, and were always available to provide welcome relief from work, moral support, and companionship in exploring this country. I cannot name them all but a few deserve a special mention: Joe Licciardi, Emily Oatney, Christy Robertson, Matt Wood, Pat Kenelly, Sharon London, Sian Mooney, Rob Neely, Sue Mauger, Id Greene, and Jean-Christophe Domec. Last but not least, I would like to thank my parents, who were always supportive and encouraging despite being thousands of miles away.

I acknowledge the funding which made this research possible from the National Science Foundation, National Earthquake Hazard Reduction Program of the U.S. Geological Survey, and, in particular, the West Coast National Undersea Research Center which provided research assistantship support for the majority of my degree program and provided the rare opportunity to explore the ocean floor by submersible during numerous research cruises.

Contribution of Authors

Chris Goldfinger, LaVerne D. Kulm, and Robert S. Yeats were the Principal Investigators of the research projects which resulted in the manuscripts presented here. Their collective contributions included assistance with initial development of the research problems, guidance in methodology, and interpretations of the final results. Their relative contributions to each of the three papers are indicated by the order of co-authorship.

Kenneth A. Piper of the Minerals Management Service first identified the listric normal faults of the Washington shelf described in Chapter II and contributed to the interpretation of fault morphology and mechanisms of extension.

The Neotectonic Map of Offshore Washington is currently unpublished but may be incorporated into a Neotectonic Map of the entire Cascadia Subduction Zone and published through the U.S. Geological Survey. This map incorporates initial mapping by Chris Goldfinger and Cheryl Hummon.

Table of Contents

	<u>Page</u>
Chapter I Introduction	1
Chapter II Listric Normal Faulting on the Cascadia Continental Margin	3
II.1 Abstract	4
II.2 Introduction and Previous Work	4
II.3 Tectonic Setting	5
II.4 Stratigraphy and Uplift History	8
II.5 Seismic Reflection Data Acquisition And Processing	13
II.6 Delineation of Seismic Stratigraphic Units	13
II.7 Distribution and Morphology of Normal Faults	19
II.8 Discussion	23
II.8.1 Isolation of Shelf Tectonics	23
II.8.2 Association of Normal Faulting with Mélange and Broken Formation	23
II.8.3 Cascadia Normal Faulting Mechanisms	24
II.8.4 Alternative Faulting Mechanisms	28
II.8.5 Extension Versus Compressional Deformation	29
II.8.6 Global Comparisons	30
II.9 Conclusions	30
II.10 Acknowledgments	31
II.11 References	32
Chapter III The Effects of Upper Plate Deformation on Records of Prehistoric Subduction Zone Earthquakes	38
III.1 Abstract	39
III.2 Introduction	39
III.3 Methods	40
III.4 Tectonic Setting	41
III.5 Regional Stratigraphy and Structure	43
III.6 Active Crustal Structures and Coastal Subsidence	45
III.6.1 Introduction	45
III.6.2 Buried Marshes in Areas of Late Quaternary Subsidence	45
III.6.3 Locations with Inconclusive Evidence for Quaternary Subsidence	65

Table of Contents, Continued

	<u>Page</u>
III.6.4 Marsh Burial Located Near Structural Uplifts	66
III.7 Discussion	67
III.7.1 Implications for the Cascadia Subduction Zone Earthquake Record	67
III.7.2 N-S Compression	74
III.8 Conclusions	75
III.9 Acknowledgments	76
III.10 References	77
 Chapter IV Evolution of the Late Neogene Central Cascadia Forearc Basin From Investigations of a Late Miocene Unconformity	 88
IV.1 Abstract	89
IV.2 Introduction	90
IV.3 Methods	91
IV.4 Cascadia Forearc Basin Stratigraphy	94
IV.5 Results	101
IV.5.1 Age of the Unconformity	101
IV.5.2 Evidence for Subaerial vs. Submarine Erosion	102
IV.5.3 Deformation of the Late Miocene Unconformity	107
IV.6 Discussion	116
IV.6.1 Regional and Global Correlations of the Late Miocene Cascadia Unconformity	116
IV.6.2 Mechanism of Erosion: Subaerial vs. Submarine	118
IV.6.3 Driving Mechanism of Erosion: Tectonics vs. Climate Change	120
IV.6.4 Evolution of the Neogene Cascadia Forearc	121
IV.6.5 Comparisons With the Washington Shelf Forearc Basin and the Eel River Basin of Northern California	133
IV.9 Conclusions	135
IV.10 Acknowledgments	137
IV.11 References	138
 Chapter V Conclusions	 148
Bibliography	150
 Appendix Neotectonic Map of Offshore Washington	 173

List of Figures

<u>Figure</u>	<u>Page</u>
Chapter II	
II.1 Map of the Cascadia subduction zone showing the study area (boxed) and underlying lithologies of the Oregon and Washington continental shelves (modified from Snively [1987] and Palmer and Lingley [1989])	6
II.2A Neotectonic map of the Washington and northern Oregon margins (modified from McCaffrey and Goldfinger [1995]) showing Quaternary (solid lines) and Pliocene and early Pleistocene (dashed lines) anticlinal fold axes and faults (synclinal fold axes removed for clarity)	7
II.2B Map of undifferentiated seismic reflection track lines from industry (public and proprietary), academic, and government sources	9
II.2C Map of the study area locating major normal faults mapped in this study	10
II.3 Stratigraphy of the Washington continental shelf as inferred from outcrops on the western Olympic Peninsula and lithologies penetrated by industry boreholes on the continental shelf [Palmer and Lingley, 1989]	11
II.4 Neotectonic and bathymetric map of the Grays Canyon outer shelf and upper slope region	14
II.5 (Top) E-W migrated multichannel seismic reflection profile A-A' on the central Washington continental shelf and upper slope with (bottom) interpretive line drawing	15
II.6 (Top) E-W migrated multichannel seismic reflection profile B-B' on the central Washington upper slope and shelf edge with (bottom) interpretive line drawing	17
II.7 (Top) E-W migrated multichannel seismic reflection profile C-C' on the southern Washington midshelf off Willapa Bay with (bottom) interpretive line drawing	18

List of Figures, Continued

	<u>Page</u>
II.8 Video frame from the Delta submersible of fault scarp A1 (see Figures II.4 and II.5) at the head of Grays Canyon	22
II.9 Development and mechanisms of listric faulting on the Cascadia outer shelf	26
 Chapter III	
III.1 Neotectonic map of active structures (late Pliocene to Holocene anticlines and faults only), including inner shelf and coastal structures outlined in this paper, and locations of coastal subsidence	42
III.2 Model showing the subduction earthquake cycle (after Darienzo & Peterson 1990)	44
III.3 Map of southern Washington coast and offshore region	47
III.4 N-S proprietary migrated multichannel seismic reflection profile 10 km west of Willapa Bay	49
III.5 Early Pleistocene terrace tidal flat sediments between Stony Point (St) and Bone River (BR) in Willapa Bay showing S-dipping palaeosols (after Clifton 1994), in agreement with the projection of the offshore synclinal axis to a position south of this location	51
III.6 Location map of northern Oregon coast and shelf, including active structures near Nehalem, Tillamook, and Netarts Bay	53
III.7 N-S proprietary multichannel seismic reflection profile between Netarts Bay and Nehalem Bay, 10 km west of the coastline	54
III.8 Location map of Siletz Bay on the central Oregon coast showing structures mapped offshore from single channel and multichannel seismic reflection profiles and onshore from Pleistocene marine terrace deformation (structures in Fig. III.9 cross section)	57

List of Figures, Continued

	<u>Page</u>
III.9 Cross section of beach exposure of Pleistocene terrace sands underlying the youngest marine terrace at Siletz Bay	58
III.10 Line drawing of N-S trending OSU single channel sparker profile, 6 km offshore Siletz Bay (bold line in Fig. III.8)	60
III.11 Central coastal Oregon between Yaquina Head and Alsea Bay, showing late Pleistocene marine terrace backedges and Quaternary faulting (after Kelsey et al. 1996)	62
III.12 Location map of the south-central Oregon coast and shelf showing Pliocene and Quaternary structures	63
III.13 Illustration of the resulting record of Taisho and Genroku subduction earthquakes on the Nankai margin (after Sugiyama 1994)	69
III.14 Coastal marsh stratigraphy in hypothetical cores showing subsided marsh and soil deposits produced by a variety of coseismic events	71

Chapter IV

IV.1 Tectonic setting of Cascadia subduction zone (inset) and study area indicating datasets used to identify late Miocene unconformity and stratigraphy of the forearc basin	92
IV.2 Generalized stratigraphy of the Eel River Basin, northern California (based on Ingle, 1987; Clark, 1992; McCrory, 1995), central Oregon coast and shelf (based on Snively, 1987; Snively and Wells, 1992; Yeats et al., 1998), and the Washington coast and shelf (based on Palmer and Lingley, 1989; McNeill et al., 1997)	95
IV.3 Extent of the late Miocene unconformity and correlative seaward conformity or disconformity	99
IV.4 E-W multichannel seismic reflection profile west of Siletz Bay (located on Fig. IV.1) showing the angular nature of the late Miocene unconformity on the inner to middle shelf	103

List of Figures, Continued

	<u>Page</u>
IV.5 E-W multichannel seismic reflection profile across the continental shelf at Stonewall Bank west of Alsea Bay (located on Fig. IV.1)	104
IV.6 Shaded relief structure contour map of the late Miocene unconformity on the central Cascadia shelf and upper slope	108
IV.7 Magnetic anomaly data (nT) of central Cascadia margin, from NGDC dataset with structure contour map of the late Miocene unconformity superimposed	112
IV.8 Gravity anomaly data (mgal) of central Cascadia margin, from NGDC dataset with structure contour map of the late Miocene unconformity superimposed	113
IV.9 Margin-parallel uplift rates and relative uplift from the continental shelf to the Coast Range	115
IV.10a E-W multichannel seismic reflection profile across Heceta Bank showing the outer-arc high of the Neogene forearc basin (located on Fig.IV.1)	123
IV.10b,c E-W multichannel seismic reflection profiles across the upper slope of the central Cascadia forearc (locations on Fig.IV.1)	124
IV.11 Tectonic history of the Neogene central Cascadia forearc depicted by time slice cross sections of the central Oregon forearc from the Cascades to the deformation front	125
IV.12 Sketch of E-W seismic reflection profile across the Astoria Fan and lower accretionary wedge at ODP Sites 174 and 175 (after von Huene and Kulm, 1973)	132

Structure and Seismic Hazards of the Offshore Cascadia Forearc and Evolution of the Neogene Forearc Basin

Chapter I

Introduction

The three manuscripts that comprise this thesis focus on different aspects of late Neogene structural deformation of the offshore and coastal Cascadia subduction zone of Oregon and Washington, northwestern United States. The seismic potential of this subduction zone has been a subject of intense debate, due to the apparent conflict between its tectonic similarity to other seismogenic subduction zones and its anomalously low seismic activity. The discovery of evidence for prehistoric subduction zone earthquakes in the last decade has furthered this debate, with the ultimate hope of determining the position and extent of the locked zone, potential magnitude of future earthquakes, and the likely timing of such potentially catastrophic events.

The Cascadia subduction zone has been characterized in the past as a typical Chilean-type subduction zone and its forearc structure has been, to some extent, oversimplified. High-quality seismic reflection data and seafloor geomorphological imaging techniques have shown that this subduction zone is characterized by complex deformation and can be divided into discrete structural regions, including regions of normal faulting, N-S compression, convergence-related compression, and mass wasting. Furthermore, investigations of the subsurface structure and stratigraphy indicate how deformation and the forearc morphology have evolved through time. Variations in deformation indicate different local and regional stress regimes, potential degree and position of interplate coupling, and regions of weakness and strength within the basement of the North American plate. An improved understanding of how the upper plate is deforming and what drives this deformation ultimately enhances our understanding of Cascadia subduction dynamics and the potential seismic and tsunami hazards that the communities of the Pacific Northwest may face from this subduction zone and forearc. Delineation of regions of distinct structural deformation style may indicate regions with differential plate coupling, individual rupture segments of the subduction zone boundary, and additional seismic sources. In addition, a more thorough understanding of the extent of heterogeneity of deformation within Cascadia is applicable to the study and understanding of active margins worldwide,

particularly where detailed studies and datasets such as those used here are currently unavailable.

Chapter II discusses evidence for and mechanisms of gravitational extension on the Washington and northern Oregon shelf and upper slope, which results in listric normal faulting, a structural phenomenon more commonly associated with passive margins. This extensional region contrasts with the predominant compression of the seaward portion of the margin. Chapter III documents evidence of N-S compression on the inner shelf and coast of the upper (North American) plate, which contrasts with predominantly northeasterly compression driven by convergence within the accretionary wedge. The evidence of prehistoric subduction zone earthquakes, in the form of rapidly subsided marsh deposits in coastal bays, coincides geographically with several of these N-S compressional structures. This association suggests that at least part of the coseismic subsidence record may be attributed to movement on upper plate structures rather than elastic rebound from the subduction zone. These structures are of critical importance to the interpretation of the paleoseismological record, and in determining the limits of the use of this record for earthquake parameters. Chapter IV investigates the origins and subsequent deformation of a late Miocene unconformity within the offshore forearc basin of the central margin. Stratigraphic and seismic reflection data are used to determine the evolution of the Cascadia forearc basin and the driving mechanisms of major changes in deposition and structural deformation, at local and regional scales and tied to global events. The deformed late Miocene surface can also be compared with data documenting coastal and Coast Range Quaternary uplift rates, to determine if rates consistently vary in time and across the margin. These data may indicate relative degrees of elastic (interplate) or permanent (interplate and upper plate) deformation.

The first paper (Chapter II), entitled "Listric Normal Faulting on the Cascadia Continental Margin" was published in June, 1997 in the *Journal of Geophysical Research*. The second paper (Chapter III), entitled "The Effects of Upper Plate Deformation on Records of Prehistoric Subduction Zone Earthquakes", will be published by the end of 1998 in a Special Publication of the Geological Society of London, "Coastal Tectonics", edited by I. Stewart and C. Vita-Finzi. The third paper (Chapter IV), entitled "Evolution of the Late Neogene Central Cascadia Forearc Basin From Investigations of a Late Miocene Unconformity", will be submitted to the *Geological Society of America Bulletin*. The Appendix, "Neotectonic Map of Offshore Washington", is currently unpublished but may be incorporated into a map of the entire Cascadia subduction zone to be compiled by the U.S. Geological Survey.

Chapter II

Listric Normal Faulting on the Cascadia Continental Margin

Lisa C. McNeill¹, Kenneth A. Piper², Chris Goldfinger³, LaVerne D. Kulm³,
and Robert S. Yeats¹

¹ Department of Geosciences,
Oregon State University, Corvallis, Oregon 97331

² Minerals Management Service,
Camarillo, California 93010

³ College of Oceanic and Atmospheric Sciences,
Oregon State University, Corvallis, Oregon 97331

McNeill, L.C., Piper, K.A., Goldfinger, C., Kulm, L.D., and Yeats, R.S.,
Listric normal faulting on the Cascadia continental margin:
Journal of Geophysical Research, v. 102, n. B6, p. 12,123-12,138, 1997.

II.1 ABSTRACT

Analysis of multichannel seismic reflection profiles reveals that listric normal faulting is widespread on the northern Oregon and Washington continental shelf and upper slope, suggesting E-W extension in this region. Fault activity began in the late Miocene and, in some cases, has continued into the Holocene. Most listric faults sole out into a subhorizontal décollement coincident with the upper contact of an Eocene to middle Miocene *mélange* and broken formation (MBF), known as the Hoh rock assemblage onshore, whereas other faults penetrate and offset the top of the MBF. The areal distribution of extensional faulting on the shelf and upper slope is similar to the subsurface distribution of the MBF. Evidence onshore and on the continental shelf suggests that the MBF is overpressured and mobile. For listric faults which become subhorizontal at depth, these elevated pore pressures may be sufficient to reduce effective stress and to allow downslope movement of the overlying stratigraphic section along a low-angle (0.1° - 2.5°) detachment coincident with the upper MBF contact. Mobilization, extension, and unconstrained westward movement of the MBF may also contribute to brittle extension of the overlying sediments. No Pliocene or Quaternary extensional faults have been identified off the central Oregon or northernmost Washington coast, where the shelf is underlain by the rigid basaltic basement of the Siletzia terrane. Quaternary extension of the shelf and upper slope is contemporaneous with active accretion and thrust faulting on the lower slope, suggesting that the shelf and upper slope are decoupled from subduction-related compression.

II.2 INTRODUCTION AND PREVIOUS WORK

Listric normal faulting is a common feature of passive margins, where fault movement contributes to crustal thinning and margin subsidence. Extension and normal faulting are also a fairly common phenomenon on convergent margins throughout the world. Examples include the forearcs of southern Peru-northern Chile [*Li*, 1995], northern Peru [*von Huene et al.*, 1989], the Middle America Trench off Costa Rica [*McIntosh et al.*, 1993] and Guatemala [*Aubouin et al.*, 1982], and the Japan Trench [*Karig et al.*, 1983; *von Huene and Lallemand*, 1990]. Extension is often associated with basal or frontal subduction erosion or nonaccretion [*von Huene and Scholl*, 1991; *McIntosh et al.*, 1993].

Decoupling by high pore pressures and reduced basal shear stress may also lead to extension in a convergent tectonic setting [Dahlen, 1984; von Huene *et al.*, 1989].

The Cascadia subduction zone (Fig. II.1) is characterized by active accretion with ample evidence of late Quaternary convergence and compressional folding on the continental slope (Fig. II.2a) [Silver, 1972; Kulm *et al.*, 1973; Carson *et al.*, 1974; Goldfinger *et al.*, 1992; MacKay *et al.*, 1992]. Older (late Pliocene to early Quaternary) compressional structures have been mapped by previous workers [Silver, 1972; Kulm and Fowler, 1974; Wagner *et al.*, 1986; Snavely, 1987; Goldfinger *et al.*, 1992] on the continental shelves of Oregon and Washington (Fig. II.2a). This study enlarges on the work of Cranswick and Piper [1992] which revealed the existence of active crustal extensional structures on the Washington and northern Oregon shelf and upper slope. The extent, morphology, and possible causes of these extensional features have been further documented by Piper [1994], Piper *et al.* [1995], and McNeill *et al.* [1995]. Discovery of these extensional structures requires a reevaluation of structures previously interpreted as folds and faults related to plate convergence. This paper will focus on the morphology, structure, stratigraphy, and inferred mechanisms of normal faulting on the Cascadia margin.

II.3 TECTONIC SETTING

The Cascadia subduction zone is formed by the subduction of the oceanic Juan de Fuca and Gorda plates beneath the North American plate off the coast of northern California, Oregon, Washington, and Vancouver Island, British Columbia (Fig. II.1). The convergence rate is 42 mm/yr. directed N69°E at the latitude of Seattle according to the NUVEL-1 plate motion model (Fig. II.1) [DeMets *et al.*, 1990]. Juan de Fuca-North American convergence is oblique, with obliquity decreasing at 5 Ma due to clockwise rotation of the convergence vector [Wilson, 1993], and with distance along the margin from south to north, due to increasing distance from the pole of rotation and change in orientation of the margin. The submarine forearc widens from 60 km off southern Oregon to 150 km off the northern Olympic Peninsula of Washington, suggesting higher regional sedimentation rates to the north. Higher Pleistocene sedimentation rates in this region are also indicated by the Astoria and Nitinat Fans on the northern Oregon and Washington abyssal plain (Fig. II.1). The accretionary complex comes onshore in Washington, where it is uplifted and eroded to form the core rocks of the Olympic Mountains. Much of onshore western Oregon and Washington and the continental shelf of Oregon are underlain

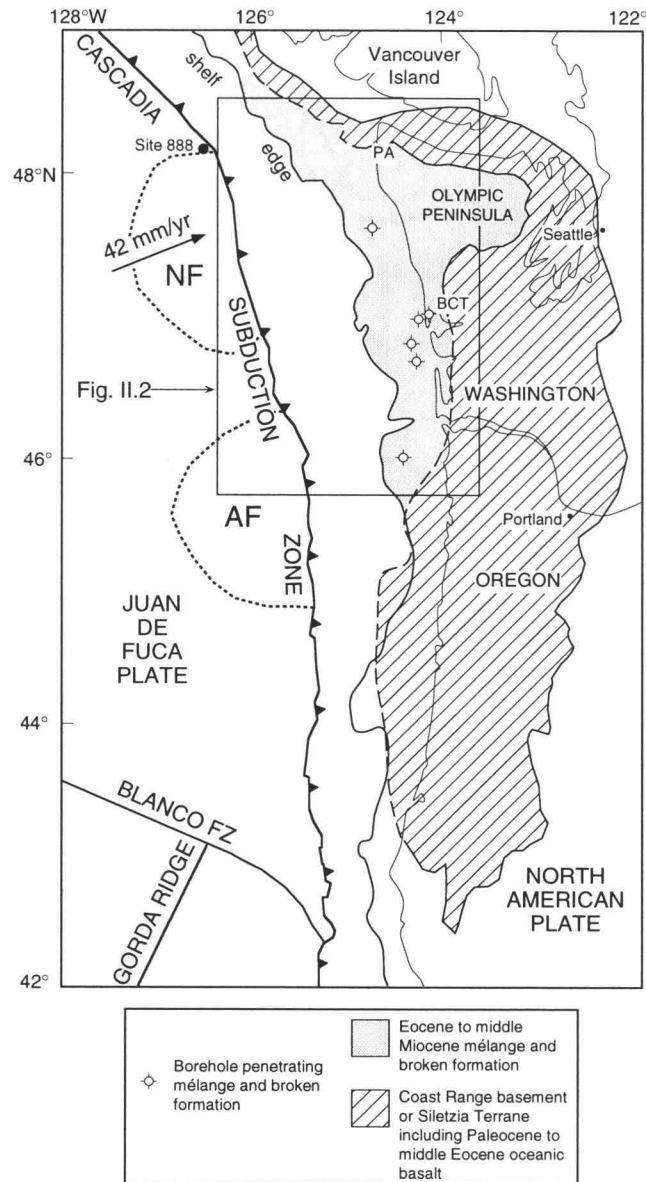


Figure II.1. Map of the Cascadia subduction zone showing the study area (boxed) and underlying lithologies of the Oregon and Washington continental shelves (modified from Snavely [1987, printed by permission from Washington Sea Grant Program, University of Washington] and Palmer and Lingley [1989]). The northern Oregon and Washington shelf are underlain by mélangé and broken formation (MBF) of the accretionary complex (Hoh rock assemblage of Rau [1973]) which extends landward onto the Olympic Peninsula, whereas the central Oregon shelf is underlain by oceanic basalt of the Siletz River Volcanics. Industry boreholes penetrating the MBF are also shown. PA, Point of the Arches, BCT, Big Creek Thrust. Submarine fans: NF, Nitinat Fan; AF, Astoria Fan. Position of Ocean Drilling Program Site 888 is shown. Plate convergence vector from De Mets et al. [1990].

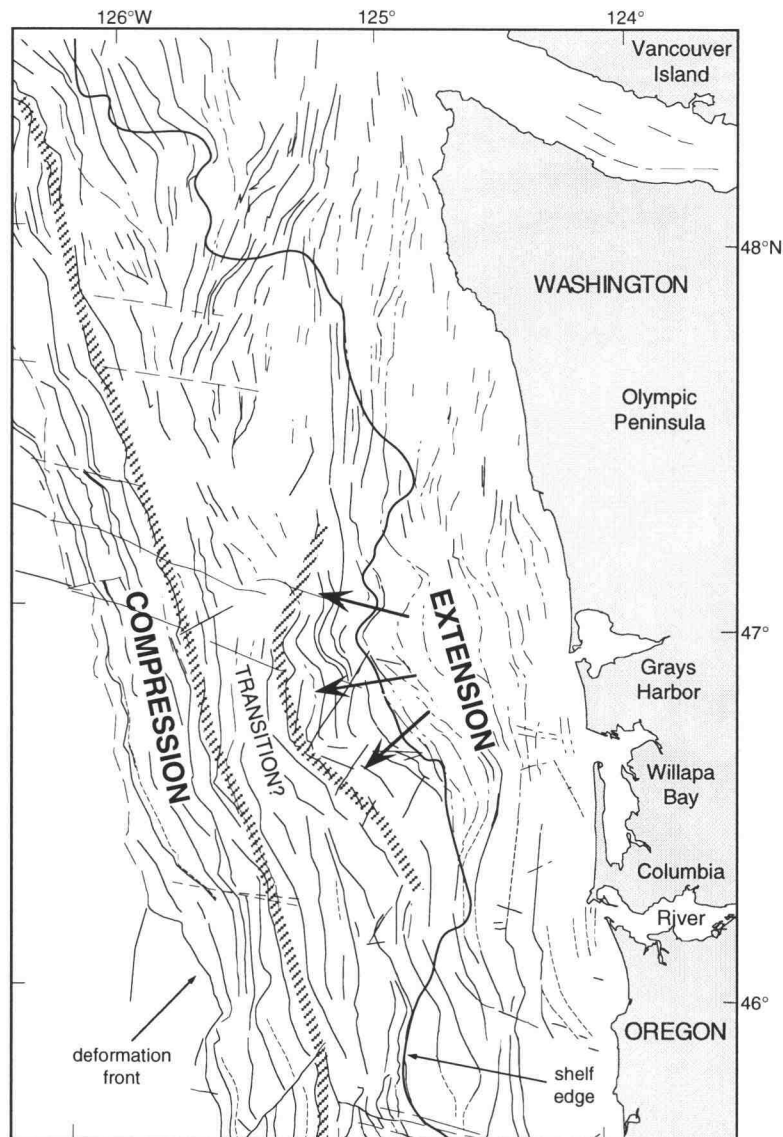


Figure II.2a. Neotectonic map of the Washington and northern Oregon margins (modified from McCaffrey and Goldfinger [1995]) showing Quaternary (solid lines) and Pliocene and early Pleistocene (dashed lines) anticlinal fold axes and faults (synclinal fold axes removed for clarity). Dashed lines also indicate inferred structures. The map was compiled from interpretations of the following data sets: industry, government, and academic seismic reflection profiles (Figure II.2b); bathymetry; side-scan sonar imagery; and submersible observations. Active compression in response to northeasterly convergence occurs on the lower slope (labeled "compression"). The shelf and upper slope are characterized by E-W extensional structures discussed in this paper (labeled "extension"), with evidence of N-S compression on the inner shelf. A zone exists where the extent of compression versus extension is presently uncertain (labeled "transition?"). Note that fold trends on the midslope wrap around a "protrusion" visible in bathymetry and the shelf edge opposite Grays Harbor, which is interpreted as the western edge of the MBF. Arrows indicate downslope movement of the MBF. North and south of the protrusion, the seaward extent of the MBF is unclear.

by a basement of Paleocene to middle Eocene oceanic basalt with minor interbedded sediments, which is known as the Coast Range basaltic basement or Siletzia terrane (Fig. II.1). Currently active accretionary thrust faults on the lower slope are characterized by seaward vergent thrusts on the Oregon margin from 42° to 44°55'N and north of 48°08'N off Vancouver Island, British Columbia, and by landward vergent thrusts between 44°55' and 48°08'N, on the northern Oregon and Washington margins.

It has been suggested that growth faulting in association with mud diapiric intrusions or piercement structures are a common phenomenon on the Washington continental shelf [Snively, 1987; Snively and Wells, 1991]. Snively and Wells [1991], Niem and others [1990, 1992] note that several seismic profiles reveal west dipping listric normal faults at the shelf edge. They attribute fault movement to downslope movement following sediment loading and collapse of the shelf margin. Analysis of an extensive data set of proprietary migrated multichannel seismic reflection profiles (Fig. II.2b) reveals that these listric normal faults and nonlistric normal faults are fairly widespread on the mid to outer continental shelf and uppermost slope of the Washington and northernmost Oregon margins (Fig. II.2c) [Piper, 1994; Piper et al., 1995; McNeill et al., 1995]. The most prominent of these faults are listric normal faults which deform as much as 3 km of the uppermost sedimentary section. Other extensional structures are not listric in the reflection data, have minimal offset, and lack prominent growth strata. These faults may or may not be listric at depth below the interpretable part of the data. These faults will be examined and discussed collectively with the more clearly listric faults.

II.4 STRATIGRAPHY AND UPLIFT HISTORY

The continental shelf of Washington and the outer to midshelf of northernmost Oregon are underlain by a thick section of Eocene to middle Miocene *mélange* and broken formation (Figs. II.1 and II.3) [Snively, 1987]. The *mélange* and broken formation may also be present elsewhere on the Cascadia margin but not immediately underlying late Tertiary strata. The *mélange* and broken formation (MBF), known as the Hoh rock assemblage on the western Olympic Peninsula [Rau, 1973, 1975, 1979; Orange et al., 1993], forms the uplifted accretionary complex of the Olympic Mountains (Fig. II.1) [Tabor and Cady, 1978]. Snively and Kvenvolden [1989] have subdivided the coastal rocks into the middle to late Eocene Ozette *mélange* and the late Oligocene to middle Miocene Hoh rock assemblage, but Orange et al. [1993] were unable to distinguish between these two units. The Eocene to middle Miocene *mélange* and broken formation is

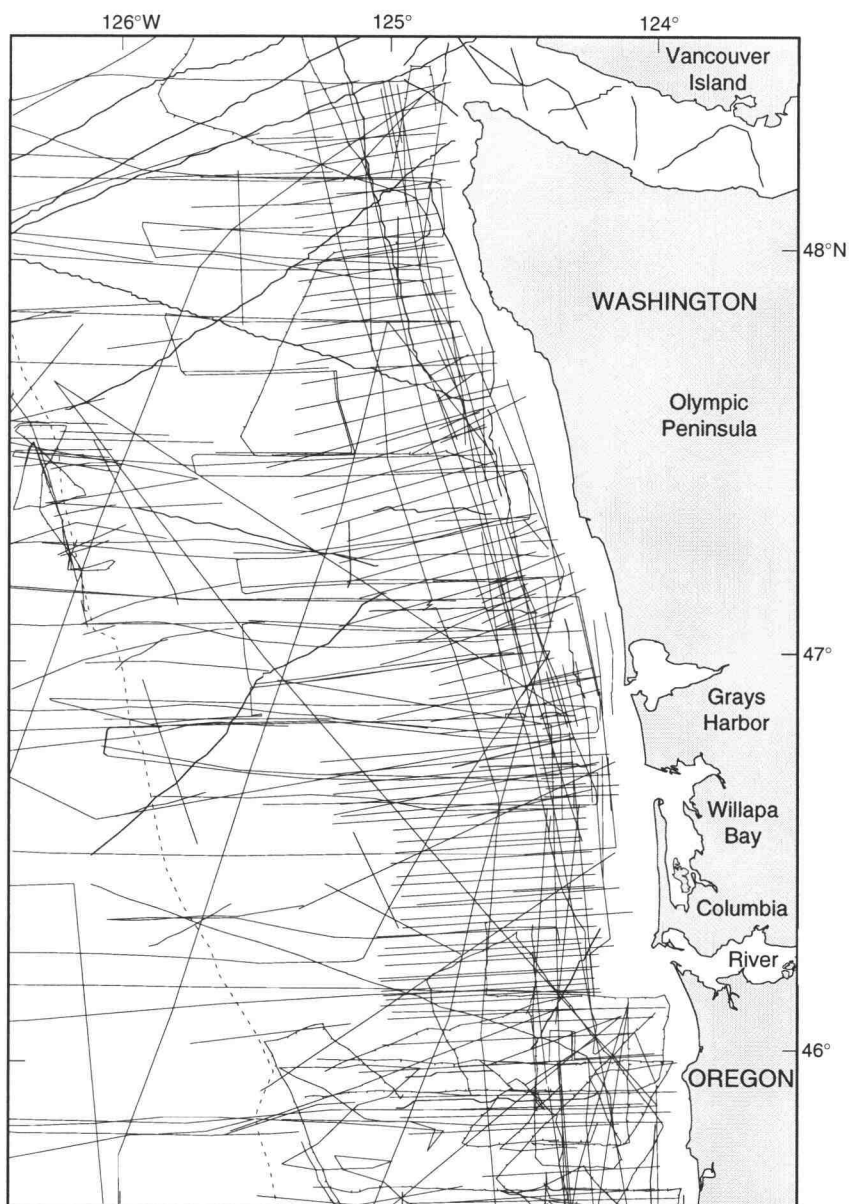


Figure II.2b. Map of undifferentiated seismic reflection track lines from industry (public and proprietary), academic, and government sources. Profiles include single and multichannel and migrated and unmigrated data. Dashed line indicates the deformation front.

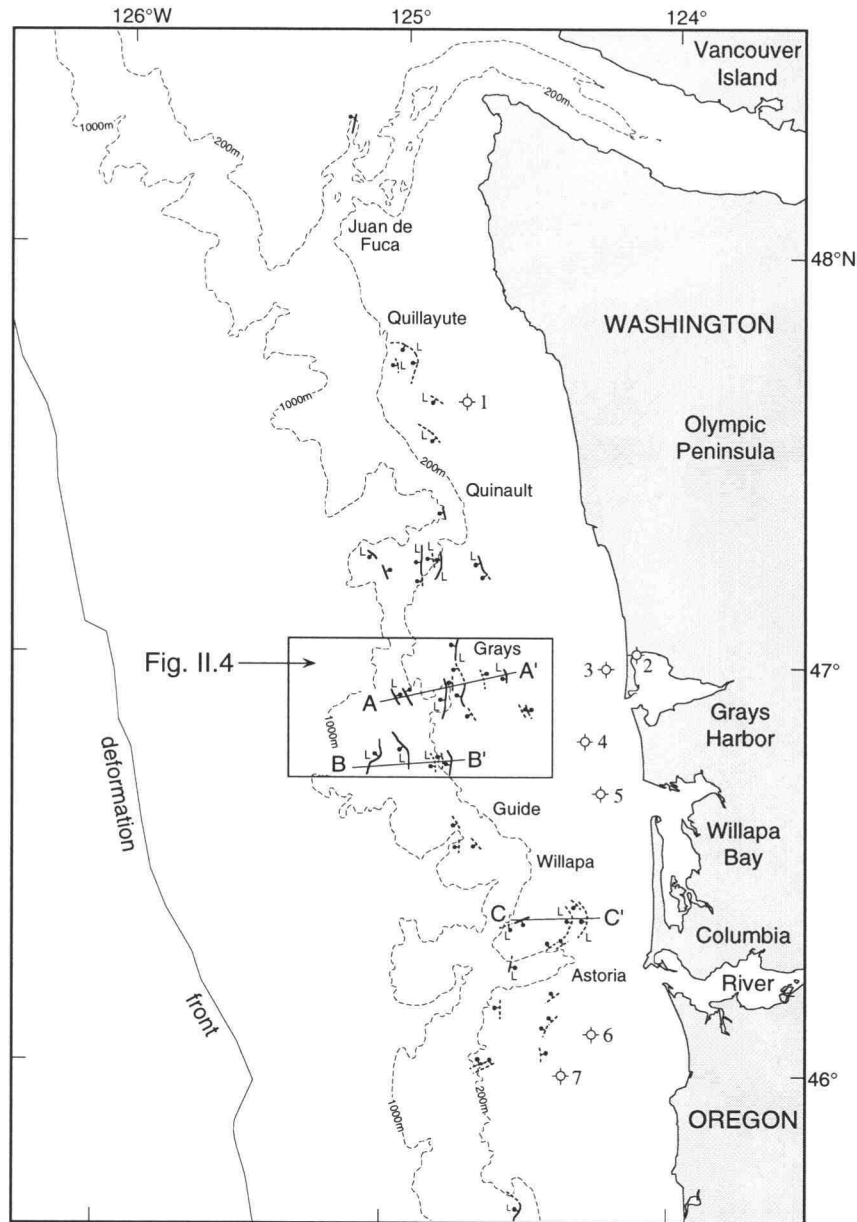


Figure II.2c. Map of the study area locating major normal faults mapped in this study. Listric normal faults indicated by "L". The 200 m (approximating the shelf edge) and 1000 m bathymetric contours represented as dashed lines. Normal faults active in the latest Pleistocene and Holocene (deforming youngest sediments and/or seafloor) shown as solid lines; normal faults active in the Pliocene and early Pleistocene shown as dashed lines. Bar and ball indicate downthrown side of fault. Submarine canyons are labeled (Juan de Fuca to Astoria) and A-A', B-B', and C-C' represent seismic reflection profiles shown in Figures II.5, II.6, and II.7, respectively. Industry boreholes on the continental shelf and in Grays Harbor area (open circles): 1, Pan American P-0141; 2, Sunshine Medina; 3, Union Tideland; 4, Shell P-0155; 5, Shell and Pan American P-0150; 6, Shell P-075; 7, Shell P-072. Grays Canyon area (Figure II.4) shown as box.


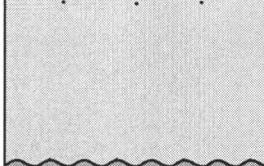
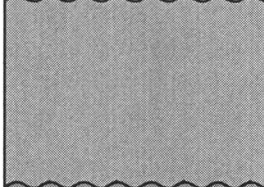
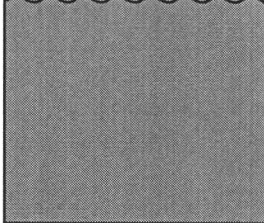
	<i>Unit</i>	<i>Age</i>	<i>Paleo Bathymetry</i>	
		Quaternary	neritic	↑ NET SHALLOWING
	Quinault Formation and equivalent	Pliocene	littoral, neritic, upper bathyal	
	Montesano Formation and equivalent	late Miocene	neritic mid bathyal	
	Mélange and broken formation (Hoh rock assemblage)	Eocene to middle Miocene	bathyal	

Figure II.3. Stratigraphy of the Washington continental shelf as inferred from outcrops on the western Olympic Peninsula and lithologies penetrated by industry boreholes on the continental shelf [Palmer and Lingley, 1989]. Paleobathymetry determined from biostratigraphic analysis of onshore and offshore wells and onshore outcrops using benthic foraminifera [Rau, 1970; Bergen and Bird, 1972] (summarized by Palmer and Lingley [1989]). The Miocene through Quaternary sequence indicates net shallowing. Shading patterns correspond to units in seismic profile interpretations of Figures II.5-II.7.

not sub-divided in this paper, according to the nomenclature of *Rau* [1973, 1975, 1979] and *Orange et al.* [1993] and is referred to as the MBF. The Hoh rock assemblage crops out along the coast approximately between Point of the Arches in the north and the Big Creek thrust in the south (Fig. II.1) [*Palmer and Lingley*, 1989]. Coastal outcrops of the Hoh rock assemblage contain both locally coherently stratified sandstones and siltstones, including turbidites, and chaotic assemblages of siltstone, sandstone, conglomerate, and altered volcanic blocks with a fine grained matrix of clay and siltstone ("tectonic mélange" of *Rau* [1973]). The weakness of the tectonic mélange is exemplified by slumping of coastal deposits and by the expansive nature of materials encountered by coastal and offshore industry boreholes [*Rau*, 1973]. To the west, beneath the Washington continental shelf, all industry boreholes reached the MBF (Fig. II.1) [*Snively*, 1987; *Palmer and Lingley*, 1989]. None of the boreholes reached units older than the Eocene MBF, but ~2 km of Eocene to middle Miocene sediments were encountered, which serves as a minimum thickness for the MBF on the midshelf. The precise extent of the MBF to the west is unclear, but its acoustic character in seismic reflection profiles, outlined below, suggests that the formation extends westward at least as far as the present shelf edge. *Snively* [1987] inferred that the MBF extends to the midslope. The Astoria Formation and Nye Mudstone are the time and lithologic correlatives of portions of the Oligocene and Miocene Hoh rock assemblage on the northern Oregon shelf [*Palmer and Lingley*, 1989].

Rapid regional uplift of the present continental margin occurred toward the end of the middle Miocene, uplifting and partly eroding the MBF. Latest middle Miocene and late Miocene strata of the Montesano Formation deposited in middle bathyal to neritic water depths (Fig. II.3) overlie the erosional angular unconformity and the MBF [*Palmer and Lingley*, 1989]. The Montesano Formation can be subdivided into three main units according to *Bergen and Bird* [1972]: lower claystone member; middle sandstone member; and upper siltstone member. Shallow water depths indicated by the sandstone member suggest that the present continental shelf developed in the late Miocene, at ~7Ma [*Palmer and Lingley*, 1989]. Development of the shelf is thought to be primarily a result of regional uplift and not simply shoaling through rapid deposition [*Bergen and Bird*, 1972]. Offshore paleobathymetry suggests primarily bathyal depths for the Montesano (S.D. Drewry et al., Minerals Management Service (MMS), unpublished work, 1993). Quinault- (and Quillayute-) equivalent Pliocene strata unconformably overlie the Montesano, as defined by *Palmer and Lingley* [1989], with onshore paleobathymetry indicating variable depositional depths, including bathyal, neritic, and neritic/littoral sequences (Fig. II.3) [*Rau*, 1970]. Offshore microfossil paleobathymetry records both bathyal and neritic depths (aforementioned MMS unpublished work). These Pliocene strata are, in turn, overlain by

Pliocene and Pleistocene gravels [*Palmer and Lingley*, 1989]. Paleobathymetry [*Rau*, 1970; *Bergen and Bird*, 1972] suggests a net progressive shallowing through the Miocene and Pliocene, from bathyal to neritic, but episodic basinal downwarping within this period is indicated by the thick section of post-MBF sediments, as much as 2 km in places [*Snively*, 1987], and variable paleowater depths within individual units (Fig. II.3).

Diapiric intrusions on the Washington continental shelf are largely rooted in the mélangé and broken formation [*Snively and Wagner*, 1982; *Snively and Wells*, 1991]. Late Miocene and younger sediments thin and onlap against these diapirs, suggesting that growth began in the late Miocene [*Snively*, 1987].

II.5 SEISMIC REFLECTION DATA ACQUISITION AND PROCESSING

Multichannel seismic reflection data used in this study were collected during three acquisition phases. Phase 1 data were acquired using a four-gun aquapulse array and 110 foot shot point interval, yielding 46-fold data. Phase 2 data were acquired using a 16-gun air gun array and 328 foot shot point interval, yielding 48-fold data. Processing for phases 1 and 2 included minimum phase inverse filter deconvolution and finite difference poststack migration, with approximate frequency filters of 10-55 Hz in the upper section and 5-25 Hz in the lower section. Phase 3 data were acquired using a 24-gun air gun array and 87.4 foot shot point interval, yielding 60-fold data. Processing included minimum phase inverse filter deconvolution and high-dip residual poststack migration, with approximate frequency filters of 8-55 Hz in the upper section and 5-25 Hz in the lower section. The seismic reflection data are shown here as migrated time sections.

II.6 DELINEATION OF SEISMIC STRATIGRAPHIC UNITS

Delineation of stratigraphic units (Fig. II.3) shown in seismic line interpretations, A-A', B-B', and C-C' (Figs. II.2c and II.4 for location; Figs. II.5, II.6, and II.7), has been determined from interpretations of the following industry boreholes on the continental shelf: Pan American P-0141; Shell P-0155; Shell/Pan American P-0150; and Shell P-075 and P-072 (locations shown in Fig. II.2c). Depths to unit surfaces were determined using available interpretations of industry borehole logs and cuttings [*Palmer and Lingley*, 1989; S.D. Drewry et al., MMS unpublished work, 1993]. Benthic foraminifera biostratigraphy

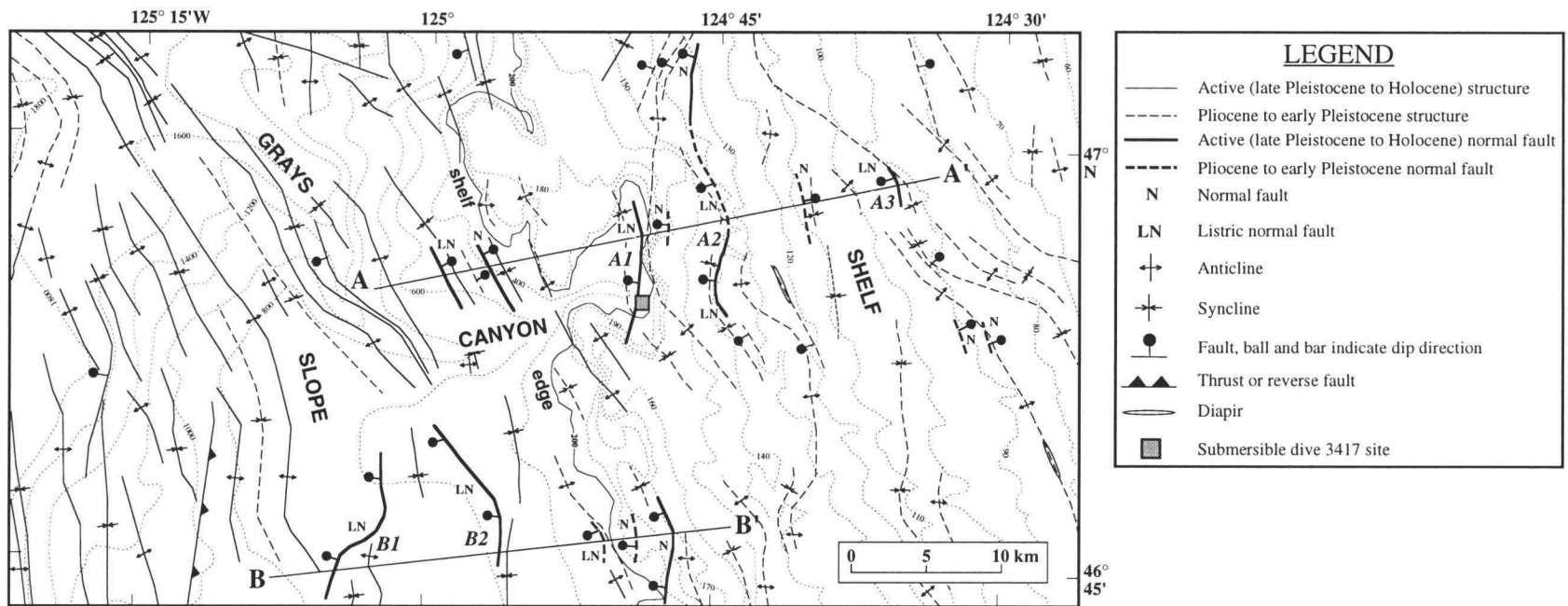


Figure II.4. Neotectonic and bathymetric map of the Grays Canyon outer shelf and upper slope region. See Figure II.2a for sources of interpretation. See Figure II.2c for location of line A-A' and B-B'. Line A-A' crosses three major seaward dipping listric normal faults, A1, A2, and A3 (see Figure II.5). Fault A1 at the head of Grays Canyon was a target for side-scan sonar surveys and submersible dives during 1994. The position of dive 3417 is indicated by the shaded box. Line B-B' crosses listric normal faults, B1 and B2 (see Figure II.6). Other normal faults are indicated by "N" (nonlistric normal faults) and "LN" (listric normal faults). Bathymetric contours are spaced every 200 m on the slope and every 10 m on the shelf. The 200 m contour broadly defines the shelf break. Owing to scale constraints, not all structures shown in seismic line interpretations (Figures II.5 and II.6) are shown.

Figure II.5. (Top) E-W migrated multichannel seismic reflection profile A-A' on the central Washington continental shelf and upper slope with (bottom) interpretive line drawing. See Figures II.2c and II.4 for location. Three major listric faults, A1, A2 and A3, are crossed by the profile including fault A1 at the head of Grays Canyon, a target of submersible dives in 1994. Listric faults deform late Miocene to Quaternary sediments with minor deformation of the uppermost *mélange* and broken formation. Faults A1 and A2 show evidence of recent activity including deformed Holocene sediments, seafloor offset, and methane-derived carbonates resulting from fluid venting. The listric faults sole out at depth into a *décollement* close to or at the upper contact of the *mélange* and broken formation. The faults are characterized by growth strata and rollover folds. TWTT, two-way travel time. Vertical exaggeration ~ 2:1 at seafloor.

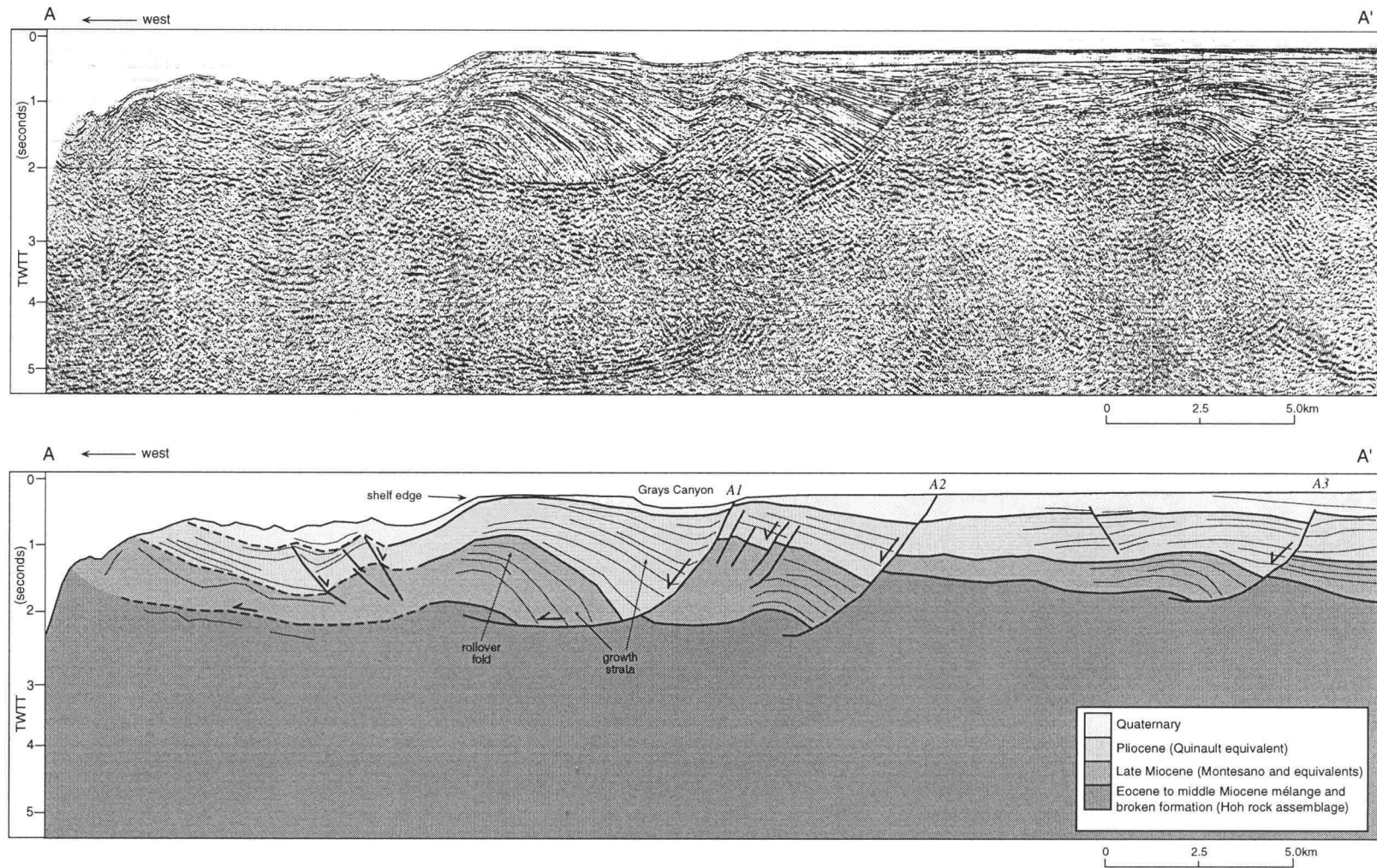


Figure II.5

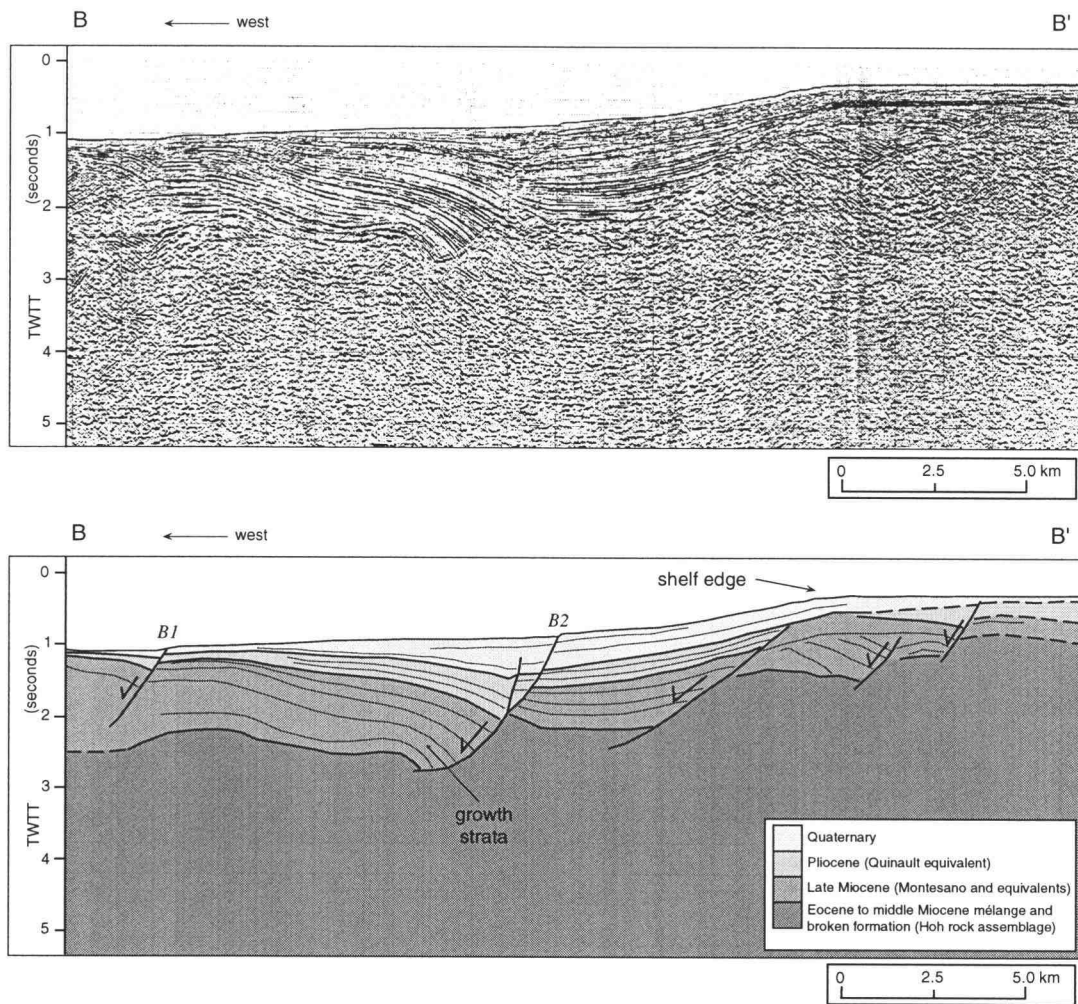


Figure II.6. (Top) E-W migrated multichannel seismic reflection profile B-B' on the central Washington upper slope and shelf edge with (bottom) interpretive line drawing. See Figures II.2c and II.4 for location. Listric faults B1 and B2 on the upper slope deform late Miocene to Holocene sediments and offset the seafloor, with seaward facing scarps of ~25 m height. Fault B2 is characterized by growth strata. TWTT, two-way travel time. Vertical exaggeration ~ 2:1 at seafloor.

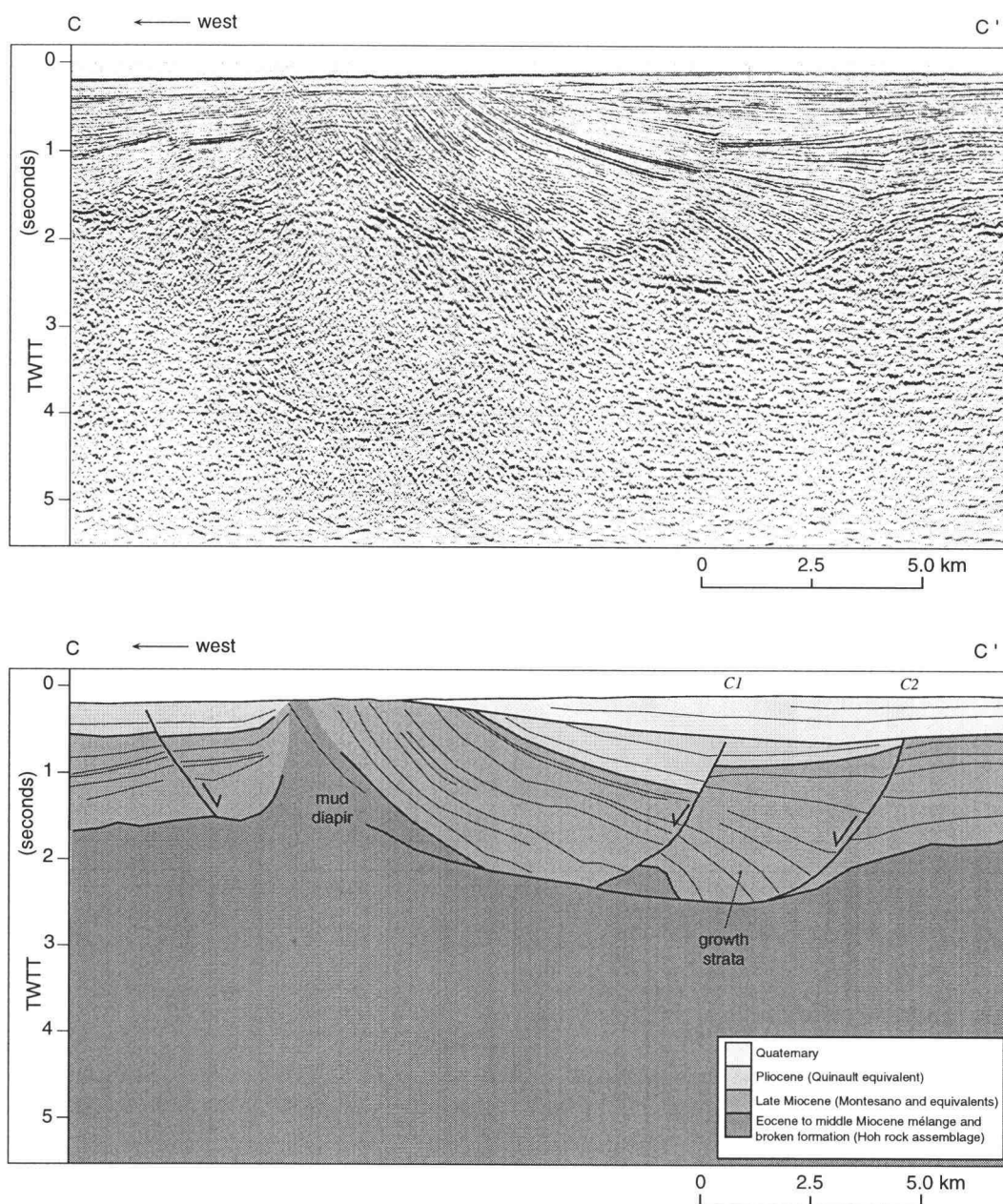


Figure II.7. (Top) E-W migrated multichannel seismic reflection profile C-C' on the southern Washington midshelf off Willapa Bay with (bottom) interpretive line drawing. See Figure II.2c for location. Listric faults C1 and C2 deform mid-Miocene (mélange and broken formation) to Pliocene sediments and are overlain by the undeformed Plio-Pleistocene unconformity. The growth strata are uplifted by a mud diapir rooted in the mélange to the west. Note also an east dipping normal fault to the west of the diapir. TWTT, two-way travel time. Vertical exaggeration ~ 2:1 at seafloor.

of the Pacific Northwest [Rau, 1981; Bergen and Bird, 1972] is based on correlations with Californian benthic foraminifera stages of Kleinpell [1938], Natland [1952], and Mallory [1959]. To locate approximate lithostratigraphic boundaries in the seismic records, these depths were converted to travel time using seismic refraction survey velocities of the Washington margin [Shor *et al.*, 1968; McClain, 1981] and sonic logs where available. Unit tops were then correlated along the network of seismic profiles. The distance of the correlation from its source was often large, and reflectors were often difficult to trace, thus introducing some degree of uncertainty into the stratigraphic interpretations shown in Figs. II.5, II.6, and II.7. However, the Eocene to middle Miocene MBF, reached by all Washington shelf industry boreholes (Fig. II.1), has a distinct acoustic character, allowing easy identification and traceability; the discontinuous and intensely sheared nature of the MBF results in similarly discontinuous seismic reflectors. This unit can be recognized below ~2 s two-way travel time (TWTT) in Fig. II.5, in contrast with the well-stratified overlying units. While correlation errors were compounded by minor differences between biostratigraphic calls reported in the literature, these correlation methods were considered sufficient and appropriate for this study. There is no evidence of the base of the MBF unit in available seismic reflection profiles or refraction velocity profiles. Thus this method cannot be used to determine the thickness of this unit.

II.7 DISTRIBUTION AND MORPHOLOGY OF NORMAL FAULTS

Well-defined normal faults occur on the middle to outer continental shelf and upper slope of the northern Oregon and Washington margins (Fig. II.2c). The most spectacular of these faults in seismic reflection profiles are listric growth faults shallowing to subhorizontal dips at depth ("L" in Fig. II.2c). In general, listric normal faults showing activity in the Pliocene (and possibly early Pleistocene) tend to be located on the midshelf and outer shelf (dashed lines); more recently active Holocene and late Pleistocene faults (solid lines), deforming uppermost sediments and/or the seafloor, occur throughout the midshelf to outer shelf and on the uppermost slope but more commonly near the shelf break. For all major normal faults (listric and apparently nonlistric), a tentative correlation can be made between age and location, with the more recently active structures located closer to the shelf break. All major extensional faults are located in < 1000 m water depth (Fig. II.2c). The distribution of normal faults in apparent E-W bands, as shown in Fig. II.2c, is not an artifact of the grid of seismic data.

Where their orientation can be determined, most normal faults identified in this study strike approximately north-south or parallel to the main trend of the shelf edge (Fig. II.2c). Those faults which can be traced across several seismic profiles often have a concave-seaward arcuate fault trace (e.g., line C-C', Fig. II.2c). More than 80% of the major normal faults mapped dip seaward. The apparent short fault length, usually < 5 km and no longer than 20 km, is not a function of the spacing of seismic reflection profiles.

A neotectonic map of the Grays Canyon region is shown in Fig. II.4, part of a map of the Oregon and Washington margin (Fig. II.2a) [Goldfinger *et al.*, 1992; McCaffrey and Goldfinger, 1995; C. Goldfinger and L.C. McNeill, manuscript in preparation, 1997]. Faults and folds are separated into those active during the Pliocene and earliest Pleistocene (dashed) and those active during the late Pleistocene and Holocene ("active", solid). Fig. II.4 also gives the locations of two seismic profiles, A-A' and B-B' (Figs. II.5 and II.6), which cross several prominent normal faults ("N" and "LN").

The listric normal faults are characterized by regular growth strata which indicates continuous rather than sporadic activity beginning in the late Miocene (Figs. II.5, II.6, and II.7). Growth faulting may be partially responsible for the thick sections of post-middle Miocene strata observed in continental shelf basins. Half-graben basins associated with these listric faults are relatively narrow [Snively and McClellan, 1987; Snively and Wells, 1991], between 4 and 10 km (perpendicular to the fault), with basinal sediment thicknesses up to 2-3 km. Normal faults deform and offset sediments of late Miocene, Pliocene, and, in some cases, Quaternary age. Rollover folds are common in hanging wall growth strata of listric faults with major offset (A1, Fig. II.5), similar to growth faults on passive margins [Busch, 1975]. In some cases, fault splays occur in the uppermost sedimentary section, producing a wedge of faulted material (B2, Fig. II.6). For the majority of listric faults, the fault dip shallows to a subhorizontal décollement, approximately coincident with the upper contact of the MBF (Figs. II.5 and II.7). This décollement occurs at travel times of up to 2.5-3.0 s TWTT, equivalent to ~ 3.0 km depth (Fig. II.5). This corresponds to about 25-30% of the total forearc sedimentary section above the subducting basaltic slab at the continental shelf edge, which is estimated to be at a depth of 10-12 km [Brandon and Calderwood, 1990]. For other listric faults (e.g., eastern end of Fig. II.6), the fault plane is more steeply dipping and apparently penetrates the top of the MBF. The fault plane may become subhorizontal within the MBF unit but is not imaged in the seismic section; faults therefore offset and deform undetermined thicknesses of the MBF unit. In both cases, extension is not a superficial effect.

Many of the normal faults cut the seafloor, indicating Holocene activity, and several produce measurable fault offsets in seismic sections (Fig. II.6). Faults B1 and B2 produce

a seafloor offset of ~ 25 m (Fig. II.6). Fault A1, which is located at the head of Grays Canyon (Figs. II.4 and II.5), also shows significant seafloor offset, although the scarp is accentuated by erosion and slumping at the head of the submarine canyon. This listric normal fault was the target of sidescan sonar and submersible investigations during an Oregon State University scientific cruise sponsored by the NOAA National Undersea Research Program (NURP) in 1994. Side-scan sonar images revealed a fault and associated scarps with a N-S trend, traceable for 5 km. Submersible dives identified a series of terraces or scarps stepping down into the canyon, the uppermost of which offsets Pleistocene and Holocene sediments [McNeill *et al.*, 1995; Piper *et al.*, 1995]. Fig. II.8 shows a video frame taken during Delta submersible dive 3417 along Fault A1 (location in Figs. II.4 and II.5) which reveals a fault scarp; the camera points to the northeast, and the scarp is ~ 0.5-1.0 m in height. Light gray Pleistocene clays and a thin cover of overlying olive-green Holocene hemipelagic sediment are exposed in the fault scarp, indicating fault movement during the Holocene. The scarp is relatively free from major bioturbation and hemipelagic sedimentation, suggesting fairly recent movement. Angular broken boulders are observed at the base of the scarp which also indicate recent breakage associated with fault movement or gravitational collapse at the head of the canyon. Side-scan sonar surveys of faults A1 and A2 provided evidence of active fluid venting in the form of precipitated calcium carbonate (high backscatter) which also suggests that these faults have been recently active [Kulm and Suess, 1990].

Where listric faulting occurs close to the shelf break and is associated with submarine canyon activity (e.g., Fig. II.4), the upper MBF contact or décollement rises to the west to become E-dipping and the MBF is commonly the source of diapiric intrusions. This reflects the mobility of the MBF unit and probably results from removal of the overlying sedimentary load on the uppermost continental slope where erosion and slumping are common, particularly at the heads of submarine canyons. This phenomenon can be seen at the western end of seismic profile A-A' (Fig. II.5). In this same profile, east dipping normal faults with associated growth strata can be seen overlying the east dipping décollement to form full graben structures with west dipping faults, e.g., A1 and A2.



Figure II.8. Video frame from the Delta submersible of fault scarp A1 (see Figures II.4 and II.5) at the head of Grays Canyon. Video camera points NE and two dots represent parallel laser beams placed 20 cm apart. The scarp is ~ 0.5-1 m in height. Scarp is relatively free from bioturbation and hemipelagic sediment, and angular boulders are observed at the base of the scarp, both suggesting recent activity.

II.8 DISCUSSION

II.8.1 Isolation of Shelf Tectonics

Normal faults in the Grays Canyon area (Fig. II.4), which indicate ~E-W extension, coexist with apparent compressional structures which suggest ~E-W shortening. Both sets of structures were apparently concurrently active throughout the Pliocene, and in some cases, during the Pleistocene and Holocene. Other workers [e.g., *Silver*, 1972; *Wagner et al.*, 1986] also suggest that this region of the Washington shelf is characterized by predominantly E-W shortening during the Neogene. However, recent coastal mapping [*McCrary*, 1994, 1996; *Thackray*, 1994] and our mapping of the inner continental shelf (C. Goldfinger and L.C. McNeill, manuscript in preparation, 1997) show evidence of active N-S shortening, suggesting that strain from oblique convergence is partitioned into arc-normal (E-W) and arc-parallel (N-S) components. This is supported by seismicity, structural data, and borehole breakouts onshore which also suggest N-S compression [e.g., *Spence*, 1989; *Zoback and Zoback*, 1989]. It is difficult to reconcile contemporaneous E-W extension and E-W shortening unless (1) the observed extension is a shallow and superficial effect, (2) predominantly nontectonic extension is occurring through some form of gravitational collapse, or (3) extension is nonsuperficial and the two tectonic regimes are isolated from one another. N-S compression and E-W extension may be dominant on much of the continental shelf, being mutually compatible stress regimes, and E-W compression is dominant on the lower slope, supporting hypothesis 3. In this scenario, N-S trending fold structures mapped on the shelf may be a result of gravitationally driven compression rather than interplate compression.

II.8.2 Association Of Normal Faulting With Mélange And Broken Formation

The majority of listric normal faults sole out at depth to a subhorizontal décollement coincident with the uppermost strata of the middle Miocene MBF, indicating a strong link between extension and the MBF. The Hoh is chaotic, highly sheared, folded, and faulted in onshore exposures [*Palmer and Lingley*, 1989; *Orange*, 1990; *Orange et al.*, 1993] and contains abundant olistostromes, tectonic inclusions, and rip-up clasts [*Rau*, 1973; *Palmer and Lingley*, 1989]. Diapiric intrusions, both on the continental shelf [*Snively and*

Wagner, 1982] and in onshore outcrops [Rau, 1973; Orange, 1990], imply that the MBF is overpressured at depth [Snively, 1987]. High mud weights required for drilling boreholes and increased mud pressure gradients in industry boreholes off northern Oregon, Washington, and southern Vancouver Island [Snively, 1987; Palmer and Lingley, 1989] both point to elevated pore pressures within the MBF.

The distribution of major normal faults mapped to date on the Washington and northern Oregon continental shelf and upper slope (Fig. II.2c) coincides with the distribution of the underlying MBF unit, where it occurs immediately below late Tertiary strata (Fig. II.1). The remainder of the northern and central Oregon continental shelf is underlain by the basaltic basement of the lower Eocene Siletz River Volcanics, part of the Coast Range basaltic basement or Siletzia terrane (Fig. II.1). The western boundary of the Siletz River Volcanics has been fairly confidently mapped from modeling magnetic and gravity anomalies, and seismic reflection profiles (Fig. II.1) [Tréhu *et al.*, 1994, 1995; Fleming, 1996]. The rigidity of the basalt contrasts with the sheared *mélange* and broken formation underlying the Washington and northernmost Oregon shelf and explains the absence of normal faulting [McNeill *et al.*, 1995]. The MBF may be underplated, in the form of sediment duplexing, beneath the Siletz River Volcanics. The Coast Range basaltic basement thins to the north and crops out onshore in Washington as the early to middle Eocene Crescent Formation, which includes the peripheral rocks of the Olympic Mountains [Tabor and Cady, 1978]. The Crescent Formation wraps around the Olympic core rocks and is found offshore as the Crescent and Metchosin Formations off the northwestern Olympic Peninsula (Fig. II.1). No listric normal faults have been identified overlying the inferred position of the northernmost Coast Range basaltic basement, but the seafloor morphology and Quaternary strata of this region are obscured by glacial outwash features from the Juan de Fuca lobe of the Cordilleran ice sheet. In southern coastal Oregon, the western boundary of the Siletz River Volcanics crosses the shoreline (Fig. II.1), and the basaltic basement is absent from the continental shelf. To date, no listric normal faults have been identified on the southern Oregon shelf or upper slope, although extremely large-scale slumping with prominent headwall scarps has been documented on the southern Oregon slope [Goldfinger *et al.*, 1995].

II.8.3 Cascadia Normal Faulting Mechanisms

The *mélange* and broken formation appears to control both the normal fault distribution and the timing of faulting, beginning in the late Miocene, following deposition,

uplift, and erosion of the middle Miocene MBF. The MBF appears to decouple the overlying continental shelf sediments, characterized by extensional deformation, from subduction-controlled E-W to NE-SW compressional deformation evident on the lower continental slope. Two related mechanisms of decoupling are described below, involving, first, detachment of the basinal shelf sediments from the MBF, and secondly, mobilization and extension of the MBF.

The upper contact of the MBF, represented by the middle to late Miocene unconformity and downward transition in acoustic character from well-stratified to discontinuous reflectors, dips very gently west throughout much of the continental shelf (Fig. II.9), with measured slopes from the midshelf to the shelf break of approximately 0.1° - 2.5° . These gentle seaward slopes represent the regional dip of this upper contact, ignoring local vertical variations due to faulting and folding. We hypothesize that such a shallow surface dip may be sufficient to allow unstable gravitational sliding on the upper MBF surface due to low basal friction and consequent detachment of the overlying sediments (Figs. II.9a and II.9b). This mechanism can be used to explain extension along only the listric normal faults which sole out at depth into the upper MBF contact. The reduced strength and effective shear stress along a fault plane or detachment associated with high pore fluid pressures has been documented by *Hubbert and Rubey* [1959] in the theory of low-angle overthrust faulting or gravitational sliding and by *Davis et al.* [1983] in the Coulomb theory of the critical tapered wedge. Seaward or downslope dipping listric normal faults also support gravitational sliding as a mechanism of extension. The upper MBF contact (middle to late Miocene unconformity) thus may act as a detachment [*Piper*, 1994], separating the mobile MBF and the more rigid post-MBF sediments, along which the late Miocene to Quaternary section moves downslope (Fig. II.9b). The listric faults on the Cascadia margin may therefore be similar to growth faults on the Texas coast, where faults flatten at depth into low-density, high fluid pressure shale masses [*Bruce*, 1973]. Normal faulting at the base of the Guatemalan slope is also thought to be a result of decoupling through elevated pore fluid pressures, as encountered during Leg 84 of the Deep Sea Drilling Project [*Aubouin et al.*, 1982], although this margin is characterized by much steeper terrain.

The subhorizontal upper contact of the MBF on the continental shelf and upper slope suggests mobilization and redistribution of this unit, aided by gravitationally driven downslope movement. The MBF may therefore be undergoing mobilization and extension to the west, where it is apparently unconstrained, with accompanying rigid or brittle extension of the overlying younger deposits (Figs. II.9a and II.9c). The upper contact may still behave as a detachment, as hypothesized above, but in this case, both the mobile MBF

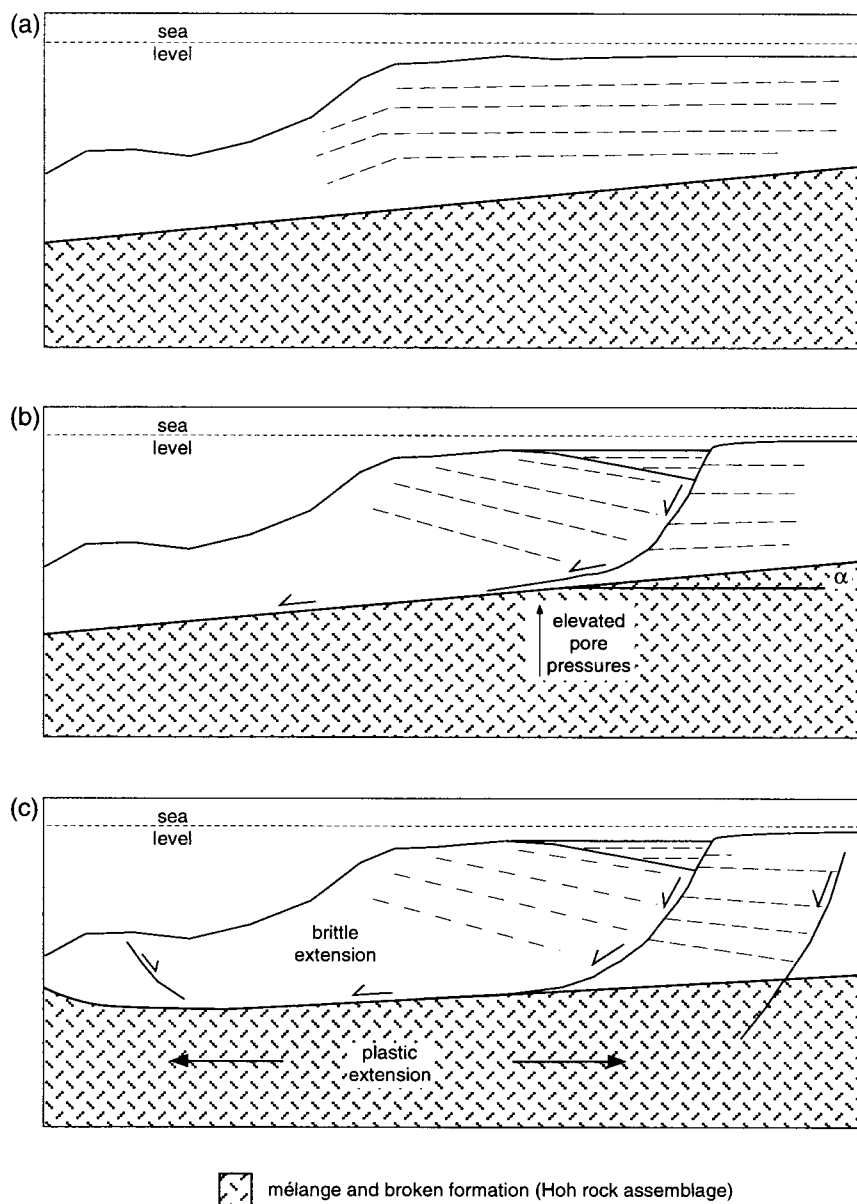


Figure II.9. Development and mechanisms of listric faulting on the Cascadia outer shelf. (a) Prior to extension: mélangé and broken formation (MBF) deposited at bathyal depths, uplifted, and eroded, and overlying late Miocene sediments deposited. The upper MBF contact dips gently seaward. (b) Extensional failure occurring through gravitational collapse along a detachment separating the MBF and overlying sediments. Elevated pore pressures within the MBF increase the chance of movement on the low-dipping failure plane. Dip of the mélangé surface, $\alpha \approx 0.1^\circ$ - 2.5° . (c) Mobilization and extension of the MBF results in brittle extension of the overlying sediments. East dipping normal faults also form.

and the overlying brittle section undergo extension, with reduced relative displacement between these two units. There may be an additional detachment at depth within the MBF, below which no extension occurs, resulting from increases in strength or decreases in pore fluid pressure. Mobilization and extension of the MBF comprise a preferred explanation for listric faults which do not flatten into a sub-horizontal décollement, but penetrate and offset the MBF unit. Diapiric intrusions throughout the shelf and evidence of upward movement of the MBF at the shelf edge (Figs. II.5 and II.9c), where the overlying sedimentary load is reduced, point to significant mobilization. Extension of both the mobile MBF and overlying brittle sediments explains the presence of east dipping and apparently upslope dipping normal faults on the shelf and upper slope (e.g., western end of Fig. II.5). These faults are less easily explained by downslope movement on a seaward-dipping detachment. Extension and thinning of the Hoh beneath the shelf might be expected to result in net subsidence, which contradicts paleobathymetric evidence of net uplift during the period of extension [Rau, 1970; Bergen and Bird, 1972]. This apparent contradiction can, however, be explained by the counteraction of other factors influencing the uplift history of the shelf, including sedimentation rates, sediment underplating, and the variation of subducting slab dip.

Extension and thinning of the MBF are supported by the increased width (Fig. II.1) and low taper angle of the Washington and northern Oregon margins relative to those of the central and southern Oregon margins. Mapped fold trends (Fig. II.2a) appear to wrap around a feature on the upper slope of the central Washington margin which is coincident with a convex-seaward "protrusion" or "bulge" in the shelf edge and is also indicated by shaded relief bathymetry [Haugerud, 1996]. We hypothesize that this protrusion and anomalous fold trends represent the expression of downslope movement and extension of the MBF (movement indicated by arrows in Fig. II.2a). The absence of similar seafloor morphology and structure to the north and south cannot be presently explained but may be the result of reduced tilting of the MBF or a constraining structure reducing seaward extension. It is interesting to note that the many of the normal faults mapped coincide with this anomaly in fold trends opposite Grays Harbor (Figs. II.2a and II.2c).

The presence of both normal faults (listric and potentially nonlistric) that cut the MBF and those that deform only overlying sediments implies that both motion on the detachment and westward flow of the MBF are occurring. Both mechanisms have been proposed as models for extension in earlier work on metamorphic core complexes of the Basin and Range Province [Wernicke, 1981].

II.8.4 Alternative Faulting Mechanisms

Westward or seaward extension resulting from both downslope movement on the upper MBF detachment and from extension within the MBF may be accentuated by uplift and westward tilting of the continental shelf and upper slope. Uplift of the shelf would increase the slope beyond a critical angle resulting in gravitational collapse. Such mechanisms are not thought necessary for extension to occur on the Washington and northern Oregon margin, but may increase the rate of movement on the MBF detachment and downslope movement of the MBF, or prolong the period of extension. Evidence of vertical tectonics on the shelf and upper slope (Fig. II.3) and the uplifted Olympic Mountains onshore [*Brandon and Calderwood, 1990*] indicate broadly contemporaneous uplift through the Miocene and Pliocene, coincident with listric normal faulting. Uplift of the shelf could be caused by underplating of subducted sediments beneath the shelf, resulting in westward tilt.

An alternative mechanism is the differential compaction or loading of the overpressured mobile MBF resulting in diapiric intrusions and growth faulting, as frequently observed on passive margins underlain by mobile sediments such as shale or salt [e.g., *Morley and Guerin, 1996*]. Diapirism is locally found in direct association with listric normal faulting on the Cascadia margin. Fig. II.7 shows two listric faults, C1 and C2, active during the late Miocene and Pliocene, associated with a diapiric intrusion rooted in the MBF below the listric faults. A requirement of differential loading is variation in the overburden mass, which is produced where basins or normal-fault-bounded depocenters exist. Therefore differential loading may only be responsible for initiation of faulting at the edges of preexisting basins or perpetuating movement on pre-existing faults. Differential loading is subsequently a self-sustaining process, with increased basinal deposition leading to further compaction and associated growth faulting and diapirism. This mechanism is a result of vertical movement of the mobile unit in contrast to that of gravity-induced downslope movement where horizontal motions are involved. Differential loading may be locally significant but secondary to horizontal mobilization of the MBF on a regional scale.

Two of the mapped listric faults are located at the heads of Grays and Quinault submarine canyons (Figs. II.2c and II.4), suggesting some association between faulting and canyon formation [*McNeill et al., 1995; Piper et al., 1995*]. The longevity of normal faulting (late Miocene to present) relative to the short lifespan of submarine canyons (present canyons were probably formed during Pleistocene lowstands) suggests that canyon formation may have been locally controlled by faulting, due to the preexisting plane of weakness along the fault, rather than canyons influencing fault location.

II.8.5 Extension Versus Compressional Deformation

Current extension of the continental shelf and upper slope is contemporaneous with accretion and thrust faulting on the lower slope of the accretionary wedge (Fig. II.2a). In addition, extensional faulting appears to be contemporaneous with mapped fold structures of C. Goldfinger and L.C. McNeill (manuscript in preparation, 1997) and other workers on the continental shelf (Figs. II.2a, II.2c, and II.4). In the light of the evidence for mobile extension, we have reexamined our earlier mapping and conclude that many of the folds in the vicinity of the normal faults are rollover folds, drape structures, and folds driven by downslope spreading of the MBF. These structures could be misinterpreted as purely convergence-related structures without the high quality data set used for this study.

E-W contractile strain is apparently low on the shelf and upper slope. We hypothesize that the extensional tectonic regime of this region is isolated by the mobile MBF from the convergence-related E-W to NE-SW compression on the lower slope. Fig. II.2a delineates zones of compression and extension determined from existing data. Extension extends seaward to the upper slope, and the prominent bulge may mark the seaward edge of the MBF, and therefore extension, on the central Washington margin. The midslope area, lying between these two regions of known compression and extension, may act as a transition zone or, more likely, a distinct change from extension to compression is located in this area. The seaward extent of the MBF is uncertain, and the resolution of available data may prevent the identification of extensional faults on much of the slope. The thickness and strength of the older MBF are unknown, and therefore the depth to which extension extends is unclear: a deeper compressional regime may underlie the extending MBF. The presence of E-W trending folds on the inner continental shelf suggests that N-S compression and E-W extension are operating simultaneously. An extreme case of decoupling extending to the plate interface (10-15 km beneath the shelf) would have significant implications for the extent of coupling on the subduction zone and hence position and width of the interplate locked zone. The extent and significance of decoupling induced by the MBF are the subject of further study and cannot be fully addressed in this paper.

II.8.6 Global Comparisons

Extension on the Cascadia margin differs significantly from the transient nature of extension observed in many other convergent margins. A commonly cited mechanism for extension in such margins is subduction erosion at the base or the front of the wedge. Forearc oversteepening, extensional faulting, and slope failure have been attributed to subduction erosion as a result of subduction of seamounts (Japan trench [von Huene and Lallemand, 1990]), a ridge (Peru trench [von Huene and Lallemand, 1990]), or horst and graben structures (Middle America Trench off Guatemala [Aubouin *et al.*, 1982] and Japan trench [von Huene and Lallemand, 1990]). The subduction of elevated basement features produces a local short-term extension or with a sweeping effect along the margin if a linear structure is subducted at an oblique angle, such as the subduction of the Nazca ridge beneath the Peru margin [von Huene and Lallemand, 1990]. However, extensional faulting in offshore Washington and northern Oregon is too regional and long-term (late Miocene to present) to be associated with the subduction of a discrete linear basement feature. In addition, subduction erosion would be accompanied by subsidence, which is not supported by paleobathymetric evidence, indicating net uplift through the Miocene and Pliocene [Rau, 1970; Bergen and Bird, 1972].

The dominance of extensional deformation on the shelf and upper slope in contrast to the expected compressional deformation of a convergent margin is common to the margins of Japan, Peru [von Huene and Lallemand, 1990], Costa Rica [McIntosh *et al.*, 1993], and the margin of Shumagin, Alaska [Bruns *et al.*, 1987], in addition to northern Cascadia. Extension and basinal deposition on the landward margin is concurrent with, and isolated from, accretion on the lower slope, as observed on the Cascadia margin. Basins on these margins, e.g., Lima Basin in Peru, Joban Basin in Japan, and Shumagin, Sanak, and Unimak Basins in Alaska, overlie a regional unconformity, suggesting rapid regional subsidence and crustal thinning. Mechanisms of extension may differ between these examples but all result in isolation of extension and compression.

II.9 CONCLUSIONS

Listric normal faulting appears to be the result of (1) downslope movement along a low-angle décollement between the uppermost middle Miocene MBF and the overlying basinal sediments and (2) mobilization and extension of the MBF and consequent brittle

extension of the overlying sediments. Miocene and Pliocene uplift of the continental shelf may have resulted in oversteepening of the shelf and further gravitational collapse but was probably not a requirement for extension. The subsurface distribution of the MBF restricts extension to the Washington and northern Oregon shelf and upper slope.

Contemporaneous compressional tectonics of the lower slope and extensional tectonics of the shelf and upper slope are apparently isolated from each other, with the latter region being decoupled from the E-W compressional forces of convergence by the underlying mobile material. Such segregation of extensional and compressional regimes on convergent margins is not unique to Cascadia, with similar observations on the Peru, Japan, Costa Rica, and Alaskan margins. Many N-S trending fold structures previously interpreted as tectonic expressions of convergence-related compression, including rollover folds, drape folds, and hanging wall synclines, can be attributed to listric faulting, with E-W extension being the dominant tectonic style. We conclude that E-W contractile strain is low on the Washington and northern Oregon shelf and that a transition from extension to compression occurs in the mid slope region, likely coincident with the seaward edge of the MBF (Fig. II.2a). The presence of long-term major extensional faults, which displace sediments to depths of 2-3 km or greater throughout much of the northern Cascadia continental shelf and upper slope, is of importance to the current stability of the margin.

II.10 ACKNOWLEDGMENTS

We acknowledge the Minerals Management Service Pacific OCS Region at Camarillo, California for supplying data necessary for this study and Scott Drewry of MMS for use of his unpublished work. We thank Steve Dickenson and Robert Lillie for helpful discussion and J.H. McBride, R. von Huene, and G.K. Westbrook for thorough and helpful reviews. We also thank the crew of the *Cavalier*, Delta submersible pilots Dave Slater and Chris Ijames, members of the 1994 scientific party (Paul Crenna, Gary Huftile, Cheryl Hummon, Alan Niem, Brad Thurber, and Hiro Tsutsumi), and Kevin Redman, David Wilson, Tim McGinness, Chris Center, and Kirk O'Donnell of Williamson and Associates, Seattle, Washington, for side-scan sonar operations. This study was supported by NOAA Undersea Research Program at the West Coast National Undersea Research Center at the University of Alaska grants UAF-92-0061 and UAF-93-0035, National Science Foundation grants OCE-8812731 and OCE-9216880, and U.S. Geological Survey National Earthquake Hazards Reduction Program awards 14-08-0001-G1800, 1434-93-G-2319, 1434-93-G-2489, and 1434-95-G-2635.

II.11 REFERENCES

Aubouin, J., et al., Leg 84 of the Deep Sea Drilling Project: Subduction without accretion: Middle America Trench off Guatemala, *Nature*, 297, 458-460, 1982.

Bergen, F.W., and K.J. Bird, The biostratigraphy of the Ocean City area, Washington, in *The Pacific Coast Miocene Biostratigraphic Symposium, Proceedings*, pp. 173-191, Econ. Paleontol. and Mineral. Pac. Sect., 1972.

Brandon, M.T., and A.R. Calderwood, High-pressure metamorphism and uplift of the Olympic subduction complex, *Geology*, 18, 1252-1255, 1990.

Bruce, C.H., Pressured shale and related sediment deformation: Mechanism for development of regional contemporaneous faults, *AAPG Bull.*, 57, 878-886, 1973.

Bruns, T.R., R. von Huene, R.C. Culotta, S.D. Lewis, and J.W. Ladd, Geology and petroleum potential of the Shumagin margin, Alaska, in *Geology and Resource Potential of the Continental Margin of Western North America and Adjacent Ocean Basins-Beaufort Sea to Baja California*, edited by D. W. Scholl, A. Grantz, and J.G. Vedder, pp. 157-189, Circum-Pac. Counc. for Energy and Miner. Resour., Houston, Tex., 1987.

Busch, D.A., Influence of growth faulting on sedimentation and prospect evaluation, *AAPG Bull.*, 59, 217-230, 1975.

Carson, B., J. Yuan, P.B. Myers Jr., and W.D. Barnard, Initial deep-sea sediment deformation at the base of the Washington continental slope: A response to subduction, *Geology*, 2, 561-564, 1974.

Cranswick, D.J., and K.A. Piper, Geologic framework of the Washington-Oregon continental shelf—Preliminary findings, in *Proceedings of the 1991 Exclusive Economic Zone Symposium on Mapping and Research: Working Together in the Pacific EEZ*, U.S. Geol. Surv. Circ., 1092, 146-151, 1992.

Dahlen, F.A., Noncohesive critical Coulomb wedges: An exact solution, *J. Geophys. Res.*, 89, 10,125-10,133, 1984.

Davis, D., J. Suppe, and F.A. Dahlen, Mechanics of fold-and-thrust belts and accretionary wedges, *J. Geophys. Res.*, 88, 1153-1172, 1983.

DeMets, C., R.G. Gordon, D.F. Argus, and S. Stein, Current plate motions, *Geophys. J. Int.*, 101, 425-478, 1990.

Fleming, S.W., Bulldozer blades and colliding submarine mountain chains: Constraints on central Oregon convergent margin tectonics from magnetics and gravity, M.S. thesis, 84 pp., Oreg. State Univ., Corvallis, 1996.

Goldfinger, C., L.D. Kulm, and R.S. Yeats, Neotectonic map of the Oregon continental margin and adjacent abyssal plain, scale 1:500,000, *Open File Rep. O-92-4*, Oreg. Dep. of Geol. and Mineral Ind., Portland, 1992.

Goldfinger, C., L.D. Kulm, and L.C. McNeill, Super-scale slumping of the southern Oregon Cascadia margin: Tsunamis, tectonic erosion, and extension of the forearc, *Eos Trans. AGU*, 76(46), Fall Meet. Suppl., F361, 1995.

Haugerud, R.A., Digital topographic-bathymetric map of Cascadia (39°N-53°N, 116°W-133°W), *Geol. Soc. Am. Abstr. Programs*, 28 (5), 73, 1996.

Hubbert, M.K., and W.W. Rubey, Role of fluid pressure in mechanics of overthrust faulting, 1, Mechanics of fluid-filled porous solids and its application to overthrust faulting, *Geol. Soc. Am. Bull.*, 70, 115-166, 1959.

Karig, D.E., H. Kagami, and DSDP Leg 87 Scientific Party, Varied responses to subduction in Nankai Trough and Japan forearc, *Nature*, 304, 148-151, 1983.

Kleinpell, R.M., *Miocene Stratigraphy of California*, 450 pp., T. Murby, London, 1938.
Kulm, L.D., and G.A. Fowler, Oregon continental margin structure and stratigraphy: A test of the imbricate thrust model, in *The Geology of Continental Margins*, edited by C.A. Burk and C.L. Drake, pp. 261-284, Springer-Verlag, New York, 1974.

Kulm, L.D., and E. Suess, Relation of carbonate deposits and fluid venting: Oregon accretionary prism, *J. Geophys. Res.*, 95, 8899-8915, 1990.

Kulm, L.D., R.A. Prince, and P.D. Snavely Jr., Site survey of the northern Oregon continental margin and Astoria Fan, *Initial Rep. Deep Sea Drill. Proj.*, 18, 979-987, 1973.

Li, C., Forearc structures and tectonics in the southern Peru-northern Chile continental margin, *Mar. Geophys. Res.*, 17, 97-113, 1995.

MacKay, M.E., G.F. Moore, G.R. Cochrane, J.C. Moore, and L.D. Kulm, Landward vergence and oblique structural trends in the Oregon margin accretionary prism: Implications and effect on fluid flow, *Earth Planet. Sci. Lett.*, 109, 477-491, 1992.

Mallory, V.S., *Lower Tertiary Biostratigraphy of the California Coast Ranges*, 416 pp., Am. Assoc. of Pet. Geol., Tulsa, Okla., 1959.

McCaffrey, R., and C. Goldfinger, Forearc deformation and great subduction earthquakes: Implications for Cascadia earthquake potential, *Science*, 267, 856-859, 1995.

McClain, K.J., A geophysical study of accretionary processes on the Washington continental margin, Ph.D. thesis, 141 pp., Univ. of Wash., Seattle, 1981.

McCrory, P.A., Quaternary crustal shortening along the central Cascadia subduction margin, Washington, *Geol. Soc. Am. Abstr. Programs*, 26(7), A-523, 1994.

McCrory, P.A., Tectonic model explaining divergent contraction directions along the Cascadia subduction margin, Washington, *Geology*, 24, 929-932, 1996.

McIntosh, K., E. Silver, and T. Shipley, Evidence and mechanisms for forearc extension at the accretionary Costa Rica convergent margin, *Tectonics*, 12, 1380-1392, 1993.

McNeill, L.C., K.A. Piper, C. Goldfinger, and L.D. Kulm, Detachment faulting on the Cascadia continental shelf: Active extension in a compressional regime?, *Eos Trans. AGU*, 76(46), Fall Meet. Suppl., F534, 1995.

Morley, C.K., and G. Guerin, Comparison of gravity-driven deformation styles and behavior associated with mobile shales and salt, *Tectonics*, 15, 1154-1170, 1996.

Natland, M.L., Pleistocene and Pliocene stratigraphy of southern California, Ph.D. thesis, 165 pp., 20 plates, Univ. of Calif., Los Angeles, 1952.

Niem, A.R., Snively, P.D., Jr., and Niem, W.A., Onshore-offshore geologic cross section from the Mist gas field, northern Oregon coast range, to the northwest Oregon continental shelf, *Oreg. Dep. of Geol. and Mineral Ind. Oil and Gas Invest.*, 17, 46 pp., 1990.

Niem, A.R., MacLeod, N.S., Snively, J., P.D., Huggins, D., Fortier, J.D., Meyer, H.J., Seeling, A., and Niem, W.A., Onshore-offshore geologic cross section, northern Oregon Coast Range to continental slope. *Oreg. Dep. of Geol. and Mineral Ind., Spec. Paper 26*, 10 pp., 1992.

Orange, D.L., Criteria helpful in recognizing shear-zone and diapiric mélanges: Examples from the Hoh accretionary complex, Olympic Peninsula, Washington, *Geol. Soc. Am. Bull.*, 102, 935-951, 1990.

Orange, D.L., D.S. Geddes, and J.C. Moore, Structural and fluid evolution of a young accretionary complex: The Hoh rock assemblage of the western Olympic Peninsula, Washington, *Geol. Soc. Am. Bull.*, 105, 1053-1075, 1993.

Palmer, S.P., and W.S. Lingley, An assessment of the oil and gas potential of the Washington outer continental shelf, *Rep. WSG 89-2*, 88 pp., Wash. Sea Grant Program, Seattle, Wash., 1989.

Piper, K.A., Extensional tectonics in a convergent margin—Pacific Northwest offshore, Washington and Oregon, *AAPG Bull.*, 78, 673, 1994.

Piper, K.A., L.C. McNeill, and C. Goldfinger, Active growth faulting on the Washington continental margin, *AAPG Bull.*, 79, 596, 1995.

Rau, W.W., Foraminifera, stratigraphy, and paleoecology of the Quinault Formation, Point Grenville-Raft River coastal area, Washington, *Wash. Div. Mines Geol. Bull.*, 62, 41 pp., 1970.

Rau, W.W., Geology of the Washington coast between Point Grenville and the Hoh River, *Wash. Div. Geol. Earth Resour. Bull.*, 66, 58 pp., 1973.

Rau, W.W., Geologic map of the Destruction Island and Taholah quadrangles, Washington, scale 1:63,360, *Geol. Map GM-13*, Wash. Div. of Geol. and Earth Resour., Olympia, Wash., 1975.

Rau, W.W., Geologic map in the vicinity of the lower Bogachiel and Hoh River valleys, and the Washington coast, scale 1:62,500, *Geol. Map GM-24*, Wash. Div. of Geol. and Earth Resour., Olympia, Wash., 1979.

Rau, W.W., Pacific Northwest Tertiary benthic foraminiferal biostratigraphic framework—An overview, *Spec. Pap. Geol. Soc. Am.*, 184, 67-84, 1981.

Shor, G.G., P. Dehlinger, H.K. Kirk, and W.S. French, Seismic refraction studies off Oregon and northern California, *J. Geophys. Res.*, 73, 2175-2194, 1968.

Silver, E.A., Pleistocene tectonic accretion of the continental slope off Washington, *Mar. Geol.*, 13, 239-249, 1972.

Snively, P.D., Jr., Tertiary geologic framework, neotectonics, and petroleum potential of the Oregon-Washington continental margin, in *Geology and Resource Potential of the Continental Margin of Western North America and Adjacent Ocean Basins-Beaufort Sea to Baja California*, edited by D. W. Scholl, A. Grantz, and J.G. Vedder, pp. 305-335, Circum-Pac. Counc. for Energy and Miner. Resour., Houston, Tex., 1987.

Snavely, P.D., Jr., and K.A. Kvenvolden, Preliminary evaluation of the petroleum potential of the Tertiary accretionary terrane, west side of the Olympic Peninsula, 1, Geology and hydrocarbon potential, *U.S. Geol. Surv. Bull.*, 1892, 1-18, 1989.

Snavely, P.D., Jr., and P.H. McClellan, Preliminary geologic interpretation of USGS S.P. Lee seismic reflection profile WO 76-7 on the continental shelf and upper slope, northwestern Oregon, *U.S. Geol. Surv. Open File Rep.*, 87-612, 12 pp., 1987.

Snavely, P.D., Jr., and H.C. Wagner, Geologic cross section across the continental margin of southwestern Washington, *U.S. Geol. Surv. Open File Rep.*, 82-459, 10 pp., 1982.

Snavely, P.D., Jr., and R.E. Wells, Cenozoic evolution of the continental margin of Oregon and Washington, *U.S. Geol. Surv. Open File Rep.*, 91-441B, 34 pp., 1991.

Spence, W., Stress origins and earthquake potential in Cascadia, *J. Geophys. Res.*, 94, 3076-3088, 1989.

Tabor, R.W., and W.M. Cady, The structure of the Olympic Mountains, Washington—Analysis of a subduction zone, *U.S. Geol. Surv. Prof. Pap.*, 1033, 38 pp., 1978.

Thackray, G. D., Deformation of middle and late Pleistocene strata on the Olympic coast of Washington, *Geol. Soc. Am. Abstr. Programs*, 26(7), A-523, 1994.

Tréhu, A.M., I. Asudeh, T.M. Brocher, J.H. Luetgert, W.D. Mooney, J.L. Nabelek, and Y. Nakamura, Crustal architecture of the Cascadia forearc, *Science*, 266, 237-243, 1994.

Tréhu, A., G. Lin, E. Maxwell, and C. Goldfinger, A seismic reflection profile across the Cascadia subduction zone offshore central Oregon: New constraints on methane distribution and crustal structure, *J. Geophys. Res.*, 100, 15,101-15,116, 1995.

von Huene, R., and S. Lallemand, Tectonic erosion along the Japan and Peru convergent margins, *Geol. Soc. Am. Bull.*, 102, 704-720, 1990.

von Huene, R., and D.W. Scholl, Observations at convergent margins concerning sediment subduction, subduction erosion, and the growth of continental crust, *Rev. Geophys.*, 29, 279-316, 1991.

von Huene, R., J. Bourgois, J. Miller, and G. Pautot, Massive collapse along the front of the Andean convergent margin off Peru, *J. Geophys. Res.*, 94, 1703-1714, 1989.

Wagner, H.C., L.D. Batatian, T.M. Lambert, and J.H. Tomson, Preliminary Geologic framework studies showing bathymetry, locations of geophysical tracklines and exploratory wells, seafloor geology and deeper geologic structures, magnetic contours, and inferred thickness of Tertiary rocks on the continental shelf and upper continental slope of southwest Washington between latitudes 46°N and 48° 30'N and from the Washington coast to 125° 30'W, *Open File Rep. 86-1*, 10 pp., Wash. Div. of Geol. and Earth Resour., Olympia, Wash., 1986.

Wernicke, B., Low-angle normal faults in the Basin and Range Province: Nappe tectonics in an extending orogen, *Nature*, 291, 645-647, 1981.

Westbrook, G.K., et al., *Proceedings of the Ocean Drilling Program, Initial Reports, 146*, 92 pp., Ocean Drill. Program, College Station, Tex., 1994.

Wilson, D.S., Confidence intervals for motion and deformation of the Juan de Fuca plate, *J. Geophys. Res.*, 98, 16,053-16,071, 1993.

Zoback, M.L., and M.D. Zoback, Tectonic stress field of the continental United States, *Mem. Geol. Soc. Am.*, 172, 523-540, 1989.

Chapter III

The Effects of Upper Plate Deformation on Records of Prehistoric Cascadia Subduction Zone Earthquakes

Lisa C. McNeill¹, Chris Goldfinger², Robert S. Yeats¹, and LaVerne D. Kulm²

¹ Department of Geosciences, Wilkinson Hall,
Oregon State University, Corvallis, Oregon 97331

² College of Oceanic and Atmospheric Sciences,
Oregon State University, Corvallis, Oregon 97331

Submitted to *Coastal Tectonics*,
Geological Society of London Special Publication,
Stewart, I. and Vita-Finzi, C. (eds.), in press.

III.1 ABSTRACT

Geophysical data from the offshore Cascadia forearc reveal many Quaternary upper-plate faults and folds. Most active structures are within the accretionary wedge, but significant deformation is also found on the continental shelf. Several faults and synclines project into adjacent coastal bays where deformation of Pleistocene marine terraces is reported. Rapidly buried marsh deposits and drowned forests in these coastal lowlands are interpreted to record coseismic deformation by prehistoric subduction zone earthquakes. The extent and amount of such coastal subsidence has been used to infer characteristic magnitudes and recurrence intervals. However, the record may incorporate both elastic strain release on the subduction zone and localized permanent upper-plate deformation. Movement on upper-plate structures may be triggered by a subduction zone earthquake, as observed in the Nankai and Alaskan forearcs. Alternatively, they may deform independently of subduction zone earthquakes. Regardless of which style of deformation predominates, the record of coseismic subsidence is likely to be affected. Crustal deformation may also contribute to the preservation of subsided marshes. Modeling of subduction zone earthquake characteristics based on coastal marsh stratigraphy is likely to be inaccurate in terms of: (a) total apparent rupture length and earthquake magnitude; (b) amount of subsidence and hence the position of the locked zone; and (c) recurrence interval. Most of these shelf and coastal structures respond to N-S compression, in contrast to convergence-related northeasterly compression in the accretionary prism, but in agreement with the regional stress field. Despite low historical coastal and continental shelf seismicity, upper-plate faults may also pose an independent seismic hazard.

III.2 INTRODUCTION

Geological and geophysical investigations of the Cascadia subduction zone during the last decade have increased public awareness of regional earthquake hazards from a subduction zone previously thought to be aseismic (Ando & Balazs 1979). Evidence for repeated abrupt subsidence in the last few thousand years is found in coastal bays along the active margin, in the form of buried marsh deposits and drowned forests (e.g., Atwater 1987, 1992; Darienzo & Peterson 1990; Atwater *et al.* 1995; Nelson *et al.* 1995; Yamaguchi *et al.* 1997). Previous workers believe these deposits to be a result of coseismic subsidence and have attributed them to subduction zone earthquakes (e.g.,

Atwater 1987, 1992; Darienzo & Peterson 1990; Atwater *et al.* 1995; Nelson *et al.* 1995; Yamaguchi *et al.* 1997). However, the similarity of these deposits to the marsh stratigraphy of tectonically inactive coasts has led to the suggestion that many abrupt burials may be non-tectonic in origin and driven by local changes in intertidal environment (e.g., Long & Shennan 1994). A non-tectonic origin cannot be eliminated except in certain cases where the event is found to be regionally widespread, is associated with other coseismic phenomenon such as tsunami deposits or liquefaction, or where the magnitude of subsidence is too large to be explained by non-tectonic mechanisms. The coseismic versus non-seismic origin of the subsidence events will not be addressed by this paper, but remains a topic of debate.

The chronology, distribution, and amount of subsidence for individual locations and events have been used to estimate recurrence intervals and magnitudes. A significant component of subsidence recorded at these sites could be attributed to localized permanent crustal deformation (Goldfinger *et al.* 1992b; Nelson 1992; Goldfinger 1994; McCaffrey & Goldfinger 1995; Nelson & Personius 1996; McCrory 1996; Clague 1997). This study shows that several bays lie within actively deforming synclines or on the downthrown side of faults mapped onshore and in the contiguous offshore inner shelf. Mapping the offshore region benefited from extensive geophysical datasets and the absence of thick vegetation and soils which often hinders coastal fieldwork. A question critical to the understanding of contributions by crustal structures to the subsidence record is: Do crustal and subduction zone earthquakes operate independently or together? Regardless of the answer to this question, localized upper plate deformation calls into question calculations of recurrence interval and earthquake magnitude obtained from records of coastal subsidence.

The objectives of this study were to consider the distribution of abruptly-buried deposits in light of upper-plate Quaternary deformation in the offshore inner shelf and onshore coastal region, and to determine the effects on and limitations of this palaeoseismic record for determination of prehistoric subduction-zone earthquake characteristics. We show that such structures reflect the predominant structural regime and stress field of the shelf and coast, and suggest that these localized structures may pose an independent seismic hazard to coastal communities.

III.3 METHODS

Structures outlined in this paper were mapped from single channel and multichannel seismic reflection profiles, sidescan sonar data, and submersible observations. Seismic

data were collected by Oregon State University, University of Washington, U.S. Geological Survey, and the petroleum industry. Many of the seismic profiles extend to within a few kilometers of the coastline.

One proprietary dataset consists of a closely spaced network (between 2 - 30 km apart) of high quality, precision-navigated, migrated multichannel profiles. This dataset covers the shelf and uppermost slope of Oregon and Washington. Acquisition details of this proprietary dataset are discussed in McNeill *et al.* (1997). Many of the structures identified in this paper were mapped from this particular dataset, with the data shown here in the form of migrated time sections.

Deep-towed sidescan sonar data were collected during several research cruises between the years of 1992 and 1995, and were navigated using GPS. Sidescan sonar data on the shelf include the AMS (Alpha Marine Systems) 150 kHz and Klein systems. Details of sidescan sonar data, and sonar processing and imaging techniques are given in Goldfinger *et al.* (1997b). The shallow-diving submersible, DELTA, was used to dive on fault targets selected from sidescan sonar images and seismic reflection data.

III.4 TECTONIC SETTING

The Cascadia subduction zone is located off the coast of the northwestern United States and southwestern Canada, a result of subduction of the Juan de Fuca and Gorda plates beneath the North American plate (Fig. III.1, inset). Convergence is oblique to the northeast at a rate of 42 mm/yr. at latitude 47° 30'N (NUVEL-1 plate motion model of DeMets *et al.* (1990)). No earthquakes have been recorded on the plate boundary during the period of recorded seismicity, with the possible exception of the 1992 Petrolia earthquake (Oppenheimer *et al.* 1993). Crustal seismicity in the North American plate and within the subducting Juan de Fuca plate is minimal but present, with greatest recorded seismicity in Washington (Puget Sound) and in the Gorda plate off northern California (e.g., Crosson & Owens 1987; Weaver & Baker 1988; Ludwin *et al.* 1991). The lack of seismicity on the megathrust led early workers to infer that subduction may have ceased or that subduction is aseismic (Ando & Balazs 1979). An alternative interpretation, that strain is currently accumulating and will be released in a future large-magnitude earthquake, was supported by evidence for abrupt potentially-coseismic coastal subsidence (Atwater 1987) and regularly-spaced turbidites, potentially earthquake-induced, in submarine channels on the Juan de Fuca abyssal plain (Adams 1990). Both lines of evidence point to several events in the last few thousand years. Coseismic subsidence in the coastal Cascadia region

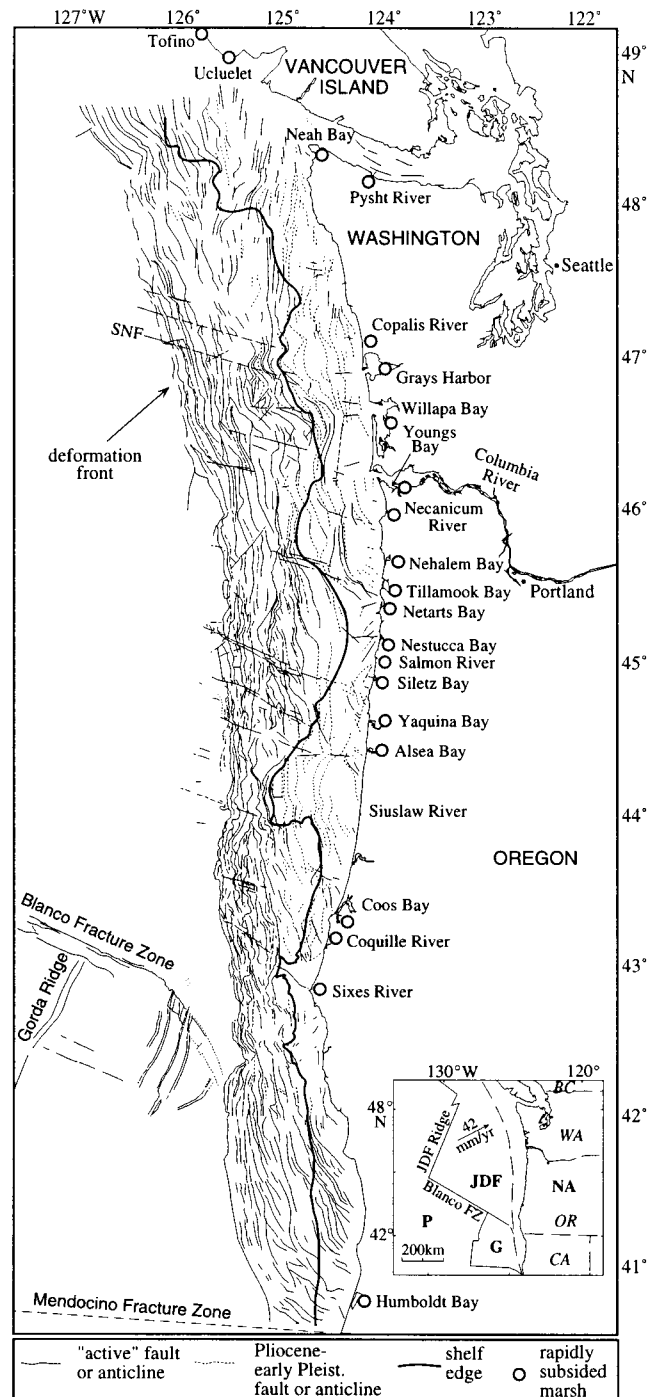


Figure III.1. Neotectonic map of recent structures (late Pliocene to Holocene anticlines and faults only), including inner shelf and coastal structures outlined in this paper, and locations of coastal subsidence. Inset shows general tectonic setting with plate convergence vector (DeMets et al. 1990). Plates: P=Pacific; JDF=Juan de Fuca; NA=North American; G=Gorda. FZ=Fracture Zone. SNF=left-lateral South Nitinat Fault. Northern California offshore structures after Clark (1990, 1992; reproduced by kind permission of AAPG and GSA).

is predicted from elastic dislocation models of the subduction zone cycle. Figure III.2 illustrates this cycle, where the land surface a certain distance from the deformation front is expected to gradually uplift during the interseismic period, followed by sudden subsidence during the seismic event. This region is expected to coincide with the coast in Cascadia. A similar elastic response was recorded accompanying the 1960 Chilean and 1964 Alaskan subduction earthquakes (Plafker 1969, 1972), with regions of coseismic uplift and subsidence identified. The earthquake potential of the Cascadia subduction zone based on coastal subsidence and abyssal plain turbidites was reinforced by analogies between Cascadia and Chilean-type subduction zones (Heaton & Kanamori 1984).

III.5 REGIONAL STRATIGRAPHY AND STRUCTURE

Cenozoic strata underlying the continental shelf consist of Eocene to Quaternary bathyal through neritic forearc basin and accretionary complex sequences resting in part on early Eocene basalt (Snively 1987; Snively & Wells 1996; Palmer & Lingley 1989). Several regional unconformities are prominent within the basinal sequence, including one of late Miocene-early Pliocene age (PM) and one of late Pliocene-Pleistocene age. The basinal sequence of the Washington shelf is underlain by a thick sequence of Eocene to middle Miocene *mélange* and broken formation, known as the Hoh Rock Assemblage and Ozette *Mélange* onshore (Rau 1973; Orange *et al.* 1993, McNeill *et al.* 1997). Eocene Coast Range basaltic formations and the middle Miocene Columbia River Basalt Group, locally interfinger with Eocene to Miocene strata in coastal Oregon and southern Washington, and extend onto the continental shelf (Niem *et al.*, 1990, 1992).

The lower continental slope is dominated by compressional tectonics within the active accretionary prism in response to plate convergence, with structural trends between N-S and NW-SE (Fig. III.1, Goldfinger *et al.* 1992a, 1997a). A set of WNW-trending left-lateral strike-slip faults, a result of oblique convergence, was mapped on the continental slope and locally on the outermost shelf of Oregon and Washington (Fig. III.1; Goldfinger 1994; Goldfinger *et al.* 1992b, 1996, 1997a). On the northern Oregon and Washington shelf and upper slope, E-W extension is common in the form of listric normal faulting related to the underlying mobile *mélange* and broken formation (McNeill *et al.* 1997). Complex fold trends on the Washington upper slope may be partially controlled by mobilization of the *mélange* and broken formation (McNeill *et al.* 1997). Structural styles are more varied on the continental shelf where many of the Miocene to early Pleistocene structures are no longer active (Fig. III.1, Goldfinger *et al.* 1992a). Active fold axes on

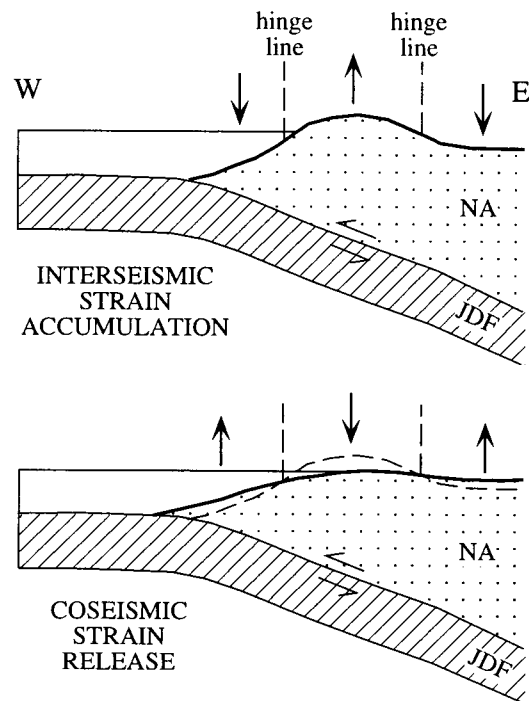


Figure III.2. Model showing the subduction earthquake cycle (after Darienzo & Peterson 1990; reproduced by kind permission of GSA). During the interseismic period (a period of hundreds of years), strain accumulates causing much of the Cascadia coastline to gradually uplift (between the two hinge lines). Coseismic strain release occurs during the subduction earthquake causing this region to rapidly subside, resulting in drowning of the coastal area. The seaward hinge line represents the zero isobase, seaward of which coseismic uplift occurs. No vertical movement occurs at the hinge lines. Under purely elastic conditions, subsidence is completely recovered with no net subsidence or uplift through the earthquake cycle. NA=North American plate, JDF=Juan de Fuca plate.

much of the inner shelf trend perpendicular to the coastline and margin (Goldfinger *et al.* 1992b; Goldfinger 1994). These fold trends suggest N-S compression rather than dominant northeasterly compression within the active accretionary prism.

III.6 ACTIVE CRUSTAL STRUCTURES AND COASTAL SUBSIDENCE

III.6.1 Introduction

To date, coastal subsidence in the form of rapidly-buried marsh deposits has been identified at the following bay and river locations along the Cascadia subduction zone, from north to south: Vancouver Island sites (Ucluelet and Tofino), Neah Bay, Pysht River, Copalis River, Grays Harbor, Willapa Bay, Columbia River, Necanicum River, Nehalem Bay, Tillamook Bay, Netarts Bay, Nestucca Bay, Salmon River, Siletz Bay, Yaquina Bay, Alsea Bay, South Slough, Coquille River, Sixes River, and Humboldt Bay (Fig. III.1; based on Atwater *et al.* 1995; Barnett 1997). Evidence of Quaternary structural downwarping is described or documented here at Grays Harbor, Willapa Bay, Nehalem Bay, Tillamook Bay, Netarts Bay, Siletz Bay, Yaquina Bay, Alsea Bay, South Slough, Coquille River, and Humboldt Bay (see table below). At these locations, buried marsh deposits are located within Quaternary synclinal folds or on the downthrown side of faults. Buried marsh locations where evidence of Quaternary deformation is inconclusive are also documented, along with two examples of buried marshes which may be located on the upthrown side of a Quaternary fault or on the crest of an anticline. The table below describes the Quaternary structures at each of these locations.

III.6.2 Buried Marshes in Areas of Late Quaternary Subsidence

III.6.2.1 Grays Harbor

Structure contours of the late Pliocene-Pleistocene unconformity west of Grays Harbor indicate a narrow E-W to NE-SW trending depression (Fig. III.3). This active syncline lies due west of Grays Harbor, which may be structurally controlled. Buried

Table of Quaternary deformation at marsh burial locations.

Presence or absence of localized Quaternary deformation at marsh burial locations documented here and in published literature. Local structures are synclines or downthrown sides of faults indicating subsidence, except for those shown in italics, which show evidence of uplift. See Figure II.1 for locations.

Site	Local Structures	Quaternary	References
Tofino	unknown	unknown	
Ucluelet	unknown	unknown	
Neah Bay	inconclusive	inconclusive	Snavely 1987
Pysht River	yes	unproven	Wagner <i>et al.</i> 1987; Gower 1960; Tabor & Cady 1978
Copalis River	yes - <i>Langley anticline</i>	yes	<i>McCrory 1996</i>
Grays Harbor	yes	yes	This study ; Grim & Bennett 1969; Palmer & Lingley 1989
Willapa Bay	yes	yes	This study
Columbia River (incl. Youngs Bay)	yes - Fern Hill fault, Youngs Bay syncline	unproven	Ryan & Stevenson 1995; Niem & Niem 1985
Necanicum River	inconclusive	inconclusive	
Nehalem Bay	yes - Neahkahnie Mountain fault	unproven	This study ; Niem & Niem 1985; Goldfinger <i>et al.</i> 1992; Wells <i>et al.</i> , 1994b
Tillamook Bay	yes - Tillamook Bay fault	unproven	This study ; Wells <i>et al.</i> 1992, 1994b; Goldfinger <i>et al.</i> 1992; Goldfinger 1994
Netarts Bay	yes - Nehalem Bank and Happy Camp faults	yes	This study ; Wells <i>et al.</i> 1992, 1994a, b; Parker 1990; Goldfinger <i>et al.</i> 1992; Goldfinger 1994
Nestucca Bay	yes	no	This study ; Goldfinger <i>et al.</i> 1992
Salmon River	inconclusive	inconclusive	
Siletz Bay	yes	yes	This study ; Goldfinger <i>et al.</i> 1992; Goldfinger 1994
Yaquina Bay	yes	yes	Kelsey <i>et al.</i> 1990; Goldfinger <i>et al.</i> 1992
Alsea Bay	yes	yes	Kelsey <i>et al.</i> 1990
South Slough	yes	yes	McInelly & Kelsey 1990; Goldfinger <i>et al.</i> 1992; Goldfinger 1994
Coquille River	yes	yes	This study ; McInelly & Kelsey 1990
Sixes River	yes, <i>anticline</i>	yes	<i>Kelsey 1990</i>
Humboldt Bay	yes - Little Salmon and Mad River faults, Freshwater syncline	yes	Clarke & Carver 1992

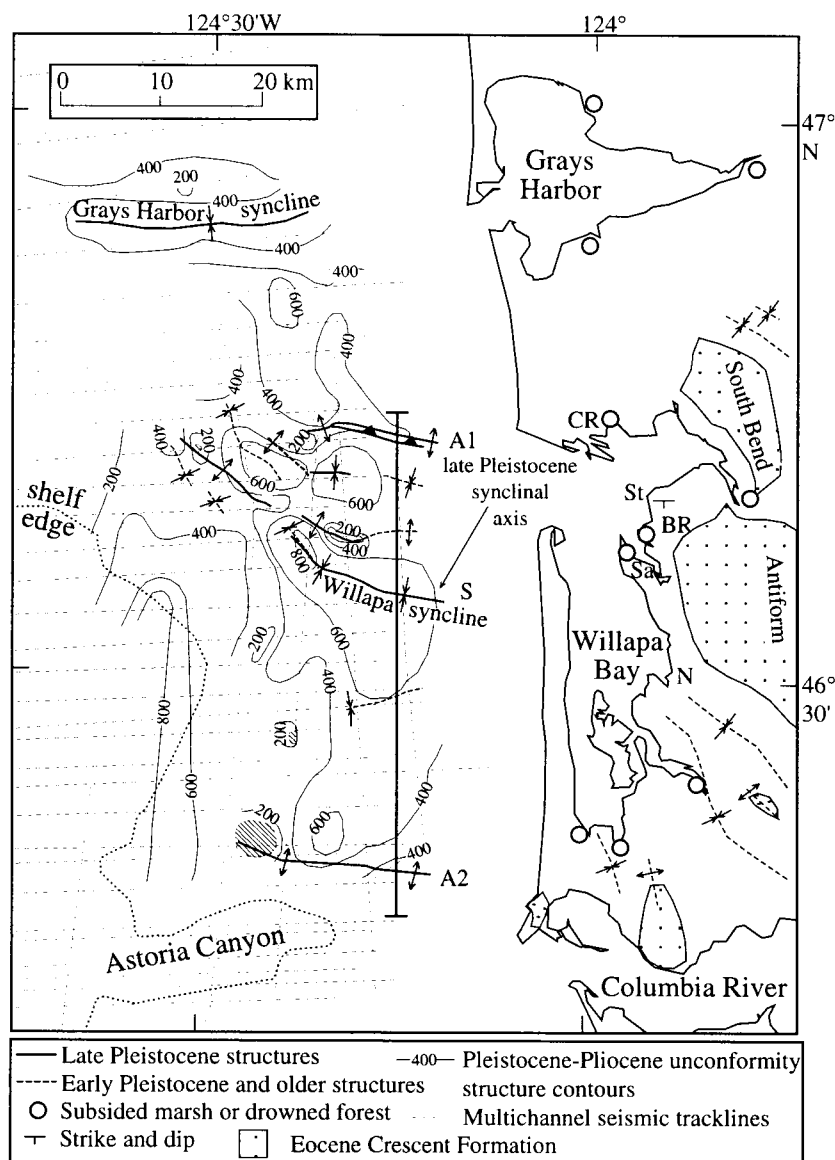


Figure III.3. Map of southern Washington coast and offshore region. Mapped shelf structures associated with the Willapa Bay syncline are active (late Quaternary, solid lines) and Pliocene-early Pleistocene (dashed lines). Structure contours of a Pliocene-Pleistocene unconformity outline Quaternary synclinal deformation (contours in meters below sea level, 200m interval, black hatching indicates the unconformity is truncated at the seafloor). Seismic tracklines used represented by dotted lines. CR=Cedar River, N=Nemah, Sa=Sandy Point, St=Stony Point, BR=Bone River. Early Pleistocene palaeosols dip to the south between Stony Point and Bone River controlled by deformation or palaeotopography. Onshore structures from Walsh et al. (1987), Atwater & Hemphill-Haley (1996), coastal subsidence locations after Atwater & Hemphill-Haley (1996). Bold line shows location of Fig. III.4, A1, A2, S are identified.

marshes have been found throughout the bay (Fig. III.3) and may not all be associated with downwarping of this particular syncline. This depression is tectonically controlled and not the simple result of backfilling of a Pleistocene lowstand channel.

III.6.2.2 Willapa Bay

Buried marshes and drowned forests provide evidence of rapid subsidence throughout Willapa Bay, southern Washington coast (Figs. III.1, III.3; e.g., Atwater 1987; Atwater & Hemphill-Haley 1996; Yamaguchi *et al.* 1997). Multichannel seismic reflection profiles 10-30 km west of the bay reveal a broad syncline 40 km in length, extending from the northern to the southern end of the bay (Figs. III.3, III.4). The synclinal axis trends NW-SE to E-W and projects into the center of Willapa Bay. To the north and south of the syncline, two bounding anticlines may be underlain by faults with reverse separation (strike-slip component unknown) (Fig. III.3). The northern N-dipping reverse fault may be blind (A1, Fig. III.4). Alternatively, this fault may be the southeastern projection of a left-lateral fault which deforms Holocene sediments on the continental slope (South Nitinat Fault of Goldfinger 1994; Goldfinger *et al.* 1997a; SNF in Fig. III.1). The Willapa Bay structures deform Eocene to late Miocene mélangé and broken formation and overlying late Miocene to Quaternary basinal sediments, and gently deform the seafloor. The northern fault was investigated during a submersible and sidescan sonar cruise in 1995. A submersible dive found no evidence of seafloor offset, possibly due to high-energy wave action in shallow water or because the fault is blind. However, evidence of carbonate cementation and algal mats was observed, suggesting fluid venting accompanying active faulting, as observed elsewhere on the margin (Kulm & Suess 1990; Goldfinger *et al.* 1997a). The southern anticline (A2) and underlying fault (or possibly diapiric intrusion) may be inactive in the Quaternary (minimal deformation of the Pliocene-Pleistocene unconformity in Fig. III.4). Structure contours of the late Pliocene-Pleistocene unconformity also outline the position of the Willapa syncline (Fig. III.3). The different positions of the late Pliocene (black dashed line), the early Pleistocene (unconformity structure contours), and the most recently active synclinal axis (black solid line) indicate that the fold axis has migrated north from Pliocene to present. Early Pliocene growth strata thicken towards the southern anticline (Fig. III.4, A2), whereas overlying late Pliocene strata thin towards the anticline, indicating that growth of this anticline occurred during the late Pliocene. Prior to this time, the syncline was formerly a larger

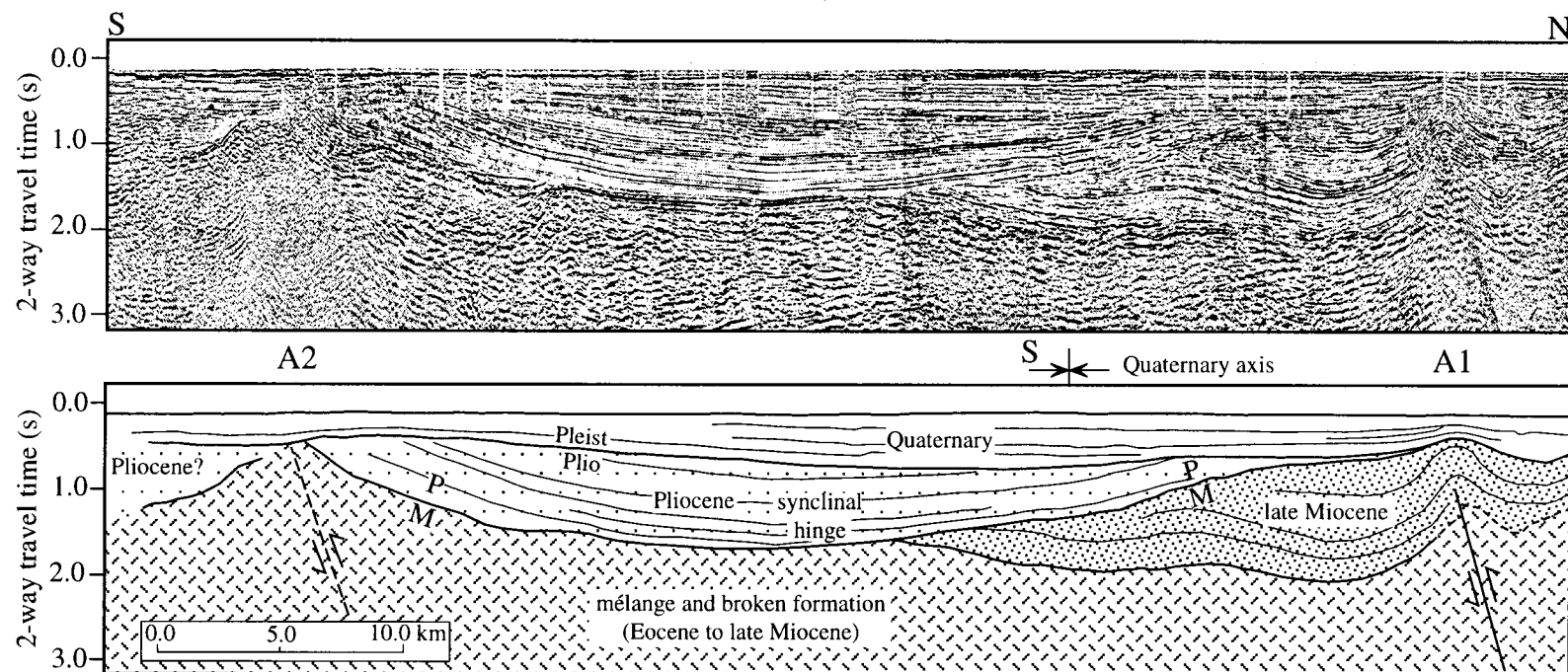


Figure III.4 N-S proprietary migrated multichannel seismic reflection profile 10 km west of Willapa Bay. The lower interpreted section shows late Miocene to Quaternary sediments and underlying mélangé are deformed by an active syncline and associated structures. To the north, Pleistocene sediments are deformed by an active N-dipping blind reverse fault. Regional angular unconformities: MP=late Miocene-Pliocene; Plio-Pleist=Pliocene-Pleistocene.

structure extending to the south. The position of synclinal folding with respect to Willapa Bay strongly suggests that the bay is structurally controlled.

Exposures of Pleistocene marine terraces and underlying Pleistocene tidal flat and Tertiary sediments are widespread and continuous throughout the central region of Willapa Bay. Amino acid racemization of shell deposits within the lowest altitude marine terrace sediments of the central bay suggest conflicting ages. Kvenvolden *et al.* (1979) identify two separate highstands, with absolute ages of 120 ka and $190 \text{ ka} \pm 40 \text{ ka}$. Amino acid ages with supporting faunal correlations and palaeoecology from Kennedy (1978) and Kennedy *et al.* (1982) suggest a more probable and precise age of 80 - 85 ka (West 1986). Despite the unresolved terrace chronology, relative altitudes of continuous and correlative terraces have been documented. The lowest terrace surface is reported to be at a constant altitude of ~ 13 -15 m above sea level in the central region of the bay (West 1986). However, reconnaissance investigation of terrace elevations for this study found that the terrace actually reaches a minimum elevation of ~ 9-10 m at Sandy Point (Sa, Fig. III.3). There are no signs of landslides or slumping in this region, and therefore terrace elevations are assumed to be undisturbed. In the northern bay, the lowest terrace, which West (1986) assumes to be the continuation of the central bay's lowest terrace (80-85 ka?), increases in altitude to 24 m (West 1986). South of Nemah (N, Fig. III.3), limited exposures of terraces of unknown age range in altitude from 12 to 18 m. These altitude changes, although only loosely constrained by age control, are in agreement with a synclinal axis close to the center of the bay. The stratigraphy of the estuarine sediments underlying the lowest and youngest central bay terrace shows no clear evidence of deformation along a N-S transect (Kvenvolden *et al.* 1979; Clifton 1983, 1994, pers. comm., 1997). However, a unit of older (early Pleistocene or late Pliocene?) well-indurated estuarine terrace sediments including a sequence of peaty muds commonly containing root or rhizome structures and thought to be palaeosols, locally exposed within the youngest terrace, may be deformed (Fig. III.5; Clifton 1994; E. Clifton, pers. comm., 1997). Between Stony Point and the Bone River (Fig. III.3), these surfaces dip gently to the south (Fig. III.5, Clifton 1994). If these surfaces were originally approximately horizontal, they are now deformed in agreement with the projection of the offshore projected synclinal axis. However, the dip of these mud layers may alternatively be controlled by palaeotopography, as we note the similar dip of the underlying (Crsecent Formation) basalt at the northern end of Figure III.5.

The WNW-trend of Quaternary structures offshore contrasts slightly with NW- to NNW-trending structures which deform Miocene and older formations mapped east of Willapa Bay (Fig. III.3; Walsh *et al.* 1987). This change in trend may reflect a change in

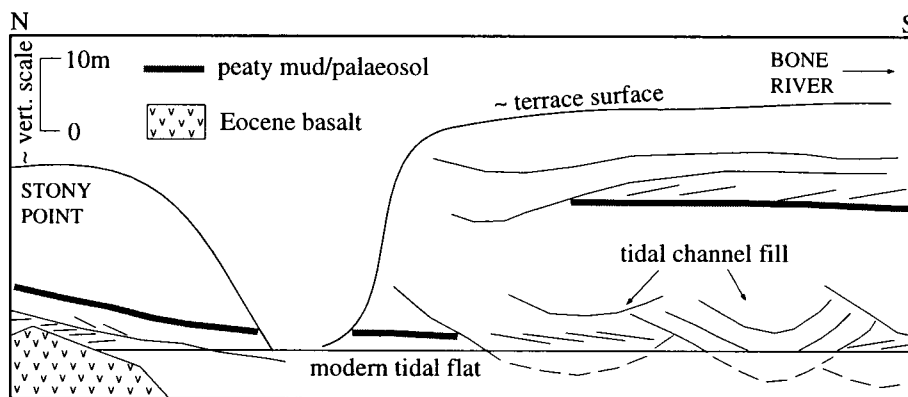


Figure III.5. Early Pleistocene terrace tidal flat sediments between Stony Point (St) and Bone River (BR) in Willapa Bay showing S-dipping palaeosols (after Clifton 1994), in agreement with the projection of the offshore synclinal axis to a position south of this location. See Fig. III.3 for locations.

compressive stress field from the early to late Tertiary, or non-linearity of mapped structures. One of two sub-parallel NW-trending synclinal axes southeast of the bay (Fig. III.3; Walsh *et al.* 1987) could be the landward projection of the offshore structure.

Atwater & Hemphill-Haley (1996) addressed the possibility of deformation by upper plate structures in Willapa Bay by studying the Holocene marsh stratigraphy on and off the N-S trending South Bend antiform (Fig. III.3). They found no difference in the amount of subsidence between these sites, although marshes are buried less deeply below the current marsh surface on, rather than off the antiform (Atwater & Hemphill-Haley 1996). However, this antiform deforms sediments no younger than Miocene and may not be currently active. However, N-S trending folds do deform Pleistocene sediments in the Columbia River (Wells, 1989). An E-W trending structure, such as the Willapa Bay syncline, should show no measurable difference in amount of subsidence along an ~E-W transect, and therefore the results of Atwater & Hemphill-Haley (1996) are not unexpected.

The offshore northern bounding anticline and thrust fault project landward towards one location of marsh burial in the northernmost bay (Fig. III.3). Evidence for subsidence at this site (Cedar River (CR in Fig. III.3) of Atwater & Yamaguchi 1991) is a western red cedar snag which died within a few months of 1700 A.D. This apparent contradiction can be explained if the crustal structure were not activated during the A.D. 1700 event, or if subsidence due to the subduction event exceeded coseismic uplift on the crustal structure with resulting net subsidence, or if the fault and anticline change strike onshore to project to the north of this particular subsidence site. In addition, the absolute vertical motion may differ from the observed relative vertical motion across this anticline.

III.6.2.3 Nehalem and Tillamook Bays

Seismic reflection profiles west of Nehalem Bay reveal synclinal deformation opposite the bay and uplift on the north side of the bay which may be equivalent to the Tertiary Neahkahnie Mountain fault of Wells *et al.* (1994b) (Fig. III.6). Movement on this fault may be oblique slip. The middle Miocene Columbia River Basalt (CRB in Fig. III.7) is deformed by these structures and exposed at Neahkahnie Mountain (Wells *et al.*, 1994b), but Quaternary deformation is unconfirmed.

The northern margin of Tillamook Bay is uplifted by the WNW-trending high-angle Tillamook Bay fault which offsets middle Miocene Columbia River Basalt sills onshore (Wells *et al.* 1992). Offset on this fault is up to the north with a significant left-lateral strike-slip component, but Quaternary deformation is unconfirmed (Wells *et al.*, 1994a, b).

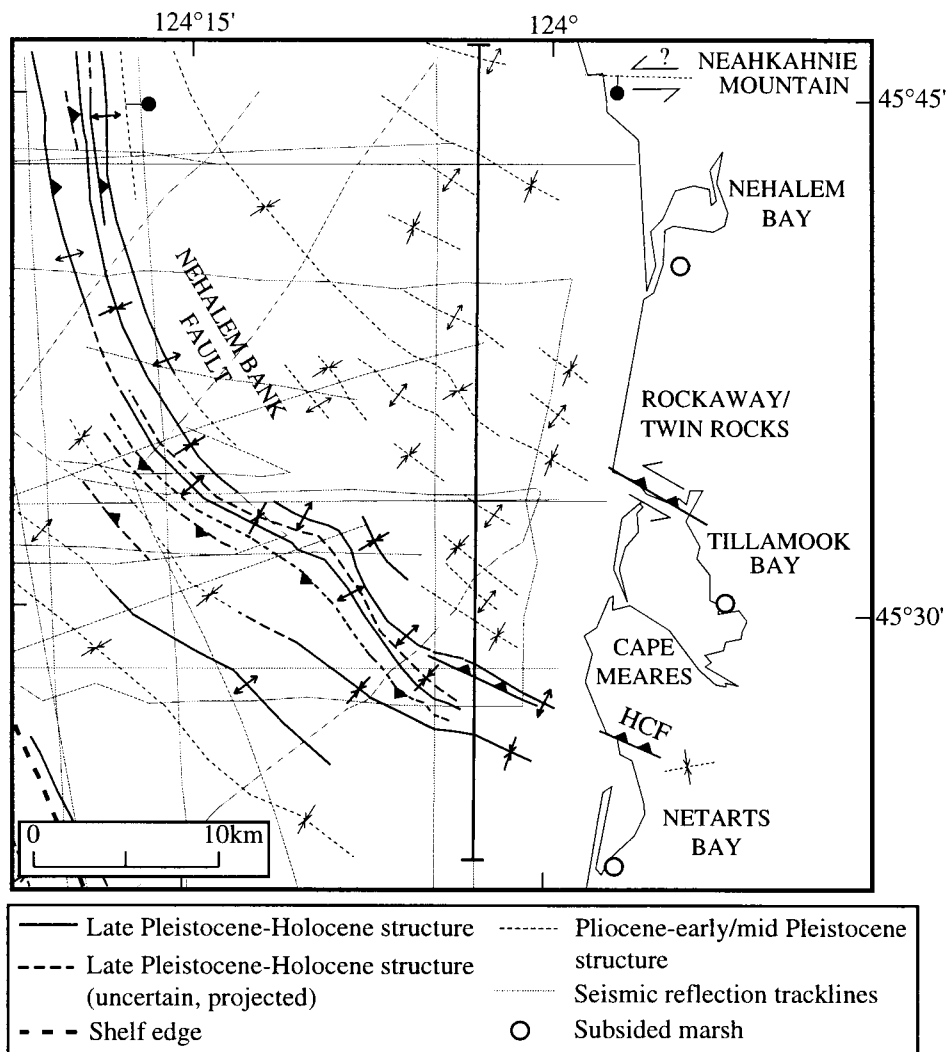


Figure III.6. Location map of northern Oregon coast and shelf, including active structures near Nehalem, Tillamook, and Netarts Bays. The offshore Nehalem Bank fault and associated syncline projects onshore as the Happy Camp fault (HCF) on the north side of Netarts Bay (Parker 1990; Wells et al. 1992, 1994a). Tillamook and Nehalem Bay may also lie within active synclines or on the downthrown side of active faults (Tillamook Bay fault of Wells et al. 1992, Neahkahnie Mountain fault of Niem & Niem 1985 and Wells et al., 1994b). Onshore structures after Parker (1990), Wells et al. (1992, 1994a, b), and Niem & Niem (1985). Heavy line represents N-S seismic reflection profile shown in Fig. III.7.

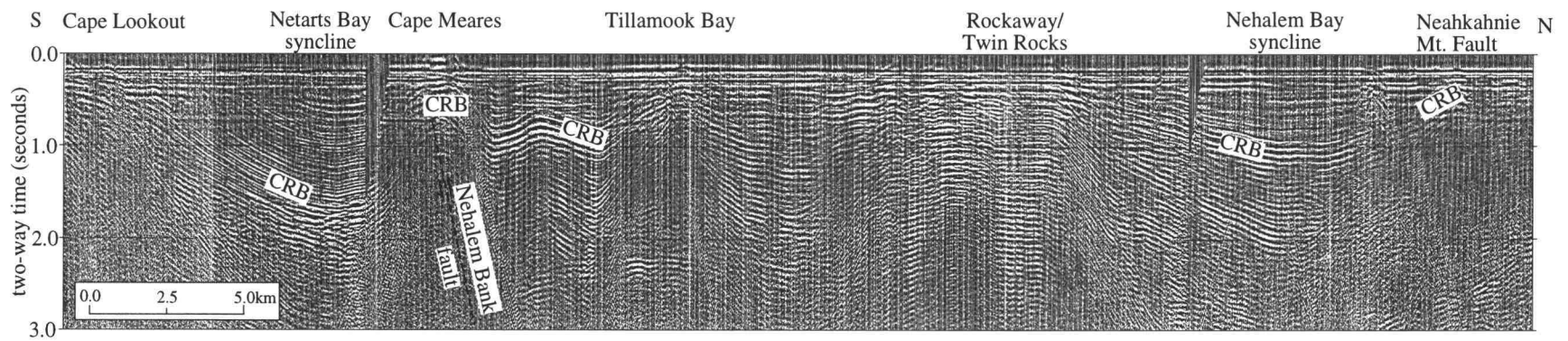


Figure III.7. N-S proprietary multichannel seismic reflection profile between Netarts Bay and Nehalem Bay, 10 km west of the coastline. The Netarts Bay syncline and Nehalem Bank fault project into Netarts Bay. This section reveals seafloor deformation by the southeasterly segment of the Nehalem Bank fault and synclinal deformation on the downthrown side of the fault. The middle Miocene Columbia River Basalt Group (CRB, bright reflector) is noticeably deformed. Sediments (assumed mostly late Miocene) show little or no thickening within the syncline, suggesting that deformation on this structure is largely post-late Miocene. Synclinal folds are also found opposite Nehalem and Tillamook Bays, although the Tillamook structure is complicated by anticlinal deformation within the broad low. Uplifted regions north of Tillamook and Nehalem Bays may be equivalent to the onshore Tillamook Bay fault and Neahkahnie Mountain fault, respectively.

Deformation opposite Tillamook Bay is more complex than at Nehalem Bay, but a broad low between the Happy Camp thrust fault south of Cape Meares and an uplifted region at Twin Rocks can be seen in Figure III.7. This low is interrupted by smaller fold axes. The uplifted region north of the bay may be related to the Tillamook Bay fault (Wells *et al.*, 1992) (Figs. III.6 and III.7).

Owing to the thin Quaternary section on the innermost shelf, offshore Quaternary deformation cannot be confirmed, but further study of the onshore Tillamook Bay fault may confirm Quaternary activity. Rapid burial of Holocene marsh deposits has been identified at both bays (Atwater *et al.*, 1995; Barnett 1997).

III.6.2.4 Netarts Bay

Netarts Bay, on the northern Oregon coast (Fig. III.1), is bounded to the north by WNW-trending, NE-dipping high-angle oblique slip (left-lateral and reverse) faults which deform coastal sediments (Wells *et al.* 1992, 1994a, b). Faults thrust middle Miocene Columbia River Basalt Group (15 Ma) over late Pleistocene alluvial gravels, and may also offset the youngest Pleistocene marine terrace surface but does not deform overlying Holocene sand dunes (Wells *et al.* 1994a). The fault is known as the Happy Camp fault onshore (Parker 1990; Wells *et al.* 1992, 1994a) and may be the southernmost extension of the prominent Nehalem Bank fault zone which deforms Miocene through Holocene sediments offshore (Fig. III.6; Goldfinger 1994). This complex zone of deformation trends roughly N-S on the outer shelf and upper slope off the northern Oregon coast (25 km west of the coastline), but changes to the southeast at its southern end to project onshore just north of Netarts Bay (Fig. III.6). No evidence of major strike-slip offset has been found along the northern segment of the offshore fault, but its N-S orientation (suggesting margin-parallel right-lateral offset where oblique convergence is partitioned into a compressional and strike-slip component), the presence of minor strike-slip faulting, and the linearity of the fault, which truncates bedding planes in AMS 150 kHz sidescan images, support a strike-slip component. However, the fault also shows significant vertical offset (both along its N-S and SE-trending segments) and we interpret it offshore as a reverse fault system downthrown to the west and south, with possible strike-slip component. As the fault trends southeasterly, the zone of deformation becomes less complex, being characterized by a N-dipping (possibly blind) reverse fault, with Miocene sediments uplifted and exposed at the seafloor, and an asymmetrical syncline to the south (S. end of Fig. III.7), which lies immediately opposite Netarts Bay. The offshore

southeast-trending fault probably has significant sinistral offset similar to the correlative fault onshore (Wells *et al.*, 1994b). Sidescan images show bedrock within the hanging wall anticline exposed on the seafloor and offset by minor N- to NNE-trending right-lateral faults. The vertical motion on the northern segment of the fault may be a flower structure or transpressional deformation.

The nearshore Nehalem Bank fault clearly deforms and offsets the middle Miocene Columbia River Basalt Group (highly reflective in seismic reflection data, S. end of Fig. III.7) and overlying sediments. Absence of structural growth of strata within the syncline in Figure III.7 suggests this fault and associated fold post-date late Miocene sedimentation. Investigation of other seismic reflection data across both the southern and northern sections of the fault shows minimal thinning in late Miocene sediments and some thinning of Pliocene sediments across the fault-controlled anticline. This indicates that the fault was active as early as the late Miocene, but the bulk of deformation has taken place during the Pliocene and Quaternary. Vertical seafloor offset of 10-20 meters across the fault zone is estimated from sidescan and seismic records, presumed to postdate late Pleistocene lowstand erosion on the shelf (Goldfinger 1994). Cooper (1981) and Parker (1990) also suggested that a west-plunging syncline that deforms middle Miocene Astoria Formation is centered about Netarts Bay. Abruptly buried marsh horizons and tree stumps have been identified at Netarts Bay (Peterson *et al.*, 1988).

III.6.2.5 Siletz Bay

Structures deforming the underlying sediments and wavecut platform of Pleistocene marine terraces (presumed 80 ka Whiskey Run terrace, West & McCrumb 1988; Kelsey 1990) have been identified in the Siletz Bay region of the central Oregon coast (McNeill *et al.*, 1993) (Figs. III.1, III.8, III.9). The wavecut platform and a locally continuous carbonaceous clay or peaty horizon, interpreted as a lagoonal marsh deposit or palaeosol and assumed to be initially sub-horizontal, were shown to be deformed. However, variations in elevation of the wavecut platform and the clay horizon/paleosol may alternatively be controlled by existing palaeotopography at the time of formation and not by deformation. Elevation of the clay horizon may also be affected by landsliding of the terrace sediments. Variations in altitude of these marker horizons indicate faulting, with vertical offsets of 5-30 m, and broad folding, with a wavelength of 8-12 km (Figs. III.8, III.9), assuming the terrace is the same age throughout. Beach exposures alone indicate trends between NNW and SSW but offshore data (see below) provide more precise trends.

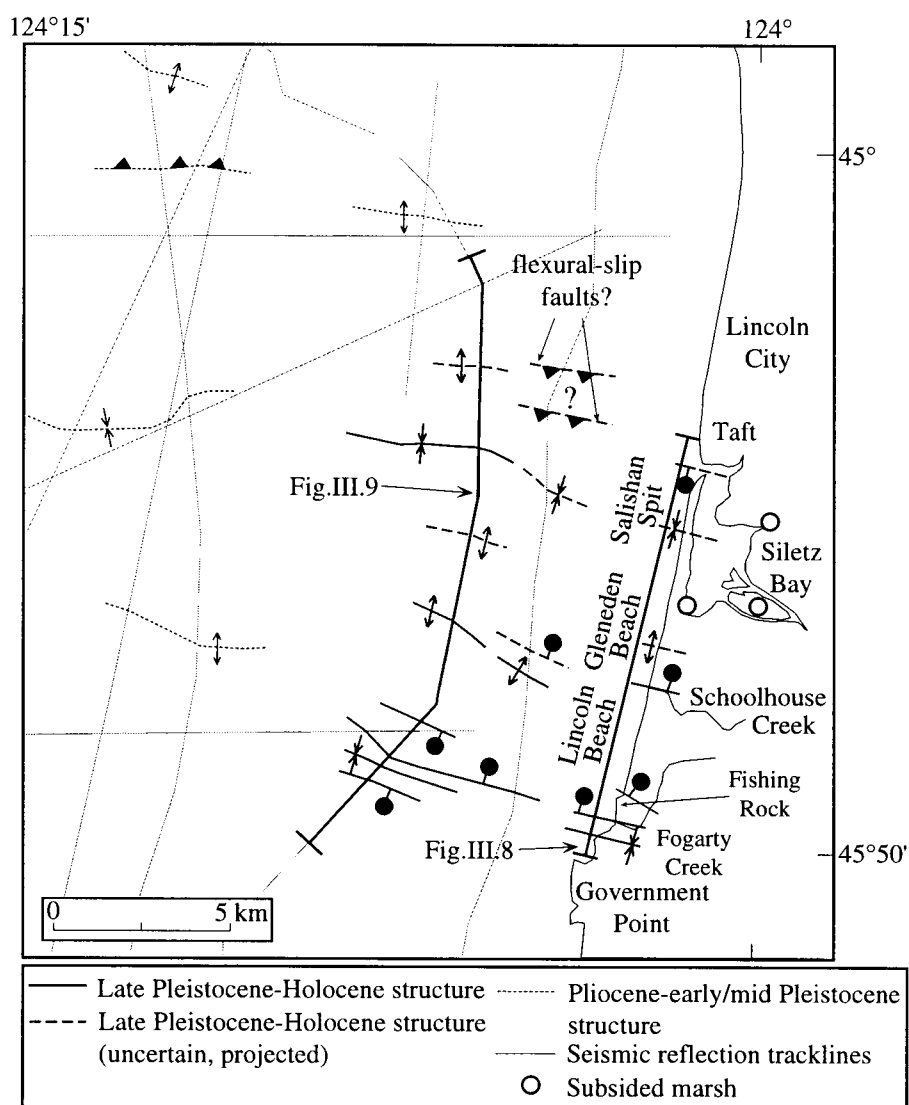


Figure III.8. Location map of Siletz Bay on the central Oregon coast showing structures mapped offshore from single channel and multichannel seismic reflection profiles and onshore from Pleistocene marine terrace deformation (structures in Fig. III.9 cross section). Bold line indicates position of single channel line in Fig. III.10. Onshore and offshore deformation suggests that Siletz Bay is structurally downwarped within a syncline or on the downthrown side of a fault. Generalised locations of subsided marshes after Darienzo et al. (1994). Orientations of onshore faults are poorly known.

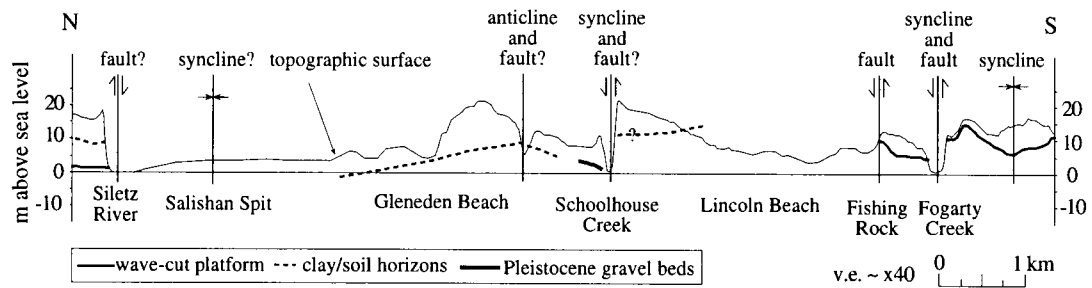


Figure III.9. Cross section of beach exposure of Pleistocene terrace sands underlying the youngest marine terrace at Siletz Bay. Marker horizons, including a clay horizon, gravel beds, and the wavecut platform were used to determine deformation of Pleistocene sediments and the location of Quaternary structures. The laterally-continuous clay horizon is apparently offset across the bay (up to the north). Faults also offset the wavecut platform at Fishing Rock and Fogarty Creek. The trends of these structures are poorly defined.

The clay horizon of the youngest terrace (80 ka) dips gently north between 5 km and 3 km south of the Siletz River mouth, where it is below beach level and projected below sea level (Fig. III.9). This clay horizon is exposed again ~10 m above sea level just north of the river mouth, where the wavecut platform is at ~2 m elevation (Fig. III.9). The platform is presumed below sea level south of the river, inferred from the elevation and dip of the clay horizon. Projection of the clay horizon below beach level suggests maximum fault offset across the Siletz River mouth of ~30 m, up to the north (offset could be a combination of folding and faulting). If this horizon is assumed to be the same age as the terrace (80 ka), this produces a late Quaternary vertical slip or subsidence rate relative to terrace levels across the river mouth of 0.4 mm/yr. This is a maximum slip rate as sediments underlying the terrace are somewhat older than 80 ka. Siletz Bay may lie in a Quaternary syncline controlled by a fault at the northern end of the bay, similar to the structure observed at Netarts Bay. Fault offset (downthrown to the north) of the Pleistocene wavecut platform and marine terrace was also documented at Fishing Rock and Fogarty Creek (Fig. III.8; Priest *et al.* 1994). Orientation of these two faults is poorly defined, but previously mapped faults onshore are oriented NW-SE and NE-SW. Poor exposure prevents the determination of any strike-slip component on onshore faults.

The possible correlative of a syncline at Siletz Bay is traced on N-S trending seismic reflection profiles 4-17 km offshore. Figure III.10 is a line drawing of a N-S single channel seismic profile 6 km west of Siletz Bay, which clearly shows synclinal deformation opposite the bay. The PM unconformity is truncated at the seafloor and therefore the age of the youngest strata is potentially late Miocene. The seafloor indicates no deformation, therefore offshore Quaternary deformation at this scale is unconfirmed. The trend of the syncline across several profiles is between E-W and ESE-WNW. Deformed synclinal sediments on middle to outer shelf profiles are truncated by the PM unconformity indicating little or no activity since the late Miocene or early Pliocene to the west, however, this unconformity is deformed by the southern bounding anticline which may project into the Gleneden Beach area. Possible onshore deformation of late Pleistocene marine terraces by the syncline suggests recent activity of these structures. Possible flexural-slip faults north of the river mouth (Fig. III.8) were poorly imaged in the single channel sparker profile and therefore have uncertain offset or dip. Faults with similar offset to those at Fishing Rock and Fogarty Creek (Fig. III.9), identified in single-channel sparker lines between 2 and 6 km offshore, may also be flexural-slip faults (Fig. III.10).

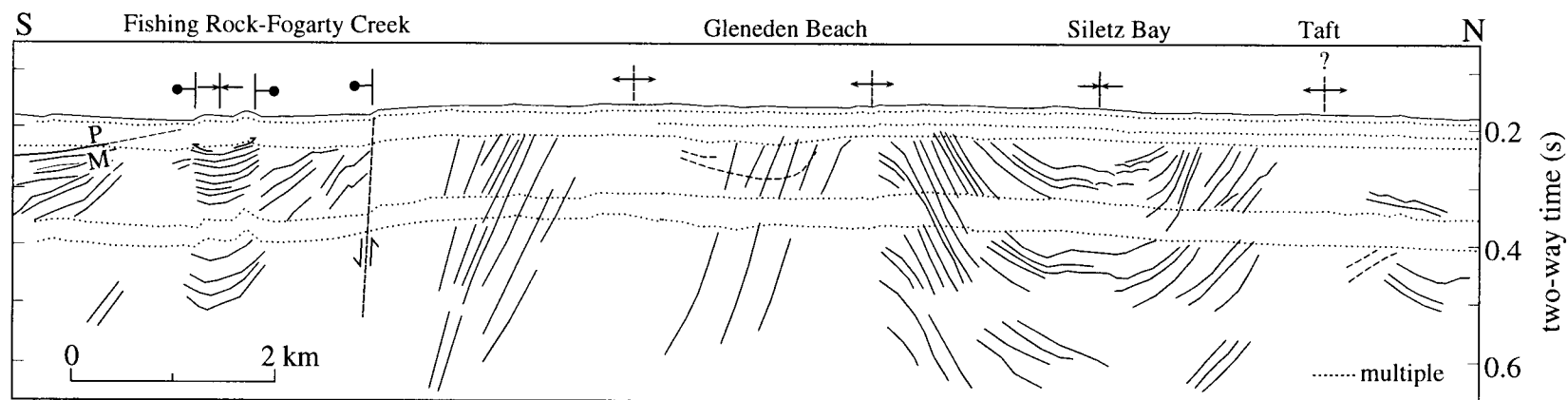


Figure III.10. Line drawing of N-S trending OSU single channel sparker profile, 6 km offshore Siletz Bay (bold line in Fig. III.8). The PM (late Miocene-early Pliocene) unconformity is projected to the seafloor at the southern end of the profile. Profile shows synclinal deformation of presumed Miocene strata off Siletz Bay, and seafloor offset by possible flexural-slip faults within an active synclinal fold west of Fishing Rock and Fogarty Creek. Fault dips and strikes are poorly constrained by seismic data.

III.6.2.6 Yaquina and Alsea Bays

A flight of uplifted Pleistocene marine terraces is preserved north and south of Yaquina Bay (Figs. III.1, III.11) on the central Oregon coast. These terraces have been differentiated by age using amino acid enantiomeric (D:L) ratios in conjunction with the palaeoecology of fossil shells (Kennedy, 1978; Kennedy *et al.*, 1982) and a soil chronosequence (Kelsey *et al.* 1996; Ticknor *et al.* 1992; Ticknor 1993). These techniques indicate offset of marine terraces on the inferred Yaquina Bay fault of 75 m down to the south (Ticknor 1993; Kelsey *et al.* 1996). The fault juxtaposes the 80 ka terrace (Qn) north of the bay against the 125 ka (Qy) terrace south of the bay (Fig. III.11; Kelsey *et al.* 1996). This offset yields a slip rate of 0.6 mm/yr. The continuation of the Yaquina Bay fault to the east was mapped by Snively *et al.* (1976), giving an ENE fault orientation (Kelsey *et al.* 1996). All core locations of buried Holocene marshes identified by Peterson & Priest (1995) are located on the south or downthrown side of the Yaquina Bay fault, although this could be due to a sampling bias.

Similar studies at Alsea Bay (Ticknor *et al.* 1992; Ticknor 1993; Kelsey *et al.* 1996) show that Quaternary faults strike generally N-S. The N-S striking Waldport fault zone vertically displaces terrace platforms down to the east (Fig. III.11), with cumulative offset apparently greatest at Alsea Bay, suggesting a structural origin for this embayment (Kelsey *et al.* 1996). All rapid subsidence sites are on the downthrown side of the Waldport fault zone.

Kelsey *et al.* (1996) conclude, from the evidence of Pleistocene terrace deformation, that both Yaquina and Alsea Bays are downwarped and structurally controlled by faults. Offshore data neither support or refute the onshore terrace evidence of deformation.

III.6.2.7 South Slough

Many active structures with N-S trends on the southern Oregon coast and shelf, where the deformation front is closer to the coastline, are interpreted to be part of accretionary prism-related deformation (Fig. III.12). One example is the South Slough syncline which deforms Quaternary sediments southwest of Coos Bay on the southern Oregon coast (Fig. III.12; Nelson 1987; Peterson & Darienzo 1989; McInelly & Kelsey 1990; Kelsey 1990) and may have produced multiple buried peats as a local structure

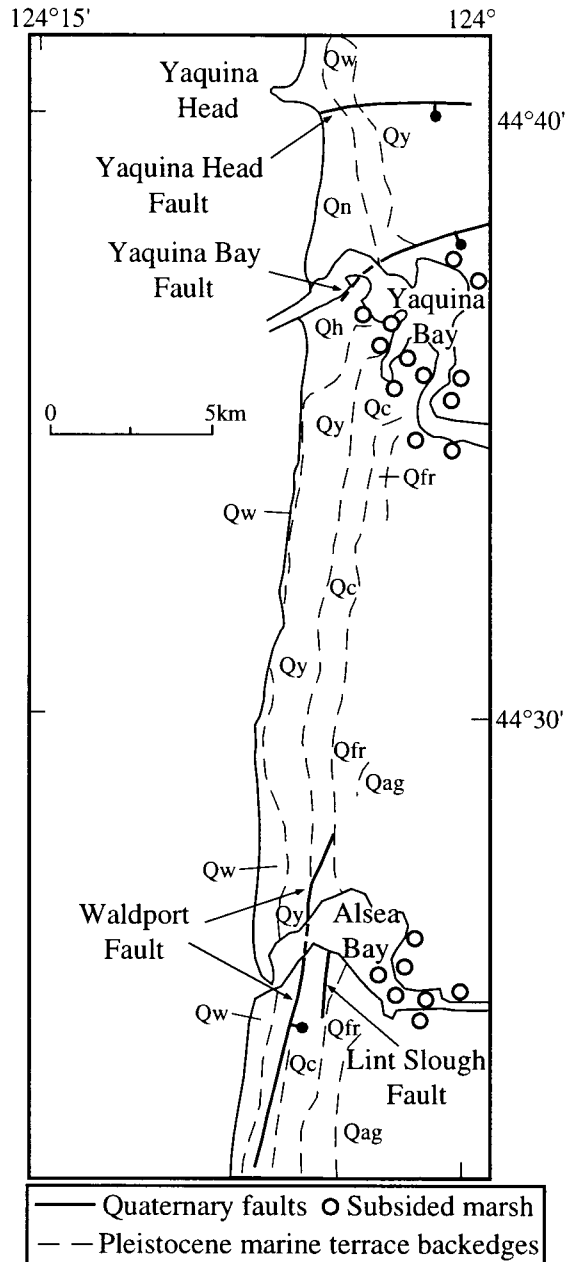


Figure III.11. Central coastal Oregon between Yaquina Head and Alsea Bay, showing late Pleistocene marine terrace backedges and Quaternary faulting (after Kelsey et al. 1996). The onshore Yaquina Bay fault (YBF) trends northeast and downdrops marine terraces to the south. The Waldport fault zone (including the Lint Slough fault) downdrop terraces to the east, with greatest offset at Alsea Bay. Marine terraces in order of increasing age based on palaeo-soil development chronology (Kelsey et al. 1996): Qn=Newport; Qw=Waconda; Qy=Yaquina; Qc=Crestview; Qfr=Fern Ridge; Qag=Alder Grove. Qh=Holocene beach and dune sands. White circles represent general subsided Holocene marsh locations (after Darienzo et al. 1994; Peterson & Priest 1995; Peterson & Darienzo 1996).

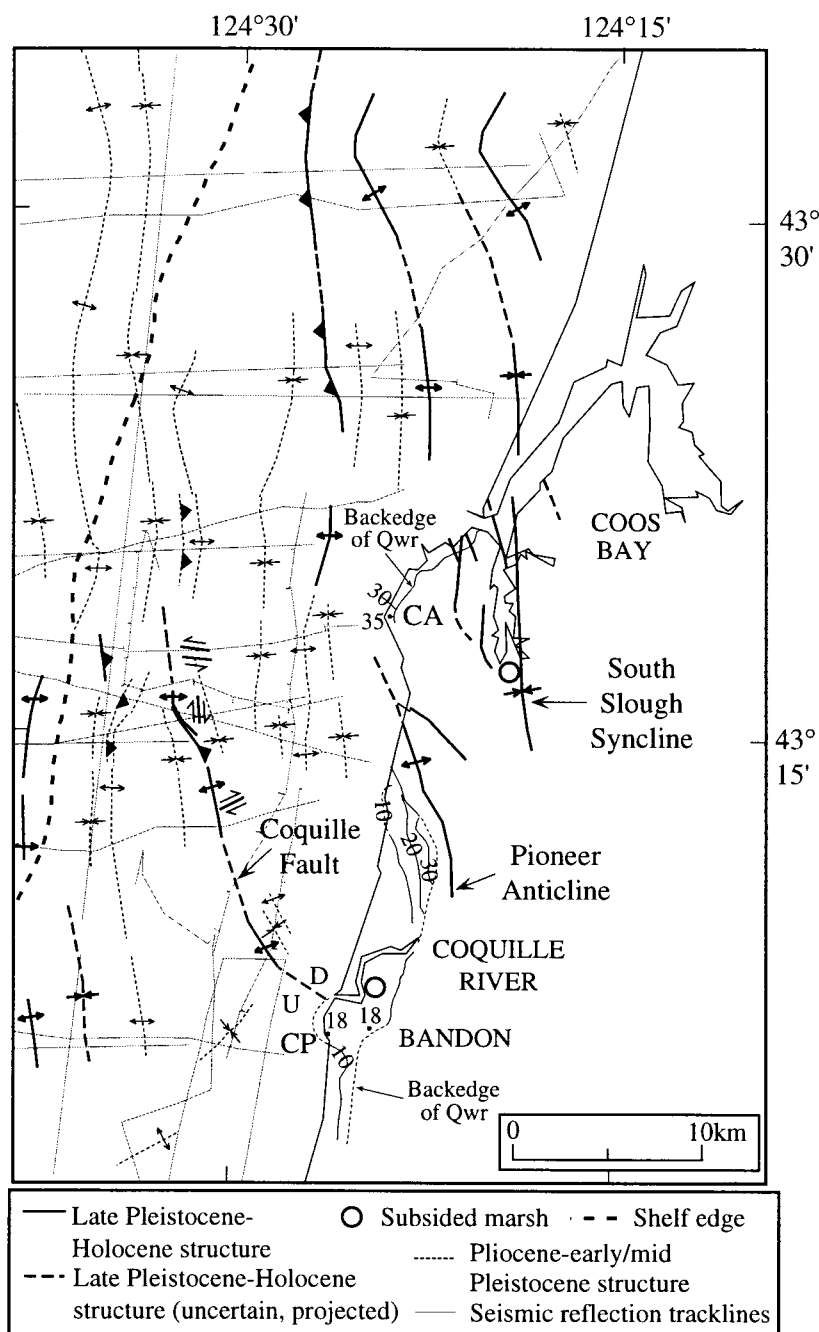


Figure III.12. Location map of the south-central Oregon coast and shelf showing Pliocene and Quaternary structures. Structures onshore based on deformed late Pleistocene terraces mapped by McInelly & Kelsey (1990) and Kelsey (1990). Offshore structures adapted from Goldfinger (1994), from seismic reflection and sidescan sonar data. Typical fractures and shears (with strike-slip offset) within Miocene and older sediments uplifted in the complex fault zone are also shown. Elevation contours of the Whisky Run wavecut platform (Qwr) shown in 10 m intervals (from McInelly & Kelsey 1990) indicate deformation by the Pioneer anticline and the Coquille fault. Coastal terrace altitudes are highest at Cape Arago (CA) and at Coquille Point (CP).

independent of elastic strain release during a subduction zone earthquake (e.g., Nelson & Personius 1996). The syncline has been traced onto the shelf on seismic reflection profiles (Fig. III.12; Goldfinger *et al.* 1992a; Goldfinger 1994). Both offshore and onshore deformation suggests that many faults are flexural-slip faults bounding active folds, such as the South Slough syncline, with fault slip parallel to bedding planes (McInelly & Kelsey 1990; Goldfinger 1994).

III.6.2.8 Coquille River

The Coquille fault (Fig. III.12; Clarke *et al.* 1985; Goldfinger 1994) comes onshore just south of the Coquille River mouth, where it deforms Pleistocene marine terraces (McInelly & Kelsey 1990). The Whisky Run (80 ka) platform descends from an altitude of 35 m at Cape Arago to sea level just north of the Coquille River, deformed by the Pioneer anticline (Fig. III.12; McInelly & Kelsey 1990). The terrace abruptly gains altitude to 18 m above sea level just south of the Coquille River at Coquille Point (Fig. III.12). This altitude change is accompanied by a change in dip of platforms from southwest north of the river to west or seaward south of the Coquille River (Fig. III.12; McInelly & Kelsey 1990). The Whisky Run platform is tilted slightly landward at Coquille Point, possibly resulting from deformation by the Coquille fault. The terrace elevation descends once again south of Coquille Point to reach sea level ~ 10 km to the south (McInelly & Kelsey 1990). Fold trends in Tertiary and Mesozoic formations underlying the Whisky Run wavecut platform vary similarly from north to south across the Coquille fault. North to south, fold trends are generally consistent with the variations in dip of the Pleistocene terraces and offshore Pleistocene fold and fault trends (Fig. III.12). No strike-slip offset or recent deformation could be determined on onshore faults in Jurassic to Eocene strata.

In seismic reflection profiles offshore, the fault zone appears as a ridge flanked by synclinal folding deforming the seafloor. Clarke *et al.* (1985) suggest the fault downdrops Pleistocene sediments to the northeast on the innermost shelf as observed in the deformed onshore marine terraces, but other seismic reflection data across the fault indicate a fairly symmetrical ridge.

III.6.2.9 Humboldt Bay

Two large thrust fault systems, the Little Salmon fault and the Mad River fault zone, deform Holocene sediments in the Humboldt Bay region of northern California (Fig. III.1), and are interpreted to be part of the onshore expression of the southern Cascadia accretionary prism (Clarke & Carver 1992). The Freshwater syncline lies between these two fault systems within Humboldt Bay and Mad River Slough, and has produced Holocene subsidence resulting in stacked buried marsh and forest horizons (Clarke & Carver 1992). The most recent subsidence event is dated at 250-300 radiocarbon yr. B.P., contemporaneous with the most recent event recorded throughout much of the subduction zone.

III.6.3 Locations with Inconclusive Evidence for Quaternary Subsidence

Other abrupt subsidence sites are characterized by inconclusive evidence or no evidence of Quaternary deformation, in the form of crustal downwarping. Marsh burials have been found in Neah Bay (Waatch River) and the Pysht River on the northernmost Olympic Peninsula (Fig. III.1; Atwater 1992). No active faults have been mapped and directly linked to evidence of rapid subsidence in Neah Bay. Buried marshes at Pysht River (Atwater 1992) lie on the downthrown side of a high-angle fault dashed through Tertiary formations (Gower 1960; Tabor & Cady 1978). This fault is mapped parallel to the river (NE), downthrown to the west, and projects offshore to a fault with similar trend in the Strait of Juan de Fuca which deforms an acoustic unit of Holocene age (Wagner and Tomson 1987). A second fault trends parallel to the coast (WNW) and projects into the bay. Buried marshes may lie on the upthrown side of this fault, but there is no evidence that it is recently active. High-resolution seismic profiles along the lower reaches of the Columbia River (Ryan & Stevenson 1995) indicate possible evidence of Quaternary faulting, including the NE-trending Fern Hill fault which offsets Miocene Astoria Formation onshore (Niem & Niem 1985). These faults have not yet been linked directly to locations of rapid marsh burial or liquefaction in the Columbia River (Atwater 1992; Atwater 1994; Obermeier 1995). Niem & Niem (1985) also map a WNW-trending syncline through Youngs Bay (Fig. III.1), south of Astoria, where a drowned forest and rapidly buried marshes have been identified (Peterson *et al.* 1997, C. Peterson, pers. comm., 1997). Quaternary deformation across this structure remains unproven. An older

syncline (deforming late Miocene and possibly Pliocene strata but with no conclusive evidence of Quaternary deformation) has been mapped on the outer shelf opposite Nestucca Bay (Fig. III.1). No evidence of Pleistocene deformation has been reported onshore, but it has been suggested that Cape Kiwanda, the headland to the north of the bay which is composed of Miocene Astoria Formation and Smugglers Cove Formation, may be a structural high (Parker 1990). Evidence of Quaternary downwarping at Vancouver Island sites, the Necanicum River, and Salmon River also remains inconclusive to judge from the available data.

III.6.4 Marsh Burial Located Near Structural Uplifts

Two possible exceptions to the hypothesis that buried marshes lie within tectonic downwarps are the Sixes River, southern Oregon, and the Copalis River, central Washington (Fig. III.1). Kelsey (1990) mapped an E-W trending anticline, which deforms Pleistocene terraces, just north of Cape Blanco and coincident with the lower reaches of the Sixes River (Fig. III.1). Buried marshes and tsunami sands have been identified on the southern limb of this anticline (Kelsey *et al.* 1993; Kelsey *et al.* 1998) in a cutoff meander of the Sixes River. Further examination of marshes in a N-S transect across the southern flank of the anticline may reveal differential subsidence (H. Kelsey, pers. comm., 1997). This apparent anomaly of local uplift and regional subsidence could be explained by subsidence being the net result of local uplift and regional subsidence, by the anticline not being triggered by every subduction zone earthquake, or by the fact that the anticline was active in the Pleistocene but not during the Holocene. A second possible exception is an ENE-trending ridge (Langley ridge) located 5 km south of the Copalis River. Deformation is interpreted as anticlinal folding and diffuse faulting above a possibly N-dipping blind thrust fault (McCrory 1996), with buried marshes at the Copalis River on the upthrown or north side of this fault. In addition to buried marshes, Atwater (1992) identified liquefaction evidence from 900-1300 years ago at Copalis River with no indication of accompanying tectonic subsidence. This event could be attributed to movement on a local crustal thrust fault such as that underlying Langley ridge. The dip of a blind fault is often difficult to determine from geomorphology and surface faulting, and this thrust fault may, in fact, dip to the south, with the Copalis River marshes lying on the downthrown side of a fault. Alternatively, a syncline to the north of this ridge may coincide with the Copalis River. This is supported by N-S single channel and multichannel seismic profiles which indicate a series of closely-spaced ~E-W trending ridges and intervening synclines on the

continental shelf. The Copalis River buried marshes may in fact lie within one of these synclines rather than being associated with the Langley Ridge structure 5 km to the south.

III.7 DISCUSSION

III.7.1 Implications for the Cascadia Subduction Zone Earthquake Record

The record of prehistoric subduction earthquakes on the Cascadia subduction zone, in the form of rapidly-buried marshes, documents sudden submergence, inundation of coastal lowlands, and burial of the former land surface. Correlation of coseismic events between coastal bays, based on radiocarbon ages and dendrochronology, has allowed rupture lengths, magnitudes, and recurrence intervals of prehistoric Cascadia earthquakes to be proposed (summarized by Atwater *et al.*, 1995). In addition, estimates of amounts of coastal subsidence can be used to approximate the position of the rupture zone and earthquake magnitude using elastic dislocation modeling. The possible non-tectonic origin of some submergence events should, however, be considered when assessing potential earthquake hazards.

In this study, it has been demonstrated that several abruptly-buried marsh locations can be linked to Pleistocene structures (synclines and downdropped side of faults) which produce downwarping. The influence of upper-plate crustal deformation on the prehistoric earthquake record may lead to inaccuracies in calculations of magnitudes and recurrence intervals if only based on the Holocene stratigraphy of coastal bays. Evidence of Quaternary deformation offshore is equivocal in some cases, but the use of offshore datasets and coastal exposures together has increased the probability of identifying recent activity. Only two possible examples of rapid subsidence coincident with crustal uplift were identified. However, these apparent anomalies could be explained by active upper plate structures not deforming during every subduction event.

III.7.1.1 Localized Upper Plate Deformation at Other Subduction Zones

Localized upper plate deformation has been documented at subduction margins worldwide, with deformation both synchronous with and independent of subduction zone

events. Examples include the Hikurangi margin of New Zealand (Berryman *et al.* 1989; Cashman and Kelsey 1990; Berryman 1993a, 1993b; Kelsey *et al.*, 1998), the Alaskan margin (Plafker 1972), the Nankai forearc of SW Japan (Sugiyama 1994; Maemoku 1988a, b; Maemoku & Tsubono 1990), and the Huon peninsula of Papua New Guinea (Pandolfi *et al.* 1994). Holocene terraces along the coastal Hikurangi margin off eastern North Island, New Zealand are uplifted by movement on steep reverse faults of the onshore accretionary prism (Berryman *et al.* 1989), with clustering of terrace ages along the coast. Stratigraphic and ecologic studies of Holocene terrace sediments on the Mahia Peninsula reveal that sedimentation was progradational between events, implying a lack of interseismic subsidence that would be expected with a subduction earthquake cycle and supporting the formation of Holocene coseismically uplifted terraces by local crustal structures (Berryman *et al.* 1997). Other earthquakes within the accretionary prism include the 1931 Hawkes Bay earthquake (Ms 7.8), caused by a fault cutting up from the megathrust (Hull 1990), and the 1855 Wairarapa earthquake, which may have originated on the megathrust and propagated into the upper plate along a blind thrust fault (Darby & Beanland 1992). In Alaska, significant deviations from the regional subsidence or uplift patterns during the 1964 earthquake (up to 12 m uplift across the Patton Bay fault on Montague Island, relative to a regional 2-4 m of uplift) were associated with movement on crustal faults contemporaneous with the subduction zone earthquake (Plafker 1969, 1972). Along the Nankai margin of Japan, two types of subduction earthquake have been inferred from coseismically-uplifted terraces (Fig. III.13; Sugiyama 1994). Subduction events where no permanent crustal deformation and therefore no uplifted terrace preservation occurred are known as Taisho type events (T, Fig. III.13). Preserved uplifted terraces resulting from the triggering of crustal deformation are known as Genroku type events (G, Fig. III.13).

III.7.1.2 Effects of Local Crustal Deformation on Subsidence Records

Recorded coseismic subsidence is the net result of regional elastic strain release from a subduction zone earthquake and local crustal deformation (permanent and/or elastic), assuming a tectonic origin for subsidence. For each event, subsidence could result from strain release on the plate boundary, on local structures, or a combination of the two. The contributions of each cannot be determined for prehistoric events, although the amount and pattern of subsidence at each location may suggest a particular mechanism. The

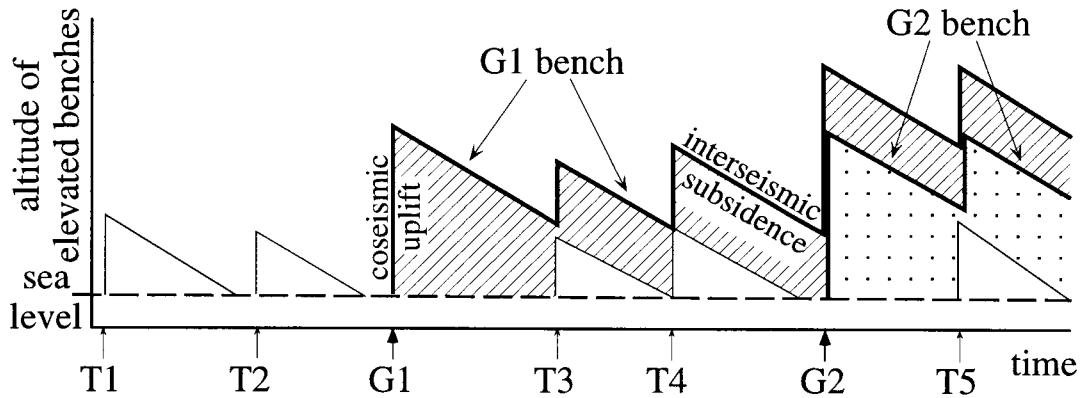


Figure III.13. Illustration of the resulting record of Taisho and Genroku subduction earthquakes on the Nankai margin (after Sugiyama 1994). No permanent inelastic crustal deformation occurs during Taisho events (T1-5); coseismic deformation is recovered in the interseismic period leaving no permanent record of the earthquake. Genroku events (G1, G2) involve local faulting or other inelastic crustal deformation leading to preservation of an uplifted bench. Note: the coseismic and interseismic vertical motions are opposite to those expected on much of the Cascadia coastline.

apparent rupture length (and hence magnitude), amount of subsidence, and timing of coseismic events can be specifically affected in the following ways:

- (1) Triggering of local crustal faults beyond (along strike) the subduction rupture zone, as the release of the elastic load on the upper plate in one area causes loading in other areas, thereby increasing the apparent rupture length and magnitude (e.g., LS2 and SZE1 in Fig. III.14). Similar patterns occurred during the Landers earthquake, where a sequence of delayed ruptures occurred within the fault zone (Sieh *et al.* 1993; Wald & Heaton 1994; Spotila & Sieh 1995), and more distant earthquakes were also triggered following the mainshock (Hill *et al.* 1993), although these events lacked surface rupture and geodetic change.
- (2) The amount of subsidence per event at each location is dependent not only on the magnitude of the subduction zone earthquake and position of the rupture zone, but also on the amount of localized upper plate deformation accompanying the earthquake. The amount of subsidence during a given earthquake cannot be used for elastic dislocation modeling of the locked zone.
- (3) Local crustal faults may move independently of subduction zone earthquakes and produce anomalous local coseismic subsidence and marsh burial (LS1 of Fig. III.14). Correlation of subsidence events from site to site is dependent on age control with sufficient precision to distinguish such events. The majority of radiocarbon ages from marsh burials have large error bars, of the order of ± 50 years to hundreds of years (e.g., Atwater 1992; Atwater *et al.* 1995), with errors often larger than the suggested recurrence intervals. More recently, AMS and high precision radiocarbon and dendrochronology ages in some locations have significantly reduced errors to ± 10 -20 years or even to within a year or season (Nelson *et al.* 1995; Yamaguchi *et al.* 1997; Jacoby *et al.* 1997), but suitable material for such precise dating techniques is often unavailable (Nelson *et al.* 1996b). The most abundant high precision data are available for the most recent subsidence event, which is dated within a few decades of 1700 A.D., and is consistent with evidence for a remote tsunami in Japan at that time (Satake *et al.* 1996). Older events are less accurately dated. Where error bars are large, it is impossible to distinguish between regional subsidence events and locally anomalous events which may have resulted from independent deformation on crustal structures. These anomalous events may be incorrectly correlated with regional coseismic subsidence events (Fig.III.14), producing an inaccurate picture of the earthquake rupture zone. In addition, subduction earthquake recurrence intervals may be underestimated if independent local subsidence events contribute to the marsh stratigraphy.

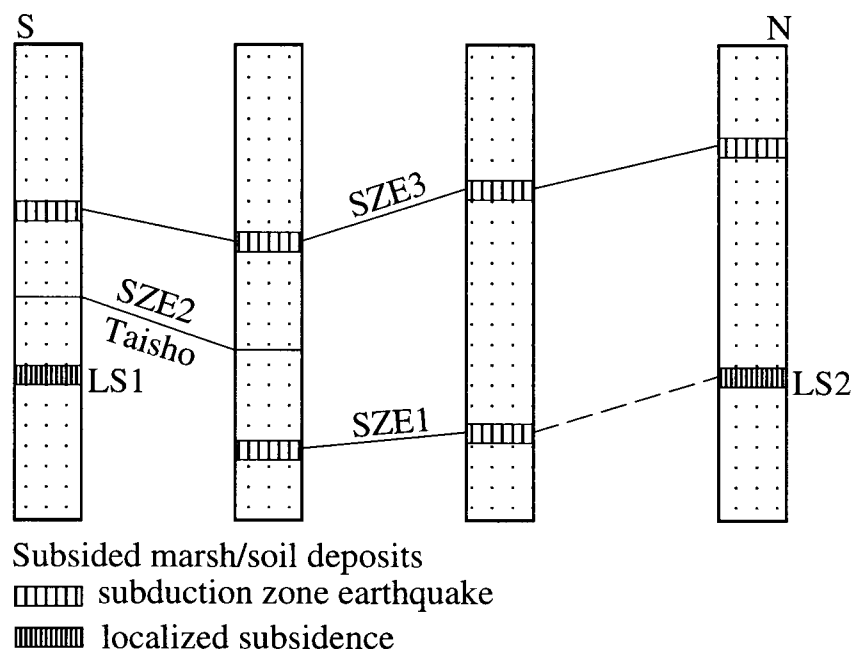


Figure III.14. Coastal marsh stratigraphy in hypothetical cores showing subsided marsh and soil deposits produced by a variety of coseismic events. LS, localized subsidence; SZE, subduction zone earthquake. SZE1 represents a small subduction earthquake which triggers localised subsidence to the north, increasing the apparent rupture length. SZE2 (Taisho type) does not trigger inelastic deformation and does not preserve coseismic subsidence. SZE3 is a widespread subduction event with subsidence at all four locations. This earthquake may also trigger local structures which may contribute to subsidence and help preserve the buried soils (Genroku type).

III.7.1.3 Synchronous vs. Independent Movement of Local Structures and Subduction Earthquakes

It is unknown, in the absence of historic subduction zone earthquakes and little upper plate seismicity, whether local crustal structures in Cascadia are triggered by subduction zone earthquakes, operate independently, or both. If movement on crustal structures is always synchronous with and triggered by subduction events, estimates of the subduction earthquake recurrence interval will be unaffected but magnitude calculations may be inaccurate. If these structures operate independently, deforming both during and between subduction events, both the magnitude and recurrence interval of subduction zone events will be affected.

If patterns of strain release are similar to those of the Alaskan and Nankai subduction zones, we might expect crustal structures to be triggered by slip on the megathrust (Plafker 1969, 1972; Sugiyama 1994). Minimal historic seismicity in the coastal and shelf region supports the hypothesis that these structures are predominantly triggered by subduction zone earthquakes, which also lack seismicity. Buried marshes similar in age to regional subsidence events have been attributed to upper plate structures in South Slough, southern Oregon coast, and Humboldt Bay, northern California coast, with little visible evidence of significant rapid subsidence in other bays in this region, such as the Siuslaw River (Nelson 1992; Nelson *et al.* 1996a; Nelson & Personius 1996; Clarke & Carver 1992). If rapid subsidence is not regionally extensive, these are examples of crustal structures that were triggered by subduction zone events. Regional subsidence in this area may be small and only detectable by biostratigraphic investigations (compare with Mathewes & Clague 1994), and pronounced sudden subsidence may only be recorded where local structures were triggered. Most upper plate structures are likely to have longer recurrence intervals than subduction zone earthquakes and may not be triggered by every subduction event.

Local structures may also produce tectonic subsidence independently of subduction events. Independent coseismic subsidence has been suggested as a likely cause of marsh burials on the southern Oregon and northern California coasts (Nelson 1992; Nelson & Personius 1996).

III.7.1.4 Preservation of Buried Marshes

The sequence of Cascadia buried marshes indicates net submergence of the land or net relative sea level rise of 2-5 m in the last 2000-4000 years (e.g., Atwater & Hemphill-Haley, 1996). If the earthquake strain cycle were completely elastic and no other factors were involved, coseismic subsidence and interseismic uplift would cancel out and no buried marshes would be preserved. This argument is used for the Nankai subduction zone, where coseismically-uplifted terraces are only preserved permanently when synchronous upper plate uplift occurs (Sugiyama 1994). If similar patterns of deformation to those at Nankai occur along the Cascadia subduction zone, permanent deformation by local structures may help to preserve marsh burial. Not all subduction zone earthquakes would be recorded (e.g., SZE2 in Fig. III.14) and subduction zone earthquakes would appear to be less frequent with longer recurrence intervals.

One major difference between the Nankai and Cascadia coastlines is the sense of elastic coseismic motion: Nankai experiences uplift whereas Cascadia experiences subsidence. Therefore, preservation of buried marshes in Cascadia may also be influenced by the following non-tectonic factors, producing relative sea level rise: (1) late Holocene eustatic sea level rise, (2) isostatic forebulge collapse following the last glacial maximum, (3) compaction, or (4) changes in the geometry of coastal estuaries (this could cause relative sea level rise or fall). These factors would not contribute to the preservation of uplifted terraces in Nankai, unless sea level was falling in the late Holocene, or this region experienced some form of isostatic uplift. Buried marsh preservation in Cascadia could also be attributed to regional tectonic subsidence resulting from, for example, subduction erosion. The rates and effects of these factors in the late Holocene are poorly known and therefore their contributions to the preservation of buried marshes can only be approximated. The rate of late Holocene global eustatic sea level rise is intensely debated, with some estimates pointing to negligible rise during the last 5000 years (P. Clark, R. Peltier, pers. comm., 1997), very low rates (Bard *et al.* 1996; Clark and Lingle 1979), or a value which is currently very difficult to separate from local and regional factors, including isostatic and tectonic factors, which dominate relative sea level rise (Bloom & Yonekura 1990; Nelson *et al.* 1996b). Estimates of forebulge collapse on much of the Cascadia margin associated with isostatic re-equilibration following the last glacial maximum (LGM) are given by the models of Peltier (1996). Subsidence rates (or relative sea level rise) for much of the Washington and Oregon coastline are estimated as 0-1 mm/yr. with a maximum on the northern Oregon coast (M2 model of Peltier 1996). However, the northern Olympic Peninsula and Vancouver Island, which underlay the Cordilleran ice

sheet during the LGM, should be experiencing isostatic rebound. Tectonic subsidence may indeed dominate the preservation of buried marshes, but until other variables are better resolved, this hypothesis remains untested.

III.7.1.5 Quantitative Subsidence Calculations

In general, subsidence patterns measured along the Cascadia subduction zone appear to be fairly consistent, with subsidence of 0.5-2 m for each burial event. Very large differences in the amount of subsidence per event, which might indicate localized subsidence contributions, have not been observed, as pointed out by Clague (1997). The large deviation in uplift magnitude recorded across the Patton Bay fault in Alaska, is not observed in subsidence on the Cascadia margin. However, the Patton Bay fault, within the coseismically uplifted zone, is within the accretionary prism and close to the deformation front, and therefore might be expected to experience more pronounced deformation. Measurements of Cascadia subsidence are invariably imprecise because biostratigraphic markers such as diatoms and plant assemblages have large vertical water depth ranges, but fairly large differences in subsidence can be detected (Atwater & Hemphill-Haley 1996). Small variations in measured subsidence through careful lithostratigraphic and biostratigraphic studies, such as those of Long and Shennan (1994), Nelson *et al.* (1996b), and Shennan *et al.* (1996), may eventually allow the contribution of local structures to the subsidence record to be determined.

The estuarine stratigraphy at many Cascadia sites is strikingly similar to that observed at passive margin sites (Long & Shennan 1994), where a coseismic origin is unlikely. Some Cascadia subsidence events may therefore have non-seismic origins such as natural succession of intertidal environments from local changes in sea level, sedimentation rates, and ocean currents (Long & Shennan 1994; Nelson *et al.* 1996a; Nelson *et al.* 1996b).

III.7.2 N-S Compression

Most active structures on the inner shelf and coast in the Cascadia subduction zone are characterized by ~ E-W trends, in contrast to the predominantly N-S to NW-SE trends which result from plate convergence on the continental slope. We agree with Snively

(1987), Goldfinger *et al.* (1992b), and Wells *et al.* (1998) that this landward region of the forearc is under N-S compression, which is in agreement with regional N-S compression throughout the continental northwestern U.S. derived from late Tertiary upper-plate fault orientations, earthquake focal mechanisms, and borehole breakouts (Werner *et al.* 1990; Zoback and Zoback 1989). The regional N-S compressional stress field extends onto the middle to outer shelf in Washington and much of Oregon. In contrast, the southern Oregon and northern California shelf and coastal region are within the active accretionary prism, and deformation is in response to plate convergence leading to structures with N-S to NW-SE trends. Wang *et al.* (1995) suggest that the NE-directed strain accumulation due to plate convergence can be considered a time-dependent local perturbation superimposed on the regional N-S compressive stress field, and thus the regional stress field and cyclic loading may coexist. The transition from regional N-S compression to predominantly plate-convergence driven compression represents a significant structural domain boundary. This transition may act as a backstop and may be related to the long-term average position of the downdip end of the seismogenic locked zone. Despite the apparent independence of upper-plate structures from subduction zone deformation, it seems likely that these structures could be triggered by rupture of the subduction zone. Independent fault movement in response to regional compression is also possible and therefore these structures pose independent seismic hazards.

III.8 CONCLUSIONS

Evidence of deformation on the Cascadia inner shelf is widespread with Pleistocene crustal downwarping or fault offset coincident with many coastal lowlands. Rapidly buried marshes at these locations may be due to elastic strain release on the subduction megathrust, downwarping or fault displacement on upper plate crustal structures, or both. Calculations of Cascadia subduction zone earthquake recurrence intervals, rupture zones, and magnitudes based on correlations of marsh burial events between sites may be complicated by the possibility of localized crustal fault movements and fold growth, in addition to non-seismic origins of the observed stratigraphy. The earthquake record is likely to be more difficult to resolve with the interaction of these multiple factors (Fig. III.14). Prehistoric subduction zone earthquakes may have been of lower magnitude than previously estimated. Recurrence intervals for such earthquakes may be overestimated, if some events are not preserved due to little permanent deformation, or underestimated, if anomalous local subsidence events are wrongly linked to similar-age regional events along

the margin. Higher resolution records of marsh chronology and estimates of subsidence, and an improved chronology of coastal fault movement may eventually lead to the separation of regional and local factors. Meanwhile, the use of these records for modeling of the subduction earthquake cycle and prediction of prehistoric earthquake rupture zones should be undertaken with caution. The inner shelf and coastal structures are consistent with the regional N-S compressional stress field and inconsistent with subduction-driven compression. Despite low seismicity, these crustal faults may be seismic and pose significant shaking and ground deformation hazards to the coastal communities.

III.9 ACKNOWLEDGMENTS

We acknowledge the Minerals Management Service Pacific OCS Region at Camarillo, California for supplying data used in this study. We thank the crews of the Jolly Roger and Cavalier, DELTA submersible pilots, Williamson and Associates of Seattle, Washington for sidescan sonar operations, and the scientific crews of the 1992-1995 research cruises. We also thank two anonymous reviewers for their helpful comments and suggestions. LCM wishes to thank B. Atwater, P. Clark, E. Clifton, H. Kelsey, P. McCrory, A. Niem, S. Obermeier, R. Peltier, C. Peterson, G. Priest, and I. Shennan for helpful discussions, however, the interpretations and conclusions of this paper are entirely the responsibility of the authors. This study was supported by NOAA Undersea Research Program at the West Coast National Undersea Research Center, University of Alaska grants UAF-92-0061 and UAF-93-0035, National Science Foundation grants OCE-8812731 and OCE-9216880, and U.S. Geological Survey National Earthquake Hazards Reduction Program awards 14-08-0001-G1800, 1434-93-G-2319, 1434-93-G-2489, and 1434-95-G-2635.

III.10 REFERENCES

ADAMS, J. 1990. Paleoseismicity of the Cascadia subduction zone: Evidence from turbidites off the Oregon-Washington Margin. *Tectonics*, **9**, 569-584.

ANDO, M. & BALAZS, E.I. 1979. Geodetic evidence for aseismic subduction of the Juan de Fuca plate. *Journal of Geophysical Research*, **84**, 3023-3027.

ATWATER, B.F. 1987. Evidence for great Holocene earthquakes along the outer coast of Washington State. *Science*, **236**, 942-944.

— 1992. Geologic evidence for earthquakes during the past 2000 years along the Copalis River, southern coastal Washington. *Journal of Geophysical Research*, **97**, 1901-1919.

— (compiler) 1994. *Geology of liquefaction features about 300 years old along the lower Columbia River at Marsh, Brush, Price, Hunting, and Wallace Islands, Oregon and Washington*. U.S. Geological Survey Open-File Report, **94-209**, 64 pp.

— & HEMPHILL-HALEY, E. 1996. *Preliminary estimates of recurrence intervals for great earthquakes of the past 3500 years at northeastern Willapa Bay, Washington*. U.S. Geological Survey Open-File Report, **96-001**, 88 pp.

— & YAMAGUCHI, D.K. 1991. Sudden, probably coseismic submergence of Holocene trees and grass in coastal Washington state. *Geology*, **19**, 706-709.

—, NELSON, A.R., CLAGUE, J.J., CARVER, G.A., YAMAGUCHI, D.K., BOBROWSKY, P.T., BOURGEOIS, J., DARIENZO, M.E., GRANT, W.C., HEMPHILL-HALEY, E., KELSEY, H.M., JACOBY, G.C., NISHENKO, S.P., PALMER, S.P., PETERSON, C.D., & REINHART, M.A. 1995. Summary Of coastal geologic evidence for past great earthquakes at the Cascadia subduction zone. *Earthquake Spectra*, **11**, 1-18.

BARD, E., HAMELIN, B., ARNOLD, M., MOTAGGIONI, L., CABIOCH, G., FAURE, G., & ROUGERIE, F. 1996. Deglacial sea-level record from Tahiti corals and the timing of global meltwater discharge. *Nature*, **382**, 241-244.

BARNETT, E.T. 1997. *Potential for coastal flooding due to coseismic subsidence in the central Cascadia margin*. M.S. Thesis, Portland State University, Portland, 144 pp.

BERRYMAN, K.R., 1993a. Age, height, and deformation of Holocene marine terraces at Mahia Peninsula, Hikurangi subduction margin, New Zealand. *Tectonics*, **12**, 1347-1364.

— 1993b. Distribution, age, and deformation of late Pleistocene marine terraces at Mahia Peninsula, Hikurangi subduction margin, New Zealand. *Tectonics*, **12**, 1365-1379.

—, BEU, A., & IRWIN, S. 1997. A high resolution model for the formation of a coseismic Holocene marine terrace sequence. *INQUA Commission on Neotectonics, Late Quaternary Coastal Tectonics Abstracts*, pp. 8 (abst.).

—, OTA, Y., & HULL, A.G. 1989. Holocene paleoseismicity in the fold and thrust belt of the Hikurangi subduction zone, eastern North Island, New Zealand. *Tectonophysics*, **163**, 185-195.

BLOOM, A.L., & YONEKURA, N. 1990. Graphic analysis of dislocated shorelines. In: NATIONAL RESEARCH COUNCIL (ed.), *Studies in Geophysics: Sea-Level Change*. National Academy Press, Washington, D.C., 104-115.

CASHMAN, S.M., & KELSEY, H.M. 1990. Forearc uplift and extension, southern Hawke's Bay, New Zealand: Mid-Pleistocene to present. *Tectonics*, **9**, 23-44.

CLAGUE, J.J. 1997. Evidence for large earthquakes at the Cascadia subduction zone. *Reviews of Geophysics*, **35**, 439-460.

CLARK, J.A., & LINGLE, C.S. 1979. Predicted relative sea level changes (18,000 B.P. to present) caused by late-glacial retreat of the Antarctic ice sheet. *Quaternary Research*, **11**, 279-298.

CLARKE, S.H., JR. 1990. *Map showing geologic structures of the northern California continental margin*. U.S. Geological Survey, Map **MF-2130**, scale 1:250 000.

— 1992. Geology of the Eel River Basin and adjacent region: Implications for late Cenozoic tectonics of the southern Cascadia subduction zone and Mendocino triple junction. *American Association of Petroleum Geologists Bulletin*, **76**, 199-224.

—, & CARVER, G.A. 1992. Late Holocene tectonics and paleoseismicity, southern Cascadia subduction zone. *Science*, **255**, 188-192.

—, FIELD, M.E., & HIROZAWA, C.A. 1985. Reconnaissance geology and geologic hazards of the offshore Coos Bay Basin, Oregon. *U.S. Geological Survey Bulletin*, **1645**, 41 pp.

CLIFTON, H.E. 1983. Discrimination between subtidal and intertidal facies in Pleistocene deposits, Willapa Bay, Washington. *Journal of Sedimentary Petrology*, **53**, 353-369.

— 1994. *Transgressive and early highstand system tracts: Pleistocene terrace deposits, Willapa Bay, Washington*. Field guide prepared in conjunction with an Society of Economic and Petroleum Geologists Research Conference, Clastic Deposits of the Transgressive Systems Tract: Facies, Stratigraphy and Reservoir Character, 70 pp.

COOPER, D.M. 1981. *Sedimentation, stratigraphy and facies variations of the lower to middle Miocene Astoria Formation in Oregon*. Ph.D. thesis, Oregon State University, Corvallis, 534 pp.

CROSSON, R.S., & OWENS, T.J. 1987. Slab geometry of the Cascadia subduction zone beneath Washington from earthquake hypocenters and teleseismic converted waves. *Geophysical Research Letters*, **14**, 824-827.

DARBY, D., & BEANLAND, S. 1992. Possible source models for the 1855 Wairarapa earthquake, New Zealand. *Journal of Geophysical Research*, **97**, 12 375-12 389.

DARIENZO, M.E., & PETERSON, C.D. 1990. Episodic tectonic subsidence of late Holocene salt marshes, northern Oregon central Cascadia margin. *Tectonics*, **9**, 1-22.

—, —, & CLOUGH, C., 1994. Stratigraphic evidence for great subduction-zone earthquakes at four estuaries in northern Oregon, U.S.A. *Journal of Coastal Research*, **10**, 850-876.

DEMETS, C., GORDON, R.G., ARGUS, D.F., & STEIN, S. 1990. Current plate motions. *Geophysical Journal International*, **101**, 425-478.

GOLDFINGER, C. 1994. *Active deformation of the Cascadia forearc: Implications for great earthquake potential in Oregon and Washington*. Ph.D. Thesis, Oregon State University, Corvallis, 202 pp.

—, KULM, L.D., & YEATS, R.S. 1992a. *Neotectonic map of the Oregon continental margin and adjacent abyssal plain*. Oregon Department of Geology and Mineral Industries, Open-File Report, **O-92-4**, scale 1:500 000.

—, —, —, APPELGATE, B., MACKAY, M., & COCHRANE, G.R. 1996. Active strike-slip faulting and folding of the Cascadia plate boundary and forearc in central and northern Oregon. In: ROGERS, A. M., WALSH, T. J., KOCKELMAN, W. J., & PRIEST, G. (eds) *Assessing and reducing earthquake hazards in the Pacific Northwest*. U.S. Geological Survey, Professional Paper, **1560**, pp. 223-256.

—, —, —, —, —, & MOORE, G.F. 1992b. Transverse structural trends along the Oregon convergent margin: implications for Cascadia earthquake potential. *Geology*, **20**, 141-144.

—, —, —, McNEILL, L.C., & HUMMON, C. 1997a. Oblique strike-slip faulting of the central Cascadia submarine forearc. *Journal of Geophysical Research*, **102**, 8217-8243.

—, McNEILL, L.C., & HUMMON, C. 1997b. Case study of GIS data integration and visualization in submarine tectonic investigations: Cascadia subduction zone. *Marine Geodesy*, **20**, 267-289.

GRIM, M.S., & BENNETT, L.C., Jr., 1969. Shallow seismic profiling of the continental shelf off Grays Harbor, Washington. *University of Washington Department of Oceanography Special Report*, **41**, 72-92.

GOWER, H.D. 1960. *Geologic map of the Pysht quadrangle, Washington*. U.S. Geological Survey Geologic Quadrangle Map, **GQ-129**, scale 1:62 500.

HEATON, T.H., & KANAMORI, H. 1984. Seismic potential associated with subduction in the northwestern United states. *Bulletin of the Seismological Society of America*, **74**, 993-941.

HILL, D.P., & 30 others 1993. Seismicity remotely triggered by the magnitude 7.3 Landers, California earthquake. *Science*, **260**, 1617-1623.

HULL, A.G. 1990. Tectonics of the 1931 Hawke's Bay earthquake. *New Zealand Journal of Geology and Geophysics*, **33**, 309-330.

JACOBY, G.C., BUNKER, D.E., & BENSON, B.E. 1997. Tree-ring evidence for an A.D. 1700 Cascadia earthquake in Washington and northern Oregon. *Nature*, **25**, 999-1002.

KELSEY, H.M. 1990. Late Quaternary deformation of marine terraces on the Cascadia subduction zone near Cape Blanco, Oregon. *Tectonics*, **9**, 983-1014.

—, TICKNOR, R.L., BOCKHEIM, J.G., & MITCHELL, C.E. 1996. Quaternary upper plate deformation in coastal Oregon. *Geological Society of America Bulletin*, **108**, 843-860.

—, WITTER, R.C., & POLENZ, M. 1993. Cascadia paleoseismic record derived from late Holocene fluvial and lake sediments, Sixes River Valley, Cape Blanco, south coastal Oregon. *Eos*, **74**, 199 (abst.).

—, —, & HEMPHILL-HALEY, E. 1998. Response of a small Oregon estuary to coseismic subsidence and postseismic uplift in the past 300 years. *Geology*, **26**, 231-234.

KENNEDY, G.L. 1978. *Pleistocene paleoecology, zoogeography and geochronology of marine invertebrate faunas of the Pacific Northwest coast (San Francisco Bay to Puget Sound)*. Ph.D. Thesis, University of California, Davis, 824 pp.

—, LAJOIE, K.R., & WEHMILLER, J.F. 1982. Aminostratigraphy and faunal correlations of late Quaternary marine terraces, Pacific Coast, USA. *Nature*, **299**, 545-547.

KULM, L.D., & SUESS, E. 1990. Relation of carbonate deposits and fluid venting: Oregon accretionary prism. *Journal of Geophysical Research*, **95**, 8899-8915.

KVENVOLDEN, K.A., BLUNT, D.J., & CLIFTON, H.E. 1979. Amino-acid racemization in Quaternary shell deposits at Willapa Bay, Washington. *Geochimica et Cosmochimica Acta*, **43**, 1505-1520.

LONG, A.J., & SHENNAN, I. 1994. Sea-level changes in Washington and Oregon and the "earthquake deformation cycle". *Journal of Coastal Research*, **10**, 825-838.

LUDWIN, R.S., WEAVER, C.S., & CROSSON, R.S. 1991. Seismicity of Washington and Oregon. In: SLEMMONS, D. B., ENGDAHL, E. R., BLACKWELL, D., & SCHWARTZ, D. (eds) *Neotectonics of North America*. Geological Society of America, DNAG CSMV-1, Boulder, Colorado, pp. 77-98.

MAEMOKU, H. 1988a. Holocene crustal movement in Muroto Peninsula, southwest Japan. *Geographical Review of Japan* *61 (Ser. A)*, **10**, 747-769.

— 1988b. Holocene crustal movement around Cape Ashizuri, southwest Japan. *Geographical Sciences*, **43**, 231-240.

—, & TSUBONO, K. 1990. Holocene crustal movements in the southern part of Kii Peninsula, outer zone of southwest Japan. *Journal of Geography*, **99**, 349-369.

MATHEWES, R.W., & CLAGUE, J.J. 1994. Detection of Large Prehistoric Earthquakes in the Pacific Northwest by Microfossil Analysis. *Science*, **264**, 688-691.

McCAFFREY, R., & GOLDFINGER, C. 1995. Forearc deformation and great subduction earthquakes: Implications for Cascadia earthquake potential. *Science*, **267**, 856-859.

McCRORY, P.A. 1996. Tectonic model explaining divergent contraction directions along the Cascadia subduction margin, Washington. *Geology*, **24**, 929-932.

McINELLY, G.W., & KELSEY, H.M. 1990. Late Quaternary tectonic deformation in the Cape Arago-Bandon region of coastal Oregon as deduced from wave cut platforms. *Journal of Geophysical Research*, **95**, 6699-6713.

MCNEILL, L.C., GOLDFINGER, C., KULM, L.D., & YEATS, R.S., 1993. Deformation of Quaternary marine terraces in the Siletz Bay region of central Oregon. *Proceedings of the Oregon Academy of Sciences*, **30**, 38 (abst.).

—, PIPER, K.A., GOLDFINGER, C., KULM, L.D., & YEATS, R.S. 1997. Listric normal faulting on the Cascadia continental shelf. *Journal of Geophysical Research*, **102**, 12 123-12 138.

NELSON, A.R. 1987. Apparent gradual rise in relative sea level on the south-central Oregon coast during the late Holocene--Implications for the great Cascadia earthquake hypothesis. *Eos*, **68**, 1240 (abst.).

— 1992. Holocene tidal-marsh stratigraphy in South-Central Oregon - Evidence for localized sudden submergence in the Cascadia subduction zone. In: Fletcher, C. H., & Wehmiller, J. F. (eds) *Quaternary Coasts of the United States: Marine and Lacustrine Systems*. Society for Sedimentary Geology Special Publication, **48**, 287-301.

—, & PERSONIUS, S.F. 1996. Great-earthquake potential in Oregon and Washington - an overview of recent coastal geologic studies and their bearing on segmentation of Holocene ruptures, central Cascadia subduction zone. In: ROGERS, A. M., WALSH, T. J., KOCKELMAN, W. J., & PRIEST, G. (eds) *Assessing and reducing earthquake hazards in the Pacific Northwest*. U.S. Geological Survey Professional Paper, **1560**, pp. 91-114.

—, ATWATER, B.F., BROBOWSKI, P.T., BRADLEY, L.A., CLAGUE, J.J., CARVER, G.A., DARIENZO, M.E., GRANT, W.C., KRUEGER, H.W., SPARKS, R., STAFFORD, T.W., & STUIVER, M. 1995. Radiocarbon evidence for extensive plate-boundary rupture about 300 years ago at the Cascadia subduction zone. *Nature*, **378**, 371-374.

—, JENNINGS, A.E., & KASHIMA, K. 1996a. An earthquake history derived from stratigraphic and microfossil evidence of relative sea-level change at Coos Bay, southern coastal Oregon. *Geological Society of America Bulletin*, **108**, 141-154.

—, SHENNAN, I., & LONG, A.J. 1996b. Identifying coseismic subsidence in tidal-wetland stratigraphic sequences at the Cascadia subduction zone of western North America. *Journal of Geophysical Research*, **101**, 6115-6135.

NIEM, A.R., & NIEM, W.A. 1985. Oil and gas investigations of the Astoria Basin, Clatsop and northernmost Tillamook Counties, northwest Oregon. *Oregon Department of Geology and Mineral Industries Oil and Gas Investigation*, **14**, scale 1:250 000.

—, MACLEOD, N.S., SNAVELY, J., P.D., HUGGINS, D., FORTIER, J.D., MEYER, H.J., SEELING, A., AND NIEM, W.A., 1992. Onshore-offshore geologic cross section, northern Oregon Coast Range to continental slope. *Oregon Department of Geology and Mineral Industries*, **26**, 10 pp.

—, SNAVELY, P.D., JR., & NIEM, W.A. 1990. Onshore-offshore geologic cross section from the Mist gas field, northern Oregon coast range, to the northwest Oregon continental shelf. *Oregon Department of Geology and Mineral Industries Oil and Gas Investigation*, **17**, 46 pp.

OBERMEIER, S.F. 1995. *Preliminary estimates of the strength of prehistoric shaking in the Columbia River valley and the southern half of coastal Washington, with emphasis for a Cascadia subduction zone earthquake about 300 years ago*. U.S. Geological Survey Open File Report, **94-589**, 34 pp.

OPPENHEIMER, D., BEROZA, G., CARVER, G., DENGLER, L., EATON, J., GEE, L., GONZALEZ, F., JAYKO, A., LI, W.H., LISOWSKI, M., MAGEE, M., MARSHALL, G., MURRAY, M., McPHERESON, R., ROMANOWICZ, B., SATAKE, K., SIMPSON, R., SOMERVILLE, P., STEIN, R., & VALENTINE, D. 1993. The Cape Mendocino, California, earthquakes of April 1992: Subduction at the triple junction. *Science*, **261**, 433-438.

ORANGE, D.L., GEDDES, D.S., & MOORE, J.C. 1993. Structural and fluid evolution of a young accretionary complex: The Hoh rock assemblage of the western Olympic Peninsula, Washington. *Geological Society of America Bulletin*, **105**, 1053-1075.

PALMER, S.P., & LINGLEY, W.S. 1989. *An assessment of the oil and gas potential of the Washington outer continental shelf*. Washington State Division of Geology and Earth Resources Report, **WSG 89-2**, 88 pp.

PANDOLFI, J.M., BEST, M.M.R., & MURRAY, S.P. 1994. Coseismic event of May 15, 1992, Huon Peninsula, Papua New Guinea: Comparison with Quaternary tectonic history. *Geology*, **22**, 239-242.

PARKER, M.J. 1990. *The Oligocene and Miocene geology of the Tillamook embayment, Tillamook County, northwest Oregon*. M.S. thesis, Oregon State University, Corvallis, 515 pp., 2 plates.

PELTIER, W.R. 1996. Mantle viscosity and ice-age topography. *Science*, **273**, 1359-1364.

PETERSON, C.D., DARIENZO, M.A., & PARKER, M., 1988. Coastal neotectonic field guide for Netarts Bay, Oregon. *Oregon Geology*, **50**, 99-106 and 117.

—, & DARIENZO, M.E. 1989. Episodic, abrupt tectonic subsidence recorded in late Holocene deposits of the South Slough syncline: An on-land expression of shelf fold belt deformation from the southern Cascadia margin. *Geological Society of America Abstracts with Programs*, **21**, 129 (abst.).

—, & PRIEST, G.R. 1995. Preliminary reconnaissance survey of Cascadia paleotsunami deposits in Yaquina Bay, Oregon. *Oregon Geology*, **57**, 33-40.

—, & DARIENZO, M.E. 1996. Discrimination of climatic, oceanic, and tectonic mechanisms of cyclic marsh burial, Alsea Bay, Oregon. In: ROGERS, A. M., WALSH, T. J., KOCKELMAN, W. J., & PRIEST, G. (eds) *Assessing and reducing earthquake hazards in the Pacific Northwest*. U.S. Geological Survey Professional Paper, **1560**, pp. 115-146.

—, BARNETT, E., BRIGGS, G.G., CARVER, G.A., CLAGUE, J.J., & DARIENZO, M.E. 1997. *Subsidence from great earthquakes in the Cascadia subduction zone, Vancouver Island, B.C., Washington, Oregon, and northernmost California*. Department of Oregon Geology and Mineral Industries, Open-File Report, **0-97-5**, 44 pp.

PLAFKER, G. 1969. *Tectonics of the March 27 Alaskan earthquake*. U.S. Geological Survey Professional Paper, **543-I**, 74 pp.

— 1972. Alaskan earthquake of 1964 and Chilean earthquake of 1960: implications for arc tectonics. *Journal of Geophysical Research*, **77**, 901-925.

PRIEST, G.R., SAUL, I., & DIEBENOW, J. 1994. *Chronic geologic hazard maps and erosion rate database, coastal Lincoln county, Oregon: Salmon River to Seal Rocks*. Oregon Department of Geology and Mineral Industries Open-File Report, **0-94-11**, 45 pp., 1:4800 scale maps.

RAU, W.W. 1973. Geology of the Washington coast between Point Grenville and the Hoh River. *Washington Division of Geology and Earth Resources Bulletin*, **66**, 58 pp.

RYAN, H. F. & STEVENSON, A. J. 1995. *Cruise report for C1-94-OW: Reconnaissance high resolution geopulse data acquired for seismic hazard studies along the Columbia River from July 18-22, 1994*. U.S. Geological Survey Open-File Report, **95-668**, 38 pp.

SATAKE, K., SHEMAZAKI, K., YOSHINOBU, T., & UEDA, K. 1996. Time and size of a giant earthquake in Cascadia inferred from Japanese tsunami records of January 1700. *Nature*, **379**, 246-249.

SHENNAN, I., LONG, A.J., RUTHERFORD, M.M., GREEN, F.M., INNES, J.B., LLOYD, J.M., ZONG, Y., & WALKER, K.J. 1996. Tidal marsh stratigraphy, sea-level change and large earthquakes, I: A 5000 year record in Washington, U.S.A. *Quaternary Science Reviews*, **15**, 1023-1059.

SIEH, K., JONES, L., HAUKSSON, E., HUDNUT, K., EBERHART-PHILLIPS, D., HEATON, T., HOUGH, S., HUTTON, K., KANAMORI, H., LILJE, A., LINDVALL, S., MCGILL, S.F., MORI, J., RUBIN, C., SPOTILA, J.A., STOCK, J., THIO, H., TREIMAN, J., WERNICKE, B., & ZACHARASEN, J. 1993. Near-field investigation of the Landers earthquake sequence, April to July, 1992. *Science*, **260**, 171-176.

SNAVELY, P.D., Jr. 1976. *Geologic map of the Yaquina and Toledo quadrangles, Lincoln County, Oregon*. U.S. Geological Survey Miscellaneous Investigations Series Map, **I-867**, scale 1:62,500.

— 1987. Tertiary geologic framework, neotectonics, and petroleum potential of the Oregon-Washington continental margin. In: Scholl, D. W., Grantz, A., & Vedder, J.G. (eds) *Geology and resource potential of the continental margin of western North America and adjacent ocean basins-Beaufort sea to Baja California*. Circum-Pacific Council for Energy and Mineral Resources, Houston, pp. 305-335.

—, & WELLS, R.E. 1996. Cenozoic evolution of the continental margin of Oregon and Washington. In: ROGERS, A. M., WALSH, T. J., KOCKELMAN, W. J., & PRIEST, G. (eds) *Assessing and reducing earthquake hazards in the Pacific Northwest*. U.S. Geological Survey, Professional Paper, **1560**, pp. 161-182.

SPOTILA, J., & SIEH, K. 1995. Geologic investigations of the "slip gap" in the surficial ruptures of the 1992 Landers earthquake, southern California. *Journal of Geophysical Research*, **100**, 543-559.

SUGIYAMA, Y. 1994. Neotectonics of Southwest Japan due to the right-oblique subduction of the Philippine Sea plate. *Geofisica Internacional*, **33**, 53-76.

TABOR, R.W., & CADY, W.M. 1978. *The Structure of the Olympic Mountains, Washington-Analysis of a subduction zone*. U.S. Geological Survey Professional Paper, **1033**, 38 pp.

TICKNOR, R.L. 1993. *Late Quaternary crustal deformation on the central Oregon coast as deduced from uplifted wave-cut platforms*. M.S. Thesis, Western Washington University, Bellingham, 70 pp.

—, KELSEY, H.M., & BOCKHEIM, J.G. 1992. Late Quaternary tectonic deformation along the central Oregon portion of the Cascadia margin as deduced from deformation of wave-cut platforms. *Geological Society of America Abstracts with Programs*, **24**, 86 (abst.).

WAGNER, H.C., & TOMSON, J.H. 1987. *Offshore geology of the Strait of Juan de Fuca, State of Washington and British Columbia, Canada*. Washington Division of Geology and Earth Resources Open File Report, **87-1**, 16 pp., 7 plates.

WALD, D., & HEATON, T. 1994. Spatial and temporal distribution of slip for the 1992 Landers, California, earthquake. *Seismological Society of America Bulletin*, **84**, 668-691.

WALSH, T.J., KOROSSEC, M.A., PHILLIPS, W.M., LOGAN, R.L., & SCHASSE, H.W. 1987. *Geologic map of Washington - Southwest quadrant*. Washington Division of Geology and Earth Resources, Geologic Map, **GM-34**, 28 pp.

WANG, K., MULDER, T., ROGERS, G.C., & HYNDMAN, R.D. 1995. Case for very low coupling stress on the Cascadia subduction fault. *Journal of Geophysical Research*, **100**, 12 907-12 918.

WEAVER, C.S., & BAKER, G.E. 1988. Geometry of the Juan de Fuca plate beneath Washington and northern Oregon from seismicity. *Bulletin of the Seismological Society of America*, **78**, 264-275.

WELLS, R.E., 1989. Geologic map of the Cape Disappointment-Naselle River area, Pacific and Wahiakum Counties, Washington. *U.S. Geological Survey, Miscellaneous Investigations Series Map*, **I-1832**.

—, SNAVELY, P.D., JR., & NIEM, A.R. 1992. Quaternary thrust faulting at Netarts Bay, northern Oregon coast. *Geological Society of America Abstracts with Programs*, **24**, 89 (abst.).

—, NIEM, A.R., & SNAVELY, P.D., JR. 1994a. Young deformation at Netarts Bay and elsewhere, northern Oregon coast. *Proceedings of the Oregon Academy of Sciences*, **XXX**, 39 (abst.).

—, SNAVELY, P.D., JR., MACLEOD, N.S., KELLY, M.M., & PARKER, M.J., 1994b. Geologic map of the Tillamook Highlands, Northwest Oregon Coast Range. *U.S. Geological Survey Open File Report*, **94-21**.

—, WEAVER, C.S., & BLAKELY, R.J., 1998. Fore-arc migration in Cascadia and its neotectonic significance. *Geology*, **26**, 759-762.

WERNER, K.S., GRAVEN, E.P., BERKMAN, T.A., & PARKER, M.J. 1990. Direction of maximum horizontal compression in northwestern Oregon determined by borehole breakouts. *Tectonics*, **10**, 948-958.

WEST, D.O. 1986. *WNP-3 geologic support services coastal terrace study*. Washington Public Power Supply System, Richland, Washington, **853-1010**, 53 pp.

—, & McCRUMB, D.R. 1988. Coastline uplift in Oregon and Washington and the nature of Cascadia subduction zone tectonics. *Geology*, **16**, 169-172.

YAMAGUCHI, D.K., ATWATER, B.F., BUNKER, D.E., BENSON, B.E., & REID, M.S. 1997. Tree-ring dating the 1700 Cascadia earthquake. *Nature*, **389**, 922-923.

ZOBACH, M.L., & ZOBACH, M.D. 1989. Tectonic stress field of the continental United States. *Geological Society of America Memoir*, **172**, 523-540.

Chapter IV

Evolution of the Late Neogene Central Cascadia Forearc Basin From Investigations of a Late Miocene Unconformity

Lisa C. McNeill¹, LaVerne D. Kulm², Chris Goldfinger², Robert S. Yeats^{1,2}

¹ Department of Geosciences, Wilkinson Hall,
Oregon State University, Corvallis, Oregon 97331

² College of Oceanic and Atmospheric Sciences,
Oregon State University, Corvallis, Oregon 97331

To be submitted to Geological Society of America Bulletin.

IV.1 ABSTRACT

The continental shelf and upper slope of the Oregon Cascadia margin are underlain by an elongate Tertiary forearc basin, equivalent to the Eel River Basin of the southernmost Cascadia margin. Seismic reflection data, seafloor samples, and oil-exploratory well and ODP drill site stratigraphy were examined to analyze the basin stratigraphy and develop a Neogene forearc history for the central Cascadia margin. Total thickness of basin strata on the central margin locally exceeds 7 km, and includes a regional angular late Miocene unconformity which may coincide with a worldwide hiatus, NH6 (~7.5-6 Ma), widespread throughout the Pacific Basin. The unconformity is angular on the inner and middle shelf, probably due to subaerial erosion despite a lack of evidence of shallow marine deposition, whereas the seaward correlative disconformity may have been produced by submarine erosion; alternatively, this horizon may be conformable. A structure contour map of the unconformity and correlated seaward reflector clearly outlines deformation into major synclines and uplift of submarine banks which modify the current shelf break position. The underlying basaltic Siletzia terrane exerts minimal influence on structural style as is evident in its lack of control (with few exceptions) on the positions of the basin outer-arc high, the shelf break, uplifted submarine banks, and the transition from arc-normal to arc-parallel compression on the middle-inner shelf. Variations in vertical tectonic uplift rates of the unconformity on the shelf in a margin-parallel direction show agreement with coastal geodetic and geomorphic data. This supports the hypothesis that the central Oregon forearc is deforming at lower rates than to the north and south, perhaps as a result of low interplate coupling. This region of reduced uplift rates may also represent a distinct segment of the subduction zone.

The forearc basin of the Willamette Valley and of the continental shelf were formerly locally connected in Paleogene and early Neogene time prior to major late Miocene uplift of the Coast Range. The shelf basin is bounded to the west by a N-S-trending outer-arc high. Rapid tectonic uplift and coincident eustatic sea level fall resulted in the formation of the late Miocene unconformity. Basin subsidence and outer-arc high uplift caused ponding of sediments (predominantly Columbia River source) within the basin, which resulted in a relatively starved outer margin and narrow Pliocene accretionary wedge. During the early-middle Pliocene, truncation of the seaward edge of the forearc basin and removal of the former outer-arc high resulted in narrowing of the basin and re-accretion of eroded older sediments within the accretionary wedge. During the Pleistocene, the central Cascadia shelf basin was filled and the outer-arc high breached by the Astoria canyon, the primary conduit of Columbia River sediments to the central Cascadia slope and abyssal

plain. Most sediments subsequently bypassed the continental shelf to be deposited in slope basins and on the abyssal plain, resulting in high growth rates of the Pleistocene accretionary wedge. This event is represented by a change in sediment provenance on the abyssal plain ~1.3-1.4 Ma, and also may be recorded by an unconformity of similar age throughout the Cascadia shelf basin. Since the late Miocene, the coastline has maintained approximately the same position acting as a hinge between Coast Range uplift and basin subsidence. Following continued submarine bank uplift and synclinal subsidence within the forearc basin, the current shelf break was formed.

IV.2 INTRODUCTION

The Cascadia continental shelf is underlain by a thick sedimentary sequence extending from the Eel River Basin in the south to offshore Vancouver Island in the north. This forearc basin was probably originally continuous in the early to middle Eocene (Christiansen and Yeats, 1992) but has subsequently been deformed and dissected into smaller basins, and eroded at its western margin. The basin stratigraphy contains several regional unconformities, suggesting a complex history of vertical tectonics, sedimentation, and sea level change. An extensive middle to late Miocene unconformity was first reported by Kulm and Fowler (1974) and Snively (1987), but the extent, origin, and deformation of this surface during the Pliocene and Quaternary have not been documented in detail. A similar regional isopach map was produced for the entire forearc basinal sequence on the Oregon margin by Cranswick and Piper (1992). The late Miocene angular unconformity is easily identifiable in seismic reflection profiles across the Oregon continental shelf. However, it is less continuously traceable where it is a disconformity on much of the Washington shelf, and it is also difficult to trace between central and southern Oregon. In these regions, the certainty of identifying and tracing the unconformity along seismic profiles is reduced, often due to poor stratigraphic control, faulting, or uplift and erosion. We therefore restricted our study to the central Cascadia margin where the unconformity is commonly angular and therefore easily identifiable, and there is stratigraphic control from exploration wells and seafloor samples. A younger regional unconformity, probable latest Pliocene or early Pleistocene age, is also recognized on the Oregon shelf, but it is less continuous than the late Miocene unconformity.

In this paper, we discuss the age, origin, and deformation of this late Miocene unconformity and incorporate this information with the stratigraphy of the forearc basin, adjacent accretionary wedge, and abyssal plain to evaluate the Neogene evolution of the

Cascadia margin. Of particular interest are the tectonic and sedimentary interaction between the accretionary wedge and forearc basin and the influence of tectonics and eustatic sea level fluctuations on sedimentation, erosion, and deformation. We also focus on how and why deformational patterns vary across and along the margin and the extent of influence of basement lithology on deformation of basin sediments. We also compare the central Cascadia forearc basin and the Washington forearc basin to the north and the Eel River Basin to the south.

A structure-contour map of the late Miocene surface on the central Cascadia margin was constructed to visualize forearc deformation. Patterns of deformation are compared with records of onshore Quaternary deformation to determine the consistency of these patterns from the late Miocene to the present and to assess the existence and significance of margin-parallel variations onshore and offshore.

IV.3 METHODS

Seismic reflection profiles alongside shelf exploration well chronology, dated seafloor samples and cores, and ODP/DSDP drill site stratigraphy (Fig. IV.1) were used to map and interpret the origin of the late Miocene unconformity within the forearc basin. The unconformity and seaward correlative reflector were traced on seismic profiles throughout the central and northern Oregon margin to produce a structure contour map. A proprietary dataset of multichannel migrated seismic reflection profiles used for the map was collected in two acquisition phases: (1) 1975, 46-channel, and (2) 1980, 96-channel, which form a network of N-S and E-W profiles across the shelf and upper slope (Fig. IV.1). Additional seismic profiles (both single channel from Shell Oil Company (Fig. IV.1) and multichannel from USGS and industry) were used to confirm the position and depth of the unconformity in data gaps of the primary dataset. The unconformity and a younger latest Pliocene or early Pleistocene unconformity and correlative seaward disconformable or conformable seismic reflector were identified and traced out on each seismic profile. The degree of uncertainty of age and position of the late Miocene unconformity was ranked to ascertain the confidence when interpreting this surface. The traced unconformities were digitized and converted to xyz values in UTM (Universal Transverse Mercator) coordinates and two-way time. Depth in time was then converted to depth using published velocities of late Neogene units from refraction experiments (Shor et al., 1968) and from sonic well logs (Palmer and Lingley, 1989; Cranswick and Piper, 1992), loosely constrained by wide-angle seismic reflection and refraction data which focused on deeper units (Tréhu et al.,

Figure IV.1 Tectonic setting of Cascadia subduction zone (inset) and study area indicating datasets used to identify late Miocene unconformity and stratigraphy of the forearc basin. Inset shows locations of relevant ODP/DSDP sites. WV=Willamette Valley, CR=Coast Range, ERB=Eel River Basin, WA submarine canyons: JF=Juan de Fuca; Ql=Quillayute; Qn=Quinault; G=Grays; Gu=Guide; W=Willapa. Main figure shows multichannel seismic (proprietary, solid) and single-channel data (dashed) used to trace the unconformity and locates dated samples at industry exploration wells, along single channel seismic lines (discontinuous samples along dashed lines) and at individual sample sites (triangles). Main structural features of the central Cascadia forearc basin are also labeled in italics. The Cascade Bench (Kulm and Fowler, 1974) extends from Heceta to Nehalem Bank along the upper slope of the Netarts Embayment. The shelf edge is defined here and in subsequent figures as a topographic break identified on seismic profiles. Bold lines represent seismic profiles illustrated in subsequent figures.

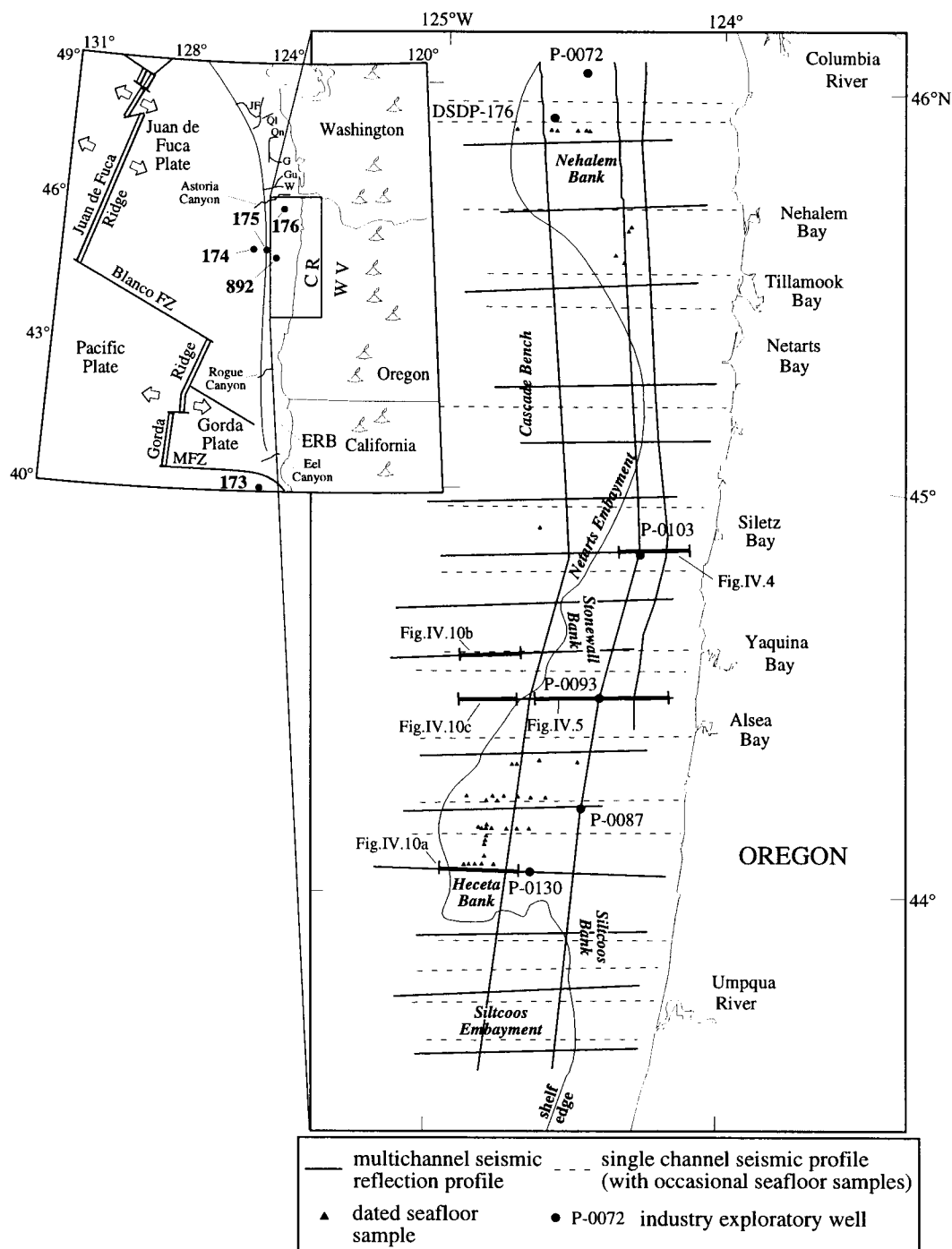


Figure IV.1

1994; Parsons et al., 1998). The overlying stratigraphic section was divided into Quaternary and Pliocene units, separated by the approximated position of the younger (earliest Pleistocene) unconformity, and assigned velocities of 1.7 km/s and 2.1 km/s, respectively. The ages of these two units are unconfirmed by biostratigraphic or radiometric age away from well or seafloor sample locations, and are therefore only approximate. Good agreement between calculated and measured depths at well locations support the methodology and values applied. Depth values represent depth to the unconformity below sea level rather than below the seafloor. The unconformity surface was initially contoured by hand within a CAD (Computer Aided Design) system rather than proceeding directly to computerized gridding to prevent the introduction of artifacts in regions of low data density (between the discrete lines of datapoints). The resulting xyz data were converted to a TIN (Triangulated Irregular Network). The TIN allows the irregularly distributed data to be densified, producing a more regular dataset with reduced potential for artifacts. The xyz TIN file was finally re-gridded (continuous curvature surface, grid cell = 300m) in GMT (Generic Mapping Tools software; Wessel and Smith, 1991), and converted to a shaded relief image. This file was also imported into and georeferenced in a GIS to compare with other datasets such as swath bathymetry, sidescan sonar, gravity and magnetic anomalies, a neotectonic map, and previous interpretations.

IV.4 CASCADIA FOREARC BASIN STRATIGRAPHY

The late Miocene unconformity lies within a sequence of forearc basinal sediments of middle Eocene to Pleistocene age on the Oregon continental shelf and late Miocene to Pleistocene age on the Washington shelf. Basinal sediments overlie early Eocene oceanic basalt of the Siletz River Volcanics (part of the Siletzia terrane) on the central Oregon margin and Eocene to middle Miocene *mélange* and broken formation of the ancient accretionary complex on the Washington and northern Oregon margin (Fig. IV.2). The magnetic gradient marking the seaward edge of the Siletzia terrane is interpreted by Snavely (1987) as the Fulmar fault, a N-S trending fault, mostly active in the Eocene with possible dextral offset.

The following stratigraphic summary is derived predominantly from Snavely (1987), Christiansen and Yeats (1992), and Snavely and Wells (1996) and is illustrated in Figure IV.2. The early Eocene basalt is overlain by early middle Eocene deep marine turbidite sandstone and siltstone of the Tyee Formation in the central Coast Range and by marine and continental units in the Puget Sound basin and faulted over the Eocene

Figure IV.2 Generalized stratigraphy of the Eel River Basin, northern California (based on Ingle, 1987; Clark, 1992; McCrory, 1995), central Oregon coast and shelf (based on Snively, 1987; Snively and Wells, 1992; Yeats et al., 1998), and the Washington coast and shelf (based on Palmer and Lingley, 1989; McNeill et al., 1997). Ages of significant unconformities and hiatuses for each region are indicated beside the stratigraphic columns. Also shown are stratigraphic columns of ODP Sites 174 on the edge of the Astoria Fan and 176 on the northern Oregon outer shelf of Nehalem Bank (locations on Fig. IV.1; based on Kulm et al., 1973; Schrader, 1973). Note that the stratigraphy is illustrated as depth columns. Ages for Site 174 are based on planktonic foraminifera (Ingle, 1973; Goldfinger et al., 1996a) and interpolation between known ages. Ages for Site 176 are based on diatoms (North Pacific Diatom Zones) with reference to other microfossils, including benthic and planktonic foraminifera, calcareous nannoplankton, and radiolarians reported in Kulm et al. (1973). CR=Columbia River, CRB=Columbia River Basalt, Pleist.=Pleistocene, NPD=North Pacific Diatom. Significant unconformities, changes in sediment provenance, and known ages are indicated beside the stratigraphic columns.

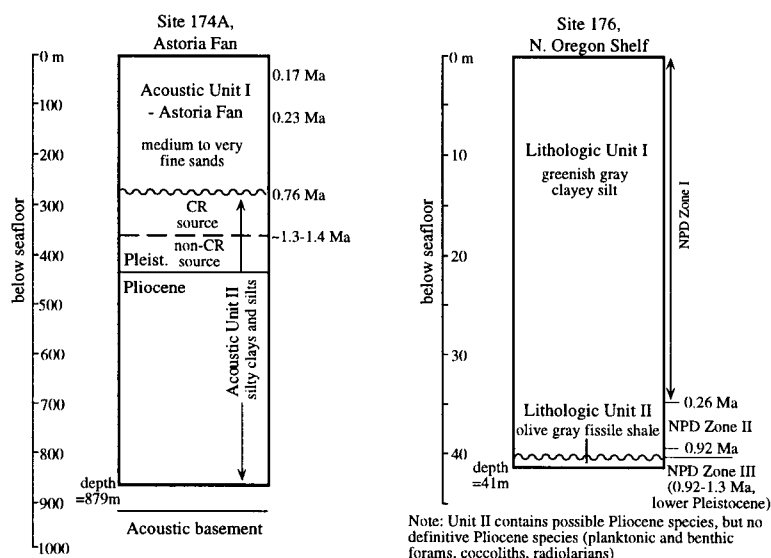
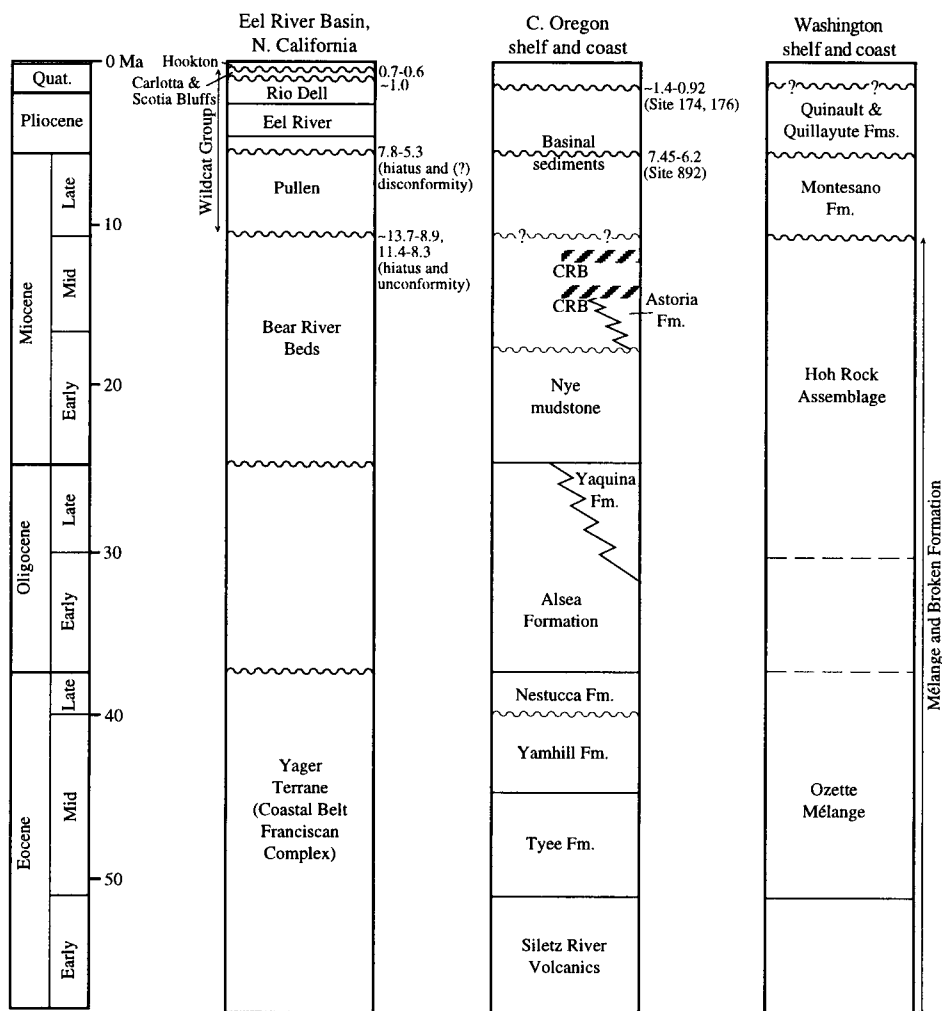


Figure IV.2

Olympic core rocks of Washington to the north. The *mélange* and broken formation of the ancient accretionary complex which constitutes the Olympic core rocks is also exposed on the western Olympic Peninsula and underlies the shelf and upper slope. It is composed of middle to late Eocene Ozette *mélange* and the late Oligocene to middle Miocene Hoh Rock Assemblage (Fig. IV.2; Rau, 1973, 1975, 1979; Orange et al., 1993). Deep marine siltstones of the upper middle Eocene Yamhill and late Eocene bedded tuffs and siltstone of the Nestucca Formation are intercalated with local Eocene submarine and subaerial basalts in the Oregon and southwest Washington Coast Range. Rapid Oligocene and early Miocene forearc basin subsidence resulted in deposition of > 2.5 km of sediments, including deep to shallow marine siltstone of the Oligocene Alsea Formation, deltaic sandstone of the Oligocene Yaquina Formation, and the early Miocene deep marine Nye mudstone on the Oregon margin. Similar thicknesses were deposited in the Tofino-Juan de Fuca Basin north of the Olympic Mountains. Basinal deposition continued into the early-middle Miocene with the Astoria Formation, a shallow marine to deltaic sandstone and siltstone (Cooper, 1981), deposited on the west flank of the uplifting Coast Range. Flows of the middle Miocene Columbia River Basalt Group unconformably overlie these units, extending onto the present continental shelf where some sills and dikes are thought to represent invasive flows interfingering with these units (Beeson et al., 1979; Niem and Niem, 1985).

Following a period of late middle Miocene deformation, up to 2 km of late Miocene and Pliocene sediment accumulated in the Oregon and Washington forearc basin. These include latest middle and late Miocene middle bathyal to neritic Montesano Formation (divided into three members: lower claystone member; middle sandstone member; and upper siltstone member) and the Pliocene and latest Miocene Quinault and Quillayute Formations (and their offshore equivalents) on the Washington coast and shelf. These units are separated by angular unconformity and are in unconformable contact with the underlying *mélange* and broken formation (Fig. IV.2; Palmer and Lingley, 1989; McNeill et al., 1997). Quaternary sediments (up to 0.5 km thickness) cover much of the Oregon and Washington continental shelf with the exception of the uplifted submarine banks where Neogene strata are exposed. An early Pleistocene (possibly latest Pliocene) unconformity is identified in both the Oregon and Washington basinal stratigraphy and in seismic reflection records (e.g., Kulm and Fowler, 1974; Palmer and Lingley, 1989). This unconformity may be equivalent to that drilled at Site 176 and 174, with an age of at least 0.92-1.4 Ma (see section IV.6.4.5, Fig. IV.2, Kulm and Fowler, 1974). Thicknesses of basinal sediments exceed 7 km (Eocene to Pleistocene) on the Oregon shelf (Snively et al., 1980) and 2 km (late Miocene to Pleistocene) on the Washington shelf (Snively, 1987).

The Eel River Basin extends from the Cape Mendocino area of coastal northern California onshore at least as far north as the latitude of Cape Sebastian (42.3°N) on the southernmost Oregon coast (Clarke, 1992). The following stratigraphic description (illustrated in Fig. IV.2) is derived primarily from the descriptions of Ingle (1987), Clarke (1992), and McCrory (1995) of the onshore exposures of basinal sediments on the northern Californian coast (including the Centerville Beach section). In contrast to the central Cascadia basin, the basinal sediments are underlain by a younger basement of accreted terranes as young as early Miocene, including the Paleocene to Eocene Yager Terrane and Eocene to Miocene King Range Terrane, part of the coastal belt of the Franciscan Complex (McCrory, 1995). Forearc basinal sediments are restricted to late Miocene and younger (similar to the Washington margin), with underlying early to middle Miocene sediments exhibiting predominantly slope basin deposition. The early to middle Miocene Bear River Beds consist of deep marine hemipelagic strata. These are unconformably overlain by basinal sediments of the late Miocene to Pleistocene Wildcat Group (Ingle, 1987; Clarke, 1992). The Wildcat Group is subdivided into the basal late Miocene Pullen Formation (containing a hiatus and disconformity between 7.5 and 5.3 Ma; Barron, 1986; McCrory, 1995), early Pliocene Eel River Formation, the Rio Dell Formation, the Scotia Bluffs sandstone, and the coarse-grained possibly non-marine (McCrory, 1986) Carlotta Formation (Ingle, 1987; Clarke, 1992; McCrory, 1995; Fig. IV.2). The Wildcat Group is unconformably overlain by the late Pleistocene non-marine Hookton Formation. These formations of the Wildcat Group show gradual shallowing and form a generally conformable sequence (Clarke, 1992). It is important to note that these units are time-transgressive and that parts of the basin had different depositional histories, therefore extrapolations to the offshore stratigraphy should be treated with caution (Clarke, 1992), both in the Eel River Basin and farther north.

The central Cascadia forearc basin is currently almost entirely filled, and most Holocene sediments bypass the continental shelf to be deposited in slope basins and on the abyssal plain. The seaward extent of basinal sediments is marked by an outer-arc high on the current outer shelf and upper slope (Fig. IV.3), but growth strata within the stratigraphic section suggest that the basin may have formerly extended farther seaward (discussed further below).

Subsequent interpretations of the Oregon and Washington basin stratigraphy are drawn from the literature, with special attention to and correlation with ODP site stratigraphy and onshore Eel River Basin stratigraphy which include detailed biostratigraphic studies which supersede the time-transgressive benthic foraminifera stratigraphy of oil-industry based studies.

Figure IV.3 Extent of the late Miocene unconformity and correlative seaward conformity or disconformity. Diagonal lines indicate where the unconformity is clearly angular. Elsewhere, the correlative reflector is non-angular or partially angular but can still be traced as a continuous reflector to the outer-arc high. Thick black line indicates the position of the outer-arc high which marks the current seaward extent of the forearc basin on the shelf and upper slope, white dots represent positions on seismic profiles, dashed lines indicate alternative outer-arc high positions. Thin dashed line represents a topographic break and change in fold orientation which may indicate the seaward extent of interplate coupling (Goldfinger et al., 1996b). White line represents present-day shelf break.

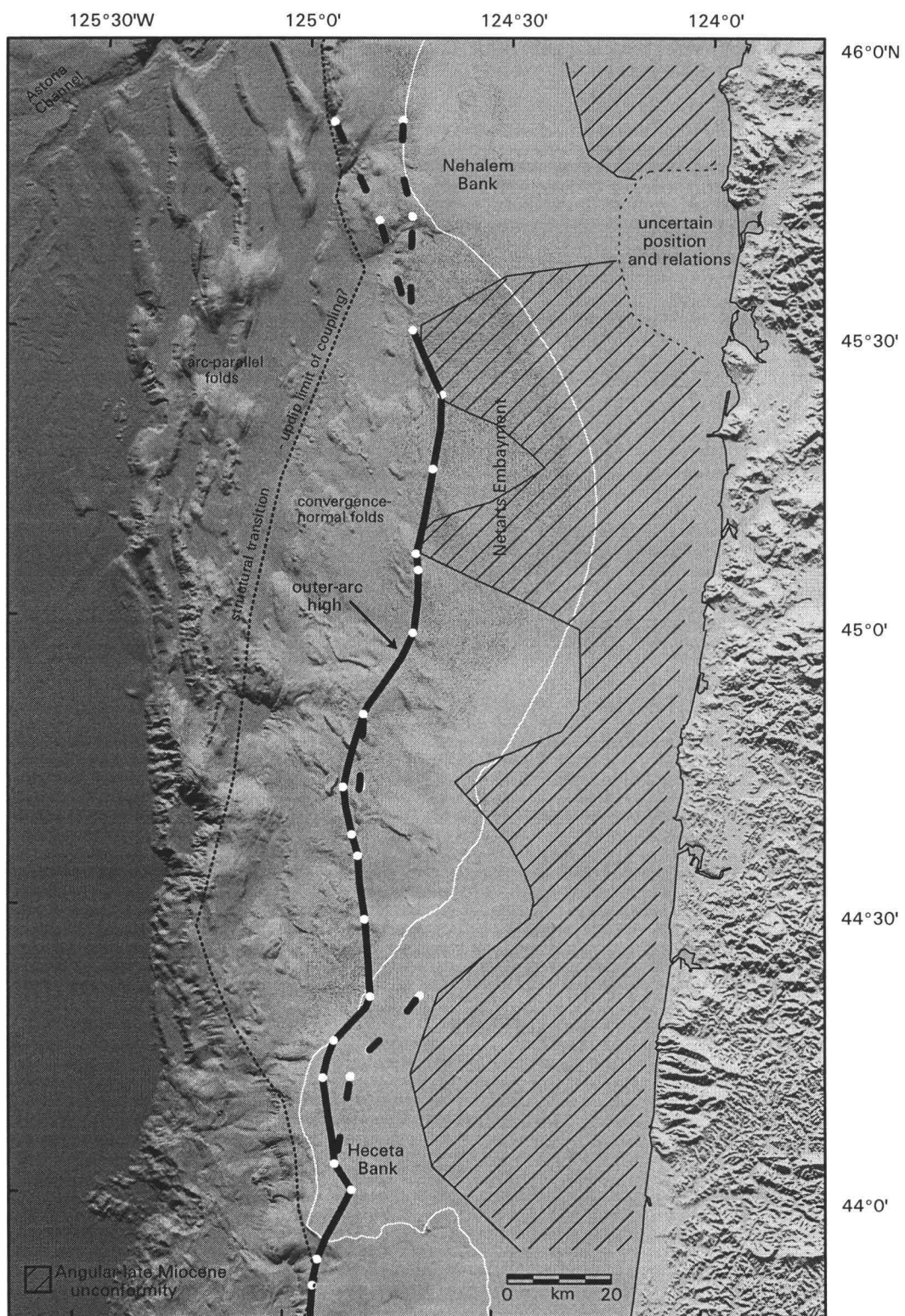


Figure IV.3

IV.5 RESULTS

IV.5.1 Age Of The Unconformity

When initially described, the age of this regional Cascadia unconformity was tentatively placed at the middle-late Miocene boundary (Kulm and Fowler, 1974). Benthic foraminifera identification on either side of the unconformity from oil-exploratory wells on the continental shelf (S.D. Drewry et al., Minerals Management Service (MMS) unpublished work, 1993) provides an approximate age ranging between middle Miocene and earliest Pliocene. Benthic foraminiferal stages are those of Kleinpell (1938) and Mallory (1959) originally defined in California stratigraphy. These stages are time-transgressive and document water depth more accurately than age based on comparisons with coccolith stratigraphy (Bukry and Snavely, 1988). Therefore, these stages are indicative of age in a general way only. How can we determine the age of the late Miocene unconformity within the Oregon and Washington stratigraphy? The youngest sediments underlying the unconformity are Mohnian (P-0130, P-0103 exploration wells, Oregon shelf) and Delmontian (P-0072, P-0075, Washington-Oregon border, P-0155, P-0141, P-0150, Washington shelf) from benthic foraminifera in wells (S.D. Drewry et al., MMS unpublished work, 1993). Delmontian fauna indicate late Miocene age, but may be equivalent to part of the middle and late Miocene Mohnian Stage and therefore somewhat older (Barron, 1986). Fauna immediately overlying the unconformity are Repettian to Wheelerian Stage of Natland (1952) (Pliocene to Pleistocene) with one example of Miocene Mohnian fauna identified (we suggest that this is reworked sediment). Paleobathymetry of benthic foraminifera immediately above and below the unconformity range between outer neritic and lower bathyal; the majority of sediments are fine- to medium-grained (clay, silt, and silty sandstone). Results from the microfossil chronologies of hiatuses in worldwide drill holes suggest a global correspondence in the Miocene-Pliocene section, with global tectonic and climatic origins (Barron and Keller, 1983; Keller and Barron, 1987). Two prominent late Miocene unconformities occur at 10.5-9.2 Ma and 7-6 Ma, Neogene Hiatuses NH4 and NH6, respectively. Both hiatuses are present at ODP drill site 892 on the Oregon upper continental slope (located on Fig. IV.1), dated at 11.4-9.0 Ma and 7.45-6.2 Ma (Fournanier and Caulet, 1995). The regional nature of the angular unconformity on the Oregon (and Washington) shelf suggests that it is related to one of these two global hiatuses. The lack of late Miocene fauna overlying the unconformity and the probable presence of late Miocene sediments underlying the unconformity suggest that the regional

unconformity on the Cascadia margin is correlative to NH6 (7-6 Ma), rather than the older NH4 (10.5-9.2 Ma). This hypothesis is supported by the presence of two unconformities within the late Miocene in offshore Washington (Fig. IV.2; Palmer and Lingley, 1989; McNeill et al., 1997), the younger (between the latest middle and late Miocene Montesano Formation and the Pliocene Quinault formation and its offshore equivalent) being the likely correlative of the Oregon regional unconformity, based on interpretation and comparison of seismic reflection records and well stratigraphy. The older angular unconformity in Washington margin stratigraphy separates the Eocene to middle Miocene *mélange* and broken formation and the late Miocene Montesano Formation. The late Miocene unconformity and its correlative seaward disconformity or conformity are likely to be time-transgressive in a seaward direction across the margin.

IV.5.2 Evidence For Subaerial Vs. Submarine Erosion

The unconformable surface is angular and relatively planar on much of the inner and middle shelf (Figs. IV.3, IV.4). The seaward correlative reflector, predominantly on the outer shelf and upper slope, is non-angular and may be disconformable and/or conformable (Figs. IV.3, IV.5). The angularity of the landward unconformity initially suggests that it was formed by subaerial erosion rather than submarine erosion. However, sediments above and below the unconformity were deposited at water depths consistent with the outer shelf (outer neritic) to lower slope (lower bathyal), 100 - 3000 m water depth (Boltovskoy and Wright, 1976), as indicated by benthic foraminifera. There is little indication of deposition in a shallow marine or high-energy environment from benthic foraminifera or coarse-grained sediments. Sample transects across the late Miocene unconformity (along Shell Oil Company single-channel profiles indicated on Fig. IV.1) indicate potential evidence of shallow marine sedimentation (carbonaceous debris, volcanic pebbles, and cobbles), but these sediments may not be in situ. The probable mechanism of erosion of the late Miocene unconformity is examined further in the discussion.

IV.5.2.1 Subaerial Erosion

If erosion was indeed subaerial, the Cascadia margin experienced a rapid change in relative sea level. Assuming that global sea level could have fallen a maximum of ~150 m,

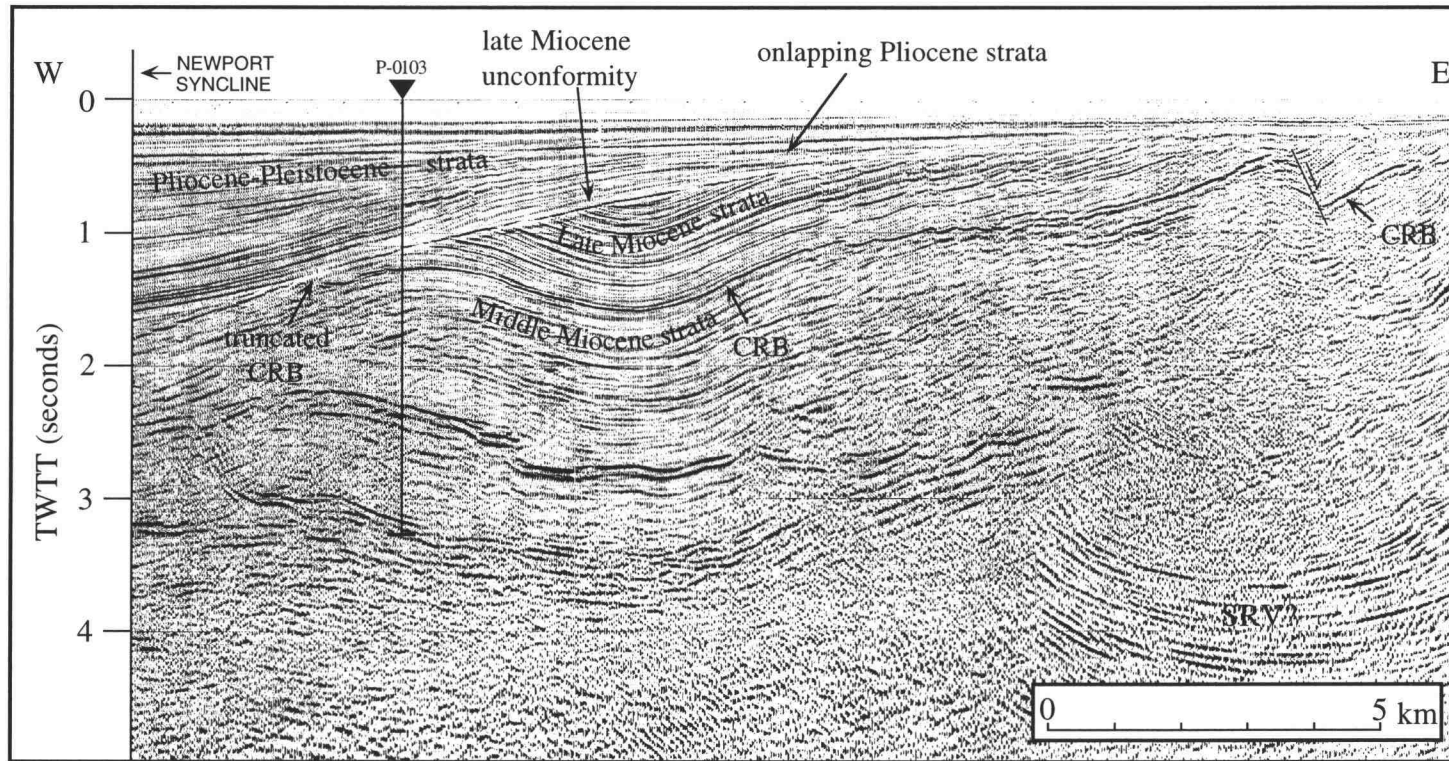


Figure IV.4. E-W multichannel seismic reflection profile west of Siletz Bay (located on Fig. IV.1) showing the angular nature of the late Miocene unconformity on the inner to middle shelf. This profile also shows the probable truncation of the Columbia River Basalt flow (CRB) just seaward of well P-0103, suggesting subaerial erosion. Pliocene sediments onlap the unconformity at very low angles suggesting a gently westward-dipping surface at the time of erosion. SRV=Siletz River Volcanics. After Yeats et al. (1998).

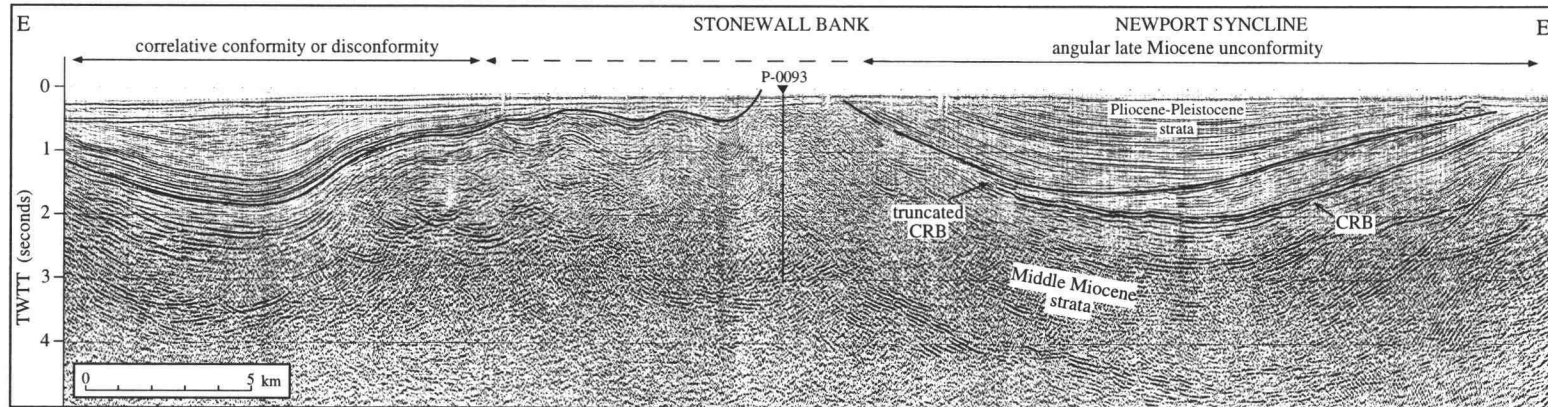


Figure IV.5. E-W multichannel seismic reflection profile across the continental shelf at Stonewall Bank west of Alsea Bay (located on Fig. IV.1). The late Miocene unconformity (bold black line) is angular landward of Stonewall Bank anticline, slightly angular just west of the bank where small wavelength folds are truncated, and conformable or disconformable seaward of these folds. This profile typifies the character of the unconformity from east to west across the shelf. Note that the unconformity truncates the late Miocene Columbia River Basalt flow (CRB) just east of well P-0093. Pliocene sediments onlap landward at a very low angle at the eastern end of the profile and are parallel to the unconformity elsewhere, indicating little relief on the unconformity at the time of erosion. After Yeats et al. (1998).

tectonic uplift is still required to bring deep marine sediments to sea level, with the exception of those deposited on the outer shelf or uppermost slope. Using paleo-water depths and ages of sediments at oil-exploratory well sites above and below the unconformity and an age of 7.5-6.2 Ma for erosion (ODP drill site 892, Fig. IV.1; Fourtanier and Caulet, 1995), uplift and subsidence rates can be approximated. Stratigraphic ages and paleobathymetry for these calculations are not restricted to wells within the study area, but also include wells on the Washington and southern Oregon shelves where the unconformity is also evident in the stratigraphy (cf. McNeill et al., 1997; Snively et al., 1980). As the amount of section eroded is unknown, some error is introduced in estimations of the onset of uplift. Calculations yield reasonable values of tectonic uplift and subsidence rates when compared with active margins with more accurate chronologies, of the order of 10's to 100's of m/Ma, the same order of magnitude as uplift rates determined for the Oregon outer shelf by Kulm and Fowler (1974) from seafloor samples. Sediments immediately overlying the unconformity indicate water depths as shallow as outer neritic to upper bathyal (~100-500 m) (Kulm and Fowler, 1974; S.D. Drewry et al., MMS unpublished work, 1993). If sea level is allowed to rise a potential maximum of 150 m, no post-erosional tectonic subsidence is required for the minimum water depths of these bathymetric zones. However, two industry wells (P-0150 and P-0141 on the Washington shelf) encountered middle-lower bathyal water depths immediately above the unconformity, which yields a significantly higher post-erosional subsidence rate if these sediments were in situ.

IV.5.2.2 Submarine Erosion

Submarine erosion and periods of reduced sedimentation rates or non-deposition have been proposed as causes of angular unconformities where evidence of a shallow marine environment is absent (e.g., Yeats, 1965; van Andel and Calvert, 1971; Teng and Gorsline, 1991). To determine whether submarine erosional currents on the Cascadia margin would be capable of eroding this stratigraphic section, we estimate current velocities required to erode sediments of certain age (and hence consolidation) and lithology, and compare these with current near-seafloor velocities measured on the present outer shelf and slope. Sediments underlying the unconformity range in age from early to middle-late Miocene, therefore eroded sediments were this age or younger. We broadly correlate maximum consolidation based on overburden with maximum sediment ages (early to middle Miocene). We approximate this overburden as between 100's of m to 1 km of

sediments eroded during the erosional event. If we assume that the period of erosion was 7.5-6.2 Ma, then the age of the oldest eroded sediments was 10.4-3.7 Ma for middle Miocene (16.6-11.2 Ma) rocks and 17.5-10.4 Ma for early Miocene (23.7-16.6 Ma) rocks at the time of erosion. Lithologies immediately above and below the unconformity were silty sandstone, silt, and clay (predominantly silt), with one example of a thin sandstone bed underlying the unconformity. Minimum velocities (flow velocity measured 1 m above seafloor, Miller et al., 1977) required to erode unconsolidated sediments, without consideration of cohesion of clays and silts, are: sand 25-80 cm/s; silt 15-25 cm/s; and clay <20 cm/s. Estimated values for cohesive clays and silts would be ~ 25-100 cm/s or possibly greater, although the exact velocities are dependent on many factors, including grain size, clay type, pore-filling cement, and the presence of organic material (P. Komar, pers. comm., 1998). Significantly greater velocities would be required to erode more consolidated or lithified older sediments, although the degree of consolidation and cementation of the central Cascadia older sediments (early to middle Miocene) at the time of erosion and its relationship to age is relatively unknown.

The predominant erosional shelf-slope current of the northeast Pacific margin is the California Current (Hickey, 1989). Recent measurements on the Oregon margin (J. Huyer and R. Smith, pers. comm., 1998) indicate near-seafloor velocities regularly reaching 20 cm/s in water depths of 600 m with maximum measured velocities of 40-50 cm/s in water depths of 250 and 600 m (corresponding to the outer shelf and upper slope region, respectively: the water depths immediately above and below the unconformity). These velocities may be exceeded in rare storm events in slightly shallower water (e.g., near-bottom velocities range up to 70 cm/s on the northern Oregon shelf at 50 - 80 m mid-shelf water depths, as reported by Smith and Hopkins (1972)). Similar studies performed by Hickey (1989) on the Washington margin suggest typical velocities of 10 cm/s, with specific mid to outer shelf near-bottom mean highs of <20 cm/s and maximum values of 20-50 cm/s. Measurements from near-bottom and mid-water sites above the middle to upper Washington slope indicate significantly reduced maximum measured velocities of 8-18 cm/s. These recent current velocities suggest that submarine abrasion of the strata (of sediment type and consolidation (based on age) determined above) on the outer shelf and upper slope underlying the late Miocene unconformity was possible but unlikely if silts and clays were cohesive.

IV.5.3 Deformation Of The Late Miocene Unconformity

Major Neogene deformational patterns of the central and northern Oregon margin can be determined from the structure contour map of the late Miocene unconformity (Fig. IV.6). Relative uplift rates along the offshore margin can also be compared with those in the coastal region over a range of timescales. The structure contour map was constructed for the central and northern Oregon margin only: extensional faulting and a less continuous angular late Miocene unconformity to the north, and difficulty in tracing the unconformity south to the Coos Bay Basin prevented the construction of a map of the entire Oregon-Washington forearc basin.

IV.5.3.1 Preserved Depositional Centers

The most prominent syncline preserving basinal sediments within the central Oregon shelf basin is the Newport syncline (20 km west of Newport) and its extension to the northwest, here named the Netarts syncline, which underlies the present-day continental slope (Fig. IV.6). The late Miocene unconformity reaches its greatest depth of ~ 2500 m below sea level within the Newport syncline. A shallower syncline to the southwest also has a northwesterly trend (Fig. IV.6). These two elongate synclines are separated by the rapidly uplifted Stonewall Bank, underlain by an active NW-trending blind reverse fault (Yeats et al., 1998). Middle Miocene and older rocks are exposed within the core of Stonewall Bank anticline. Prior to the predominantly late Pliocene (2-3 Ma) and younger uplift of Stonewall Bank (Yeats et al., 1998), strata within the Newport syncline and the syncline west of the bank were probably connected. Shallower synclines are also evident at the northern and southern ends of the gridded dataset, underlying the presently uplifted Nehalem Bank (part of the Astoria Basin) and between Heceta and Siltcoos Bank (underlying the prominent geomorphic embayment, which we refer to as the Siltcoos Embayment, Fig. IV.1).

IV.5.3.2 Late Neogene Structural Trends

The general trend of structures deforming the late Miocene unconformity is between NW-SE and N-S on the middle to outer shelf and upper slope (Fig. IV.6). This trend is in

Figure IV.6. Shaded relief structure contour map of the late Miocene unconformity on the central Cascadia shelf and upper slope. Depth in meters below sea level. Major structural and topographic features are labeled: HB (Heceta Bank); SiB (Siltcoos Bank); SB (Stonewall Bank); DBF (Daisy Bank Fault); NBF (Nehalem Bank Fault); NB (Nehalem Bank); NwS (Newport syncline); NetS (Netarts syncline). Black areas surrounding the structure contour map represent regions where the position of the unconformity are uncertain, except the region west of the outer-arc high, where the unconformity was either not present or has been eroded. The positions of seismic profiles used to produce the structure contour map are shown. Seaward margin of the Siletzia terrane (purple line), outer-arc high (red line), geodetic uplift contours from Mitchell et al. (1994, light blue lines) are also included. White line represents the modern shelf break. A-A' is position of cross section (D) shown in Fig. IV.9. B-B' is position of Coast Range cross sections (B, E) of Personius (1996) shown in Fig. IV.9.

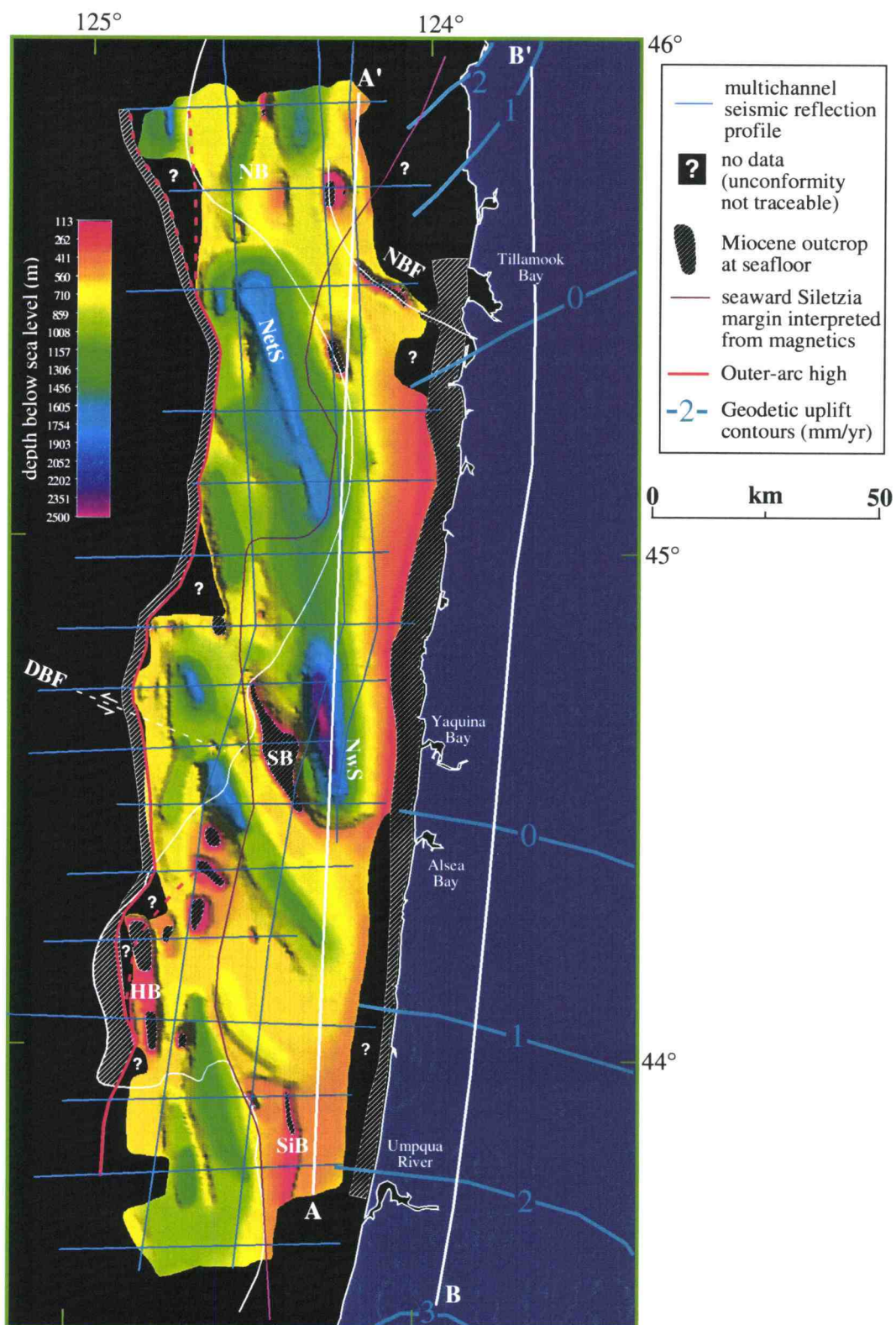


Figure IV.6

agreement with latest Quaternary structural trends in the same region (Goldfinger et al., 1992, 1997; McCaffrey and Goldfinger, 1995). These structures reflect coupling of the Juan de Fuca and North American plates beneath the shelf and upper slope, and transmission of resulting compressional forces. West of the outer-arc high, a structural transition from convergence-normal (NW) to arc-parallel (N-S) fold trends within the accretionary wedge (thin dashed line on Fig. IV.3) coincides with a topographic break and is interpreted as a structural boundary where the principal horizontal stress is rotated from convergence parallel to margin parallel. Goldfinger et al. (1992, 1996b) suggest that this "backstop" may also be the updip limit of the seismogenic plate boundary. Recent investigations of active structures deforming the innermost shelf and coastal region suggest that N-S compression may be dominant (McNeill et al., Chapter III and in press), in contrast to convergence-related E-W compression on the slope and outer shelf, but in agreement with the measured regional maximum horizontal compressive stress for the onshore northwestern U.S. (e.g., Zoback, 1992). This change in maximum compressive stress across the forearc is evident locally on the structure contour map of the late Miocene unconformity. Examples of this change include the Nehalem Bank fault (McNeill et al., in press) and the probable southeastern extension of the Stonewall Bank anticline (Fig. IV.6), whose trends change from N-S to ~ E-W as they approach the inner shelf and coastline. Yeats et al. (1998) earlier suggested that the Stonewall anticline (and reverse fault) plunges to the southeast. However, the abrupt southern termination of the Newport syncline suggests a structural origin, possibly related to the landward SE to E-W-trending extension of the Stonewall Bank structure. Both Stonewall Bank and the Nehalem Bank faults are seaward-verging, probable blind reverse faults. A similar change in trend is seen in a shallow syncline north of Siltcoos Bank (Fig. IV.6), although this structure is located in a region characterized by predominantly N-S-trending structures. Structures indicating ~E-W compression are dominant throughout much of the former shelf forearc basin, suggesting that N-S compression is restricted to the innermost shelf (supporting the conclusions of McNeill et al., in press). This is contrary to the suggestion that the edge of Siletzia represents the landward transition from convergence-related compression to regional N-S compression (Fleming, 1996). The results shown here suggest that this transition in stress fields is located landward of the seaward edge of Siletzia off central Oregon, and is also independent of this terrane in offshore northernmost Oregon and Washington where Siletzia is entirely onshore while the landward transition to N-S compression remains on the mid-inner shelf (McNeill et al., in press).

IV.5.3.3 Basin Morphology and Gravity and Magnetic Anomalies

The magnetic anomaly field underlying Heceta Bank (Fig. IV.7) is composed of a signal from the seaward-dipping Siletzia boundary and from a more westerly accreted ridge or basement sliver with similar magnetic properties (Fleming and Tréhu, submitted). The shape of the magnetic anomaly gradient echoes that of the morphological shelf break (Fig. IV.7). This similarity supports the hypothesis that the magnetic basement acts as a backstop for uplift of this submarine bank, as hypothesized by Fleming (1996) and Fleming and Tréhu (submitted). Elsewhere, the shelf edge and transitions in structural style appear to have little direct correspondence to the magnetic anomaly gradient which represents the Siletzia boundary (the magnetic anomaly is also controlled by the polarity of flows). The possible southeastern onshore projection of the Nehalem Bank fault can be seen as a magnetic high underlying the Coast Range, suggesting uplift of the underlying Siletzia basement and landward extension of the Nehalem Bank fault (Fig. IV.7).

Gravity lows are associated with Newport and Netarts synclines, the downthrown southern side of the Nehalem Bank fault, and a syncline underlying the Siltcoos Embayment (Figs. IV.1, IV.8). Moderate gravity highs are associated with the inner shelf region east of Nehalem and Heceta Banks, coincident with relative uplift of the unconformity and high uplift rates onshore (Figs. IV.6, IV.8). Heceta Bank is associated with a significant gravity high interpreted to be a result of uplifted high-density pre-Pliocene strata. However, Nehalem Bank is not associated with a similar gravity high, supporting the hypothesis that it has experienced reduced uplift rates and/or is underlain by a thicker sequence of younger, less dense sediments.

IV.5.3.4 Tectonic Influence of the Siletzia Terrane

Considering the abrupt westward change in basement lithology from the Eocene oceanic basalt of the Siletzia terrane to marine strata (Snively et al., 1980; Snively and Wells, 1996) of equivalent age and younger underlying the continental shelf and upper slope of offshore Oregon, there is minimal regional structural change in deformation across this boundary, as interpreted from deformation of the late Miocene unconformity (Figs. IV.6, IV.7). The Siletzia margin does not control the position of the outer-arc high of the shelf forearc basin, with a possible exception at Heceta Bank (Fig. IV.6). The transition from seaward convergence-driven E-W compression to landward N-S regional

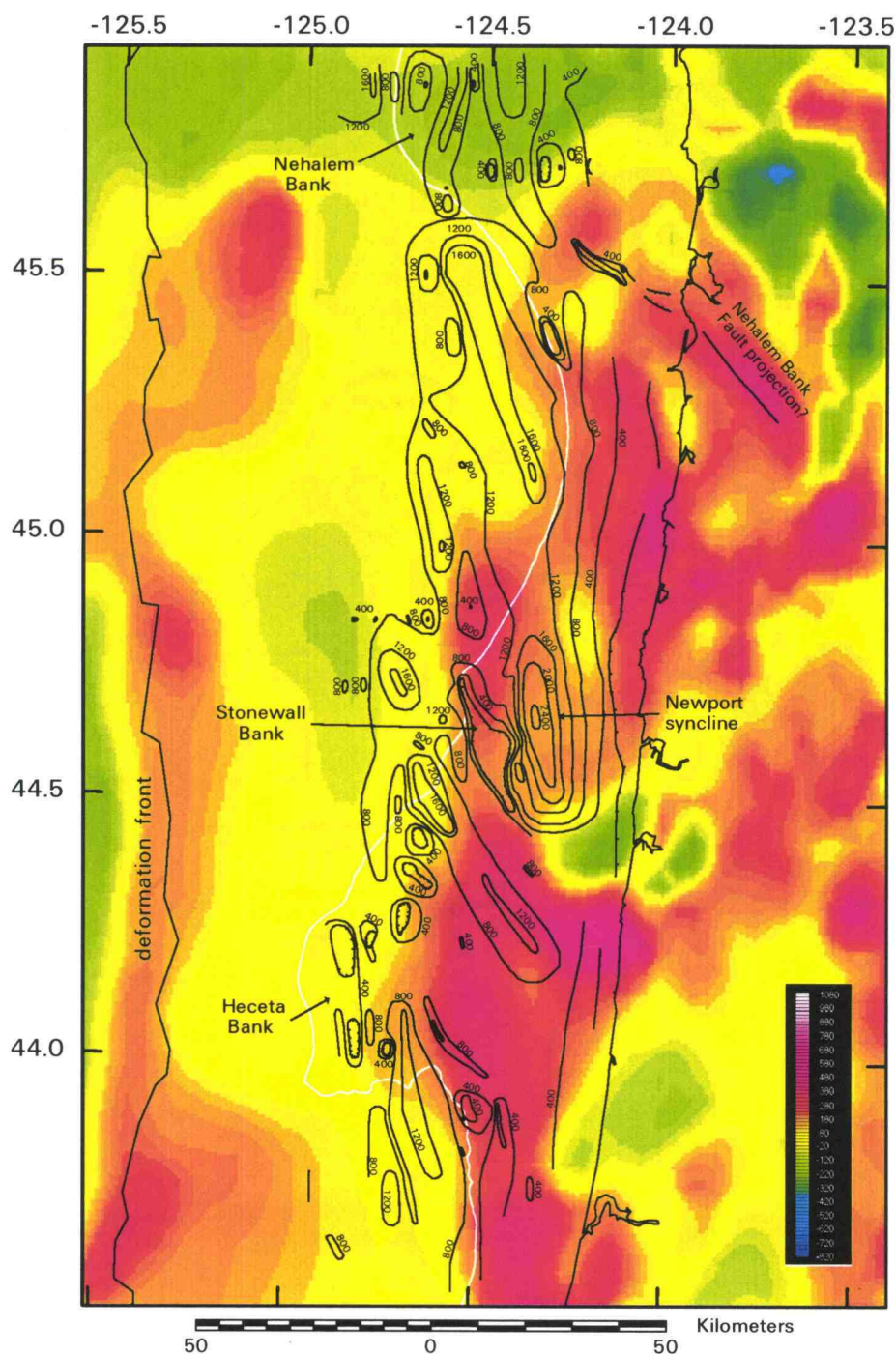


Figure IV.7 Magnetic anomaly data (nT) of central Cascadia margin, from NGDC dataset with structure contours of the late Miocene unconformity superimposed. Seaward edge of the red magnetic high represents Siletzia margin, which underlies eastern edge of Heceta Bank and western edge of Stonewall Bank. Note the magnetic high associated with the southeastern projection of the Nehalem Bank Fault. White line indicates shelf edge.

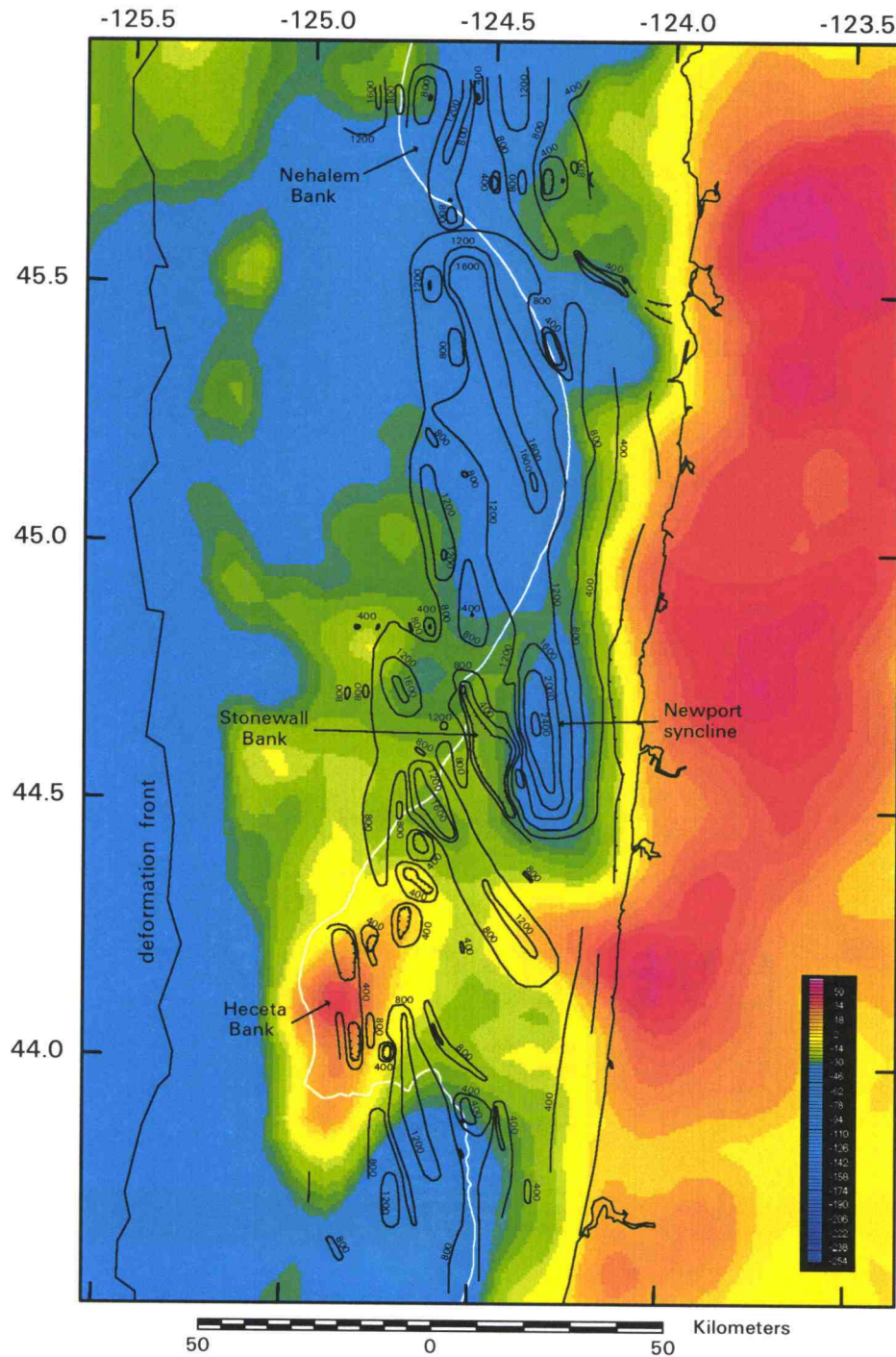


Figure IV.8 Gravity anomaly data (mgal) of central Cascadia margin, from NGDC dataset with structure contours of the late Miocene unconformity superimposed. Free air gravity offshore, Bouguer gravity onshore. White line indicates shelf edge. Note gravity highs associated with Heceta Bank and eastern Nehalem Bank. Gravity lows are associated with Newport syncline, basins underlying Netarts and Siltcoos embayments (see Fig. IV.1), and the downthrown side of the Nehalem Bank Fault.

compression does not coincide with the Siletzia margin but occurs fairly consistently on the inner to middle shelf between central Oregon and Washington (McNeill et al., in press). Finally, with the possible exceptions of Heceta Bank and Stonewall Bank (see Discussion), deformation above the Siletzia backstop does not appear to control uplift of the prominent submarine banks. It appears that the Siletzia margin does not represent as significant a structural backstop as has previously been hypothesized. However, the wavelength of compressional folding changes over the seaward margin of Siletzia, with shorter wavelength folds over the margin relative to fold wavelength on Heceta Bank to the east and the accretionary wedge to the west (Tréhu et al., 1994, 1995; Yeats et al., 1998; C. Hutto, pers. comm., 1998). The Siletzia terrane is also indirectly related to the width of the offshore forearc and tapered wedge angle, due to its control on the location of the overpressured mélange underlying the forearc basin which leads to gravitational extension of the Washington forearc (McNeill et al., 1997).

IV.5.3.5 Variations in Margin-parallel Uplift and Relative Plate Coupling

N-S trending structures deforming the late Miocene unconformity are discontinuous in a margin-parallel direction, suggesting margin-parallel variation in deformation rates. This is also suggested by variations in relative uplift rates over several time scales recorded onshore from Pleistocene marine terrace elevations (West, 1986; West and McCrumb, 1988; Kelsey et al., 1994), highway releveling surveys from this century (Mitchell et al., 1994), incision rates of Coast Range streams (Personius, 1995), and Coast Range topography (Kelsey et al., 1994; Personius, 1995) (Figs. IV.6, IV.9). The cross section A-A' of the late Miocene unconformity surface (Fig. IV.6) was chosen as a line parallel to the coastline and therefore approximately parallel to the onshore cross sections and as a line which was representative of the general features of the deformed surface. Figure IV.6 should also be referred to when considering variations in uplift rates of the unconformity to fully consider the onshore-offshore correlation of margin-parallel variations in deformation.

Several of the margin-parallel cross sections suggest low uplift rates in the central Oregon coastal region relative to the northern and southern Oregon coastal region (Figs. IV.6, IV.9). This region of low onshore uplift rates coincides with the offshore Newport and Netarts synclines (Fig. IV.6). An exception to this region of low relative uplift occurs at the Yaquina Bay fault (Fig. IV.9; Kelsey et al., 1994; McNeill et al., in press). This high is not observed in deformation of the unconformity offshore suggesting that this structure does not extend far offshore, is a very young fault (McNeill et al., in press), or

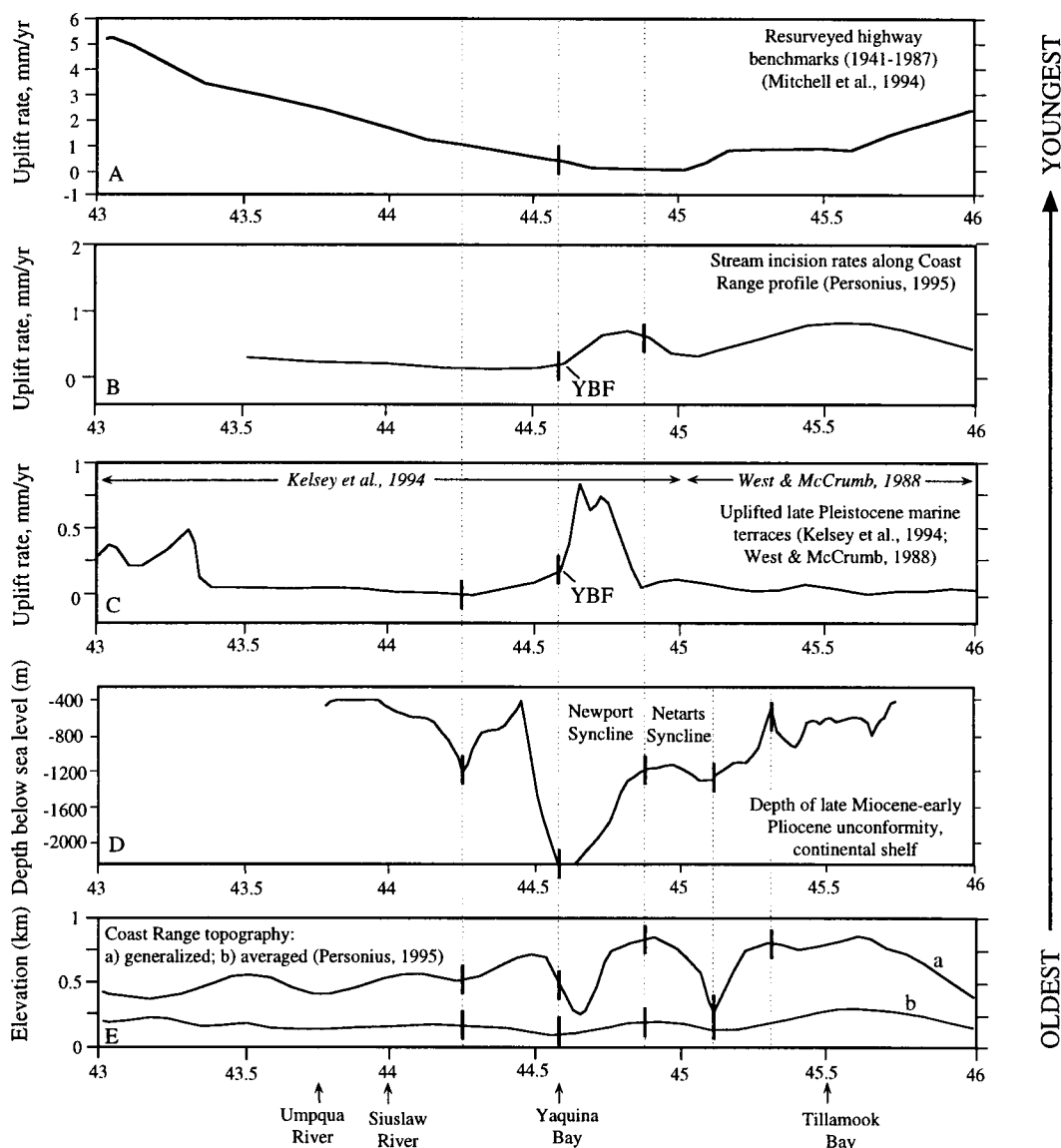


Figure IV.9. Margin-parallel uplift rates and relative uplift from the continental shelf to the Coast Range. Datasets are arranged according to age, increasing in age from top to bottom. Comparisons of these datasets indicate many similarities, such as a region of relatively low uplift centered around 44.5°N . This low is seen in resurveyed highway benchmarks (A), the deformed late Miocene unconformity on the shelf parallel to the coastline (E), and, to some extent, Coast Range topography (F) (see text for explanation of these profiles). Other local similarities are also noted - dotted lines indicate the positions of correlative lows and highs, with black heavy lines indicating where the dataset shows this trend. Local departures from these trends may be caused by local structures, such as the Yaquina Bay Fault (YBF) and possibly the Yaquina Head Fault to the north, or erosion (especially Coast Range topography). Position of unconformity cross section (A-A') and Coast Range topography and stream incision rates (B-B') shown on Fig. IV.6.

alternatively, does not exist. North and south of these prominent shelf synclines, the unconformable surface is at a relatively shallow depth. These two bordering regions are also coincident with the uplifted submarine banks, Siltcoos and Heceta to the south and Nehalem to the north. The correlation of relative uplift rates between onshore and offshore datasets measuring deformation over contrasting timescales implies that this is a long-term trend, if connected, which affects both the onshore coastal region and the continental shelf. Low uplift rates may represent a region where plate coupling is low (Mitchell et al., 1994; Goldfinger et al., 1996b) or, alternatively, a region of low permanent inelastic deformation rates. The agreement between the offshore and some onshore datasets in this region of low relative uplift supports the hypotheses that the region is deforming at a different rate from regions to the north and south and that the boundaries of this region may represent segment boundaries to rupture on the subduction zone. Local correlations can also be made between datasets: good agreement is seen between the offshore unconformity and Coast Range topography (Fig. IV.9). Local variations in topography may be dominated by erosion and bedrock lithology rather than tectonics, however, the similarities between the generalized (local) and averaged cross sections (averaging a longitudinal section of the Coast Range) suggest a tectonic signature.

IV.6 DISCUSSION

IV.6.1 Regional and Global Correlations of the Late Miocene Cascadia Unconformity

Comparisons with Neogene stratigraphy of the northeast Pacific and other continental margins allow the global significance and possible origins of the late Miocene unconformity to be established.

Post-middle Miocene Willamette Valley (and Tualatin Basin) sediments are predominantly fine-grained fluvial and lacustrine (Yeats et al., 1996) and homogeneous, therefore unlikely to reveal any significant hiatus or unconformity without accurate age control (Wilson, 1998, pers. comm., 1998). Therefore a correlation between unconformities is not possible between the shelf basin and the Willamette Valley. We would not necessarily expect stratigraphic correlation between these two basins since they were separated by Coast Range uplift. However, a late Miocene unconformity is recognized locally in the Coast Range (Armentrout, 1980; Baldwin, 1981) and in the

western Cascades (Hammond, 1979). It is important to note that contemporaneous sedimentation through the late Miocene and Pliocene (Wilson, 1998) occurred in basins east (present Willamette Valley) and west of the uplifting Coast Range. Evidence for both late Miocene hiatuses also exists on the Californian continental margin, in both onshore and offshore stratigraphy. Both the NH4 and NH6 hiatuses are identified in ODP drill site 173 on the northern California lowermost continental slope (Fig. IV.1). The stratigraphy of the onshore Eel River Basin of northern California (Fig. IV.1) reveals an unconformity and hiatus between the lower to middle Miocene Bear River beds and the overlying late Miocene Pullen Formation, the basal unit of the Wildcat Group (Fig. IV.2; Barron, 1986; Clarke, 1992; McCrory, 1989, 1995). This is coeval with an unconformity throughout California which is attributed to a major sea level lowstand at 10.5 Ma (Haq et al., 1987) and a major tectonic event (Ingle, 1986). Paleobathymetry of benthic fauna indicates in situ lower bathyal depths on either side of this hiatus (McCrory, 1995). The Wildcat Group includes a significant hiatus and possible disconformity (McCrory, 1995) at 7.8-5.3 Ma (coincident with NH6 and the proposed age of the central Cascadia unconformity), although Clarke (1992) finds the Wildcat Group to be largely conformable in this area. However, Clarke (1992) mentions an angular unconformity between the Miocene and Pliocene formations just north of Cape Mendocino in the southernmost part of the basin. This younger hiatus also corresponds to the top of the Monterey Formation of California and the Mohnian-Delmontian boundary (Keller and Barron, 1987), although the absolute age and existence of the Delmontian stage is questioned by Barron (1986) and may be equivalent to the Mohnian. The NH6 event is associated with a period of major climatic and oceanographic change, coincident with an increase in terrigenous material, increased glaciation and general cooling, intensified bottom current circulation and dissolution throughout the Pacific Basin (Ingle, 1978; Keller and Barron, 1987), and eustatic sea level fall (Barron, 1986). It is also coincident with widespread angular unconformity or disconformity throughout California, suggesting a coeval tectonic event (Barron, 1986).

On the Alaskan margin, two unconformities are present, middle-late Miocene and latest Miocene (Fisher et al., 1987), which may be the equivalents of NH4 and NH6. The younger unconformity is overlain by latest Miocene coarse-grained neritic sediments fining and deepening upwards in a typical transgressive sequence, in contrast to the Cascadia margin, where sediments indicative of a shallow marine environment (e.g., inner neritic fauna) are largely absent. The earlier unconformity is thought to be associated with tectonic erosion resulting from subduction of the Kula-Pacific ridge at 10 Ma. Stratigraphy at Bahamas Leg 166 sites indicates a prominent hiatus at ~ 8.7-6.2 Ma (Eberli et al., 1997) which may be equivalent to the 6-7 Ma hiatus in the Pacific Basin. However, this

unconformity is absent on the New Jersey slope (Leg 150) where major unconformities occur at ~ 13.5 and 11-9 Ma, both corresponding to eustatic lowstands (Lorenzo and Hesselbo, 1996). Paleobathymetry indicates transported neritic fauna and in situ bathyal fauna (Katz and Miller, 1996), suggesting these unconformities were formed below sea level. Both NH6 and NH4 appear to be globally widespread but are not always present, suggesting that, despite global driving mechanisms, regional factors are also important.

IV.6.2 Mechanism of Erosion: Subaerial vs. Submarine

IV.6.2.1 Subaerial Erosion

The absence of a regressive sequence underlying the late Miocene unconformity can be explained by erosion during the hiatus. Several hypothesized mechanisms could explain the absence of a shallow marine stratigraphic section overlying the unconformity: (1) the deposited section was sufficiently thin (low sedimentation rates) that it was not encountered during well sampling; (2) the shallow marine section, if present at all, was eroded by submarine erosion as subsidence occurred; (3) subsidence rates or rates of sea level rise were sufficiently rapid to prevent a significantly thick shallow marine section being deposited; (4) the locations of wells were such that they encountered thinner sedimentary sections on, for example, the flanks or crests of anticlines. Mechanism (1) is possible: cuttings in oil-exploratory wells were taken every 6 to 25m but identification of benthic forams and subsequent paleo-water depth calculations were not necessarily made at such frequent and regular intervals. However there is little evidence of any transgressive sequence overlying the unconformity. Mechanism (2) is possible if deposition was minimal. Submarine currents would probably be sufficiently powerful to erode these young unconsolidated sediments. Evidence of rapid sea level rise following the last glacial maximum suggests that mechanism (3) is not uncommon (Fairbanks, 1989; Bard et al., 1996) and is likely if combined with the effects of mechanisms (1) or (2). Most industry wells are located on the flanks or crests of anticlines, where accumulation rates would have been lower than within synclinal basins. However, evidence of onlapping sediments suggests that the unconformable surface was mostly planar with a gentle dip to the west, and without significant relief in most places. Therefore mechanism (4) is only likely locally.

Interestingly, sediments at the unconformable base of the Wildcat Group (~ 10 Ma) and at the 7.8-5.3 Ma hiatus within the Wildcat Group of the onshore Eel River section, in southern Cascadia, are also lower bathyal with no indication of in situ shallow marine sedimentation (McCroory, 1995).

IV.6.2.1 Submarine Erosion

Recorded current velocities on the Cascadia margin appear to be insufficient to erode older semi-consolidated cohesive silts and clays (and minor sands), although younger unconsolidated material could have been eroded and the degree of consolidation of older material is relatively unknown. In addition, two seismic reflection profiles on the inner shelf indicate that the middle Miocene Columbia River Basalts (16.5-12 Ma), were also truncated during this erosional event, if interpreted correctly (Figs. IV.4, IV.5). It seems unlikely that submarine currents would have sufficient strength to erode an intrusive basalt or basalt flow. It should also be noted that coarser grained sediments (e.g., sands and gravels) necessary for abrasion are rare in the Oregon margin stratigraphy.

Evidence of submarine-eroded angular unconformities include examples on the Walvis shelf, SW Africa (Van Andel and Calvert, 1971) and in basins of the Southern California borderlands (Teng and Gorsline, 1991). These are interpreted to result from climate change (Walvis shelf) and slow sedimentation rates during a highstand (southern California). However, the degree of angularity and truncation of underlying beds on the Cascadia margin (e.g., Fig. IV.4) far exceeds both of these examples. In addition, eroded sediments on the Walvis shelf were mostly younger and presumably less consolidated than those underlying the Cascadia unconformity. Submarine erosion is also suggested as the origin of a late Miocene-Pliocene angular unconformity in the Ventura Basin, California (Yeats, 1965) where fauna at the unconformity indicate bathyal water depths.

Positions and velocities of submarine currents may vary significantly with fluctuations in sea level. Currents would shift farther seaward as eustatic sea level fell, but variation in current strength remains uncertain. However, considering a feasible increase in velocities, it still seems unlikely that sediments of the lithology and consolidation (loosely correlated with age) indicated above could be eroded. A mechanism of slow sedimentation rates (as observed in present times in the form of glauconitic sands on uplifted highs of the Oregon shelf and upper slope) coupled with minor tectonic activity also seems unlikely. We therefore hypothesize that this unconformity was eroded subaerially, in particular

where angular truncation occurs. Seaward of the region of angular truncation (Fig. IV.3), erosion may have been submarine, or the reflector may represent a conformable contact. The presence of a landward region where the unconformity is angular versus a seaward region where the same surface is conformable or a disconformity also supports the hypothesis that this landward region was eroded subaerially. Despite the conformable appearance of this reflector in the seaward part of the basin, we hypothesize that a hiatus is still present, as at Site 892 on the continental slope.

IV.6.3 Driving Mechanism Of Erosion: Tectonics vs. Climatic Change

Significant hiatuses or unconformities are the result of regional or global tectonic effects or global climatic changes, including eustatic sea level change. If the Cascadia late Miocene unconformity was, in part, the result of subaerial erosion, as suggested above, a maximum fall in eustatic sea level of ~ 150 m is insufficient to bring these sediments to sea level and requires additional tectonic uplift. However, sea level may be a significant contributing factor.

Worldwide late Miocene eustatic lowstands (Haq et al., 1987) occurred at 10.5 (major), 8 (minor), 6.5, and 5.5 Ma, two of which coincide with global hiatuses at 10-9 Ma and 7-6 Ma. Ingle (1978) also links the Pacific Basin 7-6 Ma hiatus to a major global climatic event. The older hiatus (~10.5 Ma) is also closely linked with Pacific plate motion changes, observed in a change in orientation of the Hawaiian island-seamount chain, and rotation of the convergence vector between the Juan de Fuca and North American plates to more normal, leading to increased thrusting and uplift along this margin (McCrorry, 1995). Major plate motion changes at 7-6 Ma are not as widely reported as for the earlier event or are associated with disagreements among chronologies. Barron (1986) suggests evidence of a tectonic event linked to Pacific plate motion change at 6 Ma (Jackson et al., 1975) which is coincident with sea level fall. Wilson et al. (1984) identify a 10° clockwise rotation of the Juan de Fuca relative plate motion at 8.5 Ma, immediately preceding the NH4 hiatus, a possible result of separation of the Gorda from the Juan de Fuca plate. Wessel and Kroenke (1997, submitted) suggest that significant tectonic events throughout the Pacific Basin began at ~ 8-6 Ma, including large clockwise rotation of Juan de Fuca relative motion at 5.89 Ma (Chron 3A, Wilson, 1993, also possibly more directly connected to the separation of the Explorer Plate from the Juan de Fuca Plate). These events can be linked to the initial collision of the Ontong Java plateau with the Australian plate, resulting in anti-clockwise rotation of the absolute motion of the Pacific plate and

increased convergence rates in the northeast Pacific (Wessel and Kroenke, submitted). However, interaction intensified somewhat later at ~4-2 Ma resulting in rather more dramatic tectonic and volcanic events (Wessel and Kroenke, submitted). The NH6 event has also been loosely linked to other major tectonic events in the Pacific Basin at ~5 Ma, including the opening of the Gulf of California and the inception of the modern San Andreas system (Normark et al., 1987; Barron, 1986), though this may be a separate younger event. Riddihough (1984) suggested that a more significant clockwise rotation in Juan de Fuca plate motion occurred between 4 and 3 Ma rather than at ~5 Ma. If the offshore unconformity is associated with plate motion changes at ~10 Ma (NH4) rather than 7-6 Ma, a similar, though earlier, mechanism of uplift and erosion of the unconformity may be responsible for major uplift of the Coast Ranges (after 15 Ma, following more minor initial uplift before 15 Ma).

Potential causes of rapid vertical motions at an active margin include subduction erosion (leading to subsidence) and underplating (leading to uplift), changes in sedimentation rate, and a change in the direction, dip, or rate of the subducting plate. Subduction erosion might result from the subduction of a basement feature such as a seamount chain or ridge (e.g., von Huene and Lallemand, 1990) but would not produce the regional synchronous erosion observed here. Magnetics show that there is also little evidence of regional basement highs underlying the margin or their mirror-image equivalents west of the Juan de Fuca ridge. A change in plate motion and/or possibly plate dip is therefore the most likely cause of rapid uplift and erosion and accounts for correlation of this hiatus throughout the Pacific Basin and even globally. This global correlation may also be linked to coincident climate change (lowered sea level). Changes in Pacific plate motion around 8-6 Ma (Wessel and Kroenke, submitted), possibly resulting in clockwise rotation of the Juan de Fuca plate motion at ~8.5 Ma (Wilson et al., 1984), leading to increased normal convergence rate along the Cascadia subduction zone are a potential driving mechanism for uplift and erosion of the forearc. Relative uplift was accentuated by a simultaneous eustatic lowstand.

IV.6.4 Evolution of the Neogene Cascadia Forearc

The geometry and stratigraphy of the Cascadia forearc are a complex function of the interplay between sea level change, sedimentation, and tectonics. We attempt to determine

how the shelf forearc basin has developed through time by assessing these factors in a regional and global context.

Preserved sediments of the central Cascadia Neogene forearc basin are bound to the east by the Coast Range and to the west by a discrete outer-arc high which is parallel to the deformation front on the shelf and upper slope (Fig. IV.3). Locally the outer-arc high is a broad and complex anticlinal structure. The landward edge of the outer-arc high, i.e., the seaward limit of basinal sedimentation, or the most prominent structural and/or topographic high, is shown in Figure IV.3. At Heceta Bank, two prominent highs have been identified, although the seaward of these two structures is preferred as the main outer-arc high due to the presence of basinal sediments between them (Fig. IV.10a). Seismic evidence for ponding (westward onlap) behind the current outer-arc high is weak in older sediments, requiring the interpretation that the original western edge of the basin (former outer-arc high) was west of the westernmost preserved basin sediments. The current outer-arc high is a structural high (Figs. IV.10a, b, c) whose formation caused basinal sediments to pond behind it. Landward basinal growth strata suggest that uplift of this outer-arc high began in the early-mid Pliocene on much of the central-northern Oregon margin (Fig. IV.10b, c), but possibly slightly later (mid-Pliocene) on Heceta Bank to the south (Fig. IV.10a). Stratigraphic ages in the extreme seaward portion of the basin are uncertain, therefore, the exact timing of uplift cannot be determined. However, we are fairly certain that this outer-arc high post-dates formation of the late Miocene unconformity and correlative seaward conformity or disconformity. Prior to uplift on this structure, the forearc basin extended farther west (Fig. IV.11a, b, c), as indicated by pre-Pliocene sediments thickening slightly towards the outer-arc high (Fig. IV.10), and was bounded by an older outer-arc high. This pre-Pliocene outer-arc high is not recognized in any seismic lines. The western edge of the older basin was truncated, and eroded sediments were probably accreted or subducted. Truncation and erosion or slumping at the edge of the shelf basin is supported by the incorporation of Miocene (and possibly Eocene) bathyal sediments into the second accretionary ridge seaward of the basin (now at 700m water depth, ODP Site 892; Fourtanier and Caulet, 1995; Fourtanier, 1995; Caulet, 1995; Zellers, 1995). We hypothesize that the most recent outer-arc high (Fig. IV.3) represents a truncational structural boundary against which the mid-Pliocene to Pleistocene accretionary wedge is built (Fig. IV.11d). The truncation boundary may be represented by a region of complex, probably faulted, stratigraphy just west of the outer-arc high, observed in seismic reflection records (e.g., Fig. IV.10c). The accretionary wedge is too narrow to incorporate late Miocene to recent accreted sediments based on recent sedimentation and accretion rates (Westbrook, 1994), suggesting that either sedimentation and accretion rates have increased

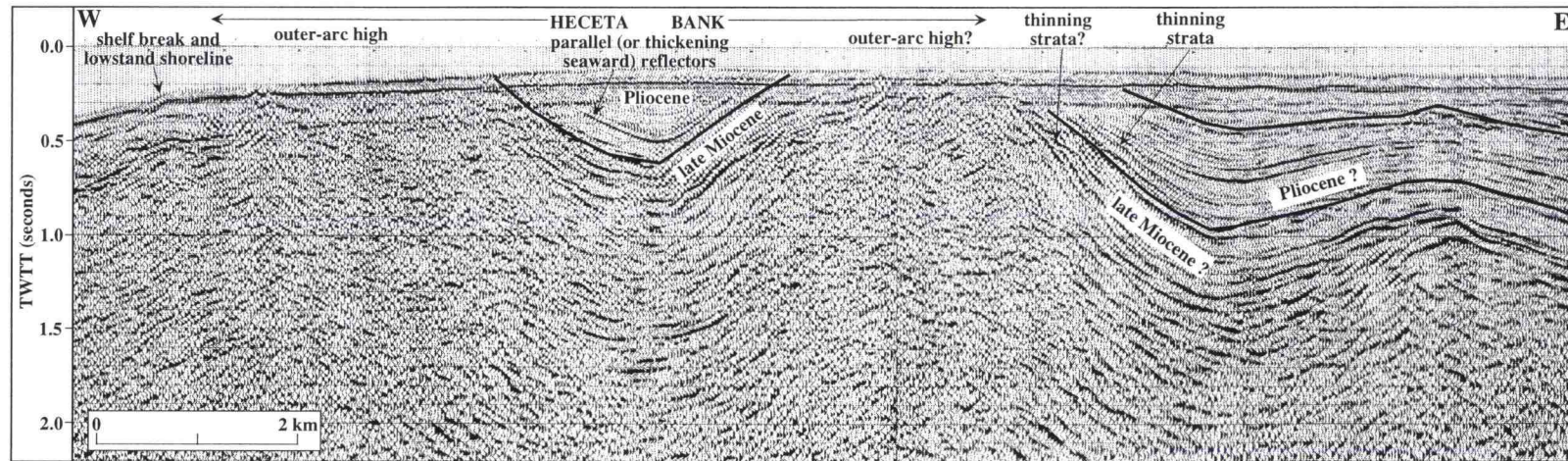


Figure IV.10a. E-W multichannel seismic reflection profile across Heceta Bank showing the outer-arc high of the Neogene forearc basin (located on Fig. IV.1). On the continental shelf, the outer-arc high has been truncated during Pleistocene lowstands, therefore it lacks topographic relief in contrast to the upper slope (Fig. IV.10b, c). The outer-arc high is composed here of two parallel anticlines (see Fig. IV.3), the outermost of which we interpret as the outer-arc high due to a small structural basin between them. On this profile, there is little evidence of growth strata in early (-mid?) Pliocene sediments in the smaller basin, suggesting uplift of the seaward major outer-arc high some time in the mid Pliocene. However, thinning of strata of the main basin suggest that major growth of the eastern outer-arc high followed the formation of the late Miocene unconformity with minor growth in the late Miocene (pre-unconformity (Pliocene) strata show some thinning and erosional truncation; overlying Pliocene strata thin towards the high). However, the exact age of sediments is unknown. From this profile and others across Heceta Bank, we interpret that growth of the main outer-arc high in this region began in the middle Pliocene.

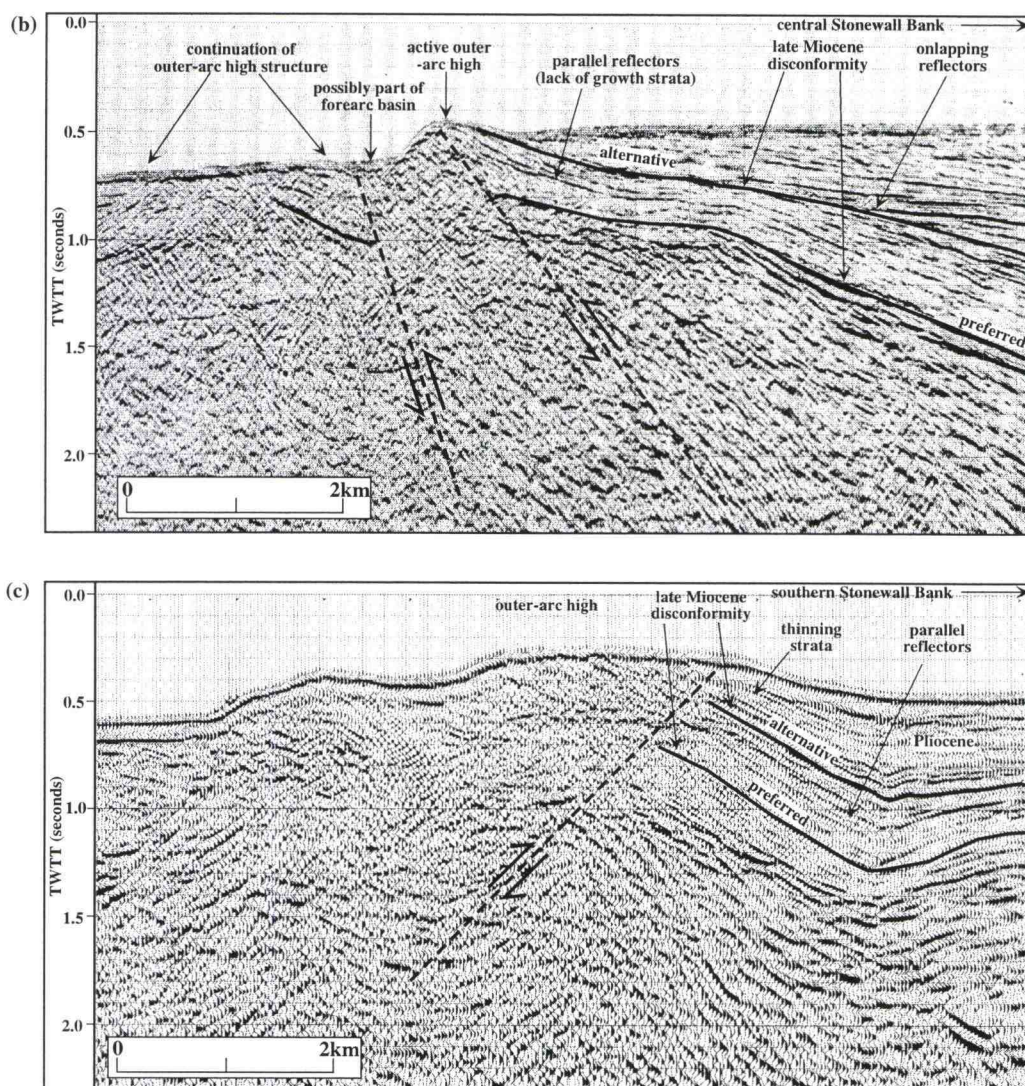
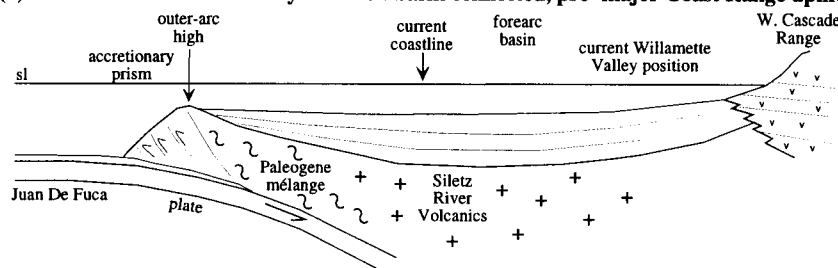


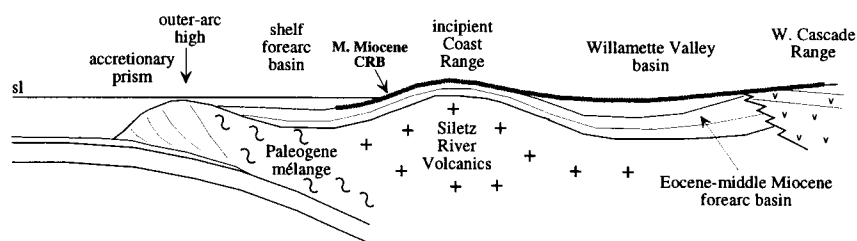
Figure IV.10b, c. E-W multichannel seismic reflection profiles across the upper slope of the central Cascadia forearc (locations on Fig. IV.1). Both profiles cross the structural outer-arc high on the upper slope west of Stonewall Bank where its relief has not been truncated during late Pleistocene lowstands. (b) crosses the outer-arc high west of central Stonewall Bank and (c) just to the south at the southern end of the bank. In both profiles, the position of the late Miocene disconformity (correlative to the landward angular unconformity) is uncertain due to poor age control and non-angularity. Preferred and alternative positions are given. Preferred positions are both overlain by parallel strata suggesting that growth of this outer-arc high did not begin until the mid-late Pliocene (indicated by seaward thinning in the upper part of the basin). Alternative positions are overlain by thinning strata suggesting that, alternatively, growth of the outer-arc high began soon after the late Miocene erosional event, in the early Pliocene. In both (b) and (c), the outer-arc high is not a simple anticline but a broader structure composed of more than one anticline: this is common in other regions of the forearc basin. Possible positions of reverse faults are also shown, underlying the high, and associated with uplift of the underlying mélangé (discontinuous reflectors).

Figure IV.11. Tectonic history of the Neogene central Cascadia forearc depicted by time slice cross sections of the central Oregon forearc from the Cascades to the deformation front. Stratigraphy and topographic features are generalized for the central Oregon forearc. (a) represents the Willamette Valley and shelf basins connected prior to major uplift of the Coast Ranges (with local highlands existing), (b) represents Columbia River Basalt emplacement and incipient Coast Range uplift, (c) represents erosion of the late Miocene unconformity, (d) represents Pliocene basin filling and truncation of the seaward edge of the offshore basin, and (e) represents shelf basin filling and submarine fan formation in the Pleistocene.

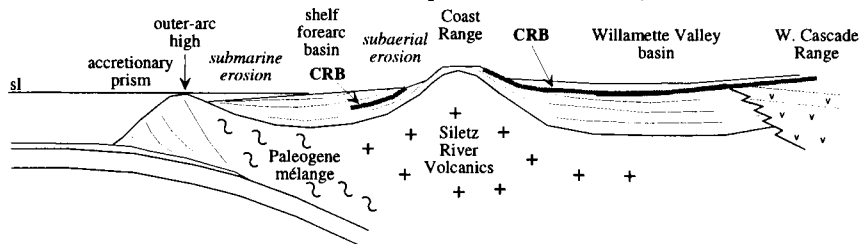
(a) > 20 Ma - Willamette Valley and shelf basin connected, pre- major Coast Range uplift



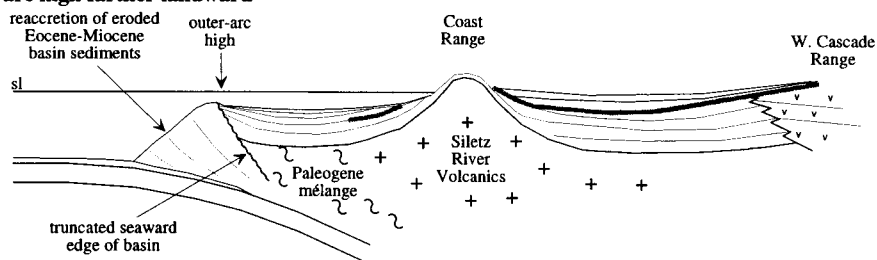
(b) 16.5-15 Ma - Broad folding of Columbia River Basalt (CRB), incipient Coast Range uplift



(c) 7.5-6 Ma - late Miocene erosion (tectonic uplift, eustatic lowstand)



(d) Early-Mid Pliocene - basin filling, truncation of seaward basin, formation of new outer-arc high farther landward



(e) ~1.3-1.4 Ma - Outer-arc high breached, sediments bypass continental shelf, submarine canyon and fan formation, accretionary prism growth

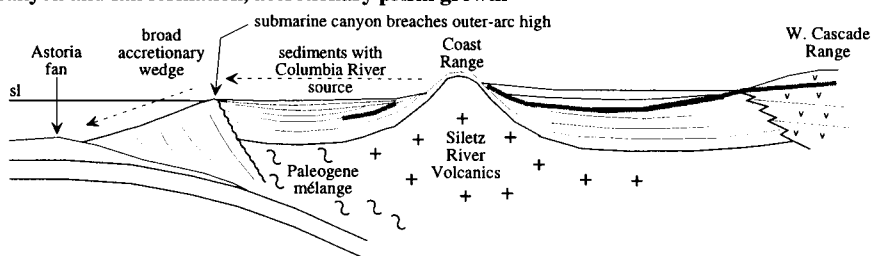


Figure IV.11

dramatically during the Quaternary or that a significant erosional event, possibly a result of subduction erosion, removed much of the late Miocene and early Pliocene wedge. The same erosional event may have been responsible for erosion of the seaward edge of the forearc basin. If the shelf forearc basin did originally extend farther seaward, the accretionary wedge was either west of its current position or narrower. The former is contrary to the general assumption that the margin and wedge have gradually built westward with time, whereas the latter may be a reflection of relative sediment budgets of the basin and the accretionary wedge, with alternating growth of the wedge and filling of the forearc basin, controlled by growth of the outer-arc high. Basin filling and growth of the outer-arc high in conjunction with sea level change and sediment input therefore control the rate of growth of the accretionary wedge.

To the east, the Willamette Valley basin was formerly partially connected to the offshore basin prior to the major late Miocene uplift of the Oregon Coast Range. Following uplift of the Oregon Coast Range (uplift underway at the time of Columbia River Basalt (CRB) flows at ~16.5-15 Ma with major uplift beginning ~15 Ma following emplacement of CRB flows which reached the Coast Range and coast (Yeats et al., 1996)), the two basins were separated (Fig. IV.11b, c). The formation of such a double forearc basin-outer arc high is unusual on continental margins, but is also present on the NE Alaskan margin, where seaward (Sanak, Shumagin, Tugidak, Albatross, Stevenson) and landward (Cook Inlet and Shelikof Strait) basins are separated by the uplifted Kodiak Island and Kenai Peninsula (von Huene et al., 1987).

IV.6.4.1 Submarine Bank Morphology and Origin

The positions of uplifted submarine banks and intervening embayments control the morphology of the current Oregon shelf break, which post-dates the formation of the shelf basin outer-arc high (in the Pliocene). Miocene rocks below the unconformity are exposed at these banks, which include Nehalem, Stonewall, Heceta, and Siltcoos Banks (Fig. IV.6), and Coquille Bank to the south. To determine the origin of the modern shelf break, we must determine what causes uplift of the submarine banks and/or the creation of the morphological embayments between these banks.

The most plausible mechanisms for localized submarine bank uplift appear to be (a) uplift above a subducted or accreted basement feature or (b) uplift above an active reverse fault or fault zone. The latter is the preferred origin of the active Stonewall Bank (Yeats et al., 1998) and probably drives the uplift of Siltcoos Bank, west of Florence, which has a

N-S trend similar to surrounding active structures. Stonewall Bank overlies the western edge of the basaltic Siletzia terrane (as modeled from magnetic anomaly data, e.g., Tréhu et al., 1994, 1995; Fleming, 1996; Fleming and Tréhu, submitted; Fig. IV.7), which may be related to its uplift mechanism. Fleming (1996) suggested that the Stonewall Bank blind reverse fault may be a reactivation of the late Eocene Fulmar fault of Snively (1987) which truncates the seaward margin of the Siletzia terrane. However, Stonewall Bank anticline trends slightly oblique (NW) to the N-S trending edge of Siletzia, therefore the two faults are probably unrelated unless the Stonewall Bank fault represents a fault splay.

Heceta and Nehalem Banks are much larger features than Stonewall or Siltcoos banks, with probable differing origins. The seaward Siletzia margin and accreted basement ridge (Fleming and Tréhu, submitted) underlie the eastern edge of Heceta Bank (although landward of the highest uplift rates, from Kulm and Fowler (1974)) and may drive the uplift of this bank. Heceta Bank is the only location where the uplifted basin outer-arc high is located on the current continental shelf: to the north and south, the high is located on the present upper slope or close to the shelf break. A Siletzia backstop may contribute to pronounced uplift associated with the outer-arc high at Heceta Bank. On the northern Oregon shelf, the outer-arc high maintains an approximately N-S trend across the upper slope and shelf break, whereas the Siletzia boundary trends northeasterly and landward (Fig. IV.6; Fleming and Tréhu, submitted). This suggests that an alternative backstop controls the position of the outer-arc high in northern Oregon and in Washington where the basaltic terrane is located entirely onshore.

Nehalem Bank is of comparable size to Heceta Bank. It is located farther seaward of Siletzia (Fig. IV.6), and uplift is less pronounced than Heceta Bank (Kulm and Fowler, 1974). The shelf basin outer-arc high is located just seaward of Nehalem Bank, with the bank itself underlain by up to 1.5 km of post-Miocene basinal sediments. Miocene sediments are only uplifted to the seafloor locally. Nehalem Bank may coincide with a region of higher sedimentation rates due to its proximity to the Columbia River. The uplift mechanism of this bank remains poorly understood, although it may be related to diapiric intrusions of the underlying *mélange* (Niem et al., 1992).

IV.6.4.2 Morphology and Origin of the Modern Shelf Break

The current shelf edge is a continuous morphological feature linking the uplifted submarine banks (Siltcoos, Heceta, Stonewall, Nehalem) and lying landward of actively subsiding synclines between these banks (forming Netarts and Siltcoos embayments). The

shelf edge follows the landward flank of the northwest extension of the Newport syncline (Netarts syncline) in Netarts Embayment (Fig. IV.6). We note that much of the eastern and southern flanks of the Netarts syncline coincide with the seaward margin of the Siletzia terrane (Fig. IV.6); possibly this syncline may, in part, be a result of subsidence just seaward of the rigid basement. The high separating Newport and Netarts synclines at 45°N may therefore also be controlled by the basement. This is one of the few examples of probable control of the location of the shelf edge by the Siletzia terrane. At Newport syncline itself, the shelf edge turns to the southwest towards Stonewall and Heceta banks. Recent uplift (late Pleistocene and (?) Holocene) of Stonewall Bank forces the shelf break seaward at this location. The shelf edge may have continued south along the landward flank of the Newport syncline prior to further uplift of Stonewall Bank. Structural trends appear to cross the shelf break at an oblique angle, e.g., west of Stonewall Bank and south of Heceta Bank (Fig. IV.6), suggesting that the modern shelf break formed recently.

IV.6.4.3 Indications of Paleo-Shelf Edge Positions

We hypothesize that the N-S-trending outer-arc high represented the former shelf edge following filling of the forearc basin. Miocene and Pliocene units uplifted at the outer-arc high within the Netarts Embayment (Fig. IV.10b, c) are truncated at sharp angles suggesting subaerial erosion. At the beginning of the Pleistocene when the basin filled and at the onset of significant sea level lowstands, the entire basin was probably abraded. Subsequent to the formation of the current shelf edge and relative subsidence within geomorphic embayments (Netarts and Siltcoos embayments), the outer-arc high was abraded on the continental shelf during more recent Pleistocene lowstands (Fig. IV.10a), but maintains topographic expression on the slope within shelf embayments (Figs. IV.10b, c) as the outer edge of the Cascade Bench of Kulm and Fowler (1974) (Figs. IV.1, IV.3). Topographic relief of the outer-arc high (Figs. IV.10b, c) must have formed subsequent to early Pleistocene abrasion and therefore indicates recent activity on this structure. A similar bench is identified north and south of Coquille Bank and on the southern Oregon upper slope (Klamath Plateau of Kulm and Fowler (1974)). We hypothesize that the seaward edge of these benches represents the southern continuation of the outer-arc high identified in central and northern Oregon, probably eventually connecting to the Eel River Basin of the southern Cascadia margin (Fig. IV.1). The present shelf break was subsequently formed as a result of continued submarine bank uplift and subsidence within intervening synclinal embayments (see IV.6.4.2).

IV.6.4.4 Paleoshoreline Position

The position of the former shoreline during the late Miocene and Pliocene can also be estimated. The distribution of sandstone and mudstone units within the coastal and offshore sequence is similar to modern seafloor distributions of sand and mud (Maloney, 1965), suggesting that the shoreline has remained in approximately the same position throughout this period, relative to eustatic sea level fluctuations. This is supported by the relative scarcity of late Miocene to early Pleistocene sediments on the Oregon coast and in the Coast Range (exceptions include the Pliocene Troutdale Formation of the ancestral Columbia River, and upper Miocene strata on the southern Oregon coast near Coos Bay; Christiansen and Yeats, 1992; Snively and Wells, 1996), indicating predominant subaerial erosion rather than deposition. These strata may also be absent due to Quaternary erosion. Interestingly, late Miocene (Montesano) and Pliocene formations (Quinalt and Quillayute) are locally preserved in the coastal regions of the Olympic Peninsula, Washington (Palmer and Lingley, 1989), suggesting that the shoreline here was somewhat farther to the east and has been migrating westward towards its present position due to uplift of the Olympic Mountains, which began at ~ 18 Ma (Brandon et al., 1998). In addition, paleobathymetry of Pliocene samples on the Oregon mid-shelf indicate water depths (45-90m) similar to current depths (Yeats et al., 1998). The shoreline appears to have acted as a hinge line during the post-middle Miocene uplift of the Oregon Coast Range and subsidence of the adjacent Neogene shelf forearc basin.

IV.6.4.5 Timing of Shelf Basin Filling and Submarine Canyon Formation

Forearc basin and abyssal plain stratigraphy suggest that the offshore Neogene forearc basin was almost entirely filled and the outer-arc high breached at some time during the Pleistocene, forming the Astoria submarine canyon, the primary conduit for Columbia River sediments to the slope and abyssal plain (Fig. IV.11e). The Astoria Canyon is the only major submarine canyon on the central Cascadia slope, in contrast to the Washington slope which is dissected by several prominent canyons (Barnard, 1978; McNeill et al., 1997). On the southern Oregon slope, the Rogue Canyon (Fig. IV.1) acts as a conduit for Rogue River sediments from the Klamath Mountains. The shelf was subsequently bypassed by sediments and truncated during Pleistocene lowstands. The base of the Astoria submarine fan was reached at 264 m below the seafloor at Site 174A (DSDP, Leg

18, Figs. IV.1, IV.2, IV.12) and was subsequently redated and recalibrated at 0.76 ± 0.5 Ma (Goldfinger et al., 1996a). However, the base of the Pleistocene fan is time transgressive and therefore somewhat older landward, where the oldest fan sediments have now been accreted. At Site 174A, a change in heavy mineral assemblage occurs below the base of the fan (Fig. IV.12), at 370 m below the seafloor (Fig. IV.2), and is dated approximately at 1.5 Ma, representing the beginning of Columbia River sediment provenance (Scheidegger et al., 1973). Prior to this time, heavy minerals suggests a non-Columbia River source from the north (British Columbia) or south (Klamath Mountains). The same change in sediment provenance between early and late Pleistocene sediments is observed in accreted deep water sediments at Leg 146 sites (e.g., site 892) on the Cascadia slope (Chamov and Murdmaa, 1995). Late Pleistocene sediments at Site 175 on the lower slope (Fig. IV.1) are also of Columbia River source (Fig. IV.12; Scheidegger et al., 1973; von Huene and Kulm, 1973). Scheidegger et al. (1973) suggested that the mineralogy change at Site 174 may have resulted from translation of the subducting plate to the northeast toward the Columbia River source. However, translation in this short period of time (~ 1 -2 Ma) would only result in 50-100 km of northeasterly migration (Chamov and Murdmaa, 1995; Westbrook, 1994). Columbia River sediments were transported southward during the late Pleistocene, as indicated by probable Columbia River source clay mineralogy in late Pleistocene sediments in the Escanaba Trough of the Gorda plate, more than 500 km to the south (McManus et al., 1970; Fowler and Kulm, 1970). This suggests that a more southerly position of Site 174 during the early Pleistocene cannot account for a significant change in mineralogy. Diagenesis of older sediments was also proposed as a possible cause of the mineralogy change (Chamov and Murdmaa, 1995), however, Scheidegger et al. (1973) found little evidence of modification of the heavy mineral assemblages at Sites 174 and 175. As an alternative hypothesis, we propose that this change in mineralogy, at ~ 1.3 -1.4 Ma (see below for details of age determination) coincides with the filling of the shelf basin in Oregon, breaching of the outer-arc high, and development of the current Astoria Canyon, as also suggested by von Huene and Kulm (1973). This change represents the onset of early submarine fan deposition in the trench and distal turbidite deposition at Site 174, followed by westward progradation of the Astoria Fan to Site 174 by 0.76 Ma. The earliest, more landward submarine fan deposits have since been accreted and incorporated into the two thrust ridges closest to the deformation front (Kulm and Fowler, 1974). At Site 176, on the seaward edge of the shelf basin off northern Oregon (Fig. IV.1), Pleistocene to possible late Pliocene sediments all indicate a Columbia River source (Scheidegger et al., 1973) as predicted from a model of basin filling. The presence of sediments of Pleistocene age within the uppermost shelf

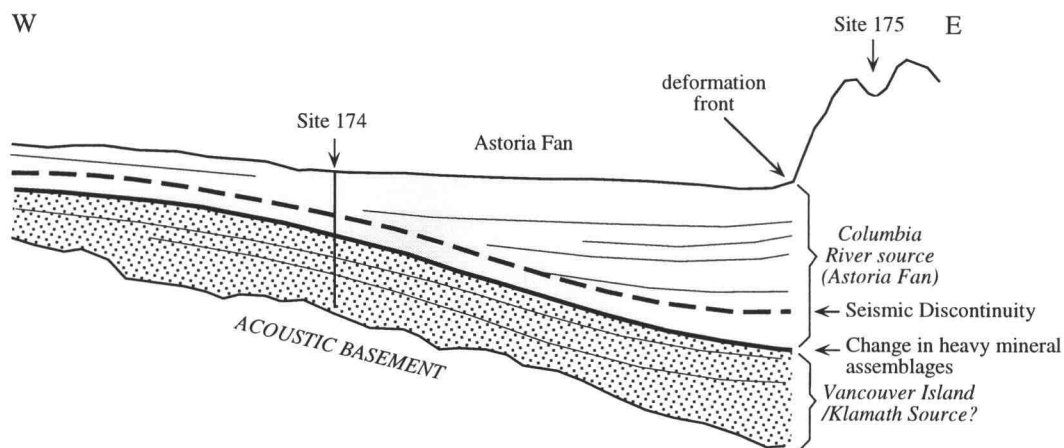


Figure IV.12. Sketch of E-W seismic reflection profile across the Astoria Fan and lower accretionary wedge at ODP Sites 174 and 175 (after von Huene and Kulm, 1973). A seismic discontinuity represents the base of the Astoria Fan sands (0.76 Ma), however, this is underlain by a change in heavy mineral assemblages. This marks the transition from upper Columbia River source to a lower more distal source (possibly Vancouver Island to the north or Klamath Mountain to the south). We hypothesize that the onset of Columbia River source sedimentation coincides with initial breaching of the forearc basin outer-arc high and inception of the Astoria submarine canyon. This transition is dated at approximately 1.3-1.4 Ma.

basin at Site 176 (Fig. IV.2) indicates that sedimentation continued to some degree within the shelf basin in the vicinity of the Columbia River mouth following initiation of the early Pleistocene Astoria submarine canyon and fan system. We cannot prove whether sedimentation within the shelf basin continued throughout the Pleistocene south of this site. Prior to this time, sedimentation rates on the abyssal plain and slope would have been significantly reduced, resulting in reduced accretion rates and a narrower accretionary wedge.

Unfortunately the change in mineralogy and sediment source was not redated along with the Astoria fan base. However, its age can be more accurately determined using Site 174A stratigraphy and assumptions concerning sedimentation rates. An assumed constant sedimentation rate for the period between the Plio-Pleistocene boundary and initial Columbia River source sediments yields an age of 1.3-1.4 Ma for the mineralogy change (Fig. IV.2). This is a maximum age for this transition as sedimentation rates at Site 174 may have increased through the Pleistocene.

The early Pleistocene unconformity, identified on the Washington, Oregon, and northern California shelf (Fig. IV.2) may be coincident with the mineralogy change and breaching of the outer-arc high. This unconformity is probably at least 0.92 Ma at Site 176 on the northern Oregon shelf (Fig. IV.2, Kulm et al., 1973), earliest Pleistocene on the Washington shelf (Palmer and Lingley, 1989), and ~ 1 Ma marking the top of the Rio Dell Formation in Eel River Basin stratigraphy off northern California. This tentative correlation suggests that filling and bypassing of the basin may have been driven by regional tectonic uplift and/or eustatic sea level fall. A slightly younger angular unconformity (0.7-0.6 Ma), clearly identifiable in stratigraphy onshore (McCrory, 1995) and in seismic records offshore (Clarke, 1992), marks the end of marine sedimentation within the Eel River Basin (the upper boundary of the Carlotta and Scotia Bluffs formations, McCrory, 1995) coincident with a significant tectonic event throughout the Pacific Basin (Ingle, 1986).

IV.6.5 Comparisons With the Washington Shelf Forearc Basin and the Eel River Basin of Northern California

The outer-arc high bounding the shelf forearc basin on the Washington margin to the north is not as prominent as on the Oregon margin, as observed in seismic reflection records (see McNeill et al., 1997). Extension along listric normal faults and pervasive gravitational failure of the outer shelf and upper slope is a result of the downslope

movement and extension of the underlying weak *mélange* and broken formation (McNeill et al., 1997). This results in an unstable shelf break and forearc basin margin which probably prevented the growth of a significant structural outer-arc high. We hypothesize that this resulted in a minor topographic barrier which was easily breached during Pleistocene lowstands forming many prominent submarine canyons (Barnard, 1978; McNeill et al., 1997). We believe this contributed to the significant number of submarine canyons on the Washington margin compared with the rest of the Cascadia margin, along with the significantly increased sediment input in Olympic Peninsula rivers from Cordilleran Ice Sheet lobes (the broad valley of the Chehalis River, which drains into Grays Harbor, drained a glacial lake in front of the Puget lobe with a discharge probably several times larger than the present Columbia River (McKee, 1972)). In north-central Oregon, only one significant submarine canyon formed during the Pleistocene: the Astoria Canyon. We presume that the Columbia River is the major source of sediments for the central Cascadia shelf forearc basin prior to inception of this canyon. The next significant submarine canyon to the south is the Rogue Canyon.

The offshore stratigraphy and structure of the offshore Eel River Basin is poorly known in contrast to the well-documented onshore Centerville Beach exposure of the southern Eel River Basin (Clarke, 1992). Therefore correlations between the offshore central and southern Cascadia forearc basins are complex. Clarke (1992) also points out the time-transgressive nature of units on an active margin, preventing direct correlation between the onshore and offshore stratigraphy. As discussed above, the onshore Eel River Basin stratigraphy suggests a similar sequence of hiatuses and unconformities to those observed on the central Cascadia margin, although it should be noted that an angular unconformity at ~ 7-6 Ma (NH6) may not be present throughout the onshore Eel River Basin sequence (Clarke, 1992; McCrory, 1995). The correspondence of hiatuses throughout the Cascadia stratigraphy (and the remaining northeast Pacific margin) support a regional tectonic driving mechanism such as changes in plate motion.

Clarke (1992) identifies an E-dipping structural discontinuity (SD) in seismic reflection records of the offshore Eel River Basin, which marks a transition in fold trends and may be similar to a transition from margin-parallel to convergence-normal fold trends observed on the Oregon slope (Fig. IV.3; Goldfinger et al., 1996b). Goldfinger et al, (1992, 1996b) suggested that this discontinuity may represent the updip limit of the interplate seismogenic zone. Is this the southern Cascadia equivalent of the outer-arc high on the central Cascadia margin? Interpreted seismic records (Clarke, 1992) indicate that basinal sediments extend west of this discontinuity, which shows little tectonic uplift, and that a more prominent structural high just to the west marks the boundary between basinal

sediments and the accretionary wedge and is coincident with the topographic shelf break (see Figure 7 of Clarke, 1992). We hypothesize that this structure may be the outer-arc high of the Eel River Basin.

IV.7 CONCLUSIONS

The Neogene central Cascadia forearc basin provides evidence for a complex history of vertical tectonics and sedimentation. This history and regional correlations are summarized below and illustrated in Figure IV.11:

- (1) Prior to initial uplift of the Coast Range between 16.5 and 15 Ma (timing of Columbia River Basalt Group eruptions which flowed to the coast through narrow valleys, Beeson et al., 1989) and onset of major uplift from 15 Ma following CRB flows, the wide forearc basin extended from the Cascade foothills to the outer-arc high and accretionary wedge with local highlands in the Oregon Coast Range. Uplift of the Oregon Coast Range subsequently separated the Willamette Valley from the shelf basin (Fig. IV.11a, b, c).
- (2) Sediments accumulated within the offshore forearc basin west of the uplifting Coast Range, ponding behind a former now-eroded outer-arc high.
- (3) Tectonic uplift (probably driven by rotation of Pacific and Juan de Fuca plate motions) and eustatic sea level fall resulted in formation of a regional unconformity at ~ 7.5-6 Ma (Fig. IV.11c), recognized as a worldwide hiatus (NH6 of Keller and Barron, 1987). The unconformity is angular close to shore, but is a disconformity or possibly conformable in the seaward part of the basin. A hiatus at this time is also observed in the Eel River Basin of the southern Cascadia margin, but without a widespread angular unconformity. This major tectonic event may be linked to events throughout the Pacific Basin associated with the docking and collision of the Ontong Java Plateau in the southwest Pacific (Wessel and Kroenke, submitted), resulting in clockwise rotation of the relative Juan de Fuca plate motion (Wilson et al., 1984).
- (4) Truncation and erosion of the seaward forearc basin and former bounding outer-arc high in the early to mid Pliocene reduced the width of the basin. Stratigraphic ages in the extreme seaward portion of the basin are uncertain, therefore, the exact timing of uplift cannot be determined. However, we are fairly certain that this outer-arc high post-dates formation of the late Miocene unconformity and correlative seaward conformity or disconformity. Basinal sediments were reaccreted and incorporated into the accretionary wedge. The more landward and current bounding outer-arc high uplifted at this time (Fig. IV.11d). The truncation event may have been a result of the subduction of basement

anomalies on the Juan de Fuca oceanic basement or oversteepening and failure of the margin.

(5) During Pliocene basin subsidence, the majority of terrigenous sediments ponded behind the outer-arc high and failed to reach the abyssal plain. The accretionary wedge at this time was probably narrow with low accretion rates.

(6) The initially planar late Miocene unconformity was deformed by localized subsidence (e.g., Newport syncline) and submarine bank uplift (e.g., Stonewall and Heceta banks) throughout the Pliocene and Quaternary.

(7) At ~ 1.3-1.4 Ma (extrapolated from Site 174A Astoria Fan stratigraphy), the outer-arc high was breached following almost complete basin filling and sediments bypassed the shelf to be deposited in slope basins and on the abyssal plain. The formation of the Astoria submarine canyon and fan system occurred at this time, with resulting growth of the Pleistocene Oregon accretionary wedge (Fig. IV.11e). This event may also be represented by an early Pleistocene unconformity throughout much of the Cascadia forearc basin. Multiple submarine canyons formed on the Washington margin at this time, possibly driven, in part, by the absence of a significant outer-arc high due to the gravitational instability and extension in this region, in addition to high sedimentation rates from the melting Cordilleran Ice Sheet lobes.

(8) Continued uplift of submarine banks and subsidence of intervening synclines produced the current sinuous shelf break morphology subsequent to 1.3 Ma. The former shelf edge probably coincided with the basin outer-arc high following initial filling of the shelf basin in the early Pleistocene. The central Cascadia shoreline has maintained its position from the late Miocene to present, acting as a hinge during Oregon Coast Range uplift and shelf basin subsidence.

(9) Variations in margin-parallel uplift rates indicated by deformation of the late Miocene unconformity continued into the Pleistocene and Holocene, as observed in comparisons between onshore and offshore datasets. A structural low common to the offshore basin and to the coastal region and Coast Range between ~ 44.5° and 45.5°N may represent a region of relatively low interplate coupling or a discrete interplate segment.

(10) Many similarities exist between the central Cascadia forearc basin and the southern Cascadia Eel River Basin. We hypothesize that these two basins were connected and their depositional and structural histories controlled by the same regional tectonic forces. Some structural differences are observed on the Washington and northernmost Oregon margin, where the underlying weak basement (mélange and broken formation) leads to partial gravitational collapse of the margin. Similarities between the stratigraphy of the central and northern Cascadia basins suggest that the elongate forearc basin initially extended the entire

length of the Cascadia margin. Subsequent deformation and segmentation has resulted in discrete smaller basins throughout.

IV.8 ACKNOWLEDGMENTS

We are grateful to Katrina Petersen for her significant contributions to the construction of the structure contour map. We wish to thank C. Hutto, J. Ingle, P. McCrory, A. Tréhu, and D.C. Wilson for helpful discussions. We also thank S. Drewry of the Minerals Management Service for the generous donation of unpublished work, and S. Snelson for making available bottom-sample data and single-channel seismic lines on the Oregon shelf. This study has been funded in part by awards from the U.S. Geological Survey National Earthquake Hazards Reduction Program: 14-08-0001-G1800, 1434-93-G-2319, 1434-93-G-2489, and 1434-95-G-2635, and from NOAA Undersea Research Program at the West Coast National Undersea Research Center: UAF-93-0035 and UAF-96-0060.

IV.9 REFERENCES

Aalto, K.R., Moley, K., and Miller, W., III, 1996, Discussion and Reply: Evolution of a trench-slope basin within the Cascadia subduction margin: The Neogene Humboldt Basin, California: *Sedimentology*, v. 43, p. 761-769.

Armentrout, J.M., 1980, Field trip road log for the Cenozoic stratigraphy of Coos Bay and Cape Blanco, southwestern Oregon, *in* Oles, K.F., Johnson, J.G., Niem, A.R., and Niem, W.R., eds., *Geologic field trips in western Oregon and southwestern Washington*, Oregon Department of Geology and Mineral Industries Bulletin, v. 101, p. 177-216.

Baldwin, E.M., 1981, *Geology of Oregon*, 3rd Ed., Dubuque, IA, Kendall/Hunt Publishing Co., 170 p.

Bard, E., Hamelin, B., Arnold, M., Motaggioni, L., Cabioch, G., Faure, G., and Rougerie, F., 1996, Deglacial sea-level record from Tahiti corals and the timing of global meltwater discharge: *Nature*, v. 382, p. 241-244.

Barnard, W.D., 1978, The Washington continental slope: Quaternary tectonics and sedimentation: *Marine Geology*, v. 27, p. 79-114.

Barron, J.A., 1986, Updated diatom biostratigraphy for the Monterey Formation of California, *in* Casey, R. E., and Barron, J. A., eds., *Siliceous Microfossil and Microplankton of the Monterey Formation and Modern Analogs*: Pacific Section, Society of Economic and Petroleum Mineralogists, v. 45, p. 105-119.

Barron, J.A. and Keller, G., 1983, Paleotemperature oscillations in the middle and late Miocene of the northeastern Pacific: *Micropaleontology*, v. 29, p. 150-181.

Beeson, M.H., Perttu, R., and Perttu, J., 1979, The origin of the Miocene basalts of coastal Oregon and Washington - An alternative hypothesis: *Oregon Geology*, v. 41, p. 159-166

Beeson, M.H., Tolan, T.L., and Anderson, J.L., 1989, The Columbia River Basalt Group in western Oregon-Geologic structures and other factors that controlled flow emplacement patterns, *in* Reidel, S. P., and Hooper, P. R., eds., *Volcanism and tectonism in the Columbia River flood-basalt province*: Geological Society of America Special Publication: v. 239 p. 223-246.

Boltovskoy, E., and Wright, R., 1976, *Recent Foraminifera*: The Hague, W. Junk.

Brandon, M.T., Roden-Tice, M.K., and Garver, J.I., 1998, Late Cenozoic exhumation of the Cascadia accretionary wedge in the Olympic Mountains, northwest Washington State: *Geological Society of America Bulletin*, v. 110, p. 985-1009.

Bukry, D., and Snavely, P.D., Jr., 1988, Coccolith zonation for Paleogene strata in the Oregon Coast Range, *in* Filewicz, M. V., and Squires, R. L., eds., *Paleogene stratigraphy, west coast of North America: Society of Economic Paleontologists and Mineralogists, Pacific Section, West Coast Paleogene Symposium*, v. 58, p. 251-263.

Caulet, J.-P., 1995, Radiolarians from the Cascadia margin, Leg 146, *in* Carson, B., Westbrook, G. K., Musgrave, R. J., and Suess, E., eds., *Proceedings of the Ocean Drilling Program, Scientific Results: College Station, TX, Ocean Drilling Program*, v. 146 (part 1) p. 47-61.

Chamov, N.P., and Murdmaa, I.O., 1995, Coarse fraction minerals of sands in Cascadia margin sediments, *in* Carson, B., Westbrook, G. K., Musgrave, R. J., and Suess, E., eds., *Proceedings of the Ocean Drilling Program, Scientific Results: College Station, TX, Ocean Drilling Program*, v. 146 (part 1), p. 33-43.

Christiansen, R.L., Yeats, R.S., Graham, S.A., Niem, W.A., Niem, A.R., and Snavely, P.D., 1992, Post-Laramide geology of the U.S. Cordilleran region, *in* Burchfiel, B. C., Lipman, P.W., and Zoback, M.L., eds., *The Geology of North America Vol. G-3, Cordilleran Orogen: Conterminous U.S.: Boulder, Colorado, Geological Society of America*, v. G-3 p. 261-406.

Clarke, S.H., Jr., 1992, Geology of the Eel River Basin and adjacent region: Implications for late Cenozoic tectonics of the southern Cascadia subduction zone and Mendocino triple junction: *American Association of Petroleum Geologists Bulletin*, v. 76, p. 199-224.

Cooper, D.M., 1981, Sedimentation, stratigraphy and facies variations of the lower to middle Miocene Astoria Formation in Oregon: Ph.D. thesis, Corvallis, Oregon State University, 534 pp.

Cranswick, D.J., and Piper, K.A., 1992, Geologic framework of the Washington-Oregon continental shelf-Preliminary findings, *in* *Proceedings of the 1991 Exclusive Economic Zone Symposium on mapping and research: Working together in the Pacific EEZ*, Portland, Oregon, 1992, U.S. Geological Survey Circular 1092: U.S. Geological Survey, p. 146-151.

Dickinson, W.R., and Snyder, W.S., 1979, The geometry of the triple junctions related to San Andreas transform: *Journal of Geophysical Research*, v. 84, p. 561-572.

Eberli, G.P., Swart, P.K., Malone, M.J., and Party, S.S., 1997, Leg synthesis: Sea-level changes and fluid flow on the Great Bahama Bank slope, *Proceedings of the Ocean Drilling Program, Initial Reports: College Station, TX, Ocean Drilling Program*, v. 166, p. 13-22.

Fairbanks, R.G., 1989, A 17,000-year glacio-eustatic sea level record: influence of glacial melting rates on the Younger Dryas event and deep-ocean circulation: *Nature*, v. 342, p. 637-642.

Fisher, M.A., Detterman, R.L., and Magoon, L.B., 1987, Tectonics and petroleum geology of the Cook-Shelikof Basin, Southern Alaska, *in* Scholl, D. W., Grantz, A., and Vedder, J.G., eds., *Geology and Resource Potential of the Continental Margin of Western North America and Adjacent Ocean Basins-Beaufort Sea to Baja California*: Houston, Circum-Pacific Council for Energy and Mineral Resources, p. 213-228.

Fleming, S.W., 1996, Bulldozer blades and colliding submarine mountain chains: Constraints on central Oregon convergent margin tectonics from magnetics and gravity: M.S. thesis, Oregon State University, Corvallis, 84 p.

Fleming, S.W., and Tréhu, A.M., submitted, Structure of the crystalline crust beneath the Oregon continental margin from potential field modeling - evidence for a buried basement ridge in local contact with a seaward-dipping backstop: submitted to *Journal of Geophysical Research*.

Fourtanier, E., 1995, Neogene diatom biostratigraphy of Site 892, Cascadia margin, *in* Carson, B., Westbrook, G. K., Musgrave, R. J., and Suess, E., eds., *Proceedings of the Ocean Drilling Program, Scientific Results*: College Station, TX, Ocean Drilling Program, v. 146 (part 1) p. 63-77.

Fourtanier, E., and Caulet, J.-P., 1995, Siliceous microfossil stratigraphic synthesis of Site 892, Cascadia Margin, *in* Carson, B., Westbrook, G. K., Musgrave, R. J., and Suess, E., eds., *Proceedings of the Ocean Drilling Program, Scientific Results*: College Station, TX, Ocean Drilling Program, v. 146 (part 1) p. 369-374.

Fowler, G.A., and Kulm, L.D., 1970, Foraminiferal and sedimentological evidence for uplift of the deep-sea floor, Gorda Rise, northeastern Pacific: *Journal of Marine Research*, v. 28, p. 321-329.

Goldfinger, C., Kulm, L.D., Yeats, R.S., Appelgate, B., MacKay, M.E., Moore, G.F., 1992, Transverse structural trends along the Oregon convergent margin: Implications for Cascadia earthquake potential and crustal rotations: *Geology*, v. 20, p. 141-144.

Goldfinger, C., Kulm, L.D., Yeats, R.S., Appelgate, B., MacKay, M., and Cochrane, G.R., 1996a, Active strike-slip faulting and folding of the Cascadia plate boundary and forearc in central and northern Oregon, *in* Rogers, A. M., Walsh, T. J., Kockelman, W. J., and Priest, G., eds., *Assessing and reducing earthquake hazards in the Pacific Northwest*: U.S. Geological Survey, Professional Paper 1560 p. 223-256.

Goldfinger, C., McNeill, L.C., Kulm, L.D., and Yeats, R.S., 1996b, Width of the seismogenic plate boundary in Cascadia: Structural indicators of strong and weak coupling: Geological Society of America Abstracts with Programs, v. 28, p. 69.

Goldfinger, C., Kulm, L.D., Yeats, R.S., McNeill, L.C., and Hummon, C., 1997, Oblique strike-slip faulting of the central Cascadia submarine forearc: Journal of Geophysical Research, v. 102, p. 8217-8243.

Hammond, P.E., 1979, A tectonic model for evolution of the Cascade Range, *in* Armentrout, J.M., Cole, M.R., and Terbest, H., Jr., eds., Cenozoic Paleogeography of the Western United States: Pacific Coast Paleogeography symposium 3, Pacific Section, Society of Economic Paleontologists and Mineralogists, p. 219-237.

Haq, B.U., Hardenbol, J., and Vail, P.R., 1987, Chronology of fluctuating sea levels since the Triassic: Science, v. 235, p. 1156-1167.

Hickey, B.M., 1989, Patterns and processes of circulation over the Washington continental shelf and slope, *in* Landrey, M. R., and Hickey, B. M., eds., Coastal Oceanography of Washington and Oregon: Amsterdam, Elsevier Oceanography Series, v. 47, p. 41-115.

Ingle, J.C., 1973, Neogene foraminifera from the northeastern Pacific ocean, Leg 18, Deep Sea Drilling Project: Initial Reports of the Deep Sea Drilling Project, v. XVIII, p. 517-567.

Ingle, J.C., 1978, Evidence of latest Miocene refrigeration and associated eustatic events in California and the North Pacific: GSA, Annual Meeting Proceedings, v. 10(7), p. 427.

Ingle, J.C., 1986, Tectonic implications of Neogene marine deposits in the Cape Mendocino area, California: Eos, v. 67(44), p. 1220.

Ingle, J.C., Jr., 1987, The depositional, tectonic, and paleoceanographic history of the Eel River (Humboldt), Point Arena, and Bodega (Point Reyes) basins of northern California: a summary of stratigraphic evidence, *in* Schymiczek, H., and Suchsland, R., eds., Tectonics, Sedimentation and Evolution of the Eel River and Associated Coastal Basins of Northern California, Misc. Publ. 37: Bakersfield, San Joaquin Geological Society, p. 49-54.

Jackson, E.D., Shaw, H.R., and Bargar, K.E., 1975, Calculated geochronology and stress field orientations along the Hawaii chain: Earth and Planetary Science Letters, v. 26, p. 145-155.

Katz, M.E., and Miller, K.G., 1996, Eocene to Miocene oceanographic and provenance changes in a sequence stratigraphic framework: benthic foraminifera of the New Jersey margin, *in* Mountain, G. S., Miller, K. G., Blum, P., Poag, C. W., and Twichell, D. C.,

eds., Proceedings of the Ocean Drilling Program, Scientific Results: College Station, Texas, Ocean Drilling Program, v. 150, p. 65-95.

Keller, G., 1979, Early Pliocene to Pleistocene planktonic foraminiferal datum levels in the North Pacific: DSDP Sites 173, 310, 296: *Marine Micropaleontology*, v. 4, p. 281-294.

Keller, G., and Barron, J.A., 1987, Paleodepth distribution of Neogene deep-sea hiatuses: *Paleoceanography*, v. 2(6), p. 697-713.

Kelsey, H.M., Engebretson, D.C., Mitchell, C.E., and Ticknor, R.L., 1994, Topographic form of the Coast Ranges of the Cascadia margin in relation to coastal uplift rates and plate subduction: *Journal of Geophysical Research*, v. 99, p. 12,245-12,255.

Kleinpell, R.M., 1938, Miocene stratigraphy of California: London, T. Murby and Company, 450 p.

Kulm, L.D., von Huene, R., and Scientific Party, 1973, Initial reports of the Deep Sea Drilling Project, v. 18: Washington, D.C., U.S. Government Printing Office, 1077 p.

Kulm, L.D., and Fowler, G.A., 1974, Oregon continental margin structure and stratigraphy: a test of the imbricate thrust model, *in* Burk, C.A., and Drake, C.L., eds., *The Geology of Continental Margins*: New York, Springer-Verlag, p. 261-284.

Le Pichon, X., 1968, Sea-floor spreading and continental drift: *Journal of Geophysical Research*, v. 73, p. 3661-3697.

Lorenzo, J.M., and Hesselbo, S.P., 1996, Seismic-to-well correlation of seismic unconformities at Leg 150 continental slope sites, *in* Mountain, G. S., Miller, K. G., Blum, P., Poag, C. W., and Twichell, D. C., eds., *Proceedings of the Ocean Drilling Program, Scientific Results*: College Station, Texas, Ocean Drilling Program, v. 150, p. 293-307.

Mallory, V.S., 1959, Lower Tertiary biostratigraphy of the California Coast Ranges: Tulsa Oklahoma, American Association of Petroleum Geologists, 416 p.

Maloney, N.J., 1965, Geology of the continental terrace off the central coast of Oregon: Ph.D. thesis, Oregon State University, Corvallis, 233 p.

McCaffrey, R., and Goldfinger, C., 1995, Forearc deformation and great subduction earthquakes: Implications for Cascadia offshore earthquake potential: *Science*, v. 267, p. 856-859.

McCrorry, P.A., 1989, Late Neogene geohistory analysis of the Humboldt Basin and its relationship to convergence of the Juan de Fuca plate: *Journal of Geophysical Research*, v. 94, p. 3126-3138.

McCrorry, P.A., 1995, Evolution of a trench-slope basin within the Cascadia subduction margin: the Neogene Humboldt Basin, California: *Sedimentology*, v. 42, p. 223-247.

McCulloch, D.S., 1987, Regional geology and hydrocarbon potential of offshore central California, *in* Scholl, D. W., Grantz, A., and Vedder, J.G., eds., *Geology and Resource Potential of the Continental Margin of Western North America and Adjacent Ocean Basins-Beaufort Sea to Baja California*: Houston, Circum-Pacific Council for Energy and Mineral Resources, p. 353-402.

McKee, B., 1972, *Cascadia: The Geological Evolution of the Pacific Northwest*: New York, McGraw-Hill.

McManus, D.A., and Scientific Party, 1970, Initial reports of the Deep Sea Drilling Project, Washington, U.S. Government Printing Office, v. 5, p. 165-202.

McNeill, L.C., Piper, K.A., Goldfinger, C., Kulm, L.D., and Yeats, R.S., 1997, Listric normal faulting on the Cascadia continental margin: *Journal of Geophysical Research*, v. 102, p. 12,123-12,138.

McNeill, L.C., Goldfinger, C., Yeats, R.S., and Kulm, L.D., in press, The Effects of Upper Plate Deformation on Records of Prehistoric Cascadia Subduction Zone Earthquakes, *in* Stewart, I., and Vita-Finzi, C., eds., *Coastal Tectonics*: Geological Society of London Special Publication.

Miller, M.C., McCave, I.N., and Komar, P.D., 1977, Threshold of sediment motion under unidirectional currents: *Sedimentology*, v. 24, p. 507-527.

Mitchell, C.E., Vincent, P., Weldon II, R.J., and Richards, M.A., 1994, Present-day vertical deformation of the Cascadia margin, Pacific northwest, U.S.A.: *Journal of Geophysical Research*, v. 99, p. 12,257-12,277.

Natland, M.L., 1952, Pleistocene and Pliocene stratigraphy of southern California [PhD Thesis]: University of California, Los Angeles, 165 p., 20 plates

Niem, A.R., and Niem, W.A., 1985, Oil and gas investigations of the Astoria Basin, Clatsop and northernmost Tillamook Counties, northwest Oregon, Oregon Department of Geology and Mineral Industries, Oil and Gas Investigation, 14, scale 1:250 000.

Niem, A.R., MacLeod, N.S., Snively, J., P.D., Huggins, D., Fortier, J.D., Meyer, H.J., Seeling, A., and Niem, W.A., 1992, Onshore-offshore geologic cross section, northern Oregon Coast Range to continental slope: Portland, OR, State of Oregon Department of Geology and Mineral Industries, Special Paper, 26, 10 pp.

Normark, W.R., Spencer, J.E., and Ingle, J.C., Jr., 1987, Geology and Neogene history of the Pacific-continental margin of Baja California Sur, Mexico, *in* Scholl, D. W., Grantz, A., and Vedder, J.G., eds., *Geology and Resource Potential of the Continental Margin of Western North America and Adjacent Ocean Basins-Beaufort Sea to Baja California*: Houston, Circum-Pacific Council for Energy and Mineral Resources, p. 449-472.

Orange, D.L., D.S. Geddes, and J.C. Moore, 1993, Structural and fluid evolution of a young accretionary complex: The Hoh rock assemblage of the western Olympic Peninsula, Washington, *Geological Society of America Bulletin*, v. 105, p. 1053-1075.

Palmer, S.P., and Lingley, W.S., 1989, An assessment of the oil and gas potential of the Washington outer continental shelf, Washington State Division of Geology and Earth Resources Report WSG 89-2, 88p.

Parsons, T., Tréhu, A.M., Luetgert, J.H., Miller, K., Kilbride, F., Wells, R.E., Fisher, M.A., Flueh, E., ten Brink, U.S., and Christensen, N.I., 1998, A new view into the Cascadia subduction zone and volcanic arc: Implications for earthquake hazards along the Washington margin: *Geology*, v. 26, p. 199-202.

Personius, S.F., 1995, Late Quaternary stream incision and uplift in the forearc of the Cascadia Subduction Zone, western Oregon: *Journal of Geophysical Research*, v. 100, p. 20,193-20,210.

Piper, D.J.W., Normark, W.R., and Ingle, J.C., Jr., 1976, The Rio Dell Formation: a Plio-Pleistocene basin slope deposit in Northern California: *Sedimentology*, v. 23, p. 309-328.

Rau, W.W., 1973, Geology of the Washington coast between Point Grenville and the Hoh River, Washington Division of Geology and Earth Resources Bulletin, v. 66, 58 p.

Rau, W.W., 1975, Geologic map of the Destruction Island and Taholah quadrangles, Washington, scale 1:63,360, Geological Map GM-13, Washington Division of Geology and Earth Resources, Olympia, Washington.

Rau, W.W., 1979, Geologic map in the vicinity of the lower Bogachiel and Hoh River valleys, and the Washington coast, scale 1:62,500, Geological Map GM-24, Washington Division of Geology and Earth Resources, Olympia, Washington.

Riddihough, R., 1984, Recent movements of the Juan de Fuca plate system: *Journal of Geophysical Research*, v. 89, p. 6980-6994.

Scheidegger, K.F., Kulm, L.D., and Piper, D.W., 1973, Heavy mineralogy of unconsolidated sands in northeastern Pacific sediments, Leg 18, Deep Sea Drilling Project, *in* Kulm, L.D., von Huene, R., et al., eds., *Initial Reports of the Deep Sea Drilling Project*, Washington, U.S. Government Printing Office, v. 18, p. 877-888.

Schrader, H.-J., 1973, Cenozoic diatoms from the northeast Pacific, Leg 18, *in* Kulm, L. D., von Huene, R., et al., eds., *Initial Reports of the Deep See Drilling Project*: Washington, U.S Government Printing Office, v. 18, p. 673-798.

Shor, G.G., Dehlinger, P., Kirk, H.K., and French, W.S., 1968, Seismic refraction studies off Oregon and northern California: *Journal of Geophysical Research*, v. 73, p. 2175-2194.

Smith, J.D., and Hopkins, T.S., 1972, Sediment transport on the continental shelf off of Washington and Oregon in light of recent current measurements, *in* Swift, D., Duane, D.B., and Pilkey, O.H., eds., *Shelf Sediment Transport: Process and Pattern*, Stroudsburg, Pennsylvania, Dowden, Hunchinson & Ross, p. 143-180.

Snively, P.D., Jr., 1987, Tertiary geologic framework, neotectonics, and petroleum potential of the Oregon-Washington continental margin, *in* Scholl, D. W., Grantz, A., and Vedder, J.G., eds., *Geology and Resource Potential of the Continental Margin of Western North America and Adjacent Ocean Basins-Beaufort Sea to Baja California*: Houston, Circum-Pacific Council for Energy and Mineral Resources, p. 305-335.

Snively, P.D., Jr., Wagner, H.C., Lander, D.L., 1980, Interpretation of the Cenozoic geologic history, central Oregon continental margin: Cross-section summary: *Geological Society of America Bulletin*, v. 91, p. 143-146.

Snively, P.D., Jr., Wagner, H.C., Lander, D.L., 1985, Land-sea geologic cross section of the southern Oregon continental margin: U.S. Geological Survey Miscellaneous Investigations Series Map-1463, scale 1:125,000.

Snively, P.D., Jr., and Wells, R.E., 1996, Cenozoic evolution of the continental margin of Oregon and Washington, *in* Rogers, A. M., Walsh, T. J., Kockelman, W. J., & Priest, G., eds., *Assessing and Reducing Earthquake Hazards in the Pacific Northwest*: U.S. Geological Survey Professional Paper, 1560, pp. 161-182.

Teng, L.S., and Gorsline, D.S., 1991, Stratigraphic framework of the continental borderland basins, southern California, *in* Dauphin, J. P., and Simoneit, B. R. T., eds., *The Gulf and Peninsular Province of Californias*: Tulsa, Oklahoma, AAPG Memoir, v. 47, p. 127-144.

Tréhu, A.M., Asudeh, I., Brocher, T.M., Luetgert, J.H., Mooney, W.D., Nabelek, J.L., and Nakumara, Y., 1994, Crustal architecture of the Cascadia forearc: *Science*, v. 266, p. 237-243.

Tréhu, A.M., Lin, G., Maxwell, E., and Goldfinger, C., 1995, A seismic reflection profile across the Cascadia subduction zone offshore central Oregon: New constraints on methane distribution and crustal structure: *Journal of Geophysical Research*, v. 100, p. 15,101-15,116.

van Andel, T.H., and Calvert, S.E., 1971, Evolution of sediment wedge, Walvis Shelf, Southwest Africa: *Journal of Geology*, v. 79, p. 585-602.

von Huene, R., and Kulm, L.D., 1973, Tectonic summary of Leg 18: *in* Kulm, L.D., von Huene, R., et al. (eds.), Initial Reports of the Deep Sea Drilling Project, Washington (U.S. Government Printing Office), v. 18, p. 961-976.

von Huene, R., and S. Lallemand, 1990, Tectonic erosion along the Japan and Peru convergent margins: *Geological Society of America Bulletin*, v. 102, p. 704-720.

von Huene, R., Fisher, M.A., and Bruns, T.R., 1987, Geology and evolution of the Kodiak margin, Gulf of Alaska, *in* Scholl, D. W., Grantz, A., and Vedder, J.G., eds., *Geology and Resource Potential of the Continental Margin of Western North America and Adjacent Ocean Basins-Beaufort Sea to Baja California*: Houston, Circum-Pacific Council for Energy and Mineral Resources, p. 191-212.

Wells, R.E., Engebretson, D.C., Snavely, P.D., Jr., and Coe, R.S., 1984, Cenozoic plate motions and the volcano-tectonic evolution of western Oregon and Washington: *Tectonics*, v. 3, p. 275-294.

Wessel, P., and Smith, W.H.F., 1991, Free software helps map and display data: *Eos Trans. AGU*, v. 72, p. 441, 445-446.

Wessel, P., and Kroenke, L.W., 1997, A geometric technique for relocating hotspots and refining absolute plate motions: *Nature*, v. 387, p. 365-369.

Wessel, P., and Kroenke, L.W., submitted, Changes in absolute plate motion: both cause and effect of global tectonism: submitted to *Science*.

West, D.O., 1986, WNP-3 geologic support services coastal terrace study, Washington Public Power Supply System, Richland, Washington 853-1010.

West, D.O., and McCrumb, D.R., 1988, Coastline uplift in Oregon and Washington and the nature of Cascadia subduction zone tectonics: *Geology*, v. 16, p. 169-172.

Westbrook, G.K., 1994, Growth of accretionary wedges off Vancouver Island and Oregon, *in* Westbrook, G. K., Carson, B., and Musgrave, R. J., et al., eds., *Proceedings of the Ocean Drilling Program, Initial Reports: v. 146 (Part 1)* p. 381-388.

Westbrook, G.K., Carson, B., Musgrave, R.J., et al., 1994, *Proceedings of the Ocean Drilling Program, Initial Reports: College Station, TX, (Ocean Drilling Program), v. 146 (Pt. 1), 92 p.*

Wilson, D.C., 1998, Post-middle Miocene geologic evolution of the Tualatin Basin, Oregon: *Oregon Geology*, v. 60, p. 99-116.

Wilson, D.S., Hey, R.N., and Nishimura, C., 1984, Propagation as a mechanism of reorientation of the Juan de Fuca Ridge: *Journal of Geophysical Research*, v. 89, p. 9215-9225.

Wilson, D.S., 1993, Confidence intervals for motion and deformation of the Juan de Fuca plate: *Journal of Geophysical Research*, v. 98, p. 16,053-16,071.

Yeats, R.S., 1965, Pliocene seaknoll at South Mountain, Ventura Basin, California: *Bulletin of the American Association of Petroleum Geologists*, v. 49, p. 526-546.

Yeats, R.S., Graven, E.P., Werner, K.S., Goldfinger, C., and Popowski, T., 1996, Tectonics of the Willamette Valley, Oregon: *U.S. Geological Survey Professional Paper 1560*, p. 183-222.

Yeats, R.S., Kulm, L.D., Goldfinger, C., and McNeill, L.C., 1998, Stonewall anticline: An active fold on the Oregon continental shelf: *Geological Society of America Bulletin*, v. 110, p. 572-587.

Zellers, S.D., 1995, Foraminiferal biofacies, paleoenvironments, and biostratigraphy of Neogene-Quaternary sediments, Cascadia margin, *in* Westbrook, G. K., Carson, B., and Musgrave, R. J., et al., eds., *Proceedings of the Ocean Drilling Program, Initial Reports: College Station, TX, Ocean Drilling Program, v. 146 (Part 1)* p. 79-113.

Zoback, M.L., 1992, First- and second-order patterns of stress in the lithosphere: The World Stress Map Project: *Journal of Geophysical Research*, v. 97, p. 11,703-11,728.

Chapter V

Conclusions

Neogene deformation of the Cascadia subduction zone is complex, with variations in structural style both across and along the margin and through time. Such variations are apparently driven by underlying basement lithology, regional versus local stress regimes, and the position and extent of plate coupling. The Washington and northern Oregon shelf and upper slope are underlain by a structurally weak basement of Eocene to Miocene *mélange* and broken formation (the ancient accretionary complex) which is mobilized and extends westward gravitationally, resulting in listric normal faulting of the overlying Neogene basinal strata. The faulted strata may be detached from the underlying *mélange* along a low-angle detachment. This region is poorly coupled from subduction-related compression and results in a broad, low-angle unstable offshore forearc cut by numerous submarine canyons. Normal faulting and concurrent compression and extension are common to other active margins but with different driving mechanisms. These faults are active in the Quaternary but we expect that fault movement is aseismic and therefore does not pose a significant seismic hazard. In contrast, the central Oregon shelf is underlain by the rigid basement of the Eocene Siletz River Volcanics, and deformation responds to the northeasterly convergence between the Juan de Fuca and North American plates. On the inner shelf and along the coast, compressional structures trend E-W reflecting N-S compression: the regional stress field. Some of these upper plate faults are active in the Quaternary and located in close proximity to coastal communities, and may therefore pose a seismic hazard in addition to the subduction zone itself.

The potential magnitudes and recurrence intervals of subduction zone earthquakes have largely been determined from the record of late Holocene coseismic submergence of marsh sediments in coastal bays. In many locations, this record may incorporate both the elastic rebound of the subduction zone earthquake and inelastic deformation on upper plate N-S compressional faults and folds. Regardless of whether upper plate structures deform concurrently or independently of elastic strain release from the subduction zone, their movement affects the coseismic subsidence record and subsequent calculations of rupture length of the subduction zone, earthquake magnitude, and recurrence interval. Their potential contribution should be considered when interpreting such calculations and predictions. Detailed stratigraphic analysis, a higher resolution chronology of the marsh

stratigraphy of each location, and improved mapping of faults deforming coastal Pleistocene terraces may allow the separation of regional (subduction zone) and local (upper plate structures) subsidence.

Deformation of and deposition within the Cascadia forearc basin reflect a complex history of interactions between tectonics, sediment supply, and climate change. These events are controlled by both regional and global events, the latter showing strong correlations in global stratigraphy including a significant late Miocene erosional event at 7.5-6 Ma driven by tectonic uplift and sea level fall. Deformation of the resulting unconformity reveals uplift at submarine banks and a region of relatively low uplift rates on the central Oregon shelf which is also observed in Quaternary uplift onshore. The offshore central Cascadia forearc basin is currently filled, and most sediments bypass the planar shelf to be deposited in slope basins and on the abyssal plain. Prior to the early Pleistocene breaching of the basin outer-arc high and formation of the Astoria submarine canyon, these sediments ponded within the basin, resulting in a thick sequence of basinal strata overlying the Eocene basement. Growth and erosion of the outer-arc high and filling of the basin are important factors in the control of sediment distribution and deposition within the forearc. To the north, extensional deformation and the absence of a significant basin outer-arc high on the Washington shelf has resulted in a contrasting forearc morphology. The Eel River Basin at the southern end of the Cascadia margin exhibits many structural and stratigraphic similarities to the central Cascadia basin. This forearc basin may have originally extended from northern California to Vancouver Island.

Bibliography

Aalto, K.R., Moley, K., and Miller, W., III, 1996. Discussion and Reply: Evolution of a trench-slope basin within the Cascadia subduction margin. *The Neogene Humboldt Basin, California: Sedimentology*, v. 43, p. 761-769.

Adams, J., 1990. Paleoseismicity of the Cascadia subduction zone: Evidence from turbidites off the Oregon-Washington Margin. *Tectonics*, v. 9, p. 569-584.

Ando, M., and Balazs, E.I., 1979. Geodetic evidence for aseismic subduction of the Juan de Fuca plate. *Journal of Geophysical Research*, v. 84, p. 3023-3027.

Armentrout, J.M., 1980. Field trip road log for the Cenozoic stratigraphy of Coos Bay and Cape Blanco, southwestern Oregon. In: *Geologic field trips in western Oregon and southwestern Washington*, Oles, K.F., Johnson, J.G., Niem, A.R., and Niem, W.R. (eds.), Oregon Department of Geology and Mineral Industries Bulletin, v. 101, p. 177-216.

Atwater, B.F., 1987. Evidence for great Holocene earthquakes along the outer coast of Washington State. *Science*, v. 236, p. 942-944.

Atwater, B.F., 1992. Geologic evidence for earthquakes during the past 2000 years along the Copalis River, southern coastal Washington. *Journal of Geophysical Research*, v. 97, p. 1901-1919.

Atwater, B.F. (compiler), 1994. Geology of liquefaction features about 300 years old along the lower Columbia River at Marsh, Brush, Price, Hunting, and Wallace Islands, Oregon and Washington. U.S. Geological Survey Open-File Report, 94-209, 64 pp.

Atwater, B.F., and Hemphill-Haley, E., 1996. Preliminary estimates of recurrence intervals for great earthquakes of the past 3500 years at northeastern Willapa Bay, Washington. U.S. Geological Survey Open-File Report, 96-001, 88 pp.

Atwater, B.F., Nelson, A.R., Clague, J.J., Carver, G.A., Yamaguchi, D.K., Bobrowsky, P.T., Bourgeois, J., Darienzo, M.E., Grant, W.C., Hemphill-Haley, E., Kelsey, H.M., Jacoby, G.C., Nishenko, S.P., Palmer, S.P., Peterson, C.D., and Reinhart, M.A., 1995. Summary of coastal geologic evidence for past great earthquakes at the Cascadia subduction zone. *Earthquake Spectra*, v. 11, p. 1-18.

Atwater, B.F., and Yamaguchi, D.K., 1991. Sudden, probably coseismic submergence of Holocene trees and grass in coastal Washington state. *Geology*, v. 19, p. 706-709.

Aubouin, J., Von Huene, R., Baltuck, M., Arnott, R., Bourgois, J., Filewicz, M., Kvenvolden, K., Leinert, B., McDonald, T., McDougall, K., Ogawa, Y., Taylor, E., and Winsborough, B., 1982, Leg 84 of the Deep Sea Drilling Project: Subduction without accretion: Middle America Trench off Guatemala. *Nature*, v. 297, p. 458-460.

Baldwin, E.M., 1981, *Geology of Oregon*, 3rd Ed., Dubuque, IA, Kendall/Hunt Publishing Co., 170 pp.

Bard, E., Hamelin, B., Arnold, M., Motaggioni, L., Cabioch, G., Faure, G., and Rougerie, F., 1996. Deglacial sea-level record from Tahiti corals and the timing of global meltwater discharge. *Nature*, v. 382, p. 241-244.

Barnard, W.D., 1978. The Washington continental slope: Quaternary tectonics and sedimentation. *Marine Geology*, v. 27, p. 79-114.

Barnett, E.T., 1997. Potential for coastal flooding due to coseismic subsidence in the central Cascadia margin. M.S. Thesis, Portland State University, Portland, 144 pp.

Barron, J.A., 1986. Updated diatom biostratigraphy for the Monterey Formation of California. In: *Siliceous Microfossil and Microplankton of the Monterey Formation and Modern Analogs*, Casey, R. E., and Barron, J. A. (eds), Pacific Section, Society of Economic and Petroleum Geologists, v. 45, p. 105-119.

Barron, J.A. and Keller, G., 1983. Paleotemperature oscillations in the middle and late Miocene of the northeastern Pacific. *Micropaleontology*, v. 29, p. 150-181.

Beeson, M.H., Perttu, R., and Perttu, J., 1979. The origin of the Miocene basalts of coastal Oregon and Washington - An alternative hypothesis. *Oregon Geology*, v. 41, p. 159-166.

Beeson, M.H., Tolan, T.L., and Anderson, J.L., 1989. The Columbia River Basalt Group in western Oregon-Geologic structures and other factors that controlled flow emplacement patterns. In: *Volcanism and tectonism in the Columbia River flood-basalt province*, Reidel, S. P., and Hooper, P. R. (eds.). Geological Society of America Special Publication, v. 239, p. 223-246.

Bergen, F.W., and Bird, K.J., 1972. The biostratigraphy of the Ocean City area, Washington. In: *The Pacific Coast Miocene Biostratigraphic Symposium, Proceedings: Economic Paleontologists and Mineralogists Pacific Section*, p. 173-191.

Berryman, K.R., 1993a. Age, height, and deformation of Holocene marine terraces at Mahia Peninsula, Hikurangi subduction margin, New Zealand. *Tectonics*, v. 12, p. 1347-1364.

Berryman, K.R., 1993b. Distribution, age, and deformation of late Pleistocene marine terraces at Mahia Peninsula, Hikurangi subduction margin, New Zealand. *Tectonics*, v. 12, p. 1365-1379.

Berryman, K.R., Beu, A., and Irwin, S., 1997. A high resolution model for the formation of a coseismic Holocene marine terrace sequence. INQUA Commission on Neotectonics, Late Quaternary Coastal Tectonics Abstracts, p. 8.

Berryman, K.R., Ota, Y., and Hull, A.G., 1989. Holocene paleoseismicity in the fold and thrust belt of the Hikurangi subduction zone, eastern North Island, New Zealand. *Tectonophysics*, v. 163, p. 185-195.

Bloom, A.L., and Yonekura, N., 1990. Graphic analysis of dislocated shorelines. In: *Studies in Geophysics: Sea-Level Change*, National Research Council (ed.), National Academy Press, Washington, D.C., p. 104-115.

Boltovskoy, E., and Wright, R., 1976. *Recent Foraminifera*. The Hague, W. Junk.

Brandon, M.T., and Calderwood, A.R., 1990. High-pressure metamorphism and uplift of the Olympic subduction complex. *Geology*, v. 18, p. 1252-1255.

Brandon, M.T., Roden-Tice, M.K., and Garver, J.I., 1998. Late Cenozoic exhumation of the Cascadia accretionary wedge in the Olympic Mountains, northwest Washington State: *Geological Society of America Bulletin*, v. 110, p. 985-1009.

Bruce, C.H., 1973. Pressured shale and related sediment deformation: mechanism for development of regional contemporaneous faults. *American Association of Petroleum Geologists Bulletin*, v. 57, p. 878-886.

Bruns, T.R., von Huene, R., Culotta, R.C., Lewis, S.D., and Ladd, J.W., 1987. Geology and petroleum potential of the Shumagin margin, Alaska. In: *Geology and Resource Potential of the Continental Margin of Western North America and Adjacent Ocean Basins-Beaufort Sea to Baja California*, Scholl, D.W., Grantz, A., and Vedder, J.G. (eds.), Circum-Pacific Council for Energy and Mineral Resources, Houston, Texas, p. 157-189.

Bukry, D., and Snively, P.D., Jr., 1988. Coccolith zonation for Paleogene strata in the Oregon Coast Range. In: *Paleogene stratigraphy, west coast of North America: Society of Economic Paleontologists and Mineralogists, Pacific Section, West Coast Paleogene Symposium*, Filewicz, M. V., and Squires, R. L. (eds.), v. 58, p. 251-263.

Busch, D.A., 1975. Influence of growth faulting on sedimentation and prospect evaluation: *American Association of Petroleum Geologists Bulletin*, v. 59, p. 217-230.

Carson, B., Yuan, J., Myers, P.B., Jr., and Barnard, W.D., 1974. Initial deep-sea sediment deformation at the base of the Washington continental slope: A response to subduction. *Geology*, v. 2, p. 561-564.

Cashman, S.M., and Kelsey, H.M., 1990. Forearc uplift and extension, southern Hawke's Bay, New Zealand: Mid-Pleistocene to present. *Tectonics*, v. 9, p. 23-44.

Caulet, J.-P., 1995. Radiolarians from the Cascadia margin, Leg 146. In: *Proceedings of the Ocean Drilling Program, Scientific Results*, Carson, B., Westbrook, G. K., Musgrave, R. J., and Suess, E. (eds), Ocean Drilling Program, College Station, Texas, v. 146 (part 1), p. 47-61.

Chamov, N.P., and Murdmaa, I.O., 1995. Coarse fraction minerals of sands in Cascadia margin sediments. In: *Proceedings of the Ocean Drilling Program, Scientific Results*, Carson, B., Westbrook, G. K., Musgrave, R. J., and Suess, E. (eds), Ocean Drilling Program, College Station, Texas, v. 146 (part 1), p. 33-43.

Christiansen, R.L., Yeats, R.S., Graham, S.A., Niem, W.A., Niem, A.R., and Snively, P.D., 1992. Post-Laramide geology of the U.S. Cordilleran region. In: *The Geology of North America Vol. G-3, Cordilleran Orogen: Conterminous U.S.*, Burchfiel, B. C., Lipman, P.W., and Zoback, M.L. (eds), Geological Society of America, Boulder, Colorado, v. G-3 p. 261-406.

Clague, J.J., 1997. Evidence for large earthquakes at the Cascadia subduction zone. *Reviews of Geophysics*, v. 35, p. 439-460.

Clark, J.A., and Lingle, C.S., 1979. Predicted relative sea level changes (18,000 B.P. to present) caused by late-glacial retreat of the Antarctic ice sheet. *Quaternary Research*, v. 11, p. 279-298.

Clarke, S.H., Jr., 1990. Map showing geologic structures of the northern California continental margin. U.S. Geological Survey, Map MF-2130, scale 1:250 000.

Clarke, S.H., Jr., 1992. Geology of the Eel River Basin and adjacent region: Implications for late Cenozoic tectonics of the southern Cascadia subduction zone and Mendocino triple junction. *American Association of Petroleum Geologists Bulletin*, v. 76, p. 199-224.

Clarke, S.H., Jr., and Carver, G.A., 1992. Late Holocene tectonics and paleoseismicity, southern Cascadia subduction zone. *Science*, v. 255, p. 188-192.

Clarke, S.H., Jr., Field, M.E., and Hirozawa, C.A., 1985. Reconnaissance geology and geologic hazards of the offshore Coos Bay Basin, Oregon. U.S. Geological Survey Bulletin, 1645, 41 pp.

Clifton, H.E., 1983. Discrimination between subtidal and intertidal facies in Pleistocene deposits, Willapa Bay, Washington. *Journal of Sedimentary Petrology*, v. 53, p. 353-369.

Clifton, H.E., 1994. Transgressive and early highstand system tracts: Pleistocene terrace deposits, Willapa Bay, Washington. Field guide prepared in conjunction with an Society of Economic and Petroleum Geologists Research Conference, Clastic Deposits of the Transgressive Systems Tract: Facies, Stratigraphy and Reservoir Character, 70 pp.

Cooper, D.M., 1981. Sedimentation, stratigraphy and facies variations of the lower to middle Miocene Astoria Formation in Oregon. Ph.D. thesis, Oregon State University, Corvallis, 534 pp.

Cranswick, D.J., and Piper, K.A., 1992. Geologic framework of the Washington-Oregon continental shelf-Preliminary findings. In: *Proceedings of the 1991 Exclusive Economic Zone Symposium on mapping and research: Working together in the Pacific EEZ*, Portland, Oregon, 1992, U.S. Geological Survey Circular, v. 1092, p. 146-151.

Crosson, R.S., and Owens, T.J., 1987. Slab geometry of the Cascadia subduction zone beneath Washington from earthquake hypocenters and teleseismic converted waves. *Geophysical Research Letters*, v. 14, p. 824-827.

Dahlen, F.A., 1984. Noncohesive critical Coulomb wedges: An exact solution. *Journal of Geophysical Research*, v. 89, p. 10,125-10,133.

Darby, D., and Beanland, S., 1992. Possible source models for the 1855 Wairarapa earthquake, New Zealand. *Journal of Geophysical Research*, v. 97, p. 12 375-12 389.

Darlenzo, M.E., and Peterson, C.D., 1990. Episodic tectonic subsidence of late Holocene salt marshes, northern Oregon central Cascadia margin. *Tectonics*, v. 9, p. 1-22.

Darlenzo, M.E., Peterson, C.D., and Clough, C., 1994. Stratigraphic evidence for great subduction-zone earthquakes at four estuaries in northern Oregon, U.S.A. *Journal of Coastal Research*, v. 10, p. 850-876.

Davis, D., Suppe, J., and Dahlen, F.A., 1983. Mechanics of fold-and-thrust belts and accretionary wedges. *Journal of Geophysical Research*, v. 88, p. 1153-1172.

DeMets, C., Gordon, R.G., Argus, D.F., and Stein, S., 1990. current plate motions. *Geophysical Journal International*, v. 101, p. 425-478.

Dickinson, W.R., and Snyder, W.S., 1979. The geometry of the triple junctions related to San Andreas transform. *Journal of Geophysical Research*, v. 84, p. 561-572.

Eberli, G.P., Swart, P.K., Malone, M.J., and Scientific Party, 1997. Leg synthesis: Sea-level changes and fluid flow on the Great Bahama Bank slope. In: *Proceedings of the Ocean Drilling Program, Initial Reports*, Ocean Drilling Program, College Station, Texas, v. 166, pp. 13-22.

Fairbanks, R.G., 1989. A 17,000-year glacio-eustatic sea level record: influence of glacial melting rates on the Younger Dryas event and deep-ocean circulation. *Nature*, v. 342, p. 637-642.

Fisher, M.A., Detterman, R.L., and Magoon, L.B., 1987 Tectonics and petroleum geology of the Cook-Shelikof Basin, Southern Alaska. In: *Geology and Resource Potential of the Continental Margin of Western North America and Adjacent Ocean Basins-Beaufort Sea to Baja California*, Scholl, D. W., Grantz, A., & Vedder, J.G. (eds), Circum-Pacific Council for Energy and Mineral Resources, Houston, p. 213-228.

Fleming, S.W., 1996. Bulldozer blades and colliding submarine mountain chains: Constraints on central Oregon convergent margin tectonics from magnetics and gravity. M.S. thesis, Oregon State University, Corvallis, 84 pp.

Fleming, S.W., and Tréhu, A.M., submitted. Structure of the crystalline crust beneath the Oregon continental margin from potential field modeling - evidence for a buried basement ridge in local contact with a seaward-dipping backstop. Submitted to *Journal of Geophysical Research*.

Fourtanier, E., 1995. Neogene diatom biostratigraphy of Site 892, Cascadia margin. In: *Proceedings of the Ocean Drilling Program, Scientific Results*, Carson, B., Westbrook, G. K., Musgrave, R. J., and Suess, E. (eds), Ocean Drilling Program, College Station, Texas, v. 146 (part 1), p. 63-77.

Fourtanier, E., and Caulet, J.-P., 1995. Siliceous microfossil stratigraphic synthesis of Site 892, Cascadia Margin. In: *Proceedings of the Ocean Drilling Program, Scientific Results*, Carson, B., Westbrook, G. K., Musgrave, R. J., and Suess, E. (eds), College Station, Texas, Ocean Drilling Program, v. 146 (part 1), p. 369-374.

Fowler, G.A., and Kulm, L.D., 1970. Foraminiferal and sedimentological evidence for uplift of the deep-sea floor, Gorda Rise, northeastern Pacific. *Journal of Marine Research*, v. 28, p. 321-329.

Goldfinger, C., 1994. Active deformation of the Cascadia forearc: Implications for great earthquake potential in Oregon and Washington. Ph.D. Thesis, Oregon State University, Corvallis, 202 pp.

Goldfinger, C., Kulm, L.D., and McNeill, L.C., 1995. Super-scale slumping of the southern Oregon Cascadia margin: Tsunamis, tectonic erosion, and extension of the forearc: EOS, Transactions of the American Geophysical Union, Fall Supplement, v. 76, p. F361.

Goldfinger, C., Kulm, L.D., and Yeats, R.S., 1992a. Neotectonic map of the Oregon continental margin and adjacent abyssal plain. Oregon Department of Geology and Mineral Industries, Open-File Report, O-92-4, scale 1:500 000.

Goldfinger, C., Kulm, L.D., Yeats, R.S., Appelgate, B., MacKay, M., and Cochrane, G.R., 1996a. Active strike-slip faulting and folding of the Cascadia plate boundary and forearc in central and northern Oregon. In: Assessing and reducing earthquake hazards in the Pacific Northwest, Rogers, A. M., Walsh, T. J., Kockelman, W. J., and Priest, G. (eds), U.S. Geological Survey, Professional Paper, 1560, p. 223-256.

Goldfinger, C., Kulm, L.D., Yeats, R.S., Appelgate, B., MacKay, M., and Moore, G.F. 1992b. Transverse structural trends along the Oregon convergent margin: Implications for Cascadia earthquake potential. *Geology*, v. 20, p. 141-144.

Goldfinger, C., Kulm, L.D., Yeats, R.S., McNeill, L.C., and Hummon, C., 1997a. Oblique strike-slip faulting of the central Cascadia submarine forearc. *Journal of Geophysical Research*, v. 102, p. 8217-8243.

Goldfinger, C., McNeill, L.C., and Hummon, C., 1997b. Case study of GIS data integration and visualization in submarine tectonic investigations: Cascadia subduction zone. *Marine Geodesy*, v. 20, p. 267-289.

Goldfinger, C., McNeill, L.C., Kulm, L.D., and Yeats, R.S., 1996b. Width of the seismogenic plate boundary in Cascadia: Structural indicators of strong and weak coupling. *Geological Society of America Abstracts with Programs*, v. 28, p. 69.

Gower, H.D., 1960. Geologic map of the Pysht quadrangle, Washington. U.S. Geological Survey Geologic Quadrangle Map, GQ-129, scale 1:62 500.

Grim, M.S., and Bennett, L.C., Jr., 1969. Shallow seismic profiling of the continental shelf off Grays Harbor, Washington. University of Washington Department of Oceanography Special Report, v. 41, p. 72-92.

Hammond, P.E., 1979. A tectonic model for evolution of the Cascade Range. In: *Cenozoic Paleogeography of the Western United States: Pacific Coast Paleogeography*

symposium 3, Armentrout, J.M., Cole, M.R., and Terbest, H., Jr. (eds.), Pacific Section, Society of Economic Paleontologists and Mineralogists, p. 219-237.

Haq, B.U., Hardenbol, J., and Vail, P.R., 1987. Chronology of fluctuating sea levels since the Triassic. *Science*, v. 235, p. 1156-1167.

Haugerud, R.A., 1996. Digital topographic-bathymetric map of Cascadia (39°N-53°N, 116°W-133°W). *Geological Society of America Abstracts with Programs*, v. 28, p. 73.

Heaton, T.H., and Kanamori, H., 1984. Seismic potential associated with subduction in the northwestern United states. *Bulletin of the Seismological Society of America*, v. 74, p. 993-941.

Hickey, B.M., 1989. Patterns and processes of circulation over the Washington continental shelf and slope. In: *Coastal Oceanography of Washington and Oregon*, Landrey, M. R., and Hickey, B. M. (eds), Elsevier Oceanography Series, Amsterdam, v. 47, p. 41-115.

Hill, D.P., and 30 others, 1993. Seismicity remotely triggered by the magnitude 7.3 Landers, California earthquake. *Science*, v. 260, p. 1617-1623.

Hubbert, M.K., and Rubey, W.W., 1959. Role of fluid pressure in mechanics of overthrust faulting, 1, Mechanics of fluid-filled porous solids and its application to overthrust faulting. *Geological Society of America Bulletin*, v. 70, p. 115-166.

Hull, A.G., 1990. Tectonics of the 1931 Hawke's Bay earthquake. *New Zealand Journal of Geology and Geophysics*, v. 33, p. 309-330.

Ingle, J.C., 1973. Neogene foraminifera from the northeastern Pacific ocean, Leg 18, Deep Sea Drilling Project: Initial Reports of the Deep Sea Drilling Project, v. 18, p. 517-567.

Ingle, J.C., Jr., 1978. Evidence of latest Miocene refrigeration and associated eustatic events in California and the North Pacific. *Geological Society of America Annual Meeting Proceedings*, v. 10(7), p. 427.

Ingle, J.C., Jr., 1986. Tectonic implications of Neogene marine deposits in the Cape Mendocino area, California. *Eos Transactions American Geophysical Union*, v. 67(44), p. 1220.

Ingle, J.C., Jr., 1987. The depositional, tectonic, and paleoceanographic history of the Eel River (Humboldt), Point Arena, and Bodega (Point Reyes) basins of northern California: a summary of stratigraphic evidence. In: *Tectonics, Sedimentation and Evolution of the Eel River and Associated Coastal Basins of Northern California*, Schymiczek, H., and

Suchsland, R. (eds), San Joaquin Geological Society, Bakersfield, Misc. Publ. 37, p. 49-54.

Jackson, E.D., Shaw, H.R., and Bargar, K.E., 1975. Calculated geochronology and stress field orientations along the Hawaii chain. *Earth and Planetary Science Letters*, v. 26, p. 145-155.

Jacoby, G.C., Bunker, D.E., and Benson, B.E., 1997. Tree-ring evidence for an A.D. 1700 Cascadia earthquake in Washington and northern Oregon. *Nature*, v. 25, p. 999-1002.

Karig, D.E., Kagami, H. and DSDP Leg 87 Scientific Party, 1983. Varied responses to subduction in Nankai Trough and Japan forearc, *Nature*, v. 304, p. 148-151.

Katz, M.E., and Miller, K.G., 1996. Eocene to Miocene oceanographic and provenance changes in a sequence stratigraphic framework: benthic foraminifers of the New Jersey margin. In: *Proceedings of the Ocean Drilling Program, Scientific Results*, Mountain, G. S., Miller, K. G., Blum, P., Poag, C. W., and Twichell, D. C. (eds), Ocean Drilling Program, College Station, Texas, v. 150, p. 65-95.

Keller, G., 1979. Early Pliocene to Pleistocene planktonic foraminiferal datum levels in the North Pacific: DSDP Sites 173, 310, 296. *Marine Micropaleontology*, v. 4, p. 281-294.

Keller, G., and Barron, J.A., 1987. Paleodepth distribution of Neogene deep-sea hiatuses. *Paleoceanography*, v. 2(6), p. 697-713.

Kelsey, H.M., 1990. Late Quaternary deformation of marine terraces on the Cascadia subduction zone near Cape Blanco, Oregon. *Tectonics*, v. 9, p. 983-1014.

Kelsey, H.M., Engebretson, D.C., Mitchell, C.E., and Ticknor, R.L., 1994. Topographic form of the Coast Ranges of the Cascadia margin in relation to coastal uplift rates and plate subduction. *Journal of Geophysical Research*, v. 99, p. 12,245-12,255.

Kelsey, H.M., Ticknor, R.L., Bockheim, J.G., and Mitchell, C.E., 1996. Quaternary upper plate deformation in coastal Oregon. *Geological Society of America Bulletin*, v. 108, p. 843-860.

Kelsey, H.M., Witter, R.C., and Hemphill-Haley, E., 1998. Response of a small Oregon estuary to coseismic subsidence and postseismic uplift in the past 300 years. *Geology*, v. 26, p. 231-234.

Kelsey, H.M., Witter, R.C., and Polenz, M., 1993. Cascadia paleoseismic record derived from late Holocene fluvial and lake sediments, Sixes River Valley, Cape Blanco, south coastal Oregon. *Eos*, v. 74, p. 199.

Kennedy, G.L., 1978. Pleistocene paleoecology, zoogeography and geochronology of marine invertebrate faunas of the Pacific Northwest coast (San Francisco Bay to Puget Sound). Ph.D. Thesis, University of California, Davis, 824 pp.

Kennedy, G.L., Lajoie, K.R., and Wehmiller, J.F., 1982. Aminostratigraphy and faunal correlations of late Quaternary marine terraces, Pacific Coast, USA. *Nature*, v. 299, p. 545-547.

Kleinpell, R.M., 1938. Miocene Stratigraphy of California, T. Murby, London, 450 pp.

Kulm, L.D., and Fowler, G.A., 1974. Oregon continental margin structure and stratigraphy: a test of the imbricate thrust model. In: *The Geology of Continental Margins*, Burk, C. A., and Drake, C.L. (eds), Springer-Verlag, New York, p. 261-284.

Kulm, L.D., and Suess, E., 1990. Relation of carbonate deposits and fluid venting: Oregon accretionary prism. *Journal of Geophysical Research*, v. 95, p. 8899-8915.

Kulm, L.D., Prince, R.A., and Snively, P.D., Jr., 1973. Site survey of the northern Oregon continental margin and Astoria Fan. In: *Initial Reports of the Deep Sea Drilling Project*, v. 18, p. 979-987.

Kulm, L.D., von Huene, R., and Scientific Party, 1973. Initial reports of the Deep Sea Drilling Project, v. 18. U.S. Government Printing Office, Washington, 1077 pp.

Kvenvolden, K.A., Blunt, D.J., and Clifton, H.E., 1979. Amino-acid racemization in Quaternary shell deposits at Willapa Bay, Washington. *Geochimica et Cosmochimica Acta*, v. 43, p. 1505-1520.

Le Pichon, X., 1968. Sea-floor spreading and continental drift. *Journal of Geophysical Research*, v. 73, p. 3661-3697.

Li, C., 1995. Forearc structures and tectonics in the southern Peru-northern Chile continental margin. *Marine Geophysical Researches*, v. 17, p. 97-113.

Long, A.J., and Shennan, I., 1994. Sea-level changes in Washington and Oregon and the "earthquake deformation cycle". *Journal of Coastal Research*, v. 10, p. 825-838.

Lorenzo, J.M., and Hesselbo, S.P., 1996. Seismic-to-well correlation of seismic unconformities at Leg 150 continental slope sites. In: *Proceedings of the Ocean Drilling Program, Scientific Results*, Mountain, G. S., Miller, K. G., Blum, P., Poag, C. W., and Twichell, D. C. (eds), Ocean Drilling Program, College Station, Texas, v. 150, p. 293-307.

Ludwin, R.S., Weaver, C.S., and Crosson, R.S., 1991. Seismicity of Washington and Oregon. In: *Neotectonics of North America*, Slemmons, D. B., Engdahl, E. R., Blackwell, D., & Schwartz, D. (eds), Geological Society of America, DNAG CSMV-1, Boulder, Colorado, p. 77-98.

MacKay, M.E., Moore, G.F., Cochrane, G.R., Moore, J.C., and Kulm, L.D., 1992. Landward vergence and oblique structural trends in the Oregon margin accretionary prism: Implications and effect on fluid flow. *Earth Planetary Science Letters*, v. 109, p. 477-491.

Maemoku, H., 1988a. Holocene crustal movement in Muroto Peninsula, southwest Japan. *Geographical Review of Japan* 61 (Ser. A), v. 10, p. 747-769.

Maemoku, H., 1988b. Holocene crustal movement around Cape Ashizuri, southwest Japan. *Geographical Sciences*, v. 43, p. 231-240.

Maemoku, H., and Tsubono, K., 1990. Holocene crustal movements in the southern part of Kii Peninsula, outer zone of southwest Japan. *Journal of Geography*, v. 99, p. 349-369.

Mallory, V.S., 1959. *Lower Tertiary Biostratigraphy of the California Coast Ranges*, American Association of Petroleum Geologists, Tulsa, Oklahoma, 416 pp.

Maloney, N.J., 1965. *Geology of the continental terrace off the central coast of Oregon*. Ph.D. thesis, Oregon State University, Corvallis, 233 pp.

Mathewes, R.W., and Clague, J.J., 1994. Detection of Large Prehistoric Earthquakes in the Pacific Northwest by Microfossil Analysis. *Science*, v. 264, p. 688-691.

McCaffrey, R., and Goldfinger, C., 1995. Forearc deformation and great subduction earthquakes: Implications for Cascadia earthquake potential. *Science*, v. 267, p. 856-859.

McClain, K.J., 1981. *A geophysical study of accretionary processes on the Washington continental margin*. Ph.D. thesis, University of Washington, Seattle, 141 pp.

McCrory, P.A., 1989. Late Neogene geohistory analysis of the Humboldt Basin and its relationship to convergence of the Juan de Fuca plate. *Journal of Geophysical Research*, v. 94, p. 3126-3138.

McCrory, P.A., 1994. Quaternary crustal shortening along the central Cascadia subduction margin, Washington. *Geological Society of America Abstracts with Programs*, v. 26, A-523.

McCrory, P.A., 1995. Evolution of a trench-slope basin within the Cascadia subduction margin: the Neogene Humboldt Basin, California. *Sedimentology*, v. 42, p. 223-247.

McCrory, P.A., 1996. Tectonic model explaining divergent contraction directions along the Cascadia subduction margin, Washington. *Geology*, v. 24, p. 929-932.

McCulloch, D.S., 1987. Regional geology and hydrocarbon potential of offshore central California. In: *Geology and Resource Potential of the Continental Margin of Western North America and Adjacent Ocean Basins-Beaufort Sea to Baja California*, Scholl, D. W., Grantz, A., and Vedder, J.G. (eds), Circum-Pacific Council for Energy and Mineral Resources, Houston, p. 353-402.

McInelly, G.W., and Kelsey, H.M., 1990. Late Quaternary tectonic deformation in the Cape Arago-Bandon region of coastal Oregon as deduced from wave cut platforms. *Journal of Geophysical Research*, v. 95, p. 6699-6713.

McIntosh, K., Silver, E., and Shipley, T., 1993. Evidence and mechanisms for forearc extension at the accretionary Costa Rica convergent margin. *Tectonics*, v. 12, p. 1380-1392.

McKee, B., 1972. *Cascadia: The Geological Evolution of the Pacific Northwest*. New York, McGraw-Hill.

McManus, D.A., and Scientific Party, 1970. Initial reports of the Deep Sea Drilling Project. Washington, U.S. Government Printing Office, v. 5 p. 165-202.

McNeill, L.C., Goldfinger, C., Yeats, R.S., and Kulm, L.D., in press. The Effects of Upper Plate Deformation on Records of Prehistoric Cascadia Subduction Zone Earthquakes. In: *Coastal Tectonics*, Stewart, I., and Vita-Finzi, C. (eds), Geological Society of London Special Publication.

McNeill, L.C., Piper, K.A., Goldfinger, C., and Kulm, L.D., 1995. Detachment faulting on the Cascadia continental shelf: Active extension in a compressional regime? *Eos Transactions American Geophysical Union*, v. 76(46), F534.

McNeill, L.C., Piper, K.A., Goldfinger, C., Kulm, L.D., and Yeats, R.S., 1997. Listric normal faulting on the Cascadia continental margin. *Journal of Geophysical Research*, v. 102, p. 12,123-12,138.

Miller, M.C., McCave, I.N., and Komar, P.D., 1977. Threshold of sediment motion under unidirectional currents. *Sedimentology*, v. 24, p. 507-527.

Mitchell, C.E., Vincent, P., Weldon II, R.J., and Richards, M.A., 1994. Present-day vertical deformation of the Cascadia margin, Pacific northwest, U.S.A. *Journal of Geophysical Research*, v. 99, p. 12,257-12,277.

Morley, C.K., and Guerin, G., 1996. Comparison of gravity-driven deformation styles and behavior associated with mobile shales and salt. *Tectonics*, v. 15, p. 1154-1170.

Natland, M.L., 1952. Pleistocene and Pliocene stratigraphy of southern California. Ph.D. thesis, University of California, Los Angeles, 165 pp., 20 plates.

Nelson, A.R., 1987. Apparent gradual rise in relative sea level on the south-central Oregon coast during the late Holocene—Implications for the great Cascadia earthquake hypothesis. *Eos*, v. 68, p. 1240.

Nelson, A.R., 1992. Holocene tidal-marsh stratigraphy in South-Central Oregon - Evidence for localized sudden submergence in the Cascadia subduction zone. In: *Quaternary Coasts of the United States: Marine and Lacustrine Systems*, Fletcher, C. H., and Wehmiller, J. F. (eds), Society for Sedimentary Geology Special Publication, v. 48, p. 287-301.

Nelson, A.R., Atwater, B.F., Brobowski, P.T., Bradley, L.A., Clague, J.J., Carver, G.A., Darienzo, M.E., Grant, W.C., Krueger, H.W., Sparks, R., Stafford, T.W., and Stuiver, M., 1995. Radiocarbon evidence for extensive plate-boundary rupture about 300 years ago at the Cascadia subduction zone. *Nature*, v. 378, p. 371-374.

Nelson, A.R., Jennings, A.E., and Kashima, K., 1996a. An earthquake history derived from stratigraphic and microfossil evidence of relative sea-level change at Coos Bay, southern coastal Oregon. *Geological Society of America Bulletin*, v. 108, p. 141-154.

Nelson, A.R., and Personius, S.F., 1996b. Great-earthquake potential in Oregon and Washington - an overview of recent coastal geologic studies and their bearing on segmentation of Holocene ruptures, central Cascadia subduction zone. In: *Assessing and Reducing Earthquake Hazards in the Pacific Northwest*, Rogers, A. M., Walsh, T. J., Kockelman, W. J., and Priest, G. (eds), U.S. Geological Survey Professional Paper, 1560, p. 91-114.

Nelson, A.R., Shennan, I., and Long, A.J., 1996c. Identifying coseismic subsidence in tidal-wetland stratigraphic sequences at the Cascadia subduction zone of western North America. *Journal of Geophysical Research*, v. 101, p. 6115-6135.

Niem, A.R., and Niem, W.A., 1985. Oil and gas investigations of the Astoria Basin, Clatsop and northernmost Tillamook Counties, northwest Oregon. Oregon Department of Geology and Mineral Industries Oil and Gas Investigation, 14, scale 1:250 000.

Niem, A.R., Snavely, P.D., Jr., and Niem, W.A., 1990. Onshore-offshore geologic cross section from the Mist gas field, northern Oregon coast range, to the northwest Oregon continental shelf. Oregon Department of Geology and Mineral Industries Oil and Gas Investigation, 17, 46 pp.

Niem, A.R., MacLeod, N.S., Snavely, J., P.D., Huggins, D., Fortier, J.D., Meyer, H.J., Seeling, A., and Niem, W.A., 1992. Onshore-offshore geologic cross section, northern Oregon Coast Range to continental slope. Oregon Department of Geology and Mineral Industries, Special Paper 26, 10 pp.

Normark, W.R., Spencer, J.E., and Ingle, J.C., Jr., 1987. Geology and Neogene history of the Pacific-continental margin of Baja California Sur, Mexico. *Geology and Resource Potential of the Continental Margin of Western North America and Adjacent Ocean Basins-Beaufort Sea to Baja California*, Scholl, D. W., Grantz, A., and Vedder, J.G. (eds), Circum-Pacific Council for Energy and Mineral Resources, Houston, p. 449-472.

Obermeier, S.F., 1995. Preliminary estimates of the strength of prehistoric shaking in the Columbia River valley and the southern half of coastal Washington, with emphasis for a Cascadia subduction zone earthquake about 300 years ago. U.S. Geological Survey Open File Report, 94-589, 34 pp.

Oppenheimer, D., Beroza, G., Carver, G., Dengler, L., Eaton, J., Gee, L., Gonzalez, F., Jayko, A., Li, W.H., Lisowski, M., Magee, M., Marshall, G., Murray, M., McPherson, R., Romanowicz, B., Satake, K., Simpson, R., Somerville, P., Stein, R., and Valentine, D., 1993. The Cape Mendocino, California, earthquakes of April 1992: Subduction at the triple junction. *Science*, v. 261, p. 433-438.

Orange, D.L., 1990. Criteria helpful in recognizing shear-zone and diapiric mélanges: Examples from the Hoh accretionary complex, Olympic Peninsula, Washington. *Geological Society of America Bulletin*, v. 102, p. 935-951.

Orange, D.L., Geddes, D.S., and Moore, J.C., 1993. Structural and fluid evolution of a young accretionary complex: The Hoh rock assemblage of the western Olympic Peninsula, Washington. *Geological Society of America Bulletin*, v. 105, p. 1053-1075.

Palmer, S.P., and Lingley, W.S., 1989. An assessment of the oil and gas potential of the Washington outer continental shelf, Washington State Division of Geology and Earth Resources Report WSG 89-2, 88pp.

Pandolfi, J.M., Best, M.M.R., and Murray, S.P., 1994. Coseismic event of May 15, 1992, Huon Peninsula, Papua New Guinea: Comparison with Quaternary tectonic history. *Geology*, v. 22, p. 239-242.

Parker, M.J., 1990. The Oligocene and Miocene geology of the Tillamook embayment, Tillamook County, northwest Oregon. M.S. thesis, Oregon State University, Corvallis, 515 pp., 2 plates.

Parsons, T., Tréhu, A.M., Luetgert, J.H., Miller, K., Kilbride, F., Wells, R.E., Fisher, M.A., Flueh, E., ten Brink, U.S., and Christensen, N.I., 1998. A new view into the Cascadia subduction zone and volcanic arc: Implications for earthquake hazards along the Washington margin. *Geology*, v. 26, p. 199-202.

Peltier, W.R., 1996. Mantle viscosity and ice-age topography. *Science*, v. 273, p. 1359-1364.

Personius, S.F., 1995. Late Quaternary stream incision and uplift in the forearc of the Cascadia Subduction Zone, western Oregon. *Journal of Geophysical Research*, v. 100, p. 20,193-20,210.

Peterson, C.D., and Darienzo, M.E., 1989. Episodic, abrupt tectonic subsidence recorded in late Holocene deposits of the South Slough syncline: An on-land expression of shelf fold belt deformation from the southern Cascadia margin. *Geological Society of America Abstracts with Programs*, v. 21, p. 129.

Peterson, C.D., and Darienzo, M.E., 1996. Discrimination of climatic, oceanic, and tectonic mechanisms of cyclic marsh burial, Alsea Bay, Oregon. In: *Assessing and Reducing Earthquake Hazards in the Pacific Northwest*, Rogers, A. M., Walsh, T. J., Kockelman, W. J., and Priest, G. (eds), U.S. Geological Survey Professional Paper, 1560, p. 115-146.

Peterson, C.D., and Priest, G.R., 1995. Preliminary reconnaissance survey of Cascadia paleotsunami deposits in Yaquina Bay, Oregon. *Oregon Geology*, v. 57, p. 33-40.

Peterson, C.D., Darienzo, M.A., and Parker, M., 1988. Coastal neotectonic field guide for Netarts Bay, Oregon. *Oregon Geology*, v. 50, p. 99-106 and 117.

Peterson, C.D., Barnett, E., Briggs, G.G., Carver, G.A., Clague, J.J., and Darienzo, M.E., 1997. Subsidence from great earthquakes in the Cascadia subduction zone, Vancouver Island, B.C., Washington, Oregon, and northernmost California. Department of Oregon Geology and Mineral Industries, Open-File Report, 0-97-5, 44 pp.

Piper, D.J.W., Normark, W.R., and Ingle, J.C., Jr., 1976. The Rio Dell Formation: a Plio-Pleistocene basin slope deposit in Northern California. *Sedimentology*, v. 23, p. 309-328.

Piper, K.A., 1994. Extensional tectonics in a convergent margin—Pacific Northwest offshore, Washington and Oregon. *American Association of Petroleum Geologists Bulletin*, v. 78, p. 673.

Piper, K.A., McNeill, L.C., and Goldfinger, C., 1995. Active growth faulting on the Washington continental margin. *American Association of Petroleum Geologists Bulletin*, v. 79, p. 596.

Plafker, G., 1969. Tectonics of the March 27 Alaskan earthquake. U.S. Geological Survey Professional Paper, 543-I, 74 pp.

Plafker, G., 1972. Alaskan earthquake of 1964 and Chilean earthquake of 1960: implications for arc tectonics. *Journal of Geophysical Research*, v. 77, p. 901-925.

Priest, G.R., Saul, I., & Diebenow, J., 1994. Chronic geologic hazard maps and erosion rate database, coastal Lincoln county, Oregon: Salmon River to Seal Rocks. Oregon Department of Geology and Mineral Industries Open-File Report, O-94-11, 45 pp., 1:4800 scale maps.

Rau, W.W., 1970. Foraminifera, stratigraphy, and paleoecology of the Quinault Formation, Point Grenville-Raft River coastal area, Washington. *Washington Division of Mines Geology Bulletin*, v. 62, 41 pp.

Rau, W.W., 1973. Geology of the Washington coast between Point Grenville and the Hoh River. *Washington Division of Geology and Earth Resources Bulletin*, v. 66, 58 pp.

Rau, W.W., 1975. Geologic map of the Destruction Island and Taholah quadrangles, Washington. Washington Division of Geology and Earth Resources, Geologic Map GM-13, Olympia, Washington, scale 1:63,360.

Rau, W.W., 1979. Geologic map in the vicinity of the lower Bogachiel and Hoh River valleys, and the Washington coast. Washington Division of Geology and Earth Resources, Geologic Map GM-24, Olympia, Washington, scale 1:62,500.

Rau, W.W., 1981. Pacific Northwest Tertiary benthic foraminiferal biostratigraphic framework—An overview. *Geological Society of America Special Paper*, v. 184, p. 67-84.

Riddihough, R., 1984, Recent movements of the Juan de Fuca plate system: *Journal of Geophysical Research*, v. 89, p. 6980-6994.

Ryan, H. F. and Stevenson, A. J., 1995. Cruise report for C1-94-OW: Reconnaissance high resolution geopulse data acquired for seismic hazard studies along the Columbia River from July 18-22, 1994. U.S. Geological Survey Open-File Report, 95-668, 38 pp.

Satake, K., Shemazaki, K., Yoshinobu, T., and Ueda, K., 1996. Time and size of a giant earthquake in Cascadia inferred from Japanese tsunami records of January 1700. *Nature*, v. 379, p. 246-249.

Scheidegger, K.F., Kulm, L.D., and Piper, D.W., 1973. Heavy mineralogy of unconsolidated sands in northeastern Pacific sediments, Leg 18, Deep Sea Drilling Project. In: *Initial Reports of the Deep Sea Drilling Project*, Kulm, L.D., von Huene, R., et al. (eds.), U.S. Government Printing Office, Washington, v. 18, p. 877-888.

Schrader, H.-J., 1973. Cenozoic diatoms from the northeast Pacific, Leg 18. In: *Initial Reports of the Deep Sea Drilling Project*, Kulm, L. D., von Huene, R., et al. (eds.), U.S. Government Printing Office, Washington, v. 18, p. 673-798.

Shennan, I., Long, A.J., Rutherford, M.M., Green, F.M., Innes, J.B., Lloyd, J.M., Zong, Y., and Walker, K.J., 1996. Tidal marsh stratigraphy, sea-level change and large earthquakes, I: A 5000 year record in Washington, U.S.A. *Quaternary Science Reviews*, v. 15, p. 1023-1059.

Shor, G.G., Dehlinger, P., Kirk, H.K., and French, W.S., 1968. Seismic refraction studies off Oregon and northern California. *Journal of Geophysical Research*, v. 73, p. 2175-2194.

Sieh, K., Jones, L., Hauksson, E., Hudnut, K., Eberhart-Phillips, D., Heaton, T., Hough, S., Hutton, K., Kanamori, H., Lilje, A., Lindvall, S., McGill, S.F., Mori, J., Rubin, C., Spotila, J.A., Stock, J., Thio, H., Treiman, J., Wernicke, B., and Zachariasen, J., 1993. Near-field investigation of the Landers earthquake sequence, April to July, 1992. *Science*, v. 260, p. 171-176.

Silver, E.A., 1972. Pleistocene tectonic accretion of the continental slope off Washington. *Marine Geology*, v. 13, p. 239-249.

Smith, J.D., and Hopkins, T.S., 1972. Sediment transport on the continental shelf off of Washington and Oregon in light of recent current measurements. In: *Shelf Sediment Transport: Process and Pattern*, Swift, D., Duane, D.B., and Pilkey, O.H. (eds.), Dowden, Hutchinson & Ross, Stroudsburg, Pennsylvania, p. 143-180.

Snavely, P.D., Jr., 1976. Geologic map of the Yaquina and Toledo quadrangles, Lincoln County, Oregon. U.S. Geological Survey Miscellaneous Investigations Series Map, I-867, scale 1:62,500.

Snavely, P.D., Jr., 1987. Tertiary geologic framework, neotectonics, and petroleum potential of the Oregon-Washington continental margin. In: *Geology and Resource Potential of the Continental Margin of Western North America and Adjacent Ocean Basins-Beaufort Sea to Baja California*, Scholl, D. W., Grantz, A., & Vedder, J.G. (eds), Circum-Pacific Council for Energy and Mineral Resources, Houston, p. 305-335.

Snavely, P.D., Jr., and Kvenvolden, K.A., 1989. Preliminary evaluation of the petroleum potential of the Tertiary accretionary terrane, west side of the Olympic Peninsula, 1, Geology and hydrocarbon potential. U.S. Geological Survey Bulletin, v. 1892, p. 1-18.

Snavely, P.D., Jr., and McClellan, P.H., 1987. Preliminary geologic interpretation of USGS S.P. Lee seismic reflection profile WO 76-7 on the continental shelf and upper slope, northwestern Oregon. U.S. Geological Survey Open File Report, 87-612, 12 pp.

Snavely, P.D., Jr., and Wagner, H.C., 1982. Geologic cross section across the continental margin of southwestern Washington. U.S. Geological Survey Open File Report, 82-459, 10 pp.

Snavely, P.D., Jr., Wagner, H.C., Lander, D.L., 1980a. Geologic cross section of the central Oregon continental margin. Geological Society of America Map and Chart Series MC-28J, scale 1:250,000.

Snavely, P.D., Jr., Wagner, H.C., Lander, D.L., 1980b. Interpretation of the Cenozoic geologic history, central Oregon continental margin: Cross-section summary. Geological Society of America Bulletin, v. 91, p. 143-146.

Snavely, P.D., Jr., Wagner, H.C., Lander, D.L., 1985. Land-sea geologic cross section of the southern Oregon continental margin. U.S. Geological Survey Miscellaneous Investigations Series Map-1463, scale 1:125,000.

Snavely, P.D., Jr., and Wells, R.E., 1996. Cenozoic evolution of the continental margin of Oregon and Washington. In: *Assessing and Reducing Earthquake Hazards in the Pacific Northwest*, Rogers, A. M., Walsh, T. J., Kockelman, W. J., & Priest, G. (eds), U.S. Geological Survey Professional Paper, 1560, p. 161-182.

Spence, W., 1989. Stress origins and earthquake potential in Cascadia. *Journal of Geophysical Research*, v. 94, p. 3076-3088.

Spotila, J., and Sieh, K., 1995. Geologic investigations of the "slip gap" in the surficial ruptures of the 1992 Landers earthquake, southern California. *Journal of Geophysical Research*, v. 100, p. 543-559.

Sugiyama, Y., 1994. Neotectonics of Southwest Japan due to the right-oblique subduction of the Philippine Sea plate. *Geofisica Internacional*, v. 33, p. 53-76.

Tabor, R.W., and Cady, W.M., 1978. The Structure of the Olympic Mountains, Washington-Analysis of a subduction zone. U.S. Geological Survey Professional Paper, 1033, 38 pp.

Teng, L.S., and Gorsline, D.S., 1991. Stratigraphic framework of the continental borderland basins, southern California. In: *The Gulf and Peninsular Province of Californias*, Dauphin, J. P., and Simoneit, B. R. T. (eds), American Association of Petroleum Geologists Memoir, Tulsa, Oklahoma, v. 47, p. 127-144.

Thackray, G. D., 1994. Deformation of middle and late Pleistocene strata on the Olympic coast of Washington. *Geological Society of America Abstracts with Programs*, v. 26(7), p. A-523.

Ticknor, R.L., 1993. Late Quaternary crustal deformation on the central Oregon coast as deduced from uplifted wave-cut platforms. M.S. Thesis, Western Washington University, Bellingham, 70 pp.

Ticknor, R.L., Kelsey, H.M., and Bockheim, J.G., 1992. Late Quaternary tectonic deformation along the central Oregon portion of the Cascadia margin as deduced from deformation of wave-cut platforms. *Geological Society of America Abstracts with Programs*, v. 24, p. 86.

Tréhu, A.M., Asudeh, I., Brocher, T.M., Luetgert, J.H., Mooney, W.D., Nabelek, J.L., and Nakumara, Y., 1994. Crustal architecture of the Cascadia forearc. *Science*, v. 266, p. 237-243.

Tréhu, A., Lin, G., Maxwell, E., and Goldfinger, C., 1995. A seismic reflection profile across the Cascadia subduction zone offshore central Oregon: New constraints on methane distribution and crustal structure. *Journal of Geophysical Research*, v. 100, p. 15,101-15,116.

van Andel, T.H., and Calvert, S.E., 1971. Evolution of sediment wedge, Walvis Shelf, Southwest Africa. *Journal of Geology*, v. 79, p. 585-602.

von Huene, R., and Kulm, L.D., 1973. Tectonic summary of Leg 18. In: *Initial Reports of the Deep Sea Drilling Project*, Kulm, L.D., von Huene, R., et al. (eds), U.S. Government Printing Office, Washington, v. 18, p. 961-976.

von Huene, R., and Lallemand, S., 1990. Tectonic erosion along the Japan and Peru convergent margins. *Geological Society of America Bulletin*, v. 102, p. 704-720.

von Huene, R., and Scholl, D.W., 1991. Observations at convergent margins concerning sediment subduction, subduction erosion, and the growth of continental crust. *Reviews of Geophysics*, v. 29, p. 279-316.

von Huene, R., Bourgois, J., Miller, J., and Pautot, G., 1989. Massive collapse along the front of the Andean convergent margin off Peru. *Journal of Geophysical Research*, v. 94, p. 1703-1714.

von Huene, R., Fisher, M.A., and Bruns, T.R., 1987. Geology and evolution of the Kodiak margin, Gulf of Alaska. In: *Geology and Resource Potential of the Continental Margin of Western North America and Adjacent Ocean Basins-Beaufort Sea to Baja California*, Scholl, D. W., Grantz, A., & Vedder, J.G. (eds), Circum-Pacific Council for Energy and Mineral Resources, Houston, p. 191-212.

Wagner, H.C., and Tomson, J.H., 1987. Offshore geology of the Strait of Juan de Fuca, State of Washington and British Columbia, Canada. Washington Division of Geology and Earth Resources Open File Report, 87-1, 16 pp., 7 plates.

Wagner, H.C., Batatian, L.D., Lambert, T.M., and Tomson, J.H., 1986. Preliminary Geologic framework studies showing bathymetry, locations of geophysical tracklines and exploratory wells, seafloor geology and deeper geologic structures, magnetic contours, and inferred thickness of Tertiary rocks on the continental shelf and upper continental slope of southwest Washington between latitudes 46°N and 48° 30'N and from the Washington coast to 125° 30'W. Washington Division of Geology and Earth Resources Open File Report, 86-1, Olympia, Washington, 10 pp.

Wald, D., and Heaton, T., 1994. Spatial and temporal distribution of slip for the 1992 Landers, California, earthquake. *Seismological Society of America Bulletin*, v. 84, p. 668-691.

Walsh, T.J., Korosec, M.A., Phillips, W.M., Logan, R.L., and Schasse, H.W., 1987. Geologic map of Washington - Southwest quadrant. Washington Division of Geology and Earth Resources, Geologic Map, GM-34, 28 pp.

Wang, K., Mulder, T., Rogers, G.C., and Hyndman, R.D., 1995. Case for very low coupling stress on the Cascadia subduction fault. *Journal of Geophysical Research*, v. 100, p. 12 907-12 918.

Weaver, C.S., and Baker, G.E., 1988. Geometry of the Juan de Fuca plate beneath Washington and northern Oregon from seismicity. *Bulletin of the Seismological Society of America*, v. 78, p. 264-275.

Wells, R.E., 1989. Geologic map of the Cape Disappointment-Naselle River area, Pacific and Wahiakum Counties, Washington. U.S. Geological Survey, Miscellaneous Investigations Series Map I-1832.

Wells, R.E., Engebretson, D.C., Snavely, P.D., Jr., and Coe, R.S., 1984. Cenozoic plate motions and the volcano-tectonic evolution of western Oregon and Washington. *Tectonics*, v. 3, p. 275-294.

Wells, R.E., Niem, A.R., and Snavely, P.D., Jr., 1994a. Young deformation at Netarts Bay and elsewhere, northern Oregon coast. *Proceedings of the Oregon Academy of Sciences*, v. 30, p. 39.

Wells, R.E., Snavely, P.D., Jr., and Niem, A.R., 1992. Quaternary thrust faulting at Netarts Bay, northern Oregon coast. *Geological Society of America Abstracts with Programs*, v. 24, p. 89.

Wells, R.E., Snavely, P.D., Jr., MacLeod, N.S., Kelly, M.M., and Parker, M.J., 1994b. Geologic map of the Tillamook Highlands, Northwest Oregon Coast Range. U.S. Geological Survey, Open File Report 94-21.

Wells, R.E., Weaver, C.S., and Blakely, R.J., 1998. Fore-arc migration in Cascadia and its neotectonic significance. *Geology*, v. 26, p. 759-762.

Werner, K.S., Graven, E.P., Berkman, T.A., and Parker, M.J., 1990. Direction of maximum horizontal compression in northwestern Oregon determined by borehole breakouts. *Tectonics*, v. 10, p. 948-958.

Wernicke, B., 1981. Low-angle normal faults in the Basin and Range Province: Nappe tectonics in an extending orogen. *Nature*, v. 291, p. 645-647.

Wessel, P., and Kroenke, L.W., 1997. A geometric technique for relocating hotspots and refining absolute plate motions. *Nature*, v. 387, p. 365-369.

Wessel, P., and Kroenke, L.W., submitted. Changes in absolute plate motion: both cause and effect of global tectonism. *Science*.

Wessel, P., and Smith, W.H.F., 1991. Free software helps map and display data. *Eos Transactions American Geophysical Union*, v. 72, p. 441, 445-446.

- West, D.O., 1986. WNP-3 geologic support services coastal terrace study, Washington Public Power Supply System, Richland, Washington 853-1010.
- West, D.O., and McCrumb, D.R., 1988. Coastline uplift in Oregon and Washington and the nature of Cascadia subduction zone tectonics. *Geology*, v. 16, p. 169-172.
- Westbrook, G.K., Carson, B., Musgrave, R.J., and Scientific Party, 1994. Proceedings of the Ocean Drilling Program, Initial Reports. Ocean Drilling Program, College Station, Texas, v. 146 (Pt. 1), 92 pp.
- Wilson, D.C., 1998. Post-middle Miocene geologic evolution of the Tualatin Basin, Oregon. *Oregon Geology*, v. 60, p. 99-116.
- Wilson, D.S., Hey, R.N., and Nishimura, C., 1984. Propagation as a mechanism of reorientation of the Juan de Fuca Ridge. *Journal of Geophysical Research*, v. 89, p. 9215-9225.
- Wilson, D.S., 1993. Confidence intervals for motion and deformation of the Juan de Fuca plate. *Journal of Geophysical Research*, v. 98, p. 16,053-16,071.
- Yamaguchi, D.K., Atwater, B.F., Bunker, D.E., Benson, B.E., and Reid, M.S., 1997. Tree-ring dating the 1700 Cascadia earthquake. *Nature*, v. 389, p. 922-923.
- Yeats, R.S., 1965. Pliocene seaknoll at South Mountain, Ventura Basin, California. *Bulletin of the American Association of Petroleum Geologists*, v. 49, p. 526-546.
- Yeats, R.S., Graven, E.P., Werner, K.S., Goldfinger, C., and Popowski, T., 1996. Tectonics of the Willamette Valley, Oregon. U.S. Geological Survey Professional Paper 1560, p. 183-222.
- Yeats, R.S., Kulm, L.D., Goldfinger, C., and McNeill, L.C., 1998. Stonewall anticline: An active fold on the Oregon continental shelf. *Geological Society of America Bulletin*, v. 110, p. 572-587.
- Zellers, S.D., 1995 Foraminiferal biofacies, paleoenvironments, and biostratigraphy of Neogene-Quaternary sediments, Cascadia margin. In: Proceedings of the Ocean Drilling Program, Initial Reports, Westbrook, G. K., Carson, B., and Musgrave, R. J., et al. (eds), Ocean Drilling Program, College Station, Texas, v. 146 (Part 1) p. 79-113.
- Zoback, M.L., 1992. First- and second-order patterns of stress in the lithosphere: The World Stress Map Project. *Journal of Geophysical Research*, v. 97, p. 11,703-11,728.

Zoback, M.L., and Zoback, M.D., 1989. Tectonic stress field of the continental United States. Geological Society of America Memoir, v. 172, p. 523-540.

Appendix

Neotectonic Map of the Washington Continental Margin

Lisa C. McNeill¹, Chris Goldfinger², and Cheryl Hummon¹

¹ Department of Geosciences,
Oregon State University, Corvallis, Oregon 97331

² College of Oceanic and Atmospheric Sciences,
Oregon State University, Corvallis, Oregon 97331

DATA SOURCES

The Neotectonic Map of the Washington Continental Margin (see accompanying plate in envelope) has been produced from the interpretation of seismic reflection profiles, with supplementary data from Hydrosweep swath bathymetry, sidescan sonar surveys, lithologies and ages of seafloor samples archived at the OSU Core Repository, gravity and magnetic anomaly maps (NGDC), and seafloor investigations by submersible.

Seismic reflection surveys used are as follows:

- (1) Oregon State University (northern Oregon, southernmost Washington margin) and University of Washington single channel sparker and airgun surveys;
- (2) U.S. Geological Survey single channel and multichannel airgun profiles;
- (3) Shell Oil Company single channel sparker profiles (shelf and upper slope, with some seafloor sample transects);
- (4) Chevron Oil Company single and multichannel profiles;
- (5) Proprietary industry migrated multichannel profiles (shelf and upper slope only);
- (6) University of California Santa Cruz single channel profiles.

The ship tracklines of these surveys are shown undifferentiated in Figure II.2B (Chapter II, McNeill et al., 1997). These data were collected using a variety of methods resulting in varying resolution, navigational accuracy, depth of penetration, and degree of processing. Details of navigational accuracy are given in Table A.1 of Goldfinger (1994). Data collection and processing details for the proprietary industry migrated multichannel survey (5) are provided in Section II.5 (Chapter II). Data with the greatest positional accuracy were used to tie interpretations from less accurate data.

Hydrosweep bathymetry is available as a narrow strip along the deformation front and along certain WNW-trending strike-slip faults which cross the margin and was therefore only locally useful for structural correlation. At the time of map construction, SeaBeam bathymetry was and continues to be classified by the Navy on the Washington margin. Recently, OSU have collected SeaBeam bathymetry in certain locations, but interpretations of most of this data have not been incorporated into the map shown here.

Sidescan sonar surveys included deep-towed high-resolution SeaMARC 1A and AMS 150 kHz collected during several OSU NOAA-NURP-sponsored research cruises, and low-resolution GLORIA sidescan collected by the U.S. Geological Survey. SeaMARC 1A surveys were restricted to the same regions as the Hydrosweep bathymetry (deformation front and WNW-trending strike-slip faults), using a frequency of 27-30 kHz, and imaging a swath of 2 or 5 km with an across-track pixel size of 1 and 2.5 m, respectively. AMS 150 kHz surveys were collected on the continental shelf, using a

frequency of 150 kHz, and imaging a swath of 1 km or 800 m with an across-track pixel size of 0.5 m. Resolution is similar to pixel size but also a function of acquisition and processing parameters. Further details of sidescan operations and processing are given within Goldfinger et al. (1997b). The GLORIA survey was restricted to the abyssal plain and continental slope but with complete coverage, and therefore provided a useful tool for correlating structures which deformed the seafloor and for mapping the complex submarine canyon and channel system. GLORIA operates at 6.2-6.8 kHz and images a 45 km swath with spatial resolution of 50 m across track and 125 m along track.

METHODS

The neotectonic map of the Washington continental margin is part of a larger map of the Cascadia margin which includes the "Neotectonic Map of the Oregon Continental Margin and Adjacent Abyssal Plain", published by the Department of Oregon Geology and Mineral Industries in 1992 (Goldfinger et al., 1992). Since 1992, this map has been and will continue to be updated as new data are acquired and as interpretations of Cascadia deformation change. Therefore, the map presented here is not a final product.

The map was constructed within the Microstation CAD (Computer Aided Design) system and Erdas Imagine GIS (for interpretation of rasterized datasets, including sidescan sonar, bathymetry, gravity and magnetics). Datasets with the greatest navigational accuracy and closely-spaced regional networks of profiles were used as the base map with additional data subsequently incorporated. The former datasets included the GLORIA sidescan sonar mosaics, the proprietary industry migrated multichannel seismic profiles (5), U.S.G.S. seismic profiles (2), and University of California Santa Cruz seismic profiles (6) (due to their regional network).

The map emphasizes predominantly active or potentially active structures: structures are differentiated by color into (a) active (Holocene and late Pleistocene), (b) early Pleistocene and Pliocene, and (c) Older or unknown age. Detailed biostratigraphy of the Washington margin is rare (restricted to seafloor samples and oil-exploratory wells on the continental shelf), and therefore most of these age assignments are simply based on depth in section and whether the seafloor is deformed by the structure (the latter refers to category (a), Holocene and late Pleistocene). These ages are therefore only loosely accurate. In some cases, recently active structures have different trends and/or overlap older structures, reflecting changes in the regional stress field. Correlation of structures between seismic reflection profiles (the predominant source of information) was hindered

by the often large distances between profiles. Crossing lines were used to correlate structures more accurately, but these often involved profiles of two different datasets with different navigational accuracies, and hence a miscorrelation at the crossing point. Some short structures have been identified on one profile only, presumed to plunge in both directions away from the line, and therefore their orientation on the map is arbitrary and largely a function of the orientation of the profile. Faults mapped and inferred from seismic reflection profiles may not always show offset of crossing structures, where this offset is not actually observed (in seafloor geomorphology or by detailed correlation between closely-spaced seismic profiles). As more seafloor bathymetry and sidescan sonar data are collected on this margin, many of these discrepancies and problems may be resolved.

GEOLOGIC INTERPRETATIONS

The Washington margin is dominated by deformation related to the Cascadia subduction zone which results from the subduction of the oceanic Juan de Fuca plate beneath the continental North American plate to the northeast (062°) at a current rate of 42 mm/yr (DeMets et al., 1994). The Washington continental margin can be topographically and geomorphically divided into the continental shelf and continental slope. Both areas are characterized by different styles of deformation. The continental slope is composed of the accretionary wedge which extends landward from the deformation front where the Juan de Fuca and North American plates meet at the seafloor. The youngest thrust ridges of the accretionary wedge in Washington are predominantly landward vergent, in contrast to the more common seaward vergent. This region of landward vergence extends from $44^\circ 51'N$ in Oregon to the northernmost Washington margin, and is seaward vergent to the north and south of this region. Landward vergence may be the result of reduced basal shear stress due to the subduction of the Pleistocene submarine fans (Astoria and Nitinat) in this region. Sediments were deposited at high rates on the fans, preventing the expulsion of fluids, and hence they are over-pressured leading to low basal shear stress. The transition (from west to east) between landward-vergent to seaward-vergent folds is represented by the dark red/black line on the plate of the neotectonic map. See Goldfinger et al. (1992b), Goldfinger et al. (1997a), McNeill et al. (1997), and MacKay et al. (1992) for further information. The deformation front is offset by left-lateral strike-slip faults which trend WNW from the abyssal plain to the mid-upper slope (Goldfinger et al., 1997a).

The majority of compressional structures on the Washington continental slope trend approximately N-S to NW reflecting convergence between the two plates, as might be

expected on a typical convergent margin. However, structural trends become more complex on the upper slope and on the shelf. Listric normal faults, trending N-S, are common on the shelf and upper slope and reflect gravitational extension of the underlying *mélange* and broken formation (see Chapter II, McNeill et al., 1997). Downslope extension of the *mélange* also produces a "bulge" in seafloor bathymetry and in fold trends west of Grays Harbor, where many of the normal faults are located. Faulting and uplift of the *mélange* and broken formation on the shelf has resulted in diapiric mud intrusions, which are also indicated on the neotectonic map. Diapirs are rare on the central and southern Oregon margin which is underlain by the basaltic Siletz River Volcanics rather than *mélange*. The innermost shelf is characterized by N-S compressional structures (trending ~E-W) which reflect the regional stress field of the Pacific Northwest. Several of these structures can be traced onshore where they may contribute to the record of coseismic subsidence in coastal bays. This is discussed fully in Chapter III and McNeill et al. (in press).

The Washington margin differs from the Oregon margin in its numerous submarine canyons. The large number of canyons are thought to be a result of the large sediment input to the margin during the Pleistocene glaciations, when the Juan de Fuca and Puget lobes of the Cordilleran ice sheet covered parts of the Olympic Peninsula and Puget Lowland of Washington. The relatively small rivers of the Olympic Peninsula would have had much higher discharge rates at this time. The Chehalis River, for example, currently occupies a very broad valley carved during increased Pleistocene volumes which emptied ice-dammed lakes similar to Lake Missoula of eastern Washington (McKee, 1972). The relative instability of the shelf break and outer shelf due to the weak underlying basement of *mélange* and broken formation in this region (see Chapters II, IV, McNeill et al., 1997) may also contribute to the formation of multiple submarine canyons.

REFERENCES

DeMets, C., Gordon, R.G., Argus, D.F., and Stein, S., 1990. current plate motions. *Geophysical Journal International*, v. 101, p. 425-478.

Goldfinger, C., 1994. Active deformation of the Cascadia forearc: Implications for great earthquake potential in Oregon and Washington. Ph.D. Thesis, Oregon State University, Corvallis, 202 pp.

Goldfinger, C., Kulm, L.D., and Yeats, R.S., 1992. Neotectonic map of the Oregon continental margin and adjacent abyssal plain. Oregon Department of Geology and Mineral Industries, Open-File Report, O-92-4, scale 1:500 000.

Goldfinger, C., Kulm, L.D., Yeats, R.S., McNeill, L.C., and Hummon, C., 1997a. Oblique strike-slip faulting of the central Cascadia submarine forearc. *Journal of Geophysical Research*, v. 102, p. 8217-8243.

Goldfinger, C., McNeill, L.C., and Hummon, C., 1997b. Case study of GIS data integration and visualization in submarine tectonic investigations: Cascadia subduction zone. *Marine Geodesy*, v. 20, p. 267-289.

McKee, B., 1972. *Cascadia: The Geological Evolution of the Pacific Northwest*. New York, McGraw-Hill.

McNeill, L.C., Goldfinger, C., Yeats, R.S., and Kulm, L.D., in press. The Effects of Upper Plate Deformation on Records of Prehistoric Cascadia Subduction Zone Earthquakes. In: *Coastal Tectonics*, Stewart, I., and Vita-Finzi, C. (eds), Geological Society of London Special Publication.

McNeill, L.C., Piper, K.A., Goldfinger, C., Kulm, L.D., and Yeats, R.S., 1997. Listric normal faulting on the Cascadia continental margin. *Journal of Geophysical Research*, v. 102, p. 12,123-12,138.